# Investigating River Ice Breakup Patterns and Snow and Ice Affected Spring Streamflow

by

Yuzhuang Chen

A thesis submitted in partial fulfillment of the requirements for the degree of

Doctor of Philosophy

in

Water Resources Engineering

Department of Civil and Environmental Engineering

University of Alberta

## Abstract

Both the observed and projected temperature in Canada increase faster than the global temperature, which has extensive implications on snow and river ice breakup regime, and then can greatly affect the timing and magnitude of snow and ice affected spring streamflow. This research is to expand our knowledge of river ice breakup timing through collecting and analyzing scientific data describing and driving such events, and simulating snow and ice induced spring streamflow through the development and application of the physics-based hydrologic and river ice models.

The biggest challenge of large-scale spatial and temporal analyses of river ice breakup timing across Canada is there are no long-time and uniform river ice breakup timing records. This study used the date of last 'B' symbol in the discharge record as breakup timing and constructed a long-term (1950-2016) and uniform river ice breakup timing dataset using nearly 200 hydrometric stations form Water Survey of Canada HYDAT database. It provides a way for researchers to construct the river ice breakup timing database and investigate the breakup timing trends under historical climate change. The spatial-temporal variations of breakup timing over terrestrial ecozones and five selected river basins of Canada were investigated based on the constructed long-term data record. The links between the discovered patterns and climatic drivers (e.g., air temperature, snowfall and rainfall), as well as elevation and anthropogenic activities were also analyzed. An overall earlier breakup trend was observed across Canada and the spring air temperature was found to be the main driver behind it. However, the most pronounced warming trends across Canada was observed in winter. Spring warming trend was not as strong as winter warming and even became weak in some periods. Other factors, such as snowfall, rainfall, elevation and flow regulation, also contributed to changes of river ice breakup in various ways.

Their combined effects made river ice breakup patterns display evident spatial and temporal differences. In addition to providing evidence of climate changes in Canada, the findings can provide theoretical support in modelling breakup processes.

The choice of proper input data and suitable calibration scheme is challenging in hydrologic modeling of higher-latitude watersheds with their unique hydro-climatic conditions. Based on the hydrologic model SWAT (Soil and Water Assessment Tool) and the calibration tool SWATCUP, this study revisited various climate data and calibration schemes, and developed a multi-objective calibration framework that can automatically eliminate unrealistic snow parameters combinations and calibrate Snow Water Equivalent (SWE) and streamflow simultaneously in a large cold region watershed, the Peace River Basin (PRB) in western Canada. It demonstrated that the proposed multi-objective calibration framework can effectively limit the uncertainty of snow-related parameters and significantly improve the simulation of snow-affected spring streamflow in the PRB. The evaluating workflow developed in this study can provide insights in modelling cold region watersheds and calibrating the hydrologic models.

Modelling snow and ice affected streamflow in cold region rivers is challenging. Ignoring the streamflow from the ungauged zones/subbasins of a river basin in preparing inflow boundaries for river ice modes could add further challenges and uncertainties. This study firstly attempted to combinedly use the river ice model River1D with the hydrologic model SWAT model to investigate the impacts of ungauged subbasin streamflow on peak flow simulation under open water and rive ice breakup conditions in the PRB. Ungauged subbasin streamflow in each inflow boundary was estimated by both simple drainage-area ratio (DAR) method and the sophisticated hydrologic model. Compared with DAR method, the hydrologic model was proved to be a promising and robust tool for estimating ungauged subbasin streamflow for the river ice model. The results

showed that ungauged subbasins of the PRB can greatly affect the peak flow simulation for both open water and river ice breakup events, especially for flood events. The peak flow simulation was significantly improved when the ungauged subbasin streamflow was properly considered and/or estimated. The findings can contribute to open water and river ice breakup flood simulation, and water resources planning and management in the PRB. The hydrologic and river ice modelling framework developed in this study can be applied into other cold region watersheds to explore the effects of the ungauged subbasins and/or forecast snow and ice induced flood events.

## Preface

The thesis is paper-based, and the major chapters are organized in article formats. Chapter 2 of this thesis had been published as Chen, Y. and She, Y., 2019. Temporal and Spatial Variation of River Ice Breakup Timing across Canada. *In Proceedings of the 20th Workshop on the Hydraulics of Ice Covered Rivers,* Ottawa, Canada, and Chen, Y. and She, Y., 2020. Long-term variations of river ice breakup timing across Canada and its response to climate change. *Cold Regions Science and Technology*, 176, p.103091. I was responsible for conceptualization, data collection and analysis, and the manuscript composition. Dr. Yuntong She was the supervisory author and was involved with conceptualization, review and editing, and funding acquisition.

Chapter 3 of this thesis is under review by *Journal of Hydrology*. I was responsible for conceptualization, data collection, methodology, results analysis, and the manuscript composition. Co-authors are Dr. Monireh Faramarzi, Thian Yew Gan and Yuntong She. Dr. Monireh Faramarzi was responsible for data collection, and review and editing. Thian Yew Gan was responsible for review and editing. Dr. Yuntong She was the supervisory author and was involved with conceptualization, review and editing, and funding acquisition.

Chapter 4 of this thesis is going to be submitted to a peer-reviewed scientific journal.

## Acknowledgement

I would like to express my deepest gratitude to my supervisor Dr. Yuntong She for her guidance, inspiration, patience, and continuous support over my whole PhD research. I would certainly not be able to accomplish this thesis without her help. I would like to thank my co-supervisor of Dr. Thian Yew Gan and my committee member of Dr. Monireh Faramarzi for their inspiring discussions, valuable suggestions, and persistent support for improving and finishing my research work. Their time and efforts are greatly appreciated.

I would like to thank the internal and external examiners, Dr. Zhehui Jin and Dr. Jueyi Sui (University of Northern British Columbia), for committing their time and efforts in reviewing this thesis, and thank Dr. Wenming (William) Zhang for chairing the exam.

I would like to acknowledge the financial support from the Natural Sciences and Engineering Research Council of Canada (NSERC), University of Alberta Graduate Entrance Scholarship, the R. (Larry) Gerard Memorial Scholarship in Ice Engineering and the teaching assistantship provided by University of Alberta. This support is gratefully acknowledged.

I would like to express my sincere gratitude to my family for their unconditional love, accompany, encouragement, understanding, and support throughout this journey. Special thanks to my sister for her encouragement, inspiration and help in pursuing and finishing my PhD research. In addition, I would like to acknowledge the help received from all my friends.

# Table of Contents

## List of Tables

## List of Figures

# Chapter 1. Introduction

Snow and ice are major elements of cold regions and play critical roles in the climatic and hydrological systems (Adam et al., 2009; Barry and Gan, 2022). In Canada, most of the land surface is covered by snow during winter and ice is present in nearly every river for some period of the year. It was reported that Canada's climate has warmed and will warm further in the future (Bush and Lemmen, 2019), which could have extensive implications on the snow and river ice regime. The increased winter temperatures generally cause less ice production, thinner ice cover, and shortened ice cover season (Burrell et al., 2021). In addition, more winter precipitation falls as rain and snow melting occurs earlier in spring as winter temperatures increase (Barnett et al., 2005). Earlier snowmelt can dramatically affect the timing of spring peak flow and river ice breakup processes.

River ice breakup may evolve as a thermal breakup or a dynamic breakup depending on the relative importance of the climatic and hydrodynamic factors (Hicks, 2016). Thermal breakup tends to occur when mild weather is accompanied by low spring runoff. In contrast, dynamic breakup is typically related to significant spring runoff events due to rapid melting of large snowpack. River ice breakup has received wide attention since it can greatly affect winter ice road system and travel safety (e.g., Clark et al., 2016; Hori et al., 2018a, 2018b), hydraulic structures and bridges (e.g. Beltaos et al., 2007; Jobe et al., 2017), aquatic ecosystem (e.g. Blackadar et al., 2020), frequency and severity of ice jam flooding (e.g., Das et al., 2020; Rokaya et al., 2019; Turcotte et al., 2019). The estimated annual costs of ice jam related damage in North America is about 300 million CAD (French, 2017).

River ice breakup and snowmelt under the changing climate have extensive and significant

implications on cold-region hydrological, ecological and river morphological systems, as well as riverine communities. It's of great importance to investigate (1) how river ice breakup timing has changed; (2) what drives the changes of river ice breakup timing; and (3) how to better simulate snow and ice affected streamflow. The objective of this thesis is to improve our knowledge of the trends and drives of river ice breakup timing, and snow and ice affected streamflow through statistical analysis and modelling.

## 1.1 Literature review

A variety of methods have been undertaken by researchers to study river ice breakup, including trend analysis of historical breakup data (de Rham et al., 2008; Fu and Yao, 2015; Rokaya et al., 2018), identification of drivers behind river ice breakup (Beltaos, 2013; Goulding et al., 2009a; Newton et al., 2017; Prowse et al., 2002), forecasting the timing and severity of breakup (Beltaos, 2003, 2013; Chandra Mahabir et al., 2006; Morales-Marín et al., 2019; Zhao et al., 2012), assessment and mapping of ice jam flood (Das et al., 2020; Lindenschmidt et al., 2016; Rokaya et al., 2020).

### *1.1.1 Trend and driver analysis of river ice breakup timing over Canada*

Many studies with respect to trends and drivers of river ice breakup timing in Canada focused on individual rivers and local regions (Beltaos, 2002; de Rham et al., 2008; Doyle and Ball, 2008; Fu and Yao, 2015; Goulding et al., 2009b; Janowicz, 2010; Jasek and Shen, 1999). The country scale breakup timing trend analysis was conducted by Zhang et al. (2001) and Lacroix et al. (2005) using ice data from approximately the second half of the 20$^{th}$ century. Researchers have examined many factors that may influence the ice breakup timing, such as air temperature (Fu and Yao, 2015; Ghanbari et al., 2009; Obyazov and Smakhtin, 2014), snowfall and rainfall (Ariano and Brown, 2019; Jensen et al., 2007; Nõges and Nõges, 2014; Vavrus et al., 1996). Cloud and elevation

(Jakkila et al., 2009; Jensen et al., 2007; Lopez et al., 2019) have also been evaluated but relevant studies mainly focused on lake ice breakup instead of river ice breakup. In general, country scale trend and driver analyses of river ice breakup timing are still very sparse in Canada.

### *1.1.2 Modelling snow and ice affected streamflow during breakup period*

In terms of forecasting the timing and severity of river ice breakup, many researchers and practitioners employed empirical or statistical methods to determine the onset and/or severity of breakup, such as the cumulative degree days of thawing (Beltaos et al., 2006; Rokaya et al., 2019b), threshold models (Shaw et al., 2013; Turcotte and Morse, 2015), multiple regression models (Mahabir et al., 2006), soft computing methods (such as fuzzy logic and artificial neural networks) (Mahabir et al., 2006; Mahabir et al., 2007; Zhao et al., 2012), partially physical equations (Beltaos, 2013), and multiple model combination methods (Sun and Trevor, 2018). Some common critics of this kind of methods are that they are site specific with high false positive results and limited warning time (Turcotte and Morse, 2015; White, 2008).

More efforts needs to be devoted into effectively coupling physics-based river ice models with hydrologic and/or climate models (Brown, 2019; Prowse et al., 2007). Generally, hydraulic models that have the capability of simulating various river ice processses, are refered as river ice models, such as River1D (Blackburn and She, 2019), CRISSP (Chen et al., 2006; Liu et al., 2006), Mike-Ice (Thériault et al., 2010), and RIVICE (Lindenschmidt, 2017). Compared with hydrologic models, river ice models can consider the detailed physical characteristics of river geometries, provide better solution for both open water and ice-related flooding, and be applied to dynamic problems, such as dam breaches and ice jam release events (Blackburn and Hicks, 2003, 2002). Nevertheless, hydrologic models can simulate many crucial climatic and hydrological processes (e.g., snowmelt) that greatly affect river ice breakup process. The streamflow simulated by a

hydrologic model can be used as indicators for breakup timing and severity or as inputs for river ice models to simulate snow and ice induced spring floods and assess the effects of climate change.

Some studies have been conducted to forecast river ice breakup timing and severity and assess future river ice regime using hydrologic models with other models, such as water temperature models, simple ice thickness models, and river ice models. Employing a 1D physics-based river ice model Mike-Ice driven by future climate forcing from the Coordinated Regional Downscaling Experiment (CORDEX, https://na-cordex.org/) and inflow data simulated with a hydrologic model (HBV), Timalsina et al. (2013) evaluated the impact of climate change on river ice regime (e.g., frazil ice and ice cover) in a regulated medium-scale river but breakup timing and severity were not their focus. Morales-Marín et al. (2019) set up a hydrologic and water temperature modelling framework to simulate the breakup timing as the time when water temperature increases above 0°C, which can be used to assess the impacts of climate change on breakup timing. The framework was also used for operational forecasting of river ice breakup timing (Rokaya et al., 2020). Brown (2019) forecasted the breakup timing and assessed the severity of breakup based on the outputs from the Raven hydrologic modelling framework (Craig et al., 2020) and Ashton's (2011) ice thickness model. Breakup timing was determined based on the timing of the initial rise on the hydrograph and its severity was evaluated with a simple threshold model based on flow, accumulated shortwave radiation and ice thickness. Hydrologic models have also been used in conjunction with river ice model for operational real-time and future ice jam flood hazard assessment and mapping in terms of probability of flood extents and depths (Das et al., 2020; Lindenschmidt et al., 2019). However, they focused on the simulation of water level profiles caused by ice jam instead of peak flow during river ice breakup period. Work towards improving the capability of the hydrologic and river ice modelling framework simulating snow and ice

induced floods in cold region river basins is in great demand.

#### *1.1.2.1 Uncertainties in hydrologic modelling*

Turcotte et al. (2019) pointed out that estimating and forecasting the river runoff during breakup season will be the most limiting factor to evaluate ice jam floods once breakup/ice jam models have reached a suitable development stage. It is vital to explore new discharge quantification methods or improve runoff simulation during the spring breakup period (i.e., snow and ice induced spring streamflow). To accurately simulate streamflow using a hydrologic model, uncertainties/errors in the input data and parameter estimation need to be reduced and relevant physical processes need to be properly accounted for. Setting up the hydrologic model properly through analyzing various combinations of input data can limit uncertainties in input data and improve overall model performance (Faramarzi et al., 2015). Ficklin and Barnhart (2014) found that the issue of hydrologic model parameter uncertainty and equifinality can lead to significantly different hydrological results. To address this, one could use multi-objective calibration methods (Hanzer et al., 2016; Rajib et al., 2016; Tuo et al., 2018a), calibrate multiple sites instead of one outlet site (Abbaspour et al., 2007; Nkiaka et al., 2018; Schuol et al., 2008), and calibrate hydrologic models under various sets of conditions (wet vs. dry) during historical period (Poulin et al., 2011). In cold regions, the land surface hydrology is dominated by winter snow accumulation and spring snowmelt (Barnett et al., 2005). Multi-objective calibration that includes both streamflow and snow measurements can be useful in improving the snow processes of hydrologic models (Tuo et al., 2018b). However, relevant studies are still sparse, especially in large cold region river basins.

*1.1.2.2 Ungauged streamflow estimation and verification*

Many river basins in the world are ungauged or poorly gauged, and the ungauged catchment streamflow estimation and/or prediction is challenging in hydrological science (Guo et al., 2021a; Hrachowitz et al., 2013; Mishra and Coulibaly, 2009; Sivapalan, 2003), which can bring huge uncertainies and/or errors into hydraulic/river ice models in simulating flood events. In 2003, the International Association of Hydrological Sciences (IAHS) launched the initiative for Predictions in Ungauged Basins (PUB) (Sivapalan et al., 2003). Numerous studies regarding ungauged catchment streamflow estimation and/or prediction have been presented since the launch of the PUB initiative, the methods range from simple draninage-area ratio (DAR) method (Asquith et al., 2006; Emerson et al., 2005; Ergen and Kentel, 2016; Gianfagna et al., 2015; Q. Li et al., 2019; McCuen and Levy, 2000) to the hydrologic model based regionalization methods (Booker and Woods, 2014; Pagliero et al., 2019; Parajka et al., 2013; Salinas et al., 2013; Singh et al., 2022; Viglione et al., 2013; Zelelew and Alfredsen, 2014; Zhang and Chiew, 2009). However, the ungauged catchment stremflow estimated by various methods can still be unsatisfactory because of the large heterogeneity of catchment attributes (e.g., soil, land cover, and slope), and uncertainties of input data and model structures and calibrations (Guo et al., 2021b; Hrachowitz et al., 2013; Sivapalan, 2003).

In the hydrologic and hydraulic modelling framework, the hydraulic models can be used to verify the hydrologic model simulated ungauged catchment streamflow. The hydrologic model estimates the ungauged catchment streamflow and provide inflows to the hydraulic model. The hydraulic model simulates water suraface area, water levels and/or flows, and by comparing to their observed values, provides verification of the ungauged streamflow estimated by the hydrologic model. For example, Liu et al. (2015) coupled the SWAT (Soil and Water Assessment Tool) hydrologic model

and the XSECT hydraulic model for estimating streamflow and water levels for ungauged subbasins in the Red River Basin (U.S. portion). Zhang et al. (2017) coupled the SWAT model and the Delft3D hydraulic model to simulate the streamflow for the ungauged zones of the Poyang Lake Basin. Despite there are a large amount of studies with respect to estimating and/or predicting streamflow in ungauged cathcments, and verifying the estimated results using the hydrologic and hydraulic modelling framework, the effects of ungauged subbasins on peak flow, especially snow and ice induced peak flow, in a large cold-region watershed is remaining to to be explored through the hydrologic and river ice modelling framework.

### *1.1.3 Summary*

The above literature review shows that large-scale trend analysis of river ice breakup timing based on long-term and uniform data across Canada is still needed because the majority of related studies focused on individual rivers and local regions. Frameworks that coupling hydrologic models with river ice and/or other models for simulating and assessing river ice regime, the timing and severity of river ice breakup, and ice jam floods have been initiated and developed, but developing a robust modelling framework that couples physics-based river ice models with hydrologic models to simulate snow and ice affected streamflow is still a challenge and in great demand. More work needs to be done to assess the uncertainties of data inputs, and hydrologic model calibration methods to better simulate the snow affected streamflow in large cold region river basins. Streamflow from ungauged subbasins of a river basin could add huge uncertainty to river ice models in simulating flood events. The effects of ungauged subbasins on peak flow, especially snow and ice induced peak flow, in a large cold region river basin is remaining to be explored through the hydrologic and river ice modelling framework.

## 1.2 Research objectives

The objectives of this research are to investigate the trends of river ice breakup timing and the potential drivers behind it, and to improve the performance of the hydrologic and river ice modelling framework in simulating snow and ice affected spring streamflow (particularly during rive ice breakup). The three specific objectives are described below:

**Objective 1**: Examine the spatial-temporal trends and drivers of river ice breakup timing across Canada (Chapter 2)

Large-scale trend analysis of river ice breakup timing based on long-term uniform data is needed to show how river ice breakup timing has changed under historical climate. Further exploration of the possible drivers of rive ice breakup is required to better understand the effects of climate change and provide reliable forecast indicators of such events. The following tasks were conducted to achieve this objective: (1) identifying the spatial and temporal variations of river ice breakup timing across major Canadian rivers; (2) analyzing detailed regional patterns over terrestrial ecozones and five selected river basins; (3) exploring the relationship between identified breakup trends/patterns and climatic factors (e.g., air temperature, rainfall and snowfall), as well as other factors (such as elevation and flow regulation).

**Objective 2**: Improve the performance of a hydrologic model in simulating snow affected streamflow in a large-scale regulated and snow-dominated river basin (Chapter 3)

Hydrologic model is a key component in hydrologic and river ice modelling framework to provide reliable inflow boundaries to river ice models. It is critical that the effects of uncertainties/errors in input data and model calibration are assessed and relevant physical processes (e.g., snowmelt) are properly accounted for. Utilizing the SWAT model, this objective was achieved by: (1)

evaluating observed and gridded climate data to find the optimal weather input; (2) automatically eliminating unrealistic snow parameter combinations, and calibrating streamflow and Snow Water Equivalent (SWE) simultaneously; (3) determining the proper calibration scheme through comparing the choice of objective function, number of simulations in each iteration, sequential calibration from upstream to downstream, and calibrating snow parameters first and then all other hydrological parameters; (4) improving the simulation of snow-affected spring streamflow using multi-objective calibration (streamflow and SWE).

**Objective 3**: Investigate the effects of ungauged subbasins on open water and river ice breakup peak flow in a large partially gauged basin with the hydrologic and river ice modelling framework (Chapter 4)

Many river basins are ungauged or partially ungauged. If the ungauged subbasin streamflow in a river basin is unconsidered or not probably estimated, it could bring large uncertainties and/or errors into the river ice models in simulating flood events. Through the combination of the SWAT hydrologic model and River1D river ice model, this objective was achieved by: (1) evaluating ungauged subbasin streamflow estimation methods, (2) investiagting the impacts of ungauged subbasins on peak flow simualtion under open water and river ice breakup conditions, and (3) analyzing the peak flow contribution of the gauged and ungauged subbasins for the open water and river ice breakup events.

## 1.3 Reference

Abbaspour, K.C., Yang, J., Maximov, I., Siber, R., Bogner, K., Mieleitner, J., Zobrist, J., Srinivasan, R., 2007. Modelling hydrology and water quality in the pre-alpine/alpine Thur watershed using SWAT. J. Hydrol. 333, 413–430. https://doi.org/10.1016/j.jhydrol.2006.09.014

Adam, J.C., Hamlet, A.F., Lettenmaier, D.P., 2009. Implications of global climate change for snowmelt hydrology in the twenty-first century. Hydrol. Process. An Int. J. 23, 962–972.

Ariano, S.S., Brown, L.C., 2019. Ice processes on medium-sized north-temperate lakes. Hydrol. Process. 33, 2434–2448.

Ashton, G.D., 2011. River and lake ice thickening, thinning, and snow ice formation. Cold Reg. Sci. Technol. 68, 3–19. https://doi.org/10.1016/j.coldregions.2011.05.004

Asquith, W.H., Roussel, M.C., Vrabel, J., 2006. Statewide analysis of the drainage-area ratio method for 34 streamflow percentile ranges in Texas. US Geological Survey.

Barnett, T.P., Adam, J.C., Lettenmaier, D.P., 2005. Potential impacts of a warming climate on water availability in snow-dominated regions. Nature 438, 303–309. https://doi.org/10.1038/nature04141

Barry, R.G., Gan, T.Y., 2022. The global cryosphere: past, present, and future. Cambridge University Press.

Beltaos, S., 2013. Hydrodynamic and climatic drivers of ice breakup in the lower Mackenzie River. Cold Reg. Sci. Technol. 95, 39–52. https://doi.org/10.1016/j.coldregions.2013.08.004

Beltaos, S., 2003. Threshold between mechanical and thermal breakup of river ice cover. Cold Reg.

Sci. Technol. 37, 1–13. https://doi.org/10.1016/S0165-232X(03)00010-7

Beltaos, S., 2002. Effects of climate on mid-winter ice jams. Hydrol. Process. 16, 789–804.

Beltaos, S., Miller, L., Burrell, B.C., Sullivan, D., 2007. Hydraulic effects of ice breakup on bridges. Can. J. Civ. Eng. 34, 539–548. https://doi.org/10.1139/L06-145

Beltaos, S., Prowse, T., 2009. River-ice hydrology in a shrinking cryosphere. Hydrol. Process. 23, 122–144.

Beltaos, S., Prowse, T., Bonsal, B., MacKay, R., Romolo, L., Pietroniro, A., Toth, B., 2006. Climatic effects on ice-jam flooding of the Peace-Athabasca Delta. Hydrol. Process. An Int. J. 20, 4031–4050.

Blackadar, R.J., Baxter, C. V., Davis, J.M., Harris, H.E., 2020. Effects of river ice break-up on organic-matter dynamics and feeding ecology of aquatic insects. River Res. Appl. 36, 480–491. https://doi.org/10.1002/rra.3585

Blackburn, J., Hicks, F., 2003. Suitability of dynamic modeling for flood forecasting during ice jam release surge events. J. Cold Reg. Eng. 17, 18–36. https://doi.org/10.1061/(ASCE)0887-381X(2003)17:1(18)

Blackburn, J., Hicks, F.E., 2002. Combined flood routing and flood level forecasting. Can. J. Civ. Eng. 29, 64–75.

Blackburn, J., She, Y., 2019. A comprehensive public-domain river ice process model and its application to a complex natural river. Cold Reg. Sci. Technol. 163, 44–58. https://doi.org/10.1016/j.coldregions.2019.04.010

Booker, D.J., Woods, R.A., 2014. Comparing and combining physically-based and empirically-based approaches for estimating the hydrology of ungauged catchments. J. Hydrol. 508, 227–239. https://doi.org/10.1016/j.jhydrol.2013.11.007

Brown, G., 2019. Application of a Hydrological Model for Predicting River Ice Breakup.

Burrell, B.C., Beltaos, S., Turcotte, B., 2021. Effects of Climate Change on River-Ice Processes and Ice Jams. Int. J. River Basin Manag. 1–78. https://doi.org/10.1080/15715124.2021.2007936

Bush, E., Lemmen, D.S., 2019. Canada's changing climate report. Government of Canada= Gouvernement du Canada.

Chen, F., Shen, H.T., Jayasundara, N., 2006. A one-dimensional comprehensive river ice model, in: Proceedings of 18th International Association of Hydraulic Research Symposium on Ice, Sapporo, Japan. Citeseer.

Clark, D.G., Ford, J.D., Berrang-Ford, L., Pearce, T., Kowal, S., Gough, W.A., 2016. The role of environmental factors in search and rescue incidents in Nunavut, Canada. Public Health 137, 44–49. https://doi.org/10.1016/j.puhe.2016.06.003

Craig, J.R., Brown, G., Chlumsky, R., Jenkinson, W., Jost, G., Lee, K., Mai, J., Serrer, M., Snowdon, A.P., Sgro, N., 2020. Flexible watershed simulation with the Raven hydrological modelling framework. Environ. Model. Softw. 104728.

Das, A., Rokaya, P., Lindenschmidt, K.E., 2020. Ice-Jam Flood Risk Assessment and Hazard Mapping under Future Climate. J. Water Resour. Plan. Manag. 146, 1–12.

https://doi.org/10.1061/(ASCE)WR.1943-5452.0001178

de Rham, L.P., Prowse, T.D., Bonsal, B.R., 2008. Temporal variations in river-ice break-up over the Mackenzie River Basin, Canada. J. Hydrol. 349, 441–454. https://doi.org/10.1016/j.jhydrol.2007.11.018

Doyle, P.F., Ball, J.F., 2008. Changing ice cover regime in southern British Columbia due to changing climate, in: Proceedings of the 19th IAHR International Symposium on Ice. St Joseph Communications, Vancouver, Canada. pp. 51–61.

Emerson, D.G., Vecchia, A. V, Dahl, A.L., 2005. Evaluation of drainage-area ratio method used to estimate streamflow for the Red River of the North Basin, North Dakota and Minnesota. US Department of the Interior, US Geological Survey.

Ergen, K., Kentel, E., 2016. An integrated map correlation method and multiple-source sites drainage-area ratio method for estimating streamflows at ungauged catchments: A case study of the Western Black Sea Region, Turkey. J. Environ. Manage. 166, 309–320. https://doi.org/10.1016/j.jenvman.2015.10.036

Faramarzi, M., Srinivasan, R., Iravani, M., Bladon, K.D., Abbaspour, K.C., Zehnder, A.J.B., Goss, G.G., 2015. Setting up a hydrological model of Alberta: Data discrimination analyses prior to calibration. Environ. Model. Softw. 74, 48–65. https://doi.org/10.1016/j.envsoft.2015.09.006

Ficklin, D.L., Barnhart, B.L., 2014. SWAT hydrologic model parameter uncertainty and its implications for hydroclimatic projections in snowmelt-dependent watersheds. J. Hydrol. 519, 2081–2090. https://doi.org/10.1016/j.jhydrol.2014.09.082

French, H.M., 2017. The periglacial environment. John Wiley & Sons.

Fu, C., Yao, H., 2015. Trends of ice breakup date in south-central Ontario. J. Geophys. Res. Atmos. 120, 9220–9236.

Ghanbari, R.N., Bravo, H.R., Magnuson, J.J., Hyzer, W.G., Benson, B.J., 2009. Coherence between lake ice cover, local climate and teleconnections (Lake Mendota, Wisconsin). J. Hydrol. 374, 282–293. https://doi.org/10.1016/j.jhydrol.2009.06.024

Gianfagna, C.C., Johnson, C.E., Chandler, D.G., Hofmann, C., 2015. Watershed area ratio accurately predicts daily streamflow in nested catchments in the Catskills, New York. J. Hydrol. Reg. Stud. 4, 583–594. https://doi.org/10.1016/j.ejrh.2015.09.002

Goulding, H.L., Prowse, T.D., Beltaos, S., 2009b. Spatial and temporal patterns of break-up and ice-jam flooding in the Mackenzie Delta, NWT. Hydrol. Process. An Int. J. 23, 2654–2670.

Goulding, H.L., Prowse, T.D., Bonsal, B., 2009a. Hydroclimatic controls on the occurrence of break-up and ice-jam flooding in the Mackenzie Delta, NWT, Canada. J. Hydrol. 379, 251–267. https://doi.org/10.1016/j.jhydrol.2009.10.006

Guo, Y., Zhang, Y., Zhang, L., Wang, Z., 2021a. Regionalization of hydrological modeling for predicting streamflow in ungauged catchments: A comprehensive review. Wiley Interdiscip. Rev. Water 8, e1487.

Guo, Y., Zhang, Y., Zhang, L., Wang, Z., 2021b. Regionalization of hydrological modeling for predicting streamflow in ungauged catchments: A comprehensive review. Wiley Interdiscip. Rev. Water 8, 1–32. https://doi.org/10.1002/wat2.1487

Hanzer, F., Helfricht, K., Marke, T., Strasser, U., 2016. Multilevel spatiotemporal validation of snow/ice mass balance and runoff modeling in glacierized catchments. Cryosphere 10, 1859–1881. https://doi.org/10.5194/tc-10-1859-2016

Hicks, F.E., 2016. An introduction to river ice engineering for civil engineers and geoscientists. CreateSpace Independent Publishing Platform.

Hori, Y., Cheng, V.Y.S., Gough, W.A., Jien, J.Y., Tsuji, L.J.S., 2018a. Implications of projected climate change on winter road systems in Ontario's Far North, Canada. Clim. Change 148, 109–122. https://doi.org/10.1007/s10584-018-2178-2

Hori, Y., Gough, W.A., Tam, B., Tsuji, L.J.S., 2018b. Community vulnerability to changes in the winter road viability and longevity in the western James Bay region of Ontario's Far North. Reg. Environ. Chang. 18, 1753–1763. https://doi.org/10.1007/s10113-018-1310-1

Hrachowitz, M., Savenije, H.H.G., Blöschl, G., McDonnell, J.J., Sivapalan, M., Pomeroy, J.W., Arheimer, B., Blume, T., Clark, M.P., Ehret, U., Fenicia, F., Freer, J.E., Gelfan, A., Gupta, H. V., Hughes, D.A., Hut, R.W., Montanari, A., Pande, S., Tetzlaff, D., Troch, P.A., Uhlenbrook, S., Wagener, T., Winsemius, H.C., Woods, R.A., Zehe, E., Cudennec, C., 2013. A decade of Predictions in Ungauged Basins (PUB)-a review. Hydrol. Sci. J. 58, 1198–1255. https://doi.org/10.1080/02626667.2013.803183

Jakkila, J., Leppäranta, M., Kawamura, T., Shirasawa, K., Salonen, K., 2009. Radiation transfer and heat budget during the ice season in Lake Pääjärvi, Finland. Aquat. Ecol. 43, 681–692. https://doi.org/10.1007/s10452-009-9275-2

Janowicz, J.R., 2010. Observed trends in the river ice regimes of northwest Canada. Hydrol. Res.

41, 462. https://doi.org/10.2166/nh.2010.145

Jasek, M.J., Shen, H.T., 1999. 1998 break-up and flood on the Yukon River at Dawson–did El Niño and climate change play a role? Ice Surf. Waters, Balkema, Rotterdam 761–768.

Jensen, O.P., Benson, B.J., Magnuson, J.J., Card, V.M., Futter, M.N., Soranno, P.A., Stewart, K.M., 2007. Spatial analysis of ice phenology trends across the Laurentian Great Lakes region during a recent warming period. Limnol. Oceanogr. 52, 2013–2026. https://doi.org/10.4319/lo.2007.52.5.2013

Jobe, A., Bhandari, S., Kalra, A., Ahmad, S., 2017. Ice-Cover and Jamming Effects on Inline Structures and Upstream Water Levels. World Environ. Water Resour. Congr. 2017 Hydraul. Waterw. Water Distrib. Syst. Anal. - Sel. Pap. from World Environ. Water Resour. Congr. 2017 270–279. https://doi.org/10.1061/9780784480625.025

Lacroix, M.P., Prowse, T.D., Bonsal, B.R., Duguay, C.R., Ménard, P., 2005. River ice trends in Canada, in: 13th Workshop on the Hydraulics of Ice Covered Rivers. pp. 41–55.

Li, Q., Peng, Y., Wang, G., Wang, H., Xue, B., Hu, X., 2019. A combined method for estimating continuous runoff by parameter transfer and drainage area ratio method in ungauged catchments. Water 11, 1104.

Lindenschmidt, K.E., 2017. RIVICE-A non-proprietary, open-source, one-dimensional river-ice model. Water (Switzerland) 9. https://doi.org/10.3390/w9050314

Lindenschmidt, K.E., Das, A., Rokaya, P., Chu, T., 2016. Ice-jam flood risk assessment and mapping. Hydrol. Process. 30, 3754–3769. https://doi.org/10.1002/hyp.10853

Lindenschmidt, K.E., Rokaya, P., Das, A., Li, Z., Richard, D., 2019. A novel stochastic modelling approach for operational real-time ice-jam flood forecasting. J. Hydrol. 575, 381–394. https://doi.org/10.1016/j.jhydrol.2019.05.048

Liu, G., Schwartz, F.W., Tseng, K., Shum, C.K., 2015. Discharge and water-depth estimates for ungauged rivers: Combining hydrologic, hydraulic, and inverse modeling with stage and water-area measurements from satellites. Water Resour. Res. 51, 6017–6035.

Liu, L., Li, H., Shen, H.T., 2006. A Two-Dimensional Comprehensive River Ice Model. Proc. 18th IAHR Int. Symp. Ice 69–76.

Lopez, L.S., Hewitt, B.A., Sharma, S., 2019. Reaching a breaking point: How is climate change influencing the timing of ice breakup in lakes across the northern hemisphere? Limnol. Oceanogr. 1–11. https://doi.org/10.1002/lno.11239

Mahabir, Chandra, Hicks, F., Fayek, A.R., 2006. Neuro-fuzzy river ice breakup forecasting system. Cold Reg. Sci. Technol. 46, 100–112. https://doi.org/10.1016/j.coldregions.2006.08.009

Mahabir, C., Hicks, F.E., Fayek, A.R., 2007. Transferability of a neuro-fuzzy river ice jam flood forecasting model. Cold Reg. Sci. Technol. 48, 188–201. https://doi.org/10.1016/j.coldregions.2006.12.004

Mahabir, C., Hicks, F.E., Robichaud, C., Fayek, A.R., 2006. Forecasting breakup water levels at Fort McMurray, Alberta, using multiple linear regression. Can. J. Civ. Eng. 33, 1227–1238. https://doi.org/10.1139/L06-067

McCuen, R.H., Levy, B.S., 2000. Evaluation of peak discharge transposition. J. Hydrol. Eng. 5,

278–289.

Mishra, A.K., Coulibaly, P., 2009. Developments in hydrometric network design: A review. Rev. Geophys. 47.

Morales-Marín, L.A., Sanyal, P.R., Kadowaki, H., Li, Z., Rokaya, P., Lindenschmidt, K.E., 2019. A hydrological and water temperature modelling framework to simulate the timing of river freeze-up and ice-cover breakup in large-scale catchments. Environ. Model. Softw. 114, 49–63. https://doi.org/10.1016/j.envsoft.2019.01.009

Newton, B.W., Prowse, T.D., de Rham, L.P., 2017. Hydro-climatic drivers of mid-winter break-up of river ice in western Canada and Alaska. Hydrol. Res. 48, 945–956. https://doi.org/10.2166/nh.2016.358

Nkiaka, E., Nawaz, N.R., Lovett, J.C., 2018. Effect of single and multi-site calibration techniques on hydrological model performance, parameter estimation and predictive uncertainty: a case study in the Logone catchment, Lake Chad basin. Stoch. Environ. Res. Risk Assess. 32, 1665–1682. https://doi.org/10.1007/s00477-017-1466-0

Nõges, P., Nõges, T., 2014. Weak trends in ice phenology of Estonian large lakes despite significant warming trends. Hydrobiologia 731, 5–18. https://doi.org/10.1007/s10750-013-1572-z

Obyazov, V.A., Smakhtin, V.K., 2014. Ice regime of Transbaikalian rivers under changing climate. Water Resour. 41, 225–231. https://doi.org/10.1134/S0097807814030130

Pagliero, L., Bouraoui, F., Diels, J., Willems, P., McIntyre, N., 2019. Investigating regionalization techniques for large-scale hydrological modelling. J. Hydrol. 570, 220–235.

https://doi.org/10.1016/j.jhydrol.2018.12.071

Parajka, J., Viglione, A., Rogger, M., Salinas, J.L., Sivapalan, M., Blöschl, G., 2013. Comparative assessment of predictions in ungauged basins-Part 1: Runoff-hydrograph studies. Hydrol. Earth Syst. Sci. 17, 1783–1795. https://doi.org/10.5194/hess-17-1783-2013

Poulin, A., Brissette, F., Leconte, R., Arsenault, R., Malo, J.S., 2011. Uncertainty of hydrological modelling in climate change impact studies in a Canadian, snow-dominated river basin. J. Hydrol. 409, 626–636. https://doi.org/10.1016/j.jhydrol.2011.08.057

Prowse, T., Bonsal, B.R., Duguay, C.R., Lacroix, M.P., 2007. River-ice break-up/freeze-up: A review of climatic drivers, historical trends and future predictions. Ann. Glaciol. 46, 443–451. https://doi.org/10.3189/172756407782871431

Prowse, T.D., Bonsal, B.R., Lacroix, M.P., 2002. Trends in River-Ice Breakup and Related Temperature Controls 2–6.

Rajib, M.A., Merwade, V., Yu, Z., 2016. Multi-objective calibration of a hydrologic model using spatially distributed remotely sensed/in-situ soil moisture. J. Hydrol. 536, 192–207. https://doi.org/10.1016/j.jhydrol.2016.02.037

Rokaya, P., Budhathoki, S., Lindenschmidt, K.-E., 2018. Trends in the Timing and Magnitude of Ice-Jam Floods in Canada. Sci. Rep. 8, 5834.

Rokaya, P., Morales-Marín, L., Bonsal, B., Wheater, H., Lindenschmidt, K.E., 2019a. Climatic effects on ice phenology and ice-jam flooding of the Athabasca River in western Canada. Hydrol. Sci. J. 64, 1265–1278. https://doi.org/10.1080/02626667.2019.1638927

Rokaya, P., Morales-Marin, L., Lindenschmidt, K.E., 2020. A physically-based modelling framework for operational forecasting of river ice breakup. Adv. Water Resour. 139, 103554. https://doi.org/10.1016/j.advwatres.2020.103554

Rokaya, P., Peters, D.L., Bonsal, B., Wheater, H., Lindenschmidt, K.E., 2019b. Modelling the effects of climate and flow regulation on ice-affected backwater staging in a large northern river. River Res. Appl. 35, 587–600. https://doi.org/10.1002/rra.3436

Salinas, J.L., Laaha, G., Rogger, M., Parajka, J., Viglione, A., Sivapalan, M., Blöschl, G., 2013. Comparative assessment of predictions in ungauged basins-Part 2: Flood and low flow studies. Hydrol. Earth Syst. Sci. 17, 2637–2652. https://doi.org/10.5194/hess-17-2637-2013

Schuol, J., Abbaspour, K.C., Yang, H., Srinivasan, R., Zehnder, A.J.B., 2008. Modeling blue and green water availability in Africa. Water Resour. Res. 44, 1–18. https://doi.org/10.1029/2007WR006609

Shaw, J.K.E., Lavender, S.T., Stephen, D., Jamieson, K., 2013. Ice Jam Flood Risk Forecasting at the Kashechewan FN Community on the North Albany River. Proc. 17th Work. River Ice 20 pages.

Singh, L., Mishra, P.K., Pingale, S.M., Khare, D., Thakur, H.P., 2022. Streamflow regionalisation of an ungauged catchment with machine learning approaches. Hydrol. Sci. J. 67, 886–897. https://doi.org/10.1080/02626667.2022.2049271

Sivapalan, M., 2003. Prediction in ungauged basins: a grand challenge for theoretical hydrology. Hydrol. Process. 17, 3163–3170.

Sivapalan, M., Takeuchi, K., Franks, S.W., Gupta, V.K., Karambiri, H., Lakshmi, V., Liang, X., McDonnell, J.J., Mendiondo, E.M., O'Connell, P.E., Oki, T., Pomeroy, J.W., Schertzer, D., Uhlenbrook, S., Zehe, E., 2003. IAHS Decade on Predictions in Ungauged Basins (PUB), 2003-2012: Shaping an exciting future for the hydrological sciences. Hydrol. Sci. J. 48, 857–880. https://doi.org/10.1623/hysj.48.6.857.51421

Sun, W., Trevor, B., 2018. Multiple model combination methods for annual maximum water level prediction during river ice breakup. Hydrol. Process. 32, 421–435.

Thériault, I., Saucet, J.-P., Taha, W., 2010. Validation of the Mike-Ice model simulating river flows in presence of ice and forecast of changes to the ice regime of the Romaine river due to hydroelectric project, in: Proceedings of the 20th IAHR International Symposium on Ice, Lahti, Finland. pp. 14–17.

Timalsina, N.P., Charmasson, J., Alfredsen, K.T., 2013. Simulation of the ice regime in a Norwegian regulated river. Cold Reg. Sci. Technol. 94, 61–73. https://doi.org/10.1016/j.coldregions.2013.06.010

Tuo, Y., Marcolini, G., Disse, M., Chiogna, G., 2018a. Calibration of snow parameters in SWAT: comparison of three approaches in the Upper Adige River basin (Italy). Hydrol. Sci. J. 63, 657–678. https://doi.org/10.1080/02626667.2018.1439172

Tuo, Y., Marcolini, G., Disse, M., Chiogna, G., 2018b. A multi-objective approach to improve SWAT model calibration in alpine catchments. J. Hydrol. 559, 347–360. https://doi.org/10.1016/j.jhydrol.2018.02.055

Turcotte, B., Burrell, B.C., Beltaos, S., 2019. The Impact of Climate Change on Breakup Ice Jams

in Canada : State of knowledge and research approaches.

Turcotte, B., Morse, B., 2015. River ice breakup forecast and annual risk distribution in a climate change perspective, in: 18th Workshop on the Hydraulics of Ice Covered Rivers, CGU HS Committee on River Ice Processes and the Environment, Quebec.

Vavrus, S.J., Wynne, R.H., Foley, J.A., 1996. Measuring the sensitivity of southern Wisconsin lake ice to climate variations and lake depth using a numerical model. Limnol. Oceanogr. 41, 822–831.

Viglione, A., Parajka, J., Rogger, M., Salinas, J.L., Laaha, G., Sivapalan, M., Blöschl, G., 2013. Comparative assessment of predictions in ungauged basins - Part 3: Runoff signatures in Austria. Hydrol. Earth Syst. Sci. 17, 2263–2279. https://doi.org/10.5194/hess-17-2263-2013

White, K.D., 2008. Breakup ice jam forecasting (Chapter 10). River ice Break. 327–348.

Zelelew, M.B., Alfredsen, K., 2014. Use of Cokriging and Map Correlation to Study Hydrological Response Patterns and Select Reference Stream Gauges for Ungauged Catchments. J. Hydrol. Eng. 19, 388–406. https://doi.org/10.1061/(asce)he.1943-5584.0000803

Zhang, L., Lu, J., Chen, X., Liang, D., Fu, X., Sauvage, S., Perez, J.M.S., 2017. Stream flow simulation and verification in ungauged zones by coupling hydrological and hydrodynamic models: A case study of the Poyang Lake ungauged zone. Hydrol. Earth Syst. Sci. 21, 5847–5861. https://doi.org/10.5194/hess-21-5847-2017

Zhang, X., David Harvey, K., Hogg, W.D., Yuzyk, T.R., 2001. Trends in Canadian streamflow. Water Resour. Res. 37, 987–998. https://doi.org/10.1029/2000WR900357

Zhang, Y., Chiew, F.H.S., 2009. Relative merits of different methods for runoff predictions in ungauged catchments. Water Resour. Res. 45. https://doi.org/10.1029/2008WR007504

Zhao, L., Hicks, F.E., Fayek, A.R., 2012. Applicability of multilayer feed-forward neural networks to model the onset of river breakup. Cold Reg. Sci. Technol. 70, 32–42. https://doi.org/10.1016/j.coldregions.2011.08.011

# Chapter 2. Long-term Variations of River Ice Breakup Timing across Canada and its Response to Climate Change

## 2.1 Introduction

The cryosphere is very sensitive to climate variability and can provide some of the most visible signatures of climate change (IPCC, 2013). River ice is one of the main components of the cryosphere, and thus its long-term records can serve as good indicators of climate change and variability in northern regions (Magnuson et al., 2000; Prowse et al., 2011, 2007). In Canada, ice is present in nearly every river for some period of the year and is an important aspect of winter hydrology. River ice breakup in particular, can greatly affect water quantity and quality of the river system, and can be both harmful and beneficial to human (Beltaos and Prowse, 2009; Hicks, 2009; Prowse et al., 2011; Weyhenmeyer et al., 2011).

Many previous studies have shown that breakup in Canadian rivers had generally become earlier. For example, Jasek and Shen (1999) discovered that breakup of the Yukon River had advanced by approximately 5 days per century from 1896 to 1998. Beltaos (2002) found that the date of breakup of the Saint John River had become 11 days earlier per century for the period of 1927-1997 and the trend had become more noticeable since late 1950s. Earlier breakup was also found in several local regions of Canada, such as southern British Columbia rivers (Doyle and Ball, 2008), Mackenzie River Basin (de Rham et al., 2008; Goulding et al., 2009b), northwest rivers (Janowicz, 2010) and south-central Ontario waterbodies (Fu and Yao, 2015). Although historical trends of rive ice breakup at a variety of spatial and temporal scales have been investigated, large-scale spatial and temporal analyses across Canada remain sparse. By far the most comprehensive such studies were conducted by Zhang et al. (2001) and Lacroix et al. (2005) using ice data from approximately

the second half of the 20th century, and both studies reported an overall trend towards earlier breakup.

Numerous studies examined the factors that may have contributed to the changes in the breakup timing. Air temperature during certain winter/spring months is probably the most significant influencing factor of river ice breakup events (Fu and Yao, 2015; Ghanbari et al., 2009; Obyazov and Smakhtin, 2014). However, river ice breakup is not controlled by a simple heat index (e.g., air temperature), other factors such as snowfall and rainfall may also be contributing factors (Beltaos and Prowse, 2009). Snow can impede heat flux into the ice cover and increase the albedo of the ice surface, and thus increased snowfall tends to delay spring breakup (Jensen et al., 2007; Vavrus et al., 1996). Rainfall during ice season may have a negative feedback on breakup timing as the heat released from rain can rapidly melt the ice (Nõges and Nõges, 2014). However, Ariano and Brown (2019) found that mid-winter rain can refreeze to form white ice, leading to increased ice thickness and delayed breakup. In addition, cloud cover and elevation can indirectly affect breakup by altering the solar radiation and air temperature (Jakkila et al., 2009; Jensen et al., 2007; Lopez et al., 2019), but these studies focused on lake ice breakup.

Most previous studies that analyzed breakup trends were based on individual river or rivers in small-scale regions. The two large-scale spatial analyses across Canada (Lacroix et al., 2005; Zhang et al., 2001) analyzed periods before 2000s. Therefore, it is of great necessity to investigate large-scale spatial and temporal patterns of river ice breakup in response to climate change, using long and uniform river ice data. This study focused on trends and changes in breakup timing for major Canadian rivers over the period of 1950-2016. Periods of 1960-2016 and 1970-2016 were also analyzed to explore how the discovered trends may change with the period of analysis. General trends and changes, as well as spatial and temporal patterns over terrestrial ecozones and

selected river basins were discussed. Studies have shown that Canada warms faster than the rest of the world and precipitation is projected to increase in most of Canada (Bush and Lemmen, 2019). Those observed trends in breakup were thus connected to the trends in climatic variables including air temperature, snowfall and rainfall since these factors are the primary drivers of the variability and change in the cryosphere. The potential effects of elevation and flow regulation on breakup timing were also evaluated as these factors further complicate how river ice breakup responds to changes in climatic factors and their effects have mainly been studied for specific rivers and from ice jam flooding perspective. Additionally, the impact of missing values in the dataset was discussed.

## 2.2 Material and methods

### *2.2.1 Data*

The dataset of breakup dates used in this study was extracted from the Water Survey of Canada (WSC) HYDAT database. The 'B' symbol in the discharge record denotes when the gauge station is affected by ice; thus the last 'B' can be considered an indication of breakup. To ensure data quality, breakup dates extracted from HYDAT database were examined by cross-checking with other sources including the National Snow and Ice Data Center (NSIDC) and Alberta Environment and Parks river ice reports (Chen and She, 2019). The dates of last 'B' had been found to be relatively consistent with the "ice off" dates obtained from these two sources.

In addition, abnormal breakup dates (those dates are notably earlier or later than the mean date in a time series) indicated by the last 'B' were checked through examining the changes of the water level or streamflow during breakup period to decrease the potential errors. The HYDAT database has good spatial and temporal coverage, and thus provide a long and uniform record of the breakup dates across Canada.

WSC gauge stations were extracted based on the following three criteria: 1) station is active at present; 2) station records are continuous instead of seasonal; and 3) the drainage area of the station is at least 5000 $km^2$. This minimum drainage area ensures the inclusion of most major rivers (including main headwaters and tributaries of those large rivers) and free floating ice (de Rham et al., 2008). However, most WSC stations located in Quebec have not been active since mid-1990s. To cover the data void region, stations from the Centre d'expertise hydrique du Québec (CEHQ) satisfying the first two criteria were also included. The third criterion was dropped because it significantly limits the number of stations for analysis in the Quebec region. Breakup dates were then determined as the last 'B' dates (WSC stations) or the last 'R' dates (CEHQ stations). Three periods (1950-2016, 1960-2016 and 1970-2016) were selected for trend analysis. Only stations with more than 70% complete record of breakup dates were used, resulting in 125, 162, and 190 stations in the three periods, respectively. Figure 2.1 shows the percentage of stations that have 70-80%, 80-90%, and >90% data records, which reflects the data quality in terms of missing values. Breakup dates were converted to day-of-year format or Julian days (e.g., January 6 = 6 Julian days) in statistical analysis.

Monthly and seasonal mean air temperature and total precipitation (snowfall and rainfall) used in this study were from the second generation adjusted historical Canadian climate data (AHCCD) database (Vincent et al., 2018, 2015, 2012). The database provides temperature data at 338 locations and precipitation data at 463 locations, and these stations have been selected and adjusted in consideration of data quality, longevity, spatial and temporal coverage (Vincent et al., 2018, 2012). For the meteorological data, only those stations with a minimum of 70% complete record of monthly and seasonal data were used in this study. The nearest meteorological station to the hydrometric station was selected to represent the climate for this breakup location. Time series of

temperature, rainfall or snowfall from this meteorological station were then correlated with the corresponding time series of breakup dates.

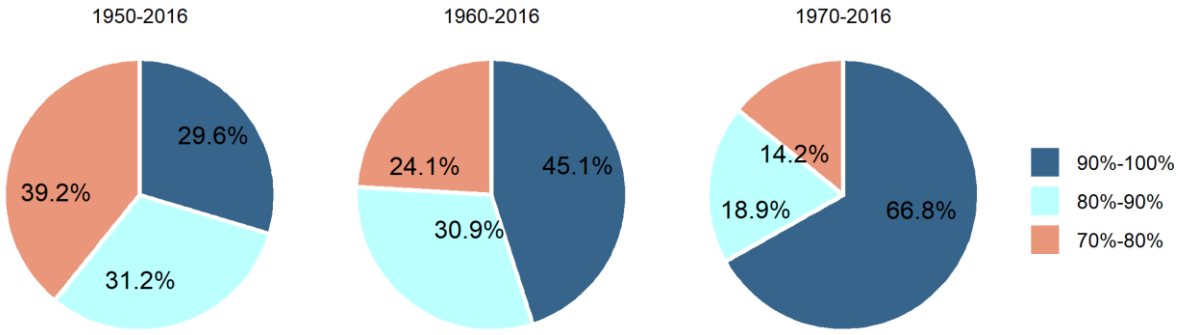


**Figure 2.1** Percentage of stations having 70%-80%, 80%-90% and 90%-100% data records in the breakup date dataset for the three analyzed periods.

### *2.2.2 Methodology*

Commonly used non-parametric Mann-Kendall (MK) trend test was used to analyze the trends of breakup dates, and climatic variables due to its resistance to the effects of extreme values (e.g., Chen et al., 2016; Zhang et al., 2001). The statistic Z-value of MK test indicates if a time series exhibits upward or downward trend. For breakup dates, positive Z indicates a trend of earlier breakup and negative Z indicates a trend of later breakup. Critical values of Z at 99%, 95% and 90% confidence level are ±2.576, ±1.96 and ±1.645, respectively. Sen's method (Sen, 1968), a robust non-parametric slope estimator, was used to estimate the rates of changes in river ice breakup timing and climatic variables. In addition, non-parametric Spearman's rank correlation coefficient was employed to assess the correlations between breakup dates and climatic or other influencing factors. When analyzing the trends over a river basin or terrestrial ecozone, change rates of breakup dates (or magnitude of breakup trends) for all the stations within the specific river basin or the terrestrial ecozone were calculated based on Sen's slope method and averaged to represent the regional trend. Similar method was applied to show the trend of temperature over a

river basin or terrestrial ecozone.

## 2.3 Historical trends in breakup timing

### *2.3.1 General trends*

Figure 2.2 shows the results from the trend analysis of the breakup date datasets. It can be seen that the majority of stations showed trend towards earlier breakup (including both significant earlier and non-significant earlier) in all three analyzed periods. During 1950-2016, about 70% or more of the stations showed earlier breakup. This is in agreement with previously studies (Lacroix et al., 2005; Vincent et al., 2015) that reported earlier breakup trends at the vast majority of locations across Canada for periods of 1950-1998 and 1950-2012. However, percentage of stations displaying later or significant later trends increased as the period of analysis became shorter and more recent.

The effect of data completeness on the trend analysis results can also be seen from Figure 2.2. For 1950-2016 and 1960-2016, the percentage of stations showing either earlier or significant earlier breakup markedly increased while the percentage of stations showing either later or significant later breakup apparently decreased with the increase of data completeness. However, the change was much subtler for 1970-2016 and was in opposite direction. The percentage of stations showing earlier breakup decreased slightly and the percentage of stations showing later breakup increased slightly as data completeness improved. This can be explained by the fact that data completeness improved in more recent years. Percentage of stations containing a minimum 90% complete record for 1950-2016, 1960-2016 and 1970-2016 was 29.6%, 45.1% and 66.8%, respectively (Figure 2.1). It indicated that the missing values were mostly concentrated in the 1950s and 1960s. Given that breakup timing was relatively later during these times, the missing values probably weakened the earlier breakup trends detected in the periods of 1950-2016 and 1960-2016. Missing values had

much less impact on the detected trend in 1970-2016 due to the high data completeness in this period.

Missing value is a common issue in river ice data due to the difficulties in documenting these events. It is often inappropriate to fill in the missing ice data by interpolation because of the highly complex non-linear ice processes. Therefore, many rive ice data were analyzed with missing values. For example, Lacroix et al. (2005) analyzed trends in river ice breakup dates using stations with a minimum 2/3 completeness, Bonsal et al. (2006) set a minimum of 20 relevant ice-date observations over 50-year period for a freshwater-ice location to be included in the trend analysis, and Schmidt et al. (2019) required at least 20 ice-off dates over various data length. The missing values in breakup data increase the uncertainties of trend analysis results and this can be seen from the data completeness analysis based on Figure 2.2. It is therefore important to consider the impact of data completeness when interpreting trend analysis results. Given that similar trends were found with data of minimum 70% and 80% completeness, the dataset with a minimum 70% completeness was used in the following discussions as it has the highest observation density.

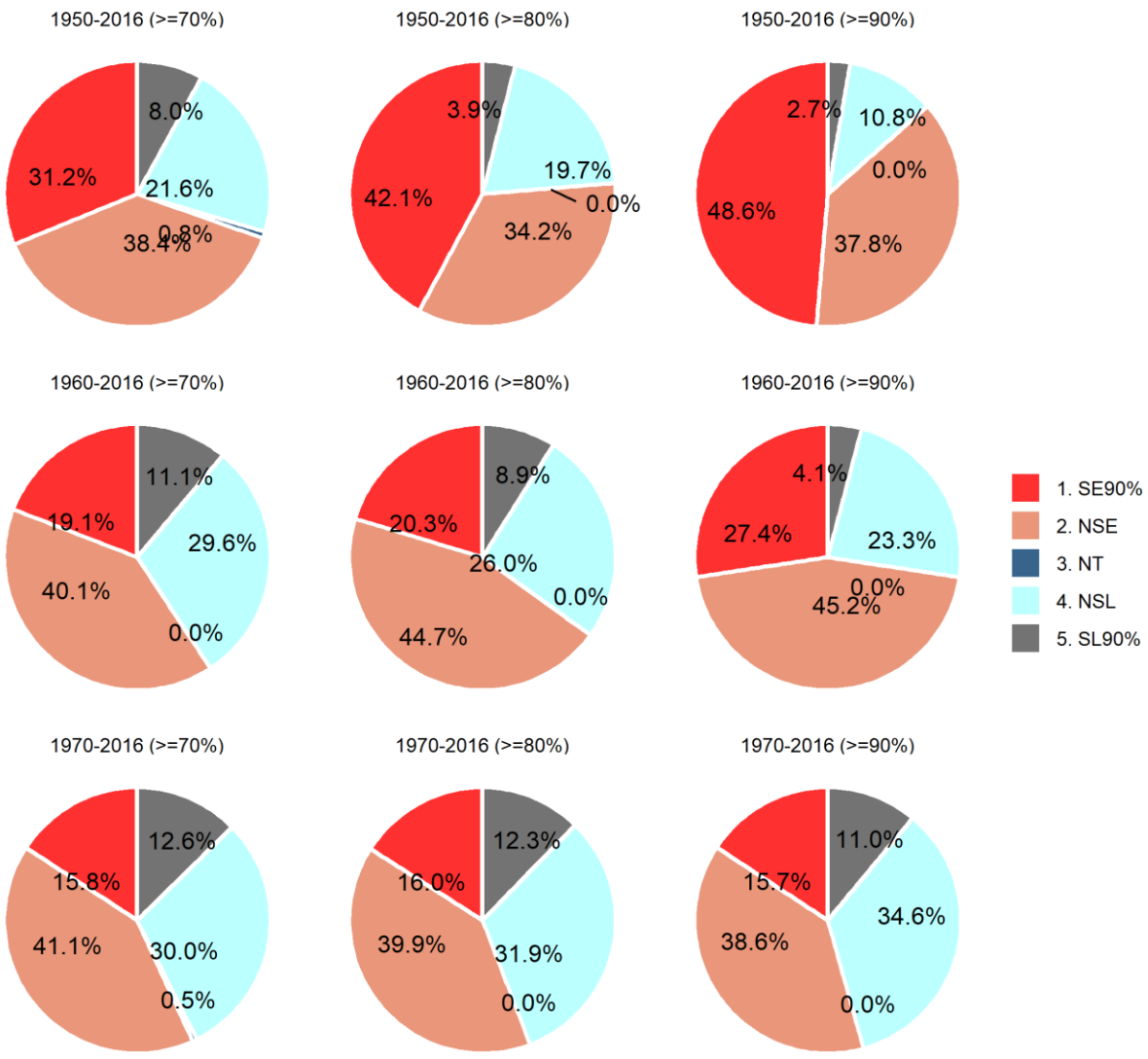


**Figure 2.2** Trends in breakup dates across Canada for different periods of analysis and with different data completeness: results presented as percentage of stations showing a specific trend. NSE, NT and NSL mean non-significant earlier trend, no trend and non-significant later trend, respectively. SE90% and SL90% indicate significant earlier and later trend at confidence level of 90% and above.

### *2.3.2 Spatial variability by terrestrial ecozones*

Spatial pattern was investigated through regional analysis in 15 terrestrial ecoregions based on the geographical areas and Canadian ecozones classified by Environment Canada (1996) (Table 2.1). The 15 ecozones were grouped into seven major ecozone groups, including the Arctic (1), Atlantic (2), Boreal (3), Central Plains (4), Great Lakes – St. Lawrence (5), Pacific and Western Mountains (6) and Taiga (7) as shown in Figure 2.3a. The ecozone groups were used to show the overall trend while the individual terrestrial ecozone was more suitable for discussing more detailed spatial pattern.

Figure 2.3 shows the trends of breakup timing over the major ecozone groups for the three periods analyzed. Three confidence levels (99%, 95% and 90%) were used to differentiate the degree of significance of earlier or later trend. It was observed that remarkable earlier breakup trends were mainly in the western part of Canada for all three periods, including the Pacific and Western Mountains, and Central Plains. However, no significant earlier breakup trend was found in the western part of the Taiga region (i.e., Taiga Plain) except one station in the period of 1970-2016. In the Arctic region, 4 of 6 stations showed earlier breakup for the period of 1960-2016 and 6 of 8 stations displayed earlier breakup for the period of 1970-2016. Two stations in these two periods showed significant earlier breakup and no station showed significant later breakup. There were mixed trends with both significant earlier and later breakup in the Atlantic and Great Lakes – St. Lawrence regions for all three periods. Zhang et al. (2001) reported similar spatial pattern that breakup had advanced in most regions of Canada except Atlantic Canada for 1947-1996, 1957-1996 and 1967-1996 using the same data source. Lacroix et al. (2005), using river ice data from the Canadian Ice Database (CID) spatially augmented with data from WSC, also found an overall earlier breakup in Canada but evenly mixed trends of earlier and later breakup in the Great lakes

– St. Lawrence regions. Figure 2.3 also shows that later breakup became more evident for 1970-2016, particularly in the eastern part of Canada. Noticeable change can be observed in the Boreal and Taiga regions where almost no stations showing significant trends for 1950-2016 and 1960-2016, but several stations with significant later or earlier breakup showed up for 1970-2016.

**Table 2.1** Summary of terrestrial ecozones and average change rate of breakup timing over each ecozone for periods of 1950-2016, 1960-2016 and 2017-2016.

| Id | Ecozone Group | Terrestrial Ecozones | T_Area ($km^2$) | L_Area ($km^2$) | FW_Area ($km^2$) | D_Cover | r_1950 (day/decade) | r_1960 (day/decade) | r_1970 (day/decade) |
|---|---|---|---|---|---|---|---|---|---|
| 1 | Arctic | Arctic Cordillera | 239,216 | 219,499 | 19,717 | Perennial Snow/Ice | / | / | / |
| 2 | Arctic | Northern Arctic | 1,433,362 | 1,283,915 | 149,447 | Barren Lands | **-1.25** | **-1.25** | -0.43 |
| 3 | Arctic | Southern Arctic | 775,734 | 716,385 | 59,349 | Arctic/Alpine Tundra | 0.53 | -0.99 | -0.83 |
| 4 | Atlantic | Atlantic Maritime | 196,449 | 176,677 | 19,772 | Mixed Forest | 0.36 | 0.33 | -0.64 |
| 5 | Boreal | Boreal Shield | 1,773,894 | 1,609,776 | 164,118 | Coniferous Forest | **1.04** | **1.32** | **1.56** |
| 6 | Central Plains | Prairie | 440,537 | 432,108 | 8,429 | Agricultural Cropland | **-1.47** | **-1.41** | -0.89 |
| 7 | Central Plains | Boreal Plains | 656,970 | 599,139 | 57,831 | Coniferous Forest | -0.59 | -0.92 | -0.68 |
| 8 | Great Lakes and St. Lawrence | Mixedwood Plains | 113,431 | 57,422 | 56,009 | Agricultural Cropland | 0.22 | 0.09 | 0.47 |
| 9 | Pacific and Western Mountains | Taiga Cordillera | 245,865 | 245,505 | 360 | Coniferous Forest | / | **1.00** | **-1.19** |
| 10 | Pacific and Western Mountains | Boreal Cordillera | 432,128 | 427,208 | 4,920 | Coniferous Forest | -0.93 | -0.35 | -0.12 |
| 11 | Pacific and Western Mountains | Montane Cordillera | 461,198 | 448,145 | 13,053 | Coniferous Forest | **-1.58** | -0.12 | -0.43 |
| 12 | Pacific and Western Mountains | Pacific Maritime | 195,554 | 181,749 | 13,805 | Coniferous Forest | -0.50 | 0.06 | -0.93 |
| 13 | Taiga | Hudson Plains | 350,318 | 341,322 | 8,996 | Transitional Forest | -0.48 | 0.06 | -0.19 |
| 14 | Taiga | Taiga Plain | 563,241 | 496,380 | 66,861 | Coniferous Forest | 0.10 | 0.15 | 0.05 |
| 15 | Taiga | Taiga Shield | 1,268,623 | 1,156,110 | 112,513 | Transitional Forest | **3.33** | **1.28** | **2.65** |

Notes: T_Area, L_Area and FW_Area are total area, land area and freshwater area. D_Cover is dominant plant/land cover. r_1950, r_1960 and r_1970 indicate the rate of change of breakup timing for 1950-2016, 1960-2016 and 1970-2016, respectively; Positive values are later breakup and negative values indicate earlier breakup. Average change rates of breakup timing over 1 day/decade are indicated in bold.

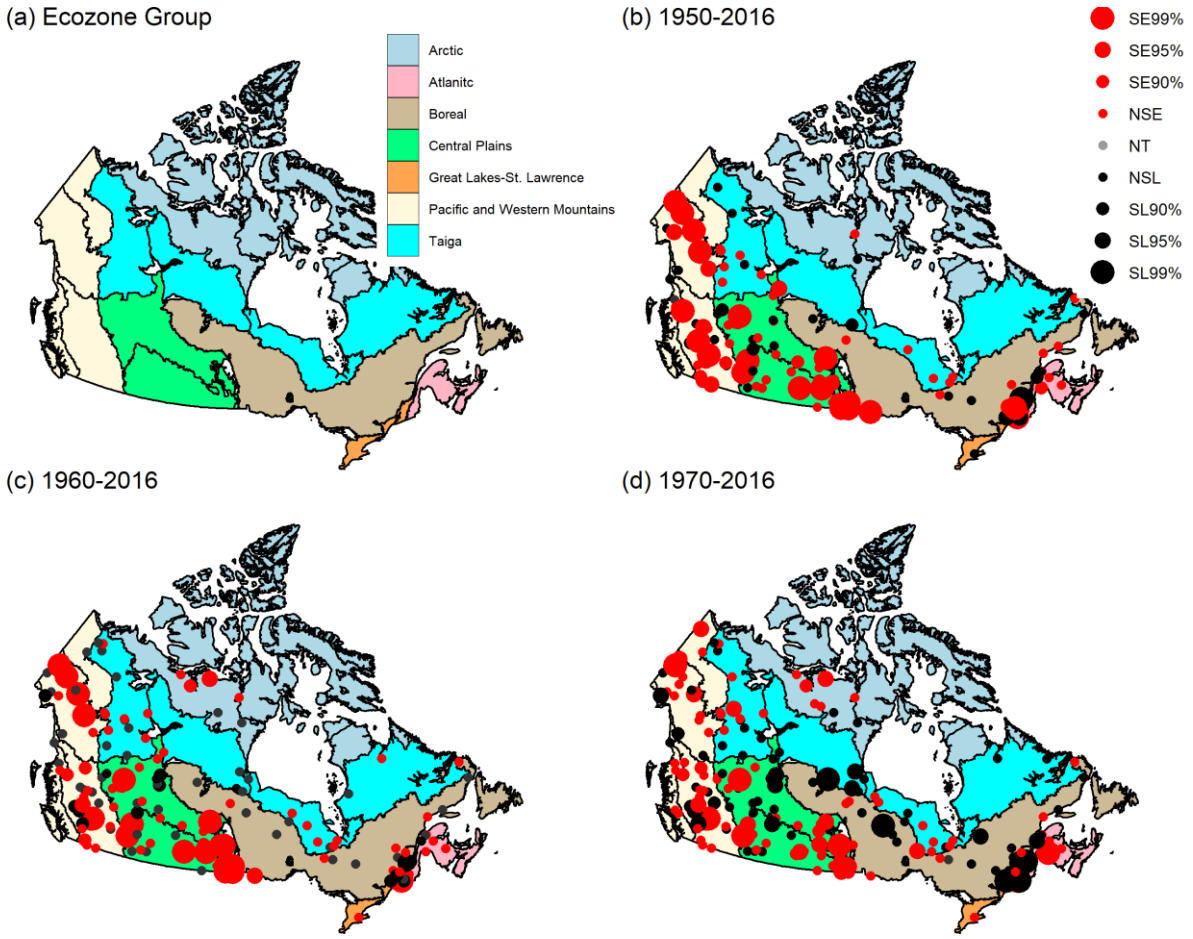


**Figure 2.3** Trends in breakup timing over ecozone groups of Canada for different periods. SE90% and SL90% indicate significant earlier and later trend at 90% confidence level (the absolute values of Z are between 1.645 and 1.96); for SE95% and SL95%, the absolute values of Z are between 1.96 and 2.576; the absolute values of Z for SE99% and SL99% are over 2.576.

Figure 2.4 shows the regional pattern of trend and change rate of breakup date over the 15 terrestrial ecozones. The values of the average rate of change for each ecozone over the three periods are given in Table 2.1. Some variabilities within specific ecozone group were noticed. Rapid advancement of breakup date was seen in Prairie and Boreal Plains (both within the Central Plain group) for all three periods, but Prairie had a much higher change rate. For 1950-2016, the rate of advancement was high in Boreal Cordillera, Montane Cordillera, and Pacific Maritime, all

were in the Pacific and Western Mountains group. However, the rates in these regions decreased for the periods of 1960-2016 and 1970-2016 except that Pacific Maritime showed a fast advancement rate of 0.93 day/decade in 1970-2016. Pacific Maritime also had the most number of stations in this period. Although all belong to the Taiga group, later breakup was seen in Taiga Plain (<0.15 day/decade) and Taiga Shield (>1 day/decade) while Hudson Plains experienced earlier breakup (1950-2016 and 1970-2016) or negligible change (1960-2016). Although there were not many stations, the Arctic region showed evidently earlier breakup. Breakup in Boreal Shield had on average become over 1 day/decade later. Later breakup with small average change rate of below 0.5 day/decade was observed in Mixedwood Plains (Great Lakes-St. Lawrence) for three periods. Atlantic Maritime had a similar small change towards later breakup for 1950-2016 and 1960-2016 but became 0.64 day/decade earlier for 1970-2016.

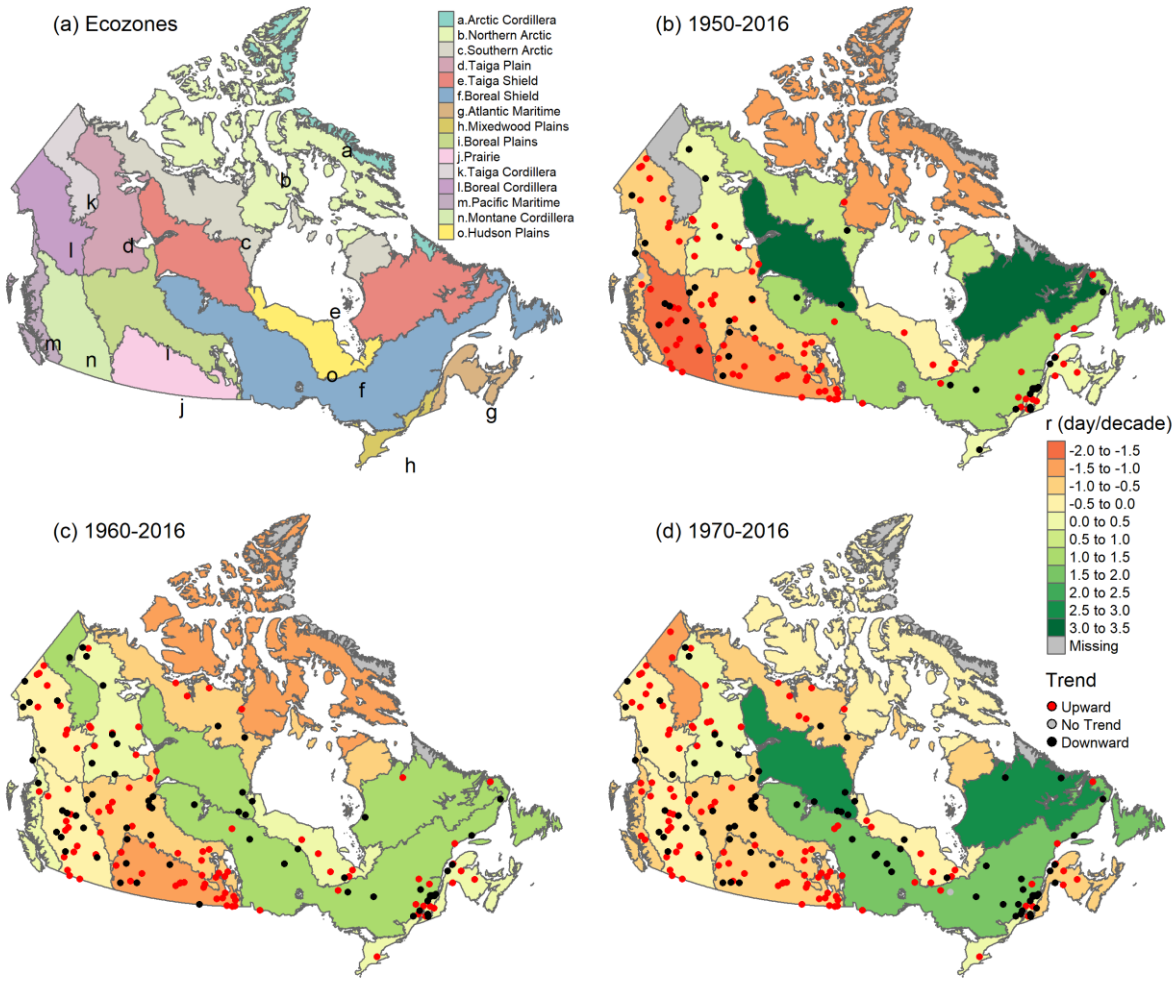


**Figure 2.4** Average rate of change in breakup timing over each terrestrial ecozone of Canada. Positive and negative values in the legend indicate later and earlier breakup, respectively.

### *2.3.3 Breakup trend in selected major river basins*

Five major river basins were selected for further analysis since the ice breakup processes are often linked with the entire river system (Figure 2.5). Table 2.2 summarizes the averaged change rate of breakup timing and its other statistical indices (such as median, range and standard deviation) to depict the changes of trends for the major river basins. The Fraser River Basin experienced remarkable change of 1.56 day/decade earlier on average during 1950-2016 while no significant overall earlier or later breakup was observed for the periods of 1960-2016 and 1970-2016. The

high standard deviations suggested significant heterogeneity of trends in this river basin. The opposite changes canceled out the overall trend, and thus no evident consistent trend was found in the Fraser River Basin for these two periods. However, it is important to note that more extreme earlier and later breakup changes were observed in this basin as period changes from 1950-2016 to 1970-2016. Heterogeneous trends were also identified in the other maritime river basin, St. Lawrence River Basin, but pronounced later breakup trends dominated and the average decadal change rates were over 1 day/decade for all three periods. The median values of the change rates were evidently less than the average values, indicating that there were some extreme later breakup trends which may have skewed the overall trend in this river basin. Heterogeneous trends were also notable in the Nelson River Basin but the trend towards earlier breakup was evident, and the mean and median change rates were over 1 day/decade for all three periods.

Smaller variation in the change rate of breakup timing was observed in the Mackenzie River and Yukon River Basins. The Yukon River Basin experienced an overall significant earlier breakup trend with regional change rates ranging from 0.82-1.27 day/decade for the different periods. Jasek and Shen (1999) found that the breakup of Yukon River had become ~0.5 day/decade earlier during 1896-1998. The earlier breakup trend in the Yukon River Basin had greatly enhanced recently. There was no significant regional earlier or later breakup trend in the Mackenzie River Basin and the average change rate was small.

**Table 2.2** Summary of change rate of breakup timing in five selected river basins for the three periods of analysis.

| Period | River Basin | Mean_r (day/decade) | Median_r (day/decade) | Range_r (day/decade) | std_r | Number of Station |
|---|---|---|---|---|---|---|
| 1950-2016 | Fraser | **-1.56** | **-1.20** | -7 to 2.3 | 2.8 | 11 |
| | Mackenzie | -0.34 | -0.30 | -3 to 1.4 | 0.9 | 25 |
| | Nelson | **-1.29** | **-1.20** | -5.2 to 1.4 | 1.4 | 33 |
| | St. Lawrence | **1.14** | 0.40 | -4.1 to 10.9 | 3.2 | 22 |
| | Yukon | **-1.27** | **-1.30** | -2.1 to -0.5 | 0.6 | 6 |
| 1960-2016 | Fraser | 0.24 | 0.19 | -6 to 6.1 | 3.3 | 14 |
| | Mackenzie | -0.09 | 0.00 | -3.4 to 1.8 | 1.0 | 36 |
| | Nelson | **-1.69** | **-1.43** | -14.3 to 1.5 | 2.6 | 36 |
| | St. Lawrence | **1.38** | 0.44 | -3.8 to 10.9 | 2.9 | 25 |
| | Yukon | -0.83 | -0.95 | -2.1 to 0.5 | 0.9 | 8 |
| 1970-2016 | Fraser | -0.08 | -0.15 | -7 to 6.1 | 3.7 | 14 |
| | Mackenzie | 0.01 | 0.00 | -3.3 to 1.8 | 1.0 | 41 |
| | Nelson | **-1.36** | **-1.64** | -12.3 to 3.3 | 2.3 | 40 |
| | St. Lawrence | **2.08** | **1.07** | -4 to 12.8 | 3.4 | 26 |
| | Yukon | -0.82 | **-1.00** | -2 to 0.5 | 0.8 | 10 |

Notes: Mean_r, Median_r, Range_r and std_r, are mean, median, range and standard deviation of the change rate of breakup timing of each river basin, respectively. Mean and median change rates over 1 day/decade are in bold.

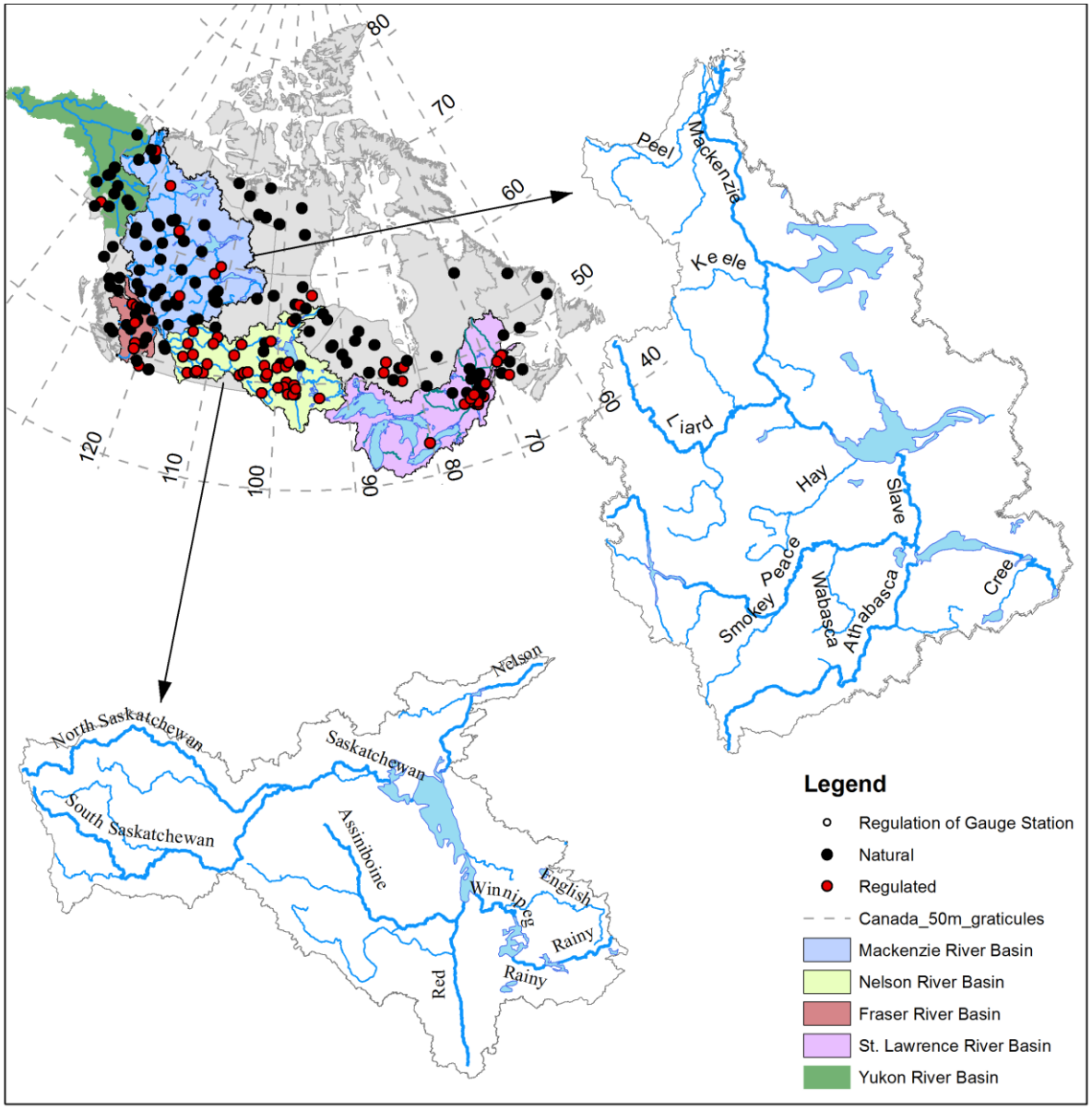


**Figure 2.5** Five selected river basins. Gauge stations with regulation condition for the period of 1970-2016 are also shown. For international river basins (e.g., Yukon River Basin), only gauge stations in Canada are analyzed. The mainstreams and major tributaries of Mackenzie and Nelson River Basins are highlighted for the following analysis.

Detailed changes of breakup pattern in five selected river basins were further explored for 1970-2016 as this period had the most number of stations and least missing values (Figure 2.6). Most

stations in the Mackenzie River Basin showed no significant change in breakup timing, but some stations in the headwaters and smaller tributaries showed remarkable changes. Stations showing significant earlier breakup of over 1 day/decade were mainly observed in the Peace River basin while significant later breakup of over 1 day/decade were mainly identified in the Athabasca River Basin. Most stations in the Yukon River Basin experienced earlier breakup, with 5 of 10 stations showing significant changes of over 1 day/decade earlier. These bigger changes were all on the tributaries of the Yukon River while the only available station on the mainstream showed negligible change.

In the Fraser River Basin, significant later breakup changes were identified mainly in the upper reach of the Fraser River (2.6 day/decade), the Nechakon River Basin (1.6 day/decade), and the Chilcotin River Basin (3.3 and 6.1 day/decade). Breakup dates were significantly earlier for the middle reach of Fraser River (-3.9 day/decade) and the Thompson River Basin (-1.4, -3.6 and -7.0 day/decade), except that one station showed a change of 5.1 day/decade later.

Most stations in the Nelson River Basin experienced earlier breakup of 1 to 2.5 day/decade. One station (Fairford River near Fairford) showed dramatic change of 12.3 day/decade earlier. Only 6 of 40 stations displayed later breakup and these are mainly in the upper Nelson River Basin (North Saskatchewan River and North Saskatchewan River Basins); 5 of the 6 stations showed rapid change of over 1 day/decade later. Significant trends towards later breakup dominated the St. Lawrence River Basin with only 5 of 26 stations showing earlier breakup. Some dramatic delays in breakup dates were found in this basin, including the stations at North Arm (12.8 day/decade), Saint Anne (6.7 day/decade), Rimouski (6 day/decade), Red (5.5 day/decade), and Montmorency (5 day/decade). Obvious earlier breakup was only identified in Richelieu (Riviere) Aux Rapides Fryers (-4 day/decade).

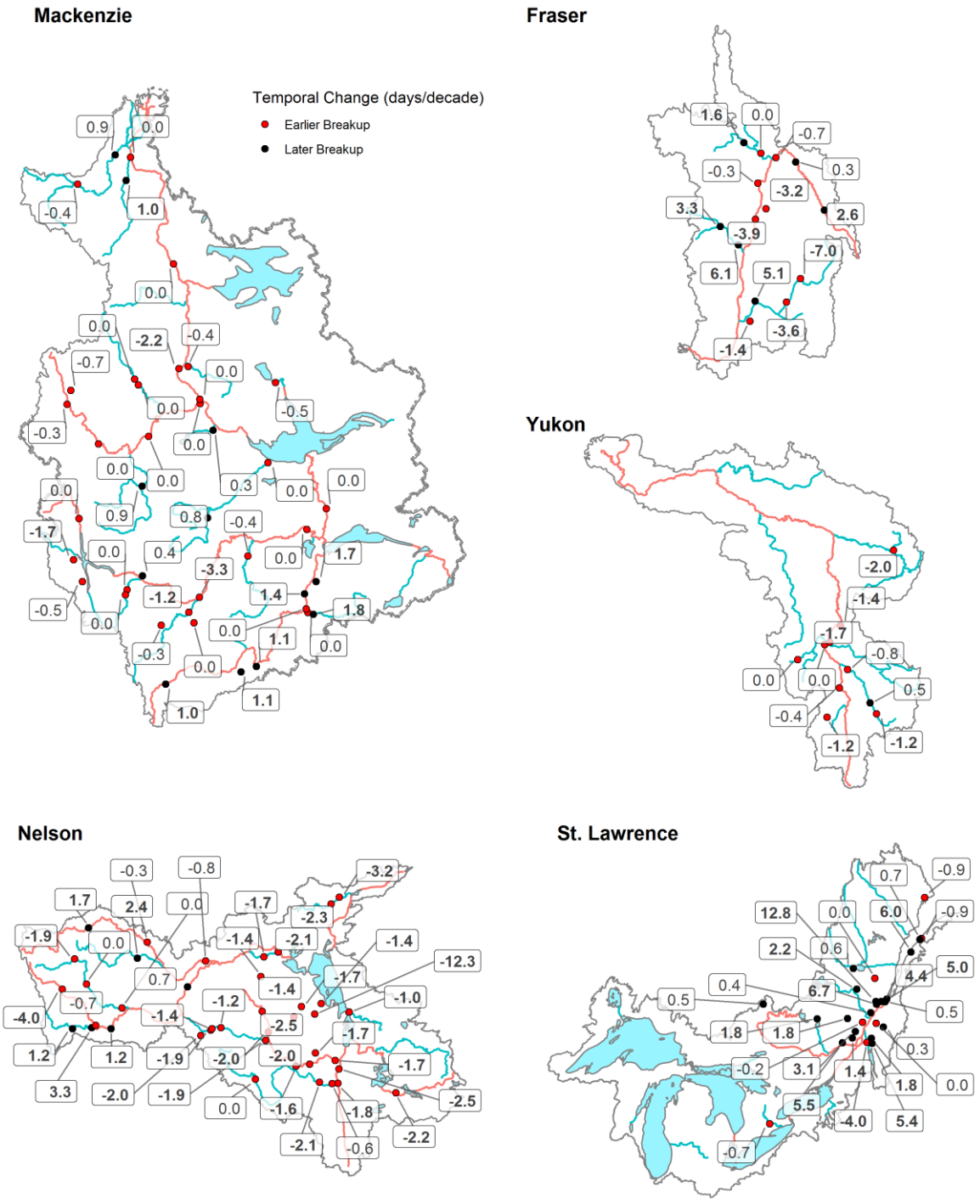


**Figure 2.6** Changes in breakup dates within five selected river basins during 1970-2016; numbers indicate the change rate in day/decade, positive and negative values mean later and earlier breakup respectively, and the absolute values greater than or equal to 1 day/decade are in bold.

## 2.4 Influencing factors of river ice breakup

This section assesses the influencing factors on the observed trends in breakup dates. Five parameters, air temperature, snowfall, rainfall, elevation, and flow regulation, were selected based on the literature review. Other factors, such as large-scale atmospheric and oceanic circulation patterns (e.g., NAO, PNA and ENSO), may also contribute to the change of river ice breakup (Bonsal et al., 2006; Schmidt et al., 2019) but are not discussed here.

### *2.4.1 Surface air temperature*

#### *2.4.1.1 Relationship with monthly/seasonal air temperature*

The relationships between breakup dates and monthly (October-May) and seasonal (winter, spring and autumn) mean air temperature were analyzed for all three periods. Three periods showed similar results and breakup timing was negatively correlated with air temperature. It was found that 84.9% of the correlations were significant at 95% confidence interval when the correlation coefficients of breakup and monthly/seasonal air temperature were below -0.5, and thus the correlation coefficient < -0.5 was considered good correlation and used as a criterion to evaluate the correlations with other parameters in the following sections. Breakup date was mainly correlated with monthly mean air temperature from February-May, particularly March and April. Mean air temperature during March-April and spring (March-May) also had good correlation with breakup date. There seemed to be weaker or no discernible correlation with monthly mean air temperature from October-December and mean air temperature during autumn (September-November) and winter (December-February). The results are consistent with previous studies (Benson et al., 2012; Fu and Yao, 2015; Hodgkins et al., 2005) which reported that breakup date is closely correlated with air temperature for March through April or spring.

Figure 2.7 provides the spatial pattern of the correlation between breakup date and

monthly/seasonal mean air temperature. Breakup of most stations analyzed in this study occurred sometime in March or April, which explained why the breakup date was better correlated with March and April mean air temperature. Moving towards the high latitude regions, good correlations were found with later month as breakup tended to occur later. This is generally consistent with previous studies which consider the air temperature of 1-3 months before breakup as the dominant factor for lake ice phenology (Duguay et al., 2006; Livingstone, 2000; Nõges and Nõges, 2014). It is also important to note that the correlation between breakup date and air temperature in higher latitude regions (roughly north of 58°N) was not as good as those in lower latitude regions.

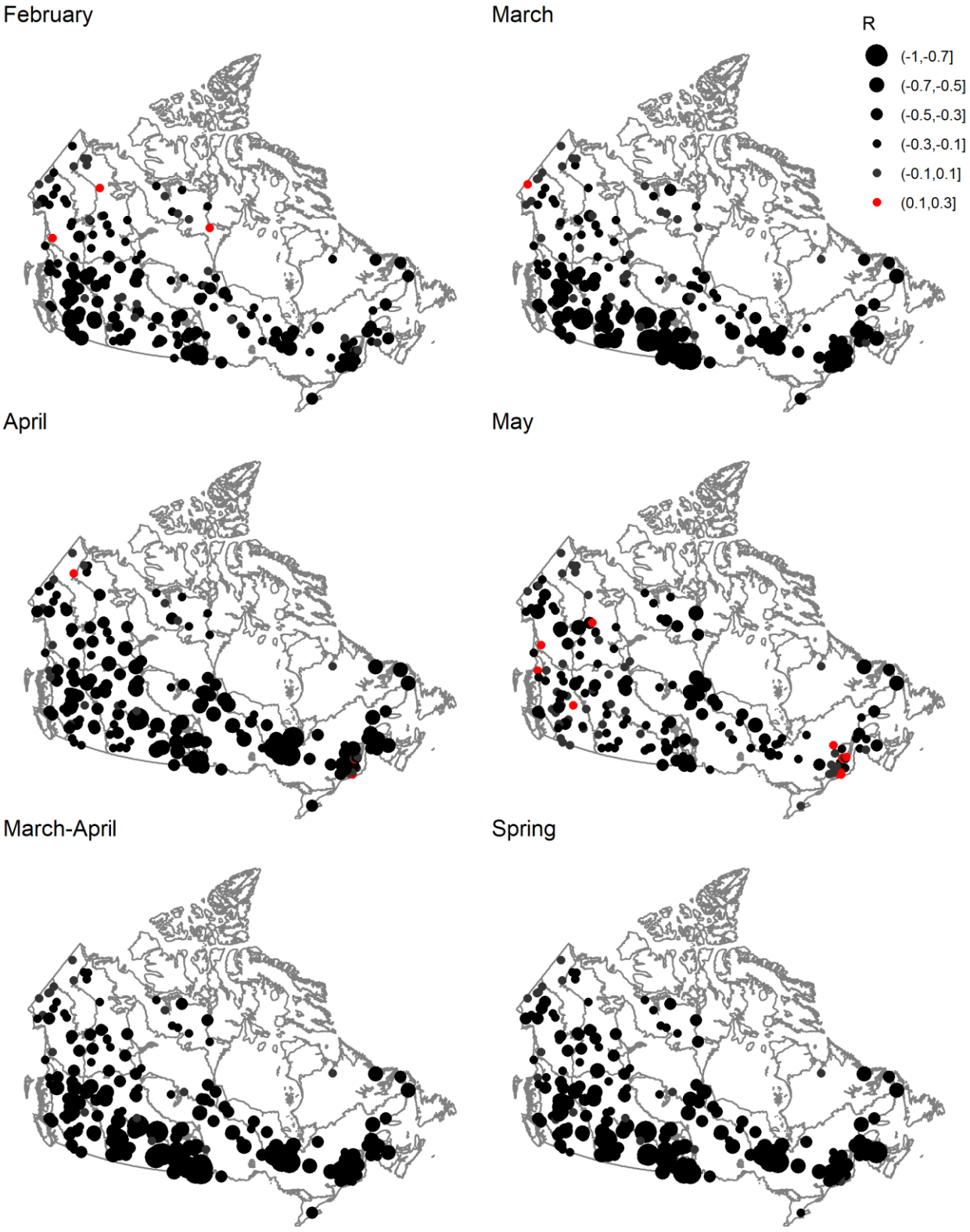


**Figure 2.7** Spatial pattern of correlation between breakup date and monthly/seasonal mean air temperature for the period of 1970-2016.

*2.4.1.2 Trends in winter and spring air temperature*

The trend and magnitude of trend in winter and spring air temperature are shown in Figures 2.8 and 2.9. Only the results of 1950-2016 and 1970-2016 were displayed because significant differences were identified between these two periods. Strong winter warming trends were observed almost all over Canada for 1950-2016, especially for the western part where most stations had warmed by 0.5-1°C/decade. The spring warming pattern was similar although most stations had relatively lower warming rates of 0.05-0.5°C/decade. The spring warming trend explains the general trend towards earlier breakup across Canada that was found in 1950-2016 and 1960-2016 (see Figure 2.3). Relative weaker spring warming trend in the Atlantic and Great Lakes – St. Lawrence to some degree explains the mixed signals in these regions. River ice breakup in these regions may still be sensitive to climate change as both significant earlier and significant later trends were found here. Vincent et al. (2015) observed a modest cooling over 1940-1970s, but a markedly rapid warming afterwards. Figures 2.8 and 2.9 show that winter warming trends became stronger in terms of magnitude and coverage from 1950-2016 to 1970-2016. However, significant spring warming trends (0.5-1°C/decade) were only identified in the Arctic and part of Pacific regions for 1970-2016. Spring warming trends in other regions became weak and some stations in Atlantic and Great Lakes – St. Lawrence, and Central Plains even showed apparent cooling trends as compared to the period of 1950-2016. This was consistent with more stations showing later breakup during 1970-2016.

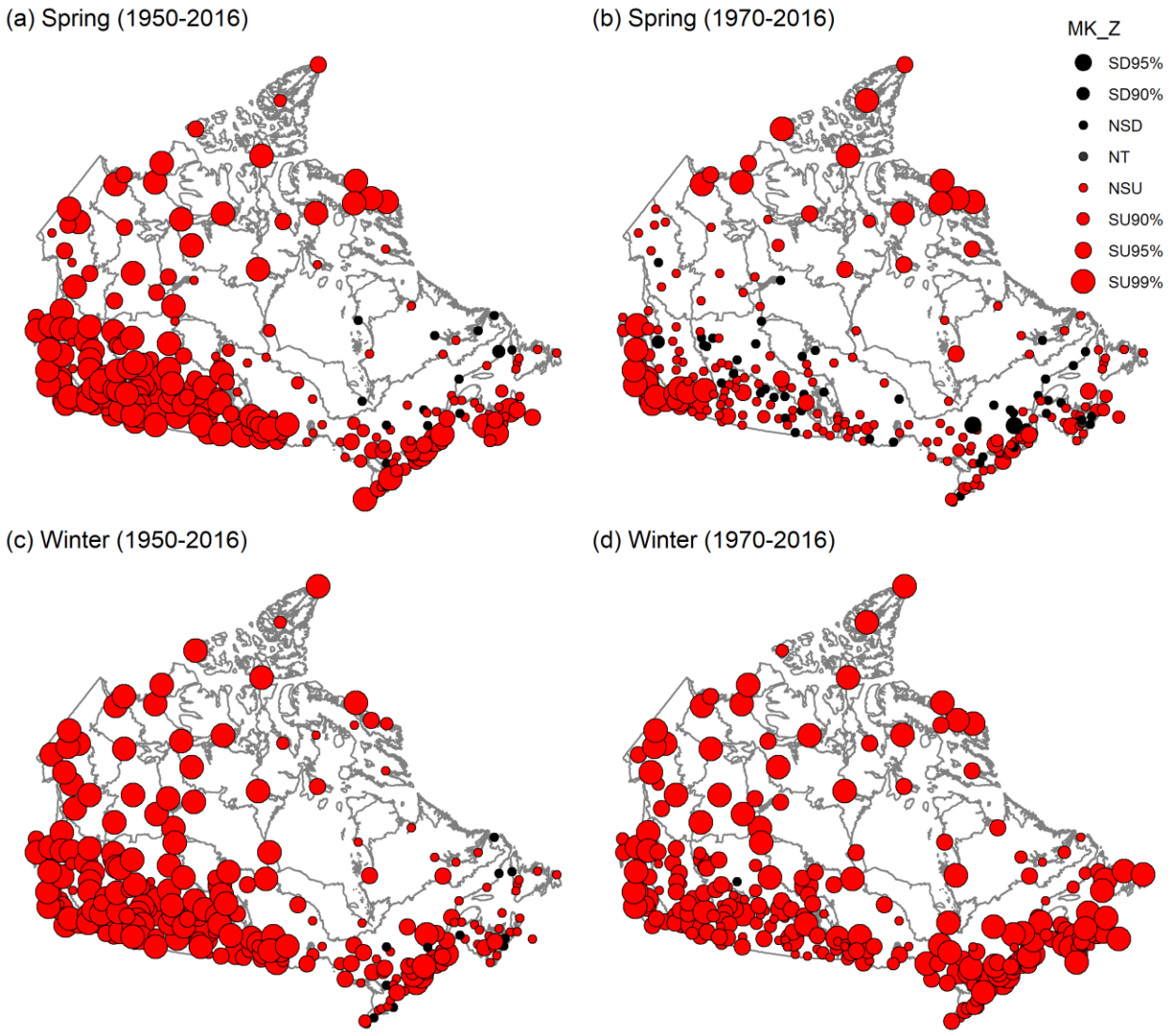


**Figure 2.8** Trends in winter and spring mean air temperature for the periods of 1950-2016 and 1970-2016. SU90% and SD90% indicate significant upward (warming) and downward (cooling) trends at 90% confidence level (the absolute values of Z are between 1.645 and 1.96); for SU95% and SD95%, the absolute values of Z are between 1.96 and 2.576; the absolute values of Z for SU99% are over 2.576.

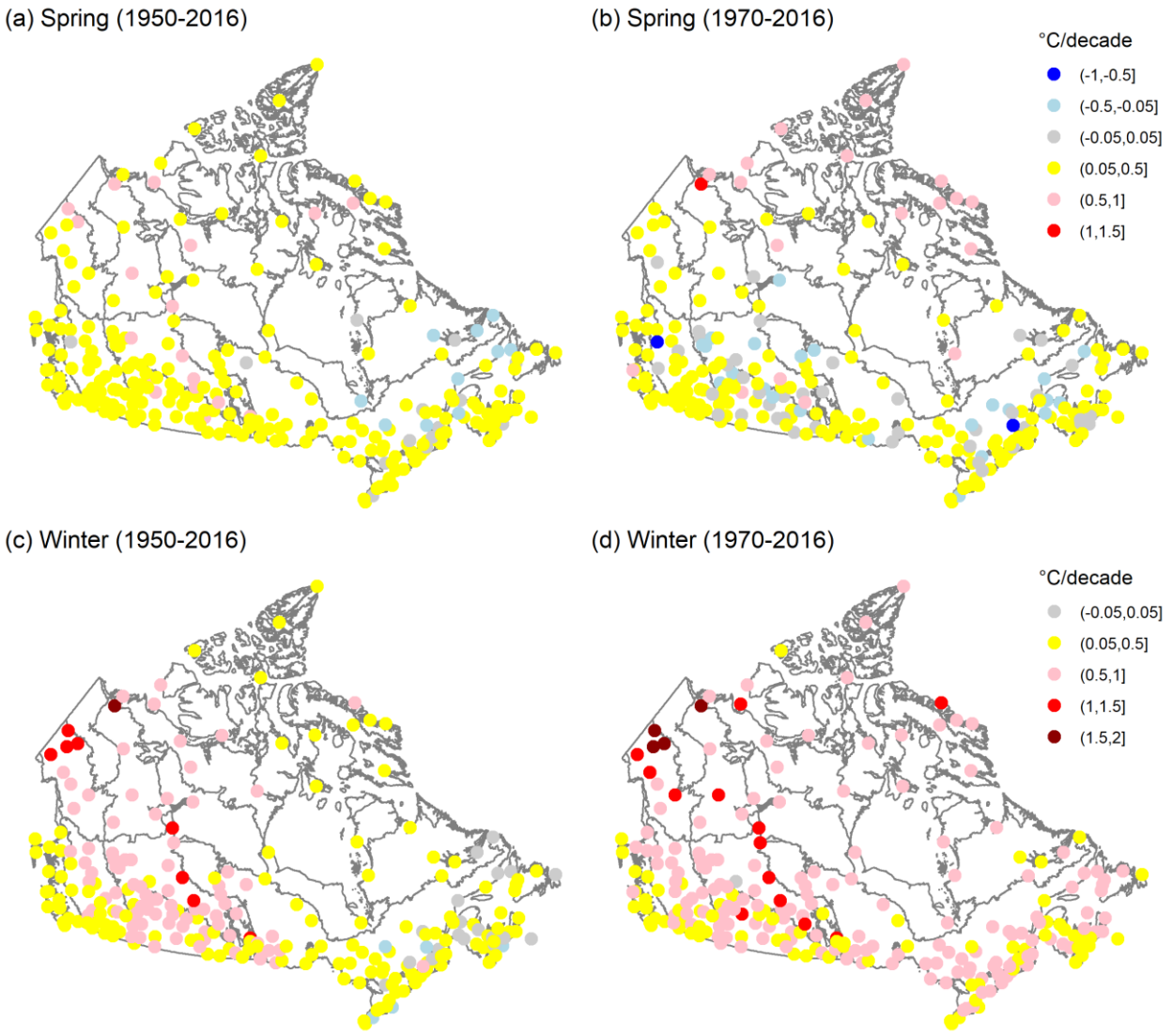


**Figure 2.9** Rate of change in winter and spring mean air temperature for the periods of 1950-2016 and 1970-2016.

*2.4.1.3 Regional sensitivity of breakup timing to spring warming*

Regional spring warming rates over 15 terrestrial ecozones of Canada for different periods are shown in Figure 2.10. The most rapid warming rates were mainly observed in the Arctic region for all three periods. Multiple factors, such as ice-albedo feedback due to diminishing sea ice, ocean heat transport and cloud feedback, have been proposed to be the potential causes of the faster warming in the Arctic (Rantanen et al., 2022). The spring warming rates in the western Canada (e.g., Pacific Maritime, Montane Cordillera, Boreal Cordillera, Taiga Plain, Prairie, and Boreal Plains) were evidently greater than the southeast (e.g., Taiga Shield, Boreal Shield, Mixed wood Plains, and Atlantic Maritime), especially for 1950-2016 and 1960-2016. Prominent spring warming trend was mainly observed in the north part of Canada and Pacific Maritime during 1970-2016. The spring warming pattern was in good agreement with the pattern of the change in breakup timing (see Figure 2.4), especially for 1950-2016 and 1960-2016. There were strong correlations between regional warming rate and the change rate of breakup timing for 1950-2016 (R = -0.79) and 1960-2016 (R = -0.73). This suggested that temperature was a main driver behind river ice breakup. The correlation was not as good for the period of 1970-2016 (R = -0.42). It is likely due to breakup was more sensitive to air temperature in southern regions, while noticeable spring warming was only identified in the north part of Canada for 1970-2016.

Average rates of change in spring air temperature for the selected five major river basins are given in Table 2.3. Fast spring warming was observed in the Yukon River Basin which was consistent with the significant earlier breakup found earlier. The Mackenzie River Basin also had fast spring warming rate (for 1950-2016 and 1960-2016) but the average change of breakup date in this watershed was not apparent (see Table 2.2). About half of the Mackenzie River Basin is in the north of 58°. As discussed above, breakup in this region was not very sensitive to warming trends.

Additionally, it was found that breakups in larger rivers were not very sensitive to warming trend as compared to smaller rivers and headwaters. Beltaos and Burrell (2003) pointed out that the ice regime could be modified by climate change in different ways over various parts of Canada because regional and local climates are also greatly affected by topography, latitude, altitude, and the proximity of large water bodies (e.g., Great Bear Lake and Great Slave Lake). Those factors may support the weak earlier breakup trend found in the Mackenzie River Basin, as well as Taiga Plain which is mainly in the north of the Mackenzie River Basin and contains the mainstream of Mackenzie River.

The spring warming rate in the Fraser River Basin was relatively high during 1950-2016 while decreased for 1960-2016 and 1970-2016. This corresponded well to the significant trend towards earlier breakup found in 1950-2016 and mixed trends observed in the other two periods. In the Nelson River Basin, breakup at most stations advanced by over 1 day/decade even for the relatively low spring warming rate of 0.13°C/decade. The least significant spring warming rate was found in the St. Lawrence River Basin, where the regional mean change rate of breakup timing was over 1 day/decade later.

Magnuson et al. (2000) reported earlier breakup trend of 0.65 day/decade for Northern Hemisphere waterbodies during 1846-1995 along with warming rate of 0.12°C/decade. In this study, the average change rates of breakup date observed in the Fraser, Nelson and Yukon River Basins during 1950-2016 are evidently faster than the rate reported by Magnuson et al. (2000). In addition, the spring warming trends became weaker for almost all river basins as the period of analysis changed from 1950-2016 to 1970-2016.

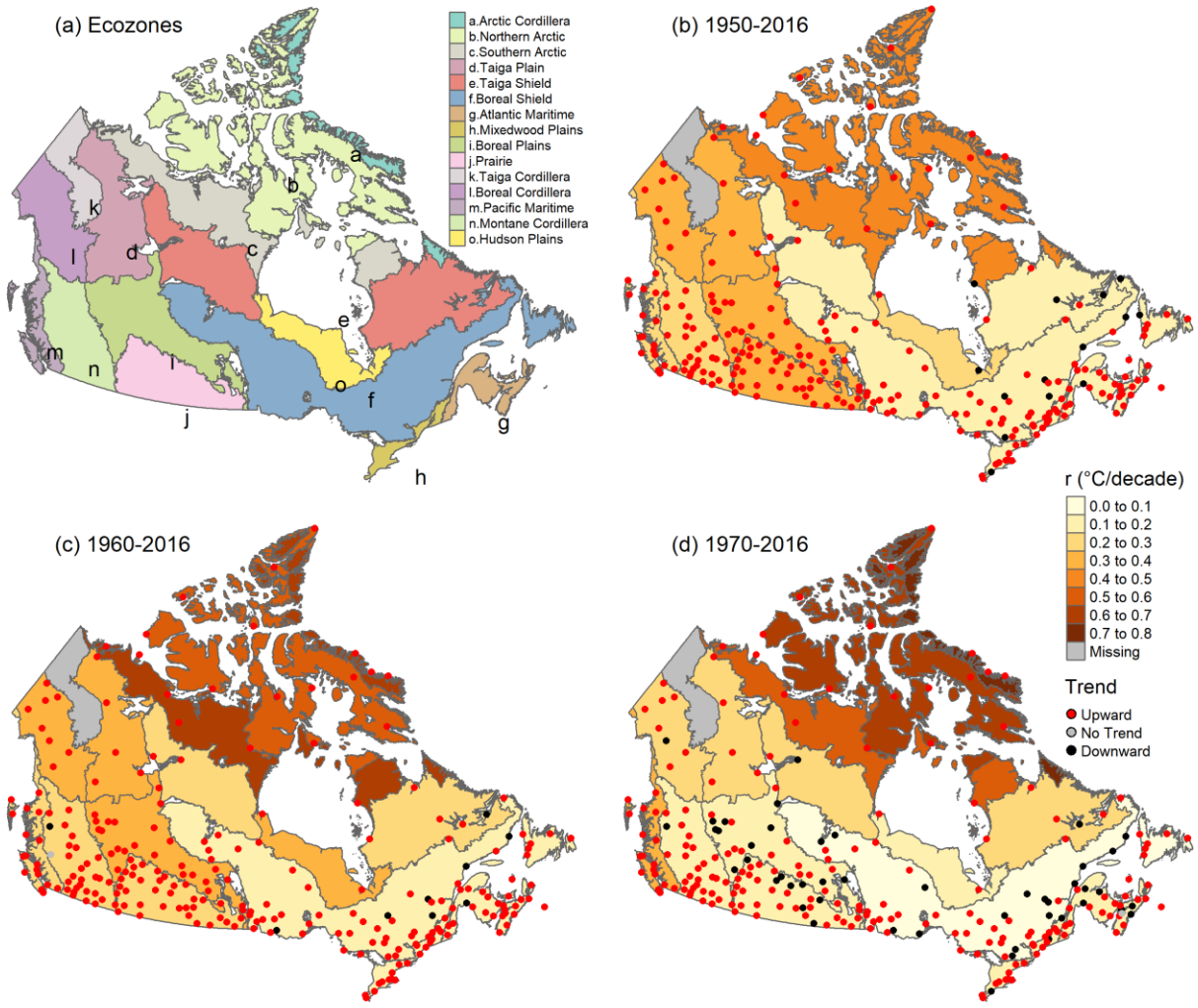


**Figure 2.10** Average spring warming rates over each terrestrial ecozone of Canada.

**Table 2.3** Summary of spring air temperature changes in five river basins for periods of 1950-2016, 1960-2016 and 2017-2016.

| Period | River Basin | Mean_Q (°C/decade) | Median_Q (°C/decade) | Range_Q (°C/decade) | std_Q | Number of Station |
|---|---|---|---|---|---|---|
| 1950-2016 | Fraser | 0.30 | 0.30 | 0.02 to 0.43 | 0.11 | 12 |
| | Mackenzie | 0.38 | 0.35 | 0.11 to 1 | 0.17 | 23 |
| | Nelson | 0.37 | 0.37 | 0.05 to 0.66 | 0.12 | 58 |
| | St. Lawrence | 0.13 | 0.14 | -0.18 to 0.31 | 0.11 | 47 |
| | Yukon | 0.39 | 0.39 | 0.16 to 0.62 | 0.21 | 6 |
| 1960-2016 | Fraser | 0.24 | 0.24 | -0.16 to 0.42 | 0.16 | 12 |
| | Mackenzie | 0.34 | 0.30 | 0.03 to 1.1 | 0.20 | 23 |
| | Nelson | 0.30 | 0.29 | -0.06 to 0.6 | 0.13 | 58 |
| | St. Lawrence | 0.16 | 0.18 | -0.32 to 0.38 | 0.13 | 47 |
| | Yukon | 0.38 | 0.39 | 0.16 to 0.61 | 0.19 | 6 |
| 1970-2016 | Fraser | 0.16 | 0.18 | -0.5 to 0.4 | 0.24 | 12 |
| | Mackenzie | 0.12 | 0.09 | -0.3 to 1.18 | 0.28 | 23 |
| | Nelson | 0.13 | 0.13 | -0.24 to 0.6 | 0.16 | 58 |
| | St. Lawrence | 0.12 | 0.14 | -0.53 to 0.38 | 0.17 | 47 |
| | Yukon | 0.22 | 0.25 | 0 to 0.33 | 0.12 | 6 |

Notes: Mean_Q, Median_Q, Range_Q and std_Q, are mean, median, range and standard deviation of spring warming rates over each river basin, respectively.

### *2.4.2 Snowfall*

Snowfall generally affects ice breakup through insulation (reduce heat transfer between ice and air) and/or albedo effects (higher albedo reflects more solar radiation) (Jensen et al., 2007). Vavrus et al. (1996) found that an increase in snowfall results in a monotonic delay in breakup timing due to higher albedo of snowfall, the increased creation of snow ice, and the added mass of the frozen snow and ice layers. In addition, a decrease in snowfall generally advances breakup. These explain the positive correlation between breakup timing and snowfall shown in Figure 2.11, though the impacts of snowfall on the breakup timing were not as strong as those with the air temperature. Breakup date had better correlation with monthly total snowfall from February-May, particularly during March-April and spring (March-May). Snowfall during winter (December-February) and autumn (September-November) contributed slightly or negligibly to breakup timing. The spatial pattern of correlation between breakup date and monthly/seasonal total snowfall shown in Figure 2.11 was similar to that with air temperature, and breakup timing was closely correlated with the total snowfall for about 1-3 months before breakup. However, it is important to note that the correlation between breakup date and total snowfall was relatively good in higher latitude regions (roughly north of 58°N) which was not the case for the correlation pattern with air temperature.

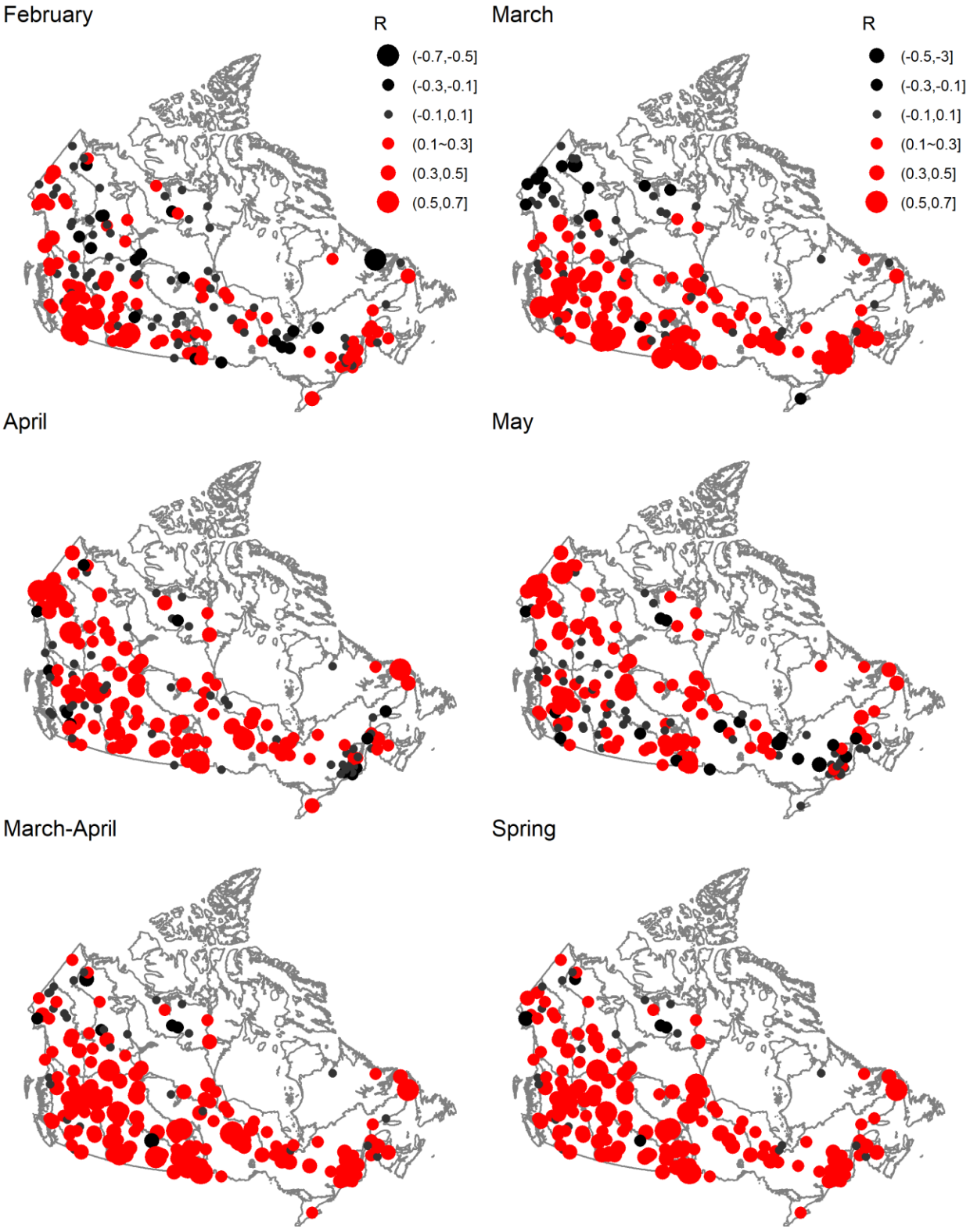


**Figure 2.11** Spatial pattern of correlation between breakup date and monthly/seasonal total snowfall for the period of 1970-2016.

The trends and rates of change in spring and winter total snowfall are shown in Figures 2.12 and 2.13. Significant increasing trends of snowfall in spring and winter were mainly found in northern Canada for the period of 1950-2016. Remarkable decreasing trends of snowfall were observed in the south part of the Pacific and Western Mountains, and Central Plains. Decreasing rate of snowfall in winter was faster as compared to in spring. Mixed trends of significant increasing and decreasing snowfall were seen in Great Lakes – St. Lawrence regions. Increased snowfall in the higher latitude regions may impede heat flux from air to the ice through insulation and/or albedo effects. On the other hand, decreased snowfall in the lower latitude regions makes heat flux from air to the ice easier. This may partly explain why breakup timing in the higher latitude regions is less sensitive to climatic warming than the lower latitude regions.

The snowfall pattern for the period of 1970-2016 was similar to 1950-2016, but the increasing trends in the north became weaker while the decreasing trends in the south became stronger, especially for spring. This may be attributed to a rapid increase in temperature after 1970s, but snowfall pattern tended to be more complicated and there were more chances of extreme events. For example, both pronounced increase and decrease in snowfall were observed in Atlantic and Great Lakes – St. Lawrence, and Central Plains (Figure 2.13), which in part contributed to the mixed trends of breakup timing mentioned above.

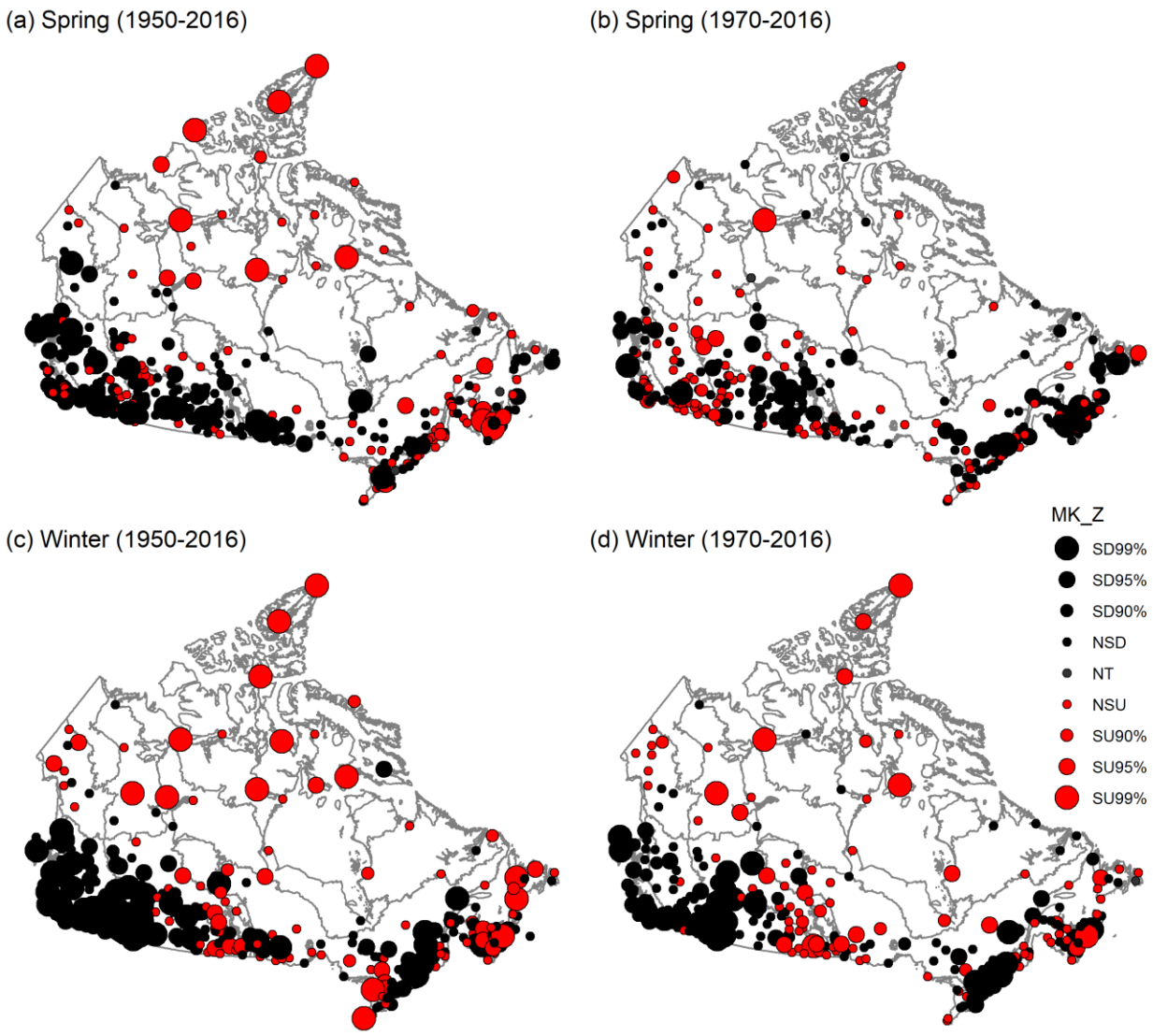


**Figure 2.12** Trends in winter and spring total snowfall for the periods of 1950-2016 and 1970-2016.

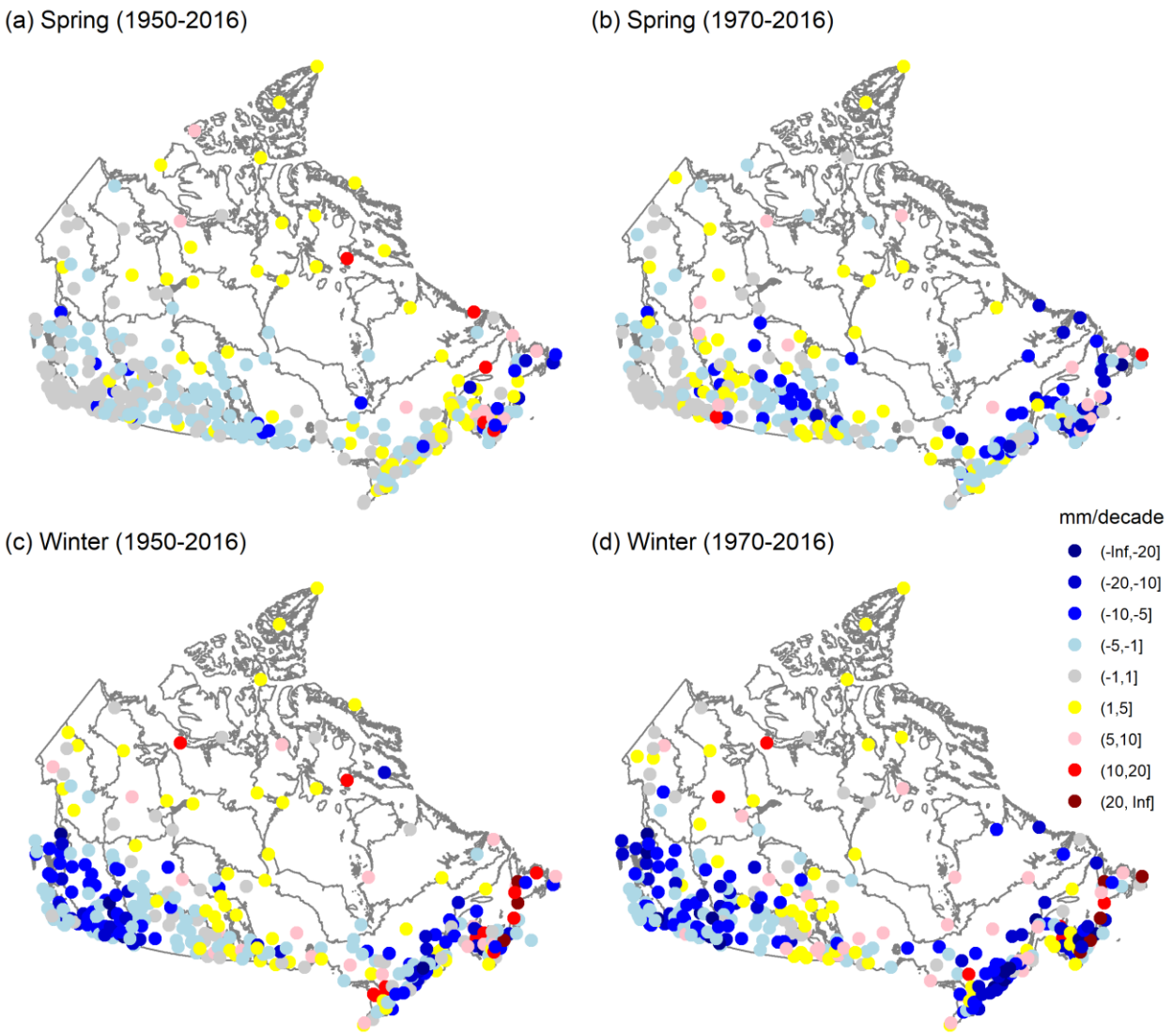


**Figure 2.13** Rate of change in winter and spring total snowfall for the periods of 1950-2016 and 1970-2016.

### *2.4.3 Rainfall*

The correlation between breakup date and monthly (October-May) and seasonal (winter, spring and autumn) total rainfall were investigated. It was found that breakup date was mainly negatively correlated with monthly total rainfall from January-May, especially for March and spring. The results are consistent with Nõges and Nõges (2014) who found that increased rainfall during ice season can contribute to ice breakup. However, no significant negative correlation between breakup timing and rainfall was found during October-December, autumn (September-November) and winter (December-February). Mid-winter (e.g., January and February) rain during ice season may also contributed to later breakup (red point in Figure 2.14). These positive correlations were mainly observed in high latitude regions and east part of Canada where mean air temperature was very low or warming trend was weak. The positive feedback of rainfall on breakup timing may be attributed to that midwinter rain can also favor white ice formation through refreezing, and thus delay breakup (Ariano and Brown, 2019). However, those positive correlations observed in Maritime and temperate regions from March to May probably have no physical meanings since river ice probably has already melted out in these regions in those months (Figure 2.14).

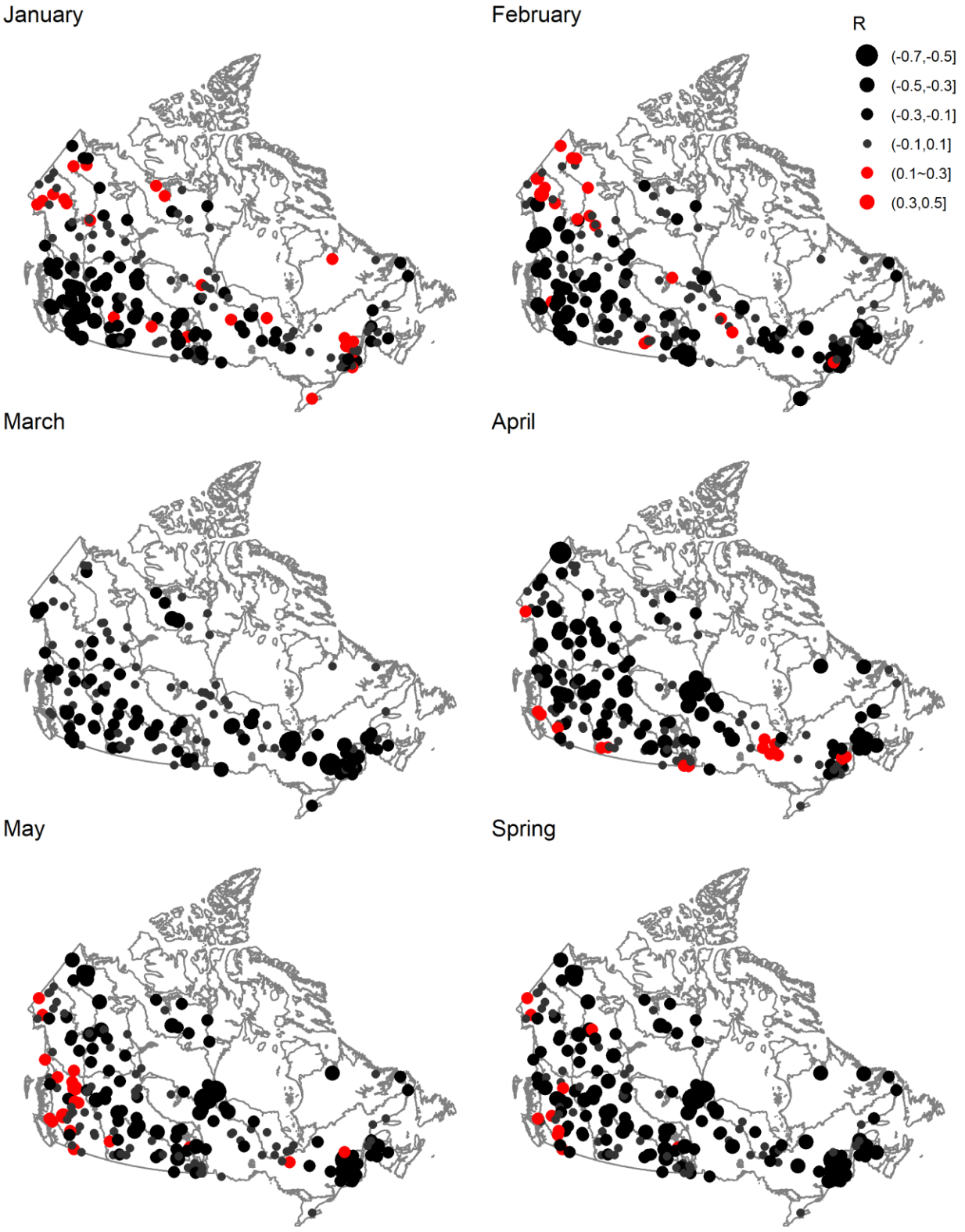


**Figure 2.14** Spatial pattern of correlation between breakup date and monthly/seasonal total rainfall for the period of 1970-2016.

Figures 2.15 and 2.16 show the trends and rates of change in spring and winter total rainfall, respectively. Both spring and winter total rainfall showed remarkable increasing trends across Canada during 1950-2016, especially for spring total rainfall in the southern Canada. The increasing trend in spring and winter total rainfall became weak for the period of 1970-2016, and some significant decreasing changes in spring total rainfall showed up. For the northern Canada, noticeable increase (over 1-3 mm/decade) in spring total rainfall were only observed in the north part of the Pacific and Western Mountains. Overall increased spring rainfall in the southern Canada may also advance breakup and thus breakup timing in the lower latitude regions appeared to be more sensitive to climatic warming than the higher latitude regions.

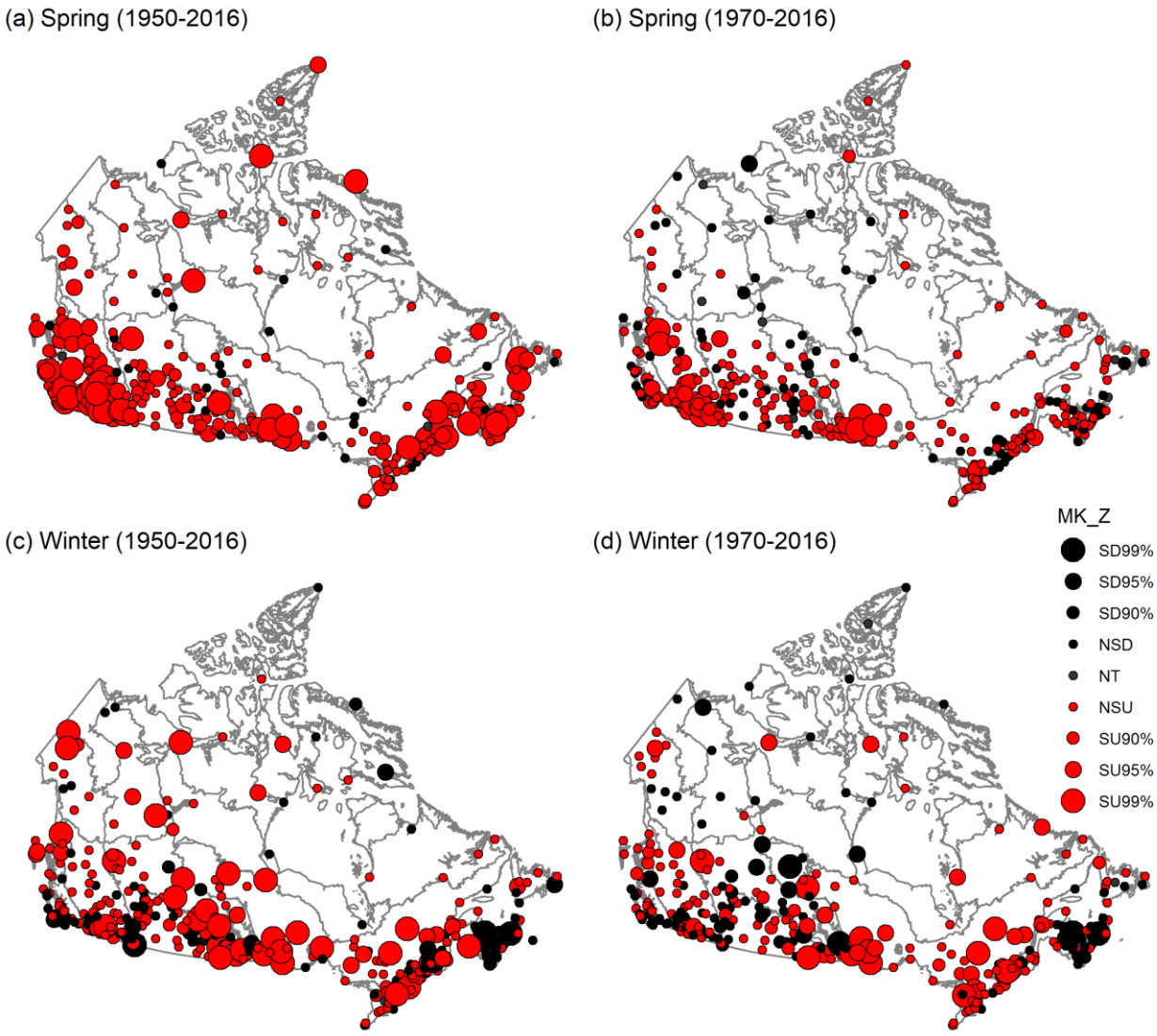


**Figure 2.15** Trends in winter and spring total rainfall for the periods of 1950-2016 and 1970-2016.

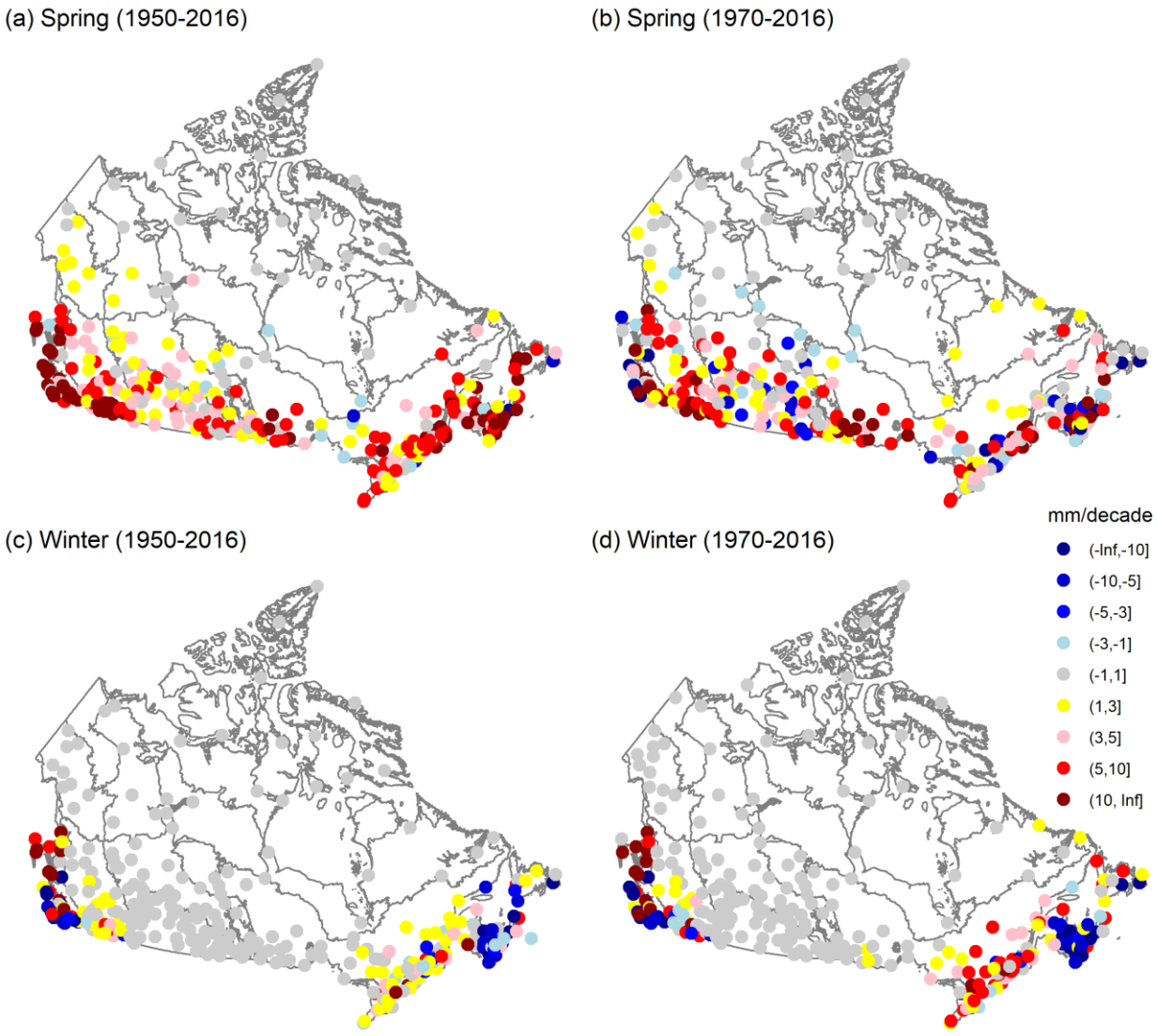


**Figure 2.16** Temporal changes in winter and spring total rainfall for the periods of 1950-2016 and 1970-2016.

### *2.4.4 Elevation*

Table 2.4 shows the correlations between elevation and the change rate of breakup date in the five selected river basins. Two correlation methods both suggested strong positive correlations (over 0.7) in the Fraser River Basin for all three periods. Higher elevations generally experience colder temperature because of adiabatic cooling. It is not difficult to understand that those stations in maritime and temperate regions with higher elevations often experience later breakup. Similar findings had been reported for lake ice, for example, Williams and Stefan (2006) reported weak positive correlation between lake ice breakup dates and elevations in North America, and Lopez et al. (2019) found that 46% of the variation in lake ice breakup trends can be explained by spring air temperature and elevation across the Northern Hemisphere. However, the impacts of elevations were not evident in other river basins. Poor positive and negligible correlations were found in the Nelson River Basin and the St. Lawrence River Basin, respectively. In addition, weak negative correlations were observed in high latitude regions, such as Mackenzie and Yukon River Basins. It indicated that breakup tended to occur earlier at higher elevations in high latitude regions. A possible explanation for this is that stations at high elevations are generally those stations in the headwaters and smaller tributaries. As discussed earlier, these stations are more sensitive to climate change. Breakup at higher elevations may occur earlier in high latitude regions when spring warmed rapidly (see temperature change in Figure 2.9).

**Table 2.4** Correlation between elevation and change rate of breakup timing (day/decade) in five river basins for the three periods of analysis.

| Period | River Basin | r_Spearman | r_Pearson | Range_elev (m) | std_elev | Number of Station |
|---|---|---|---|---|---|---|
| 1950-2016 | Fraser | **0.83** | **0.84** | 466 to 806 | 112 | 11 |
| | Mackenzie | -0.28 | -0.21 | 57 to 1,027 | 242 | 25 |
| | Nelson | 0.19 | 0.03 | 205 to 1,073 | 219 | 33 |
| | St. Lawrence | 0.05 | 0.20 | 18 to 354 | 87 | 22 |
| | Yukon | -0.43 | -0.28 | 349 to 907 | 216 | 6 |
| 1960-2016 | Fraser | **0.78** | **0.72** | 466 to 806 | 107 | 14 |
| | Mackenzie | -0.34 | -0.30 | 6 to 1,027 | 239 | 36 |
| | Nelson | 0.44 | 0.23 | 201 to 1,073 | 217 | 36 |
| | St. Lawrence | 0.08 | 0.09 | 18 to 633 | 131 | 25 |
| | Yukon | 0.21 | 0.19 | 358 to 907 | 192 | 8 |
| 1970-2016 | Fraser | **0.78** | **0.72** | 466 to 806 | 107 | 14 |
| | Mackenzie | -0.34 | -0.30 | 6 to 1,027 | 239 | 41 |
| | Nelson | 0.44 | 0.23 | 201 to 1,073 | 217 | 40 |
| | St. Lawrence | 0.08 | 0.09 | 18 to 633 | 131 | 26 |
| | Yukon | 0.21 | 0.19 | 358 to 907 | 192 | 10 |

Notes: r_Spearman and r_Pearson are correlation coefficients using Spearman and Person correlations methods separately; Correlation coefficients over 0.5 were indicated in bold. Range_elev and std_elev indicate range and standard deviation of elevations over each river basin, respectively.

### *2.4.5 Human activities*

The smallest warming rate was found in the St. Lawrence River Basin. However, it cannot fully explain why many stations in this river basin show extreme later breakup trends and the regional change rate can be as high as 1.1 day/decade. Nilsson et al. (2005) assessed the effects of fragmentation (by dams) and flow regulation (resulting from reservoir operation, irrigation, and inter-basin diversion) on the world's large river systems. They grouped those large river systems into unaffected, moderately affected, and strongly affected river watersheds. The St. Lawrence and the Nelson River Basins are both strongly affected river watersheds, the Fraser and Mackenzie

River Basins are moderately affected, and the Yukon River Basin is unaffected. The effects of flow regulation for those river basins also can be assessed using the regulation conditions of WSC gauge stations (Figure 2.5). For example, most gauge stations in the St. Lawrence and Nelson River Basins are regulated, which is consistent with the labels of strongly affected river watersheds by Nilsson et al. (2005). Flow regulation by dams modulates changes in flood frequency due to climate change typically by reducing spring floods resulting from snowmelt and increasing winter flows (Ashmore and Church, 2001). This increases the chance of thermal ice breakup instead of mechanical ice breakup in those regulated rivers. In other words, flow regulation to some degree delays river ice breakup or prolongs the breakup period. Many large and small tributaries in the basin are fragmented by dams and only 25% to 49% of the main channel segments lack dams in St. Lawrence River (Dynesius and Nilsson, 1994). Therefore, the significant later breakup trends occurring at many stations in the St. Lawrence River Basin is likely due to the combined effects of climatic factors and human activities. Flow regulation also can advance river ice breakup or contributes to mechanical breakup. For instance, the flow regulated station of Peace River at Peace River trended towards earlier breakup of over 3 day/decade for all three periods. This significant earlier breakup trend is probably due to the winter releases and regulation thermal effects (Prowse and Conly, 1998). Other extreme earlier breakup trends were also observed in flow regulated stations, such as Bow River at Calgary (4 day/decade earlier), Fraser River near Marguerite (3.9 day/decade earlier), and Fairford River near Fairford (12.3 day/decade earlier) during 1970-2016. The impacts of human activities on rive ice breakup are yet to be further explored and quantified based on more detailed data and sophisticated methods.

## 2.5 Conclusion

This study constructed a long-term and uniform river ice breakup timing dataset and explored large-scale spatial and temporal variations of river ice breakup timing across Canada. An overall earlier breakup trend was found across Canada, especially for the Pacific and Western Mountains, Central Plains and Arctic. Mixed trends were identified in the Atlantic and Great Lakes – St. Lawrence regions while later breakup trends were observed in Boreal Shield and Taiga Shield. Breakup date was found to be mainly correlated with spring air temperature even though warming trend was stronger for winter than for spring. Breakup pattern tended to be consistent with the spring warming pattern, especially for 1950-2016 and 1960-2016. Later breakup trends became more evident for 1970-2016 in accordance with the weaker spring warming trend found in the south and west parts of the country during this period. Evident spring warming was mainly found in the north part of Canada (Arctic) for this period. However, in higher latitude regions, the breakup timing appeared to be less sensitive to spring warming mainly because its effect was counteracted by the increased spring snowfall, which delays breakup. This explained why the breakup and spring warming patterns were not in as good agreement for 1970-2016 than for the other two periods. Rainfall generally advances breakup during ice-covered season though midwinter rainfall also can contribute to later breakup through refreezing in some colder or weak warming regions. Increased rainfall in southern Canada in part explained why breakup in lower latitude regions are more sensitive to climate change and variability. Additionally, river ice breakup in headwaters and small tributaries appeared to be more sensitive to climate change as compared to main streams and large rivers. Higher elevation tended to delay river ice breakup through adiabatic cooling in regions with large elevation variations and maritime or temperate climate, but can also experience earlier breakup in high latitude regions. Flow regulation and fragmentation can both advance and delay

river ice breakup. Extreme later breakup trends in the St. Lawrence River Basin and earlier breakup trends in the Peace River basin are likely due to the combined effect of climatic factors and flow regulations. Furthermore, large number of missing values in the breakup dataset can lead to biased trend analysis results and thus data completeness should be considered when interpreting trend analysis results. This study offers a way to construct long-term and uniform river ice breakup timing database in Canada. The findings from this study not only highlight the temporal and spatial variations of river ice breakup across Canada and the drivers behind the observed patterns, but also provide theoretical support for modelling the breakup process.

## 2.6 References

Ariano, S.S., Brown, L.C., 2019. Ice processes on medium-sized north-temperate lakes. Hydrol. Process. 33, 2434–2448.

Ashmore, P., Church, M.A., 2001. The impact of climate change on rivers and river processes in Canada. Geological Survey of Canada Ottawa, Ontario.

Beltaos, S., 2002. Effects of climate on mid-winter ice jams. Hydrol. Process. 16, 789–804.

Beltaos, S., Burrell, B.C., 2003. Climatic change and river ice breakup. Can. J. Civ. Eng. 30, 145–155. https://doi.org/10.1139/l02-042

Beltaos, S., Prowse, T., 2009. River-ice hydrology in a shrinking cryosphere. Hydrol. Process. 23, 122–144.

Benson, B.J., Magnuson, J.J., Jensen, O.P., Card, V.M., Hodgkins, G., Korhonen, J., Livingstone, D.M., Stewart, K.M., Weyhenmeyer, G.A., Granin, N.G., 2012. Extreme events, trends, and variability in Northern Hemisphere lake-ice phenology (1855-2005). Clim. Change 112, 299–323. https://doi.org/10.1007/s10584-011-0212-8

Bonsal, B.R., Prowse, T.D., Duguay, C.R., Lacroix, M.P., 2006. Impacts of large-scale teleconnections on freshwater-ice break/freeze-up dates over Canada. J. Hydrol. 330, 340–353. https://doi.org/10.1016/j.jhydrol.2006.03.022

Bush, E., Lemmen, D.S., 2019. Canada's changing climate report. Government of Canada= Gouvernement du Canada.

Chen, Y., Guan, Y., Shao, G., Zhang, D., 2016. Investigating trends in streamflow and precipitation

in Huangfuchuan basin with wavelet analysis and the Mann-Kendall test. Water (Switzerland) 8. https://doi.org/10.3390/w8030077

Chen, Y., She, Y., 2019. Temporal and Spatial Variations of River Ice Breakup Timing across Canada, in: 20th Workshop on the Hydraulics of Ice Covered Rivers.

de Rham, L.P., Prowse, T.D., Bonsal, B.R., 2008. Temporal variations in river-ice break-up over the Mackenzie River Basin, Canada. J. Hydrol. 349, 441–454. https://doi.org/10.1016/j.jhydrol.2007.11.018

Doyle, P.F., Ball, J.F., 2008. Changing ice cover regime in southern British Columbia due to changing climate, in: Proceedings of the 19th IAHR International Symposium on Ice. St Joseph Communications, Vancouver, Canada. pp. 51–61.

Duguay, C.R., Prowse, T.D., Bonsal, B.R., Brown, R.D., Lacroix, M.P., Ménard, P., 2006. Recent trends in Canadian lake ice cover. Hydrol. Process. 20, 781–801. https://doi.org/10.1002/hyp.6131

Dynesius, M., Nilsson, C., 1994. Fragmentation and flow regulation of river systems in the northern third of the world. Science (80-. ). 266, 753–762.

Fu, C., Yao, H., 2015. Trends of ice breakup date in south-central Ontario. J. Geophys. Res. Atmos. 120, 9220–9236.

Ghanbari, R.N., Bravo, H.R., Magnuson, J.J., Hyzer, W.G., Benson, B.J., 2009. Coherence between lake ice cover, local climate and teleconnections (Lake Mendota, Wisconsin). J. Hydrol. 374, 282–293. https://doi.org/10.1016/j.jhydrol.2009.06.024

Goulding, H.L., Prowse, T.D., Beltaos, S., 2009b. Spatial and temporal patterns of break-up and ice-jam flooding in the Mackenzie Delta, NWT. Hydrol. Process. An Int. J. 23, 2654–2670.

Hicks, F., 2009. An overview of river ice problems: CRIPE07 guest editorial.

Hodgkins, G.A., Dudley, R.W., Huntington, T.G., 2005. Changes in the number and timing of days of ice-affected flow on northern New England rivers, 1930-2000. Clim. Change 71, 319–340. https://doi.org/10.1007/s10584-005-5926-z

IPCC, 2013. IPCC, 2013: climate change 2013: the physical science basis. Contribution of working group I to the fifth assessment report of the intergovernmental panel on climate change.

Jakkila, J., Leppäranta, M., Kawamura, T., Shirasawa, K., Salonen, K., 2009. Radiation transfer and heat budget during the ice season in Lake Pääjärvi, Finland. Aquat. Ecol. 43, 681–692. https://doi.org/10.1007/s10452-009-9275-2

Janowicz, J.R., 2010. Observed trends in the river ice regimes of northwest Canada. Hydrol. Res. 41, 462. https://doi.org/10.2166/nh.2010.145

Jasek, M.J., Shen, H.T., 1999. 1998 break-up and flood on the Yukon River at Dawson–did El Niño and climate change play a role? Ice Surf. Waters, Balkema, Rotterdam 761–768.

Jensen, O.P., Benson, B.J., Magnuson, J.J., Card, V.M., Futter, M.N., Soranno, P.A., Stewart, K.M., 2007. Spatial analysis of ice phenology trends across the Laurentian Great Lakes region during a recent warming period. Limnol. Oceanogr. 52, 2013–2026. https://doi.org/10.4319/lo.2007.52.5.2013

Lacroix, M.P., Prowse, T.D., Bonsal, B.R., Duguay, C.R., Ménard, P., 2005. River ice trends in

Canada, in: 13th Workshop on the Hydraulics of Ice Covered Rivers. pp. 41–55.

Livingstone, D.M., 2000. Large-scale climatic forcing detected in historical observations of lake ice break-up. Int. Vereinigung für Theor. und Angew. Limnol. Verhandlungen 27, 2775–2783.

Lopez, L.S., Hewitt, B.A., Sharma, S., 2019. Reaching a breaking point: How is climate change influencing the timing of ice breakup in lakes across the northern hemisphere? Limnol. Oceanogr. 1–11. https://doi.org/10.1002/lno.11239

Magnuson, J.J., Robertson, D.M., Benson, B.J., Wynne, R.H., Livingstone, D.M., Arai, T., Assel, R.A., Barry, R.G., Card, V., Kuusisto, E., 2000. Historical trends in lake and river ice cover in the Northern Hemisphere. Science (80-. ). 289, 1743–1746.

Nilsson, C., Reidy, C.A., Dynesius, M., Revenga, C., 2005. Fragmentation and flow regulation of the world's large river systems. Science (80-. ). 308, 405–408.

Nõges, P., Nõges, T., 2014. Weak trends in ice phenology of Estonian large lakes despite significant warming trends. Hydrobiologia 731, 5–18. https://doi.org/10.1007/s10750-013-1572-z

Obyazov, V.A., Smakhtin, V.K., 2014. Ice regime of Transbaikalian rivers under changing climate. Water Resour. 41, 225–231. https://doi.org/10.1134/S0097807814030130

Prowse, T., Alfredsen, K., Beltaos, S., Bonsal, B., Duguay, C., Korhola, A., McNamara, J., Pienitz, R., Vincent, W.F., Vuglinsky, V., Weyhenmeyer, G.A., 2011. Past and future changes in arctic lake and river ice. Ambio 40, 53–62. https://doi.org/10.1007/s13280-011-0216-7

Prowse, T., Bonsal, B.R., Duguay, C.R., Lacroix, M.P., 2007. River-ice break-up/freeze-up: A review of climatic drivers, historical trends and future predictions. Ann. Glaciol. 46, 443–451.

https://doi.org/10.3189/172756407782871431

Prowse, T.D., Conly, F.M., 1998. Effects of climatic variability and flow regulation on ice-jam flooding of a northern delta. Hydrol. Process. 12, 1589–1610.

Rantanen, M., Karpechko, A.Y., Lipponen, A., Nordling, K., Hyvärinen, O., Ruosteenoja, K., Vihma, T., Laaksonen, A., 2022. The Arctic has warmed nearly four times faster than the globe since 1979. Commun. Earth Environ. 3, 1–10.

Schmidt, D.F., Grise, K.M., Pace, M.L., 2019. High-frequency climate oscillations drive ice-off variability for Northern Hemisphere lakes and rivers. Clim. Change 152, 517–532. https://doi.org/10.1007/s10584-018-2361-5

Sen, P.K., 1968. Estimates of the regression coefficient based on Kendall's tau. J. Am. Stat. Assoc. 63, 1379–1389.

Vavrus, S.J., Wynne, R.H., Foley, J.A., 1996. Measuring the sensitivity of southern Wisconsin lake ice to climate variations and lake depth using a numerical model. Limnol. Oceanogr. 41, 822–831.

Vincent, L.A., Milewska, E.J., Wang, X.L., Hartwell, M.M., 2018. Uncertainty in homogenized daily temperatures and derived indices of extremes illustrated using parallel observations in Canada. Int. J. Climatol. 38, 692–707. https://doi.org/10.1002/joc.5203

Vincent, L.A., Wang, X.L., Milewska, E.J., Wan, H., Yang, F., Swail, V., 2012. A second generation of homogenized Canadian monthly surface air temperature for climate trend analysis. J. Geophys. Res. Atmos. 117, 1–13. https://doi.org/10.1029/2012JD017859

Vincent, L.A., Zhang, X., Brown, R.D., Feng, Y., Mekis, E., Milewska, E.J., Wan, H., Wang, X.L., 2015. Observed trends in Canada's climate and influence of low-frequency variability modes. J. Clim. 28, 4545–4560. https://doi.org/10.1175/JCLI-D-14-00697.1

Weyhenmeyer, G.A., Livingstone, D.M., Meili, M., Jensen, O., Benson, B., Magnuson, J.J., 2011. Large geographical differences in the sensitivity of ice-covered lakes and rivers in the Northern Hemisphere to temperature changes. Glob. Chang. Biol. 17, 268–275. https://doi.org/10.1111/j.1365-2486.2010.02249.x

Williams, S.G., Stefan, H.G., 2006. Modeling of lake ice characteristics in North America using climate, geography, and lake bathymetry. J. Cold Reg. Eng. 20, 140–167. https://doi.org/10.1061/(ASCE)0887-381X(2006)20:4(140)

Zhang, X., David Harvey, K., Hogg, W.D., Yuzyk, T.R., 2001. Trends in Canadian streamflow. Water Resour. Res. 37, 987–998. https://doi.org/10.1029/2000WR900357

# Chapter 3. Evaluation and Uncertainty Assessment of Weather Data and Model Calibration on Daily Streamflow Simulation in a Large-scale Regulated and Snow-dominated River Basin

## 3.1 Introduction

Distributed and/or semi-distributed hydrologic models are crucial in water resources planning and management and have been widely used in investigating the effects of climate and land-use change on water quantity and quality (Faramarzi et al., 2017; Gizaw et al., 2017; Loiselle et al., 2020; Scheepers et al., 2018; Yan et al., 2013). The reliability and robustness of hydrologic models generally depend on accurate model representations, appropriate input data, and proper model calibration (Abbaspour et al., 2017; Beven, 2000; Faramarzi et al., 2015). An accurate model setup is the prerequisite of a successful hydrologic model. Calibration might be of little help if pre-calibrated model performance is very poor (Abbaspour et al., 2017). Various types of input data (e.g., climate, soil, and land-use) could bring in different sources of uncertainties in model results, and each type often has more than one data source for a region. Climate data is crucial for hydrologic modelling; however, it is often difficult to collect high-quality observed climate data for large-scale regions, especially in mountains (Zaremehrjardy et al., 2021). In addition to meteorological data, there are numerous gridded climate data products available, such as Climate Forecast System Reanalysis (CFSR), gridded climate data provided by Natural Resources Canada (NRCan), and ERA5 (Dile and Srinivasan, 2014; Hersbach et al., 2020; McKenney et al., 2011), but their applicability for reliable hydrologic modeling in large snow-dominated watersheds remains challenging. The performance of the recently released ERA5 reanalysis data (Hersbach et al., 2020) in hydrologic models has drawn lots of attention globally (Champagne et al., 2021; Tarek

et al., 2020; Xiang et al., 2021). However, studies regarding the performance of ERA5 data in distributed and/or semi-distributed hydrologic modeling and in reproducing daily streamflow in mid-to-high latitude watersheds are still very sparse.

Hydrologic models can be unreliable if not correctly calibrated. Model calibration involves several considerations including calibration algorithm, parameters to be calibrated and their range, calibrating all the parameters together or separately, choice of objective function, number of simulations, number of objective variables to calibrate the model, and sequential calibration of a river basin from upstream to downstream versus calibrating the watershed as a whole (Arsenault et al., 2014; Kouchi et al., 2017; Muleta, 2012; Yang et al., 2008). While most of the studies reported that different choices can lead to different calibration results, the choice of proper input data, realistic parameter combination, and suitable calibration scheme has remained challenging in hydrologic modeling of higher-latitude watersheds with their unique hydro-climatic conditions. Despite a wide range of studies on model calibration and uncertainties, applying a particular approach or data is often extemporary in process representation, particularly in the cold watersheds. Moreover, less attention has been paid to the effects of the number of simulations through iterations of the calibration processes. The inherent model equifinality issue, i.e. multiple parameter sets provide equally good model performance (Beven, 2006; Beven and Binley, 2014), introduces uncertainty that can deteriorate the reliability of hydrologic models in forecasting future water resources (Ficklin and Barnhart, 2014; Her and Seong, 2018). This issue can be more critical in cold regions where hydrological cycle is governed by snow processes (Zaremehrjardy et al., 2021). Multi-site (Abbaspour et al., 2007; Nkiaka et al., 2018; Schuol et al., 2008) and multi-objective calibration (Hanzer et al., 2016; Rajib et al., 2016; Tuo et al., 2018a) schemes have been reported as useful means in limiting model equifinality. Although multiple variables (e.g., soil moisture,

evapotranspiration, and water quality) have been used in multi-objective calibration (Cao et al., 2006; Molina-Navarro et al., 2017; Puertes et al., 2019; Rajib et al., 2016; Rientjes et al., 2013), snow data is seldom utilized in simulation of cold watersheds. Snowfall is a vital source of streamflow in cold regions, and thus multi-objective calibration that considers both streamflow and snow measurements can be beneficial in improving the snow processes of hydrologic models (Tuo et al., 2018b). However, relevant studies are minimal, especially in large-scale watersheds of mid-to-high latitude regions.

The Soil and Water Assessment Tool (SWAT) (Arnold et al., 1998), a semi-distributed hydrologic model and public domain software, has been widely used in various regions from small catchments to continental scale to simulate the streamflow and water quality (Abbaspour et al., 2015; Faramarzi et al., 2015; Ficklin et al., 2012; Musau et al., 2015; Neupane et al., 2018; Tuo et al., 2016). The model delineates a basin into many subbasins, which are further divided into hydrologic response units (HRUs), each consisting of unique soil, land cover, and slope combinations. The Sequential Uncertainty Fitting Program (SUFI2) of SWATCUP is often employed to calibrate the SWAT model (Abbaspour, 2015; Ha et al., 2017; Yang et al., 2008). SMFMX and SMFMN, the maximum and minimum snowmelt rates, are among the most sensitive parameters in snow mass balance simulations in the SWAT model. However, the standard SUFI2-SWATCUP approach does not systematically assess nor control the relationship between various snow parameters (for example, if SMFMX is greater than SMFMN). Consequently, the parameter set generated by SWATCUP can contain parameter combinations where SMFMX is less than SMFMN, which does not make physical sense. In general, previous studies either did not control or exclude such unrealistic snow parameter combinations, or manually calibrated for Snow Water Equivalent (SWE) after completing an automatic streamflow calibration (Liu et al., 2020; Peker and Sorman,

2021; Tuo et al., 2018a, 2018b). This laborious effort may reduce the reliability of the final calibrated model. Therefore, developing an automatic calibration scheme to reject unrealistic parameter combinations related to snow simulation and simultaneously calibrate streamflow and SWE in a multi-objective calibration framework is necessary (Tuo et al., 2018b).

The main objective of this study is to revisit the commonly used climate data and calibration approaches and develop a more automatic calibration framework for a thorough analysis and assessment of model performance in simulation of snow processes and resulting streamflow in cold region watersheds. Our specific objectives include: (1) evaluate observed and gridded (e.g., ERA5) climate data to find the optimal weather input, as the first necessary step to drive the semi-distributed hydrologic model (SWAT model) before calibration; (2) modify SWAT and/or SWATCUP for automatic elimination of unrealistic snow parameter combinations resulted from SUFI2-SWATCUP parameter sampling, and for multi-objective calibration of streamflow and SWE; (3) find the proper calibration scheme through investigating the uncertainties of the objective function, number of simulations in each iteration, sequential calibration from upstream to downstream, and calibrating snow parameters first and then all other hydrological parameters; (4) improve the simulation of snow-affected spring streamflow using multi-objective calibration (streamflow and SWE). We focused our modeling efforts on the Peace River Basin (PRB) in western Canada. The PRB is characterized by heterogeneous soil, land use and geospatial conditions, and represent cold region hydrology (e.g., Pomeroy et al., 2007). The basin has also been regulated by several large dams in the upstream. Therefore, the PRB is a suitable study area for assessing our research objectives and a watershed worth to be explored.

## 3.2 Data and methodology

### *3.2.1 Study area*

The Peace River Basin (PRB) is in western Canada, and its area is about 306,000 $km^2$. It begins from the Rocky Mountains in the east-central British Columbia and extends towards the northeast side of Alberta. The modelled area in this study is around 277,286 $km^2$ (Figure 3.1). The altitude varies from 3,286 m in the west to about 200 m in the east side of the PRB. The river basin is mainly covered by forests (over 60%), and the majority are evergreen needle leaf and deciduous forests. Based on the historical climate data from Environment and Climate Change Canada (ECCC) for the 2004-2013 period, the air temperature ranged from around -50 ℃ in winter to about 30 ℃ in summer, and the average annual temperature in the basin was from -1.8 to 3.9 ℃. The range of average annual total precipitation was between 386 mm to 1,278 mm across the study area. The low temperature in the PRB generally lasts from October to April, during which snowfall dominates the river basin. The watershed typically experiences peak flows during spring due to snowpack melting (Toth et al., 2006). The PRB has been regulated by the W.A.C. Bennett Dam, at the Williston Lake reservoir, in the upstream tributaries since 1968. Williston Reservoir covers approximately 1,773 $km^2$ at full pool and has active storage of 39,471 million $m^3$. The Peace Canyon Dam was constructed in 1980, forming the 23 km long Dinosaur Reservoir just behind W.A.C. Bennett Dam. The Dinosaur Reservoir covers approximately 9 $km^2$ at full pool and has limited active storage of 24.69 million $m^3$. The Site C dam, the third dam and hydroelectric generating station located downstream of the two existing dams, was approved in December 2014 and construction is expected to be completed in 2025 (https://www.sitecproject.com/about-site-c/project-overview).

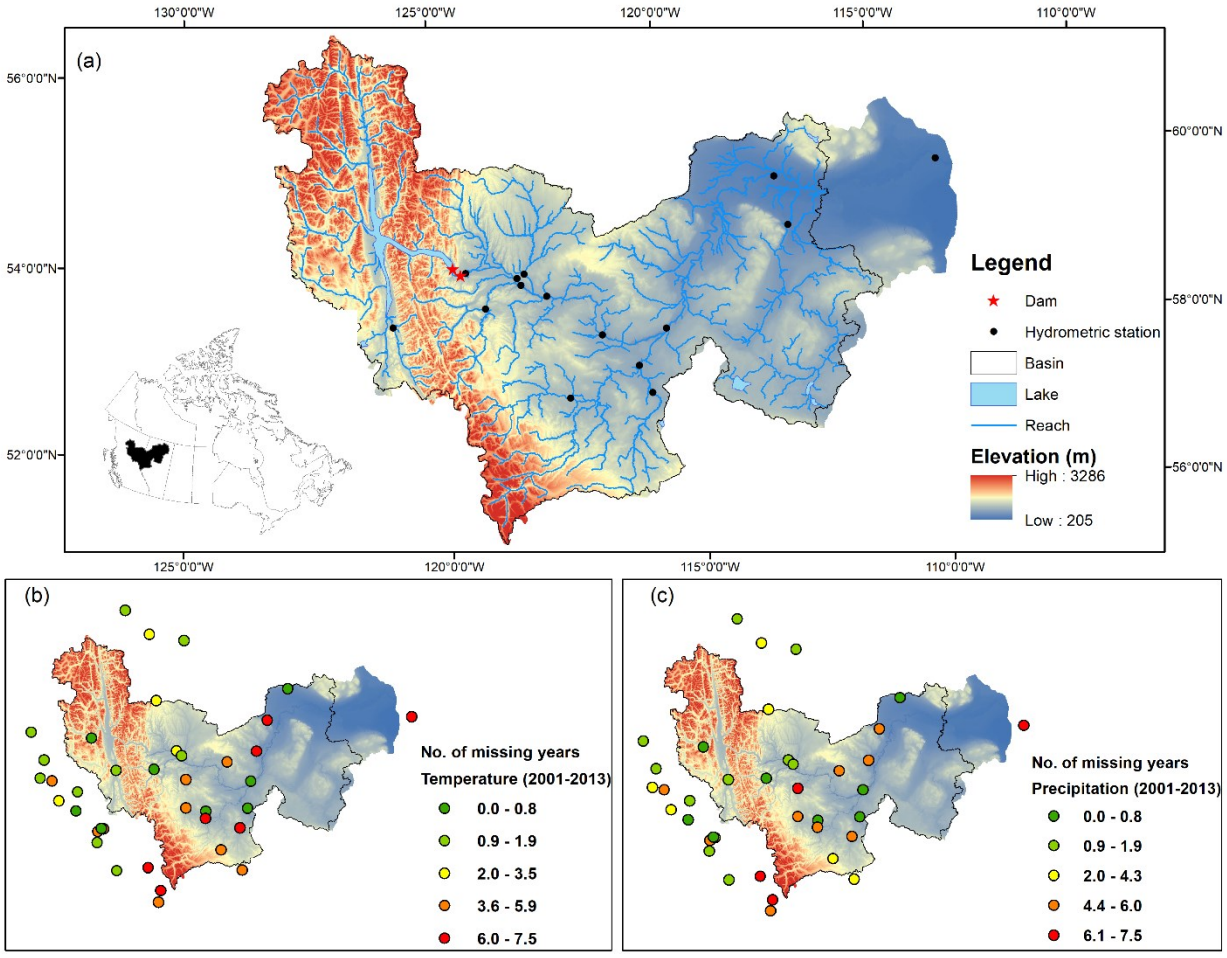


**Figure 3.1** Map of Peace River Basin and the black line encloses the study area: (a) location of dams, lakes, and hydrometric stations; (b) & (c) location of ECCC meteorological stations (temperature and precipitation); color of circles indicates the number of years with missing daily data during 2001-2013.

### *3.2.2 SWAT model*

The SWAT2012 model (version 670) is a daily continuous-time, semi-distributed, and watershed-scale hydrologic model (Arnold et al., 1998; Neitsch et al., 2011). Simulation of watershed hydrology in SWAT contains the land phase and the routing phase of the hydrological cycle. The first phase controls the amount of water in each subbasin to the main channel, and the second phase routes the water to the outlet through the channel network of the watershed. The climatic inputs

for the model include daily precipitation, maximum and minimum air temperature, solar radiation, relative humidity, and wind speed, which provide the moisture and energy that drive all other hydrological processes in the watershed.

The model categorizes rain or snow using a user-specified threshold value of the mean daily air temperature. The stored format of snowfall at the ground surface is a snowpack, and the amount of water stored in it is expressed as SWE. The snowpack increases with snowfall and accumulation or decreases with snowmelt or sublimation. The air and snowpack temperature, areal coverage of snow, and melting rate are the main factors that control the snowmelt process. Snowmelt and rainfall are contained in the computation of runoff and percolation. To account for the orographic effects on both precipitation and temperature, the model allows up to 10 elevation bands to be defined in each subbasin. Temperature (maximum and minimum) and precipitation are computed for each band as a function of the respective lapse rate and the difference between the station elevation and the average elevation specified for the band. Reservoirs are impoundments located on the main channel network, and they receive water from all upstream subbasins. SWAT provides four methods to calculate the volume of outflow, including measured daily outflow, measured monthly outflow, average annual release rate for the uncontrolled reservoir, and controlled outflow with target release. More details about the theory of the model can be found in Neitsch et al. (2011).

To automatically calibrate streamflow and subbasin-scale SWE, some changes in the original code of SWAT were made. SWAT only calculates the SWE at the HRU scale. Therefore, the SWAT code was modified to calculate the subbasin SWE based on the existing HRU data, and output to output.sub file based on SUFI2-SWATCUP requirements so that the SWE can be automatically calibrated together with streamflow.

### *3.2.3 Data and model setup*

Data used for building the SWAT model of the PRB are summarized in Table 3.1. The digital elevation model (DEM) at 90 m resolution (Jarvis et al., 2008) was used for sub-basin delineation, while a detailed stream network was initially delineated using a 30 m resolution DEM and used for watershed delineation. With the threshold of 100 $km^2$, the study basin was delineated into 808 subbasins, which were further divided into 6,243 HRUs. Five elevation bands were defined for each subbasin, mainly in the upstream regions, to account for the orographic effects on precipitation and temperature. The land-use map was obtained from the GeoBase Land Cover Product, which identified 23 classes of land-use and land-cover for the study area. Soil data were from two sources, including Soil Landscapes of Canada (SLC) V3.2 from the Agriculture Agri-Food Canada and FAO soil database. SLC was pre-processed by Cordeiro et al. (2017) in a format that can be easily used in SWAT, and it has a more detailed soil classification and parameterization scheme. However, the existing SLC data does not cover a small portion of the upstream areas and the global FAO soil map and its attributed parameters (Fischer et al., 2008) were used to fill this gap.

For the study period, the Williston and Dinosaur Reservoirs need to be considered on the Peace River Basin. The outflow from the Williston Reservoir flows immediately into the Dinosaur Reservoir. The storage of the Dinosaur Reservoir can be ignored compared with the storage of the Williston Reservoir. Therefore, the two reservoirs were considered a combined reservoir in the hydrologic model. The reservoir was simulated using the measured daily outflow method, and the reservoir input data for SWAT (Table 3.2) was extracted and/or estimated from the Williston and Dinosaur Reservoir specifications in a BC Hydro report ("Peace River Water Use Plan - Revised for Acceptance by the Comptroller of Water Rights",

http://www.bchydro.com/content/dam/hydro/medialib/internet/documents/environment/pdf/peace_river_water_use_plan.pdf). The volume of water and surface area at the emergency/principal spillway elevation are not provided in the report. In this study, the volume of water needed to fill the reservoir to the emergency and principal spillways was estimated based on the stage-storage relationship for the Williston Reservoir provided in the report. The reported surface area of the Williston Reservoir at full pool (maximum normal operation elevation) is 1,773 $km^2$. We used these information to estimate the reservoir surface area at the emergency/principal spillway elevation assuming the reservoir is a conical frustum. Water level data at the WSC station 07EF002 for the Williston Reservoir was used to estimate the initial reservoir storage on a given date. Streamflow data at Hudson Hope (07EF001), several kilometers downstream the Peace Canyon Dam, was used as reservoir outflow.

Weather inputs for SWAT model include precipitation, temperature (maximum and minimum temperature), solar radiation, relative humidity, and wind speed. Three data sources were used to assess the uncertainty in weather data, including ECCC, National Centers for Environmental Prediction's Climate Forecast System Reanalysis (CFSR), and the ERA5. Daily precipitation and temperature data of 136 meteorological stations were obtained from ECCC. For the study period (2001-2013), only 38 stations have less than 60% missing values and these were used in the model. The meteorological stations available from ECCC do not have reasonable spatial distribution across the PRB as only a few of them are in the mountainous regions and the downstream part of the basin, and the observed climate data collected from these stations are dominated by many missing values (see Figure 3.1b, c). CFSR has all the required weather data for the model. In this study, the missing solar radiation, relative humidity, and wind speed data in ECCC and ERA5 were completed from the nearest CFSR grid stations and combined with their precipitation and

temperature data to drive the SWAT model. In addition, the missing values in the precipitation and temperature data of ECCC meteorological stations were filled using the weather generator module built in the SWAT model. Daily streamflow and SWE were used for model calibration and validation. 14 WSC stations that had less than 20% missing values of daily flow, and 14 point stations near the streamflow stations from ERA5 providing daily SWE data during 2004-2013 were used in this study (Table 3.3).

**Table 3.1** Data sources used in SWAT Model

| Data Type | Sources | Resolution | Region | Reference |
|---|---|---|---|---|
| DEM | OpenTopography | 30m | Global | https://portal.opentopography.org |
| | SRTM | 90m | Global | http://srtm.csi.cgiar.org |
| Weather data | ECCC | / | Canadian | http://climate.weather.gc.ca/ |
| | CFSR | 0.3° grid | Global | https://globalweather.tamu.edu/ |
| | ERA5 | 30km×30km | Global | https://www.ecmwf.int/en/forecasts/datasets/reanalysis-datasets/era5 |
| Landuse and land cover map | circa 2000 | 30m×30m | Canadian | https://open.canada.ca/data/en/dataset/97126362-5a85-4fe0-9dc2-915464cfdbb7 |
| Soil data | Soil Landscapes of Canada V3.2 | 1:1,000,000 | Canadian | http://sis.agr.gc.ca/cansis/nsdb/slc/index.html |
| | FAO soil map | 1:5,000,000 | Global | http://www.fao.org/geonetwork/srv/en/metadata.show?id=14116 |
| Streamflow | WSC | / | Canadian | https://www.canada.ca/en/environment-climate-change/services/water-overview/quantity/monitoring/survey.html |
| Daily operation of reservoirs/dams | BC Hydro | / | Local | https://www.bchydro.com/toolbar/about/sustainability/conservation/water_use_planning/northern_interior/peace_river.html |
| SWE | ERA5 | 30km×30km | Global | https://www.ecmwf.int/en/forecasts/datasets/reanalysis-datasets/era5 |

**Table 3.2** SWAT reservoir input parameters and data

| Reservoir/Dam Specifications | Input |
|---|---|
| Volume of water needed to fill the reservoir to the emergency spillway (RES_EVOL $10^4$ $m^3$) | 4,120,001 |
| Reservoir surface area when the reservoir is filled to the emergency spillway (RES_ESA ha=$10^4$ $m^2$) | 177,300 |
| Reservoir surface area when the reservoir is filled to the principal spillway (RES_PVOL $10^4$ $m^3$) | 1,432,411 |
| Volume of water needed to fill the reservoir to the principal spillway (RES_PSA ha=$10^4$ $m^2$) | 114,728 |
| Initial reservoir volume (RES_PVOL $10^4$ $m^3$) | 2,740,320 |
| The year the reservoir become operational | 1967 |
| Daily outflow of the reservoir (IRESCO=3) | Hudson Hope station |
| Emergency spillway elevation (m) | 672.02 |
| Principal spillway elevation (m) | 653.53 |

**Table 3.3** Hydrometric station information of Peace River Basin.

| ID | Station Number | Subbasin ID | Station Name | Latitude | Longitude | Gross Drainage Area ($km^2$) |
|---|---|---|---|---|---|---|
| 1 | 07HF001 | 115 | Peace River at Fort Vermilion | 58.388 | -116.029 | 227,000 |
| 2 | 07JD002 | 223 | Wabasca River at Highway No. 88 | 57.875 | -115.389 | 35,800 |
| 3 | 07EF001 | 364 | Peace River at Hudson Hope | 56.027 | -121.909 | 73,100 |
| 4 | 07FA004 | 399 | Peace River above Pine River | 56.199 | -120.815 | 87,200 |
| 5 | 07FD002 | 421 | Peace River near Taylor | 56.139 | -120.672 | 101,000 |
| 6 | 07FC001 | 422 | Beatton River near Fort St. John | 56.278 | -120.7 | 15,600 |
| 7 | 07FD010 | 436 | Peace River above Alces River | 56.127 | -120.057 | 121,000 |
| 8 | 07FB001 | 464 | Pine River at East Pine | 55.718 | -121.212 | 12,100 |
| 9 | 07EE007 | 523 | Parsnip River above Misinchinka River | 55.082 | -122.913 | 4,930 |
| 10 | 07HA001 | 524 | Peace River at Peace River | 56.245 | -117.314 | 194,000 |
| 11 | 07FD003 | 572 | Peace River at Dunvegan Bridge | 55.919 | -118.607 | 135,000 |
| 12 | 07GJ001 | 637 | Smoky River at Watino | 55.715 | -117.623 | 50,300 |
| 13 | 07GH002 | 702 | Little Smoky River near Guy | 55.456 | -117.162 | 11,100 |
| 14 | 07GE001 | 717 | Wapiti River near Grande Prairie | 55.071 | -118.803 | 11,300 |

### *3.2.4 Model calibration and evaluation schemes*

The examination of the performance of the SWAT models in this study is based on their ability to reproduce historical SWE and streamflow data. The input data of 2001-2003 was used to warm up the models and then the models were calibrated with 2004-2009 and validated for 2010-2013. The commonly used SUFI2 of SWATCUP was used to perform the sensitivity analysis, calibration, and validation (Abbaspour, 2015). For the purpose of uncertainty analysis, a total of 25 parameters were selected based on an extensive literature review and their values were constrained by the published or physically realistic ranges (Anand et al., 2018; Grusson et al., 2015; Sospedra-Alfonso et al., 2015; Zaremehrjardy et al., 2021). A sensitivity analysis was performed for three SWAT projects driven by the CFSR, ECCC, and ERA5 climate data, respectively. Specifically, we used a Latin Hypercube Sampling Technique within the SUFI2 algorithm to generate 1,000 samples of parameter sets from the given ranges and fed them into the models to perform 1,000 simulations for each model. Based on P-value and t-Statistic provided by Global Sensitivity analysis of the SWATCUP (Abbaspour, 2015), four insensitive parameters were dropped, and the remaining 21 parameters shown in Table 3.4 were used for calibration. To evaluate the effects of the objective function on model calibration, two commonly used efficiency coefficients, the Nash–Sutcliffe efficiency (NS) and a modified version of the efficiency criterion ($bR^2$) defined by Krause et al. (2005), were selected as the objective functions.

**Table 3.4** Selected parameters for calibration.

| ID | Name | Description | Range |
|---|---|---|---|
| *Snow parameters* | | | |
| 1 | v__SFTMP | Snowfall temperature (ºC) | [-5, 5] |
| 2 | v__SMTMP | Snowmelt base temperature (ºC) | [-5, 5] |
| 3 | v__SMFMX | Maximum melt rate for snow during the year (mm/ºC-day) | [0, 10] |
| 4 | v__SMFMN | Minimum melt rate for snow during the year (mm/ºC-day) | [0, 10] |
| 5 | v__TIMP | Snowpack temperature lag factor | [0, 1] |
| *Elevation band parameters* | | | |
| 6 | v__TLAPS | Temperature lapse rate (°C/km) | [-7.5, -5.5] |
| 7 | v__PLAPS | Precipitation lapse rate (mm $H^2O$/km) | [0, 250] |
| *Hydrological parameters* | | | |
| 8 | v__ALPHA_BF | Base flow alpha factor (days) | [0, 1] |
| 9 | v__REVAPMN | Threshold depth of water in the shallow aquifer for 'revap' to occur (mm) | [0, 500] |
| 10 | v__GW_DELAY | Groundwater delay time (days) | [0, 500] |
| 11 | v__GWQMN | Threshold depth of water in the shallow aquifer required for return flow to occur (mm) | [0, 5000] |
| 12 | v__RCHRG_DP | Deep aquifer percolation fraction | [0, 1] |
| 13 | r__SOL_AWC | Soil available water storage capacity (mm $H^2O$/mm soil) | [-0.5, 0.5] |
| 14 | r__SOL_K | Soil conductivity (mm/hr) | [-0.8, 0.8] |
| 15 | r__SOL_BD | Soil bulk density ($g/cm^3$) | [-0.5, 0.6] |
| 16 | v__EPCO | Plant uptake compensation factor | [0, 1] |
| 17 | v__ESCO | Soil evaporation compensation factor | [0, 1] |
| 18 | r__OV_N | Manning's n value for overland flow | [-0.2, 0] |
| 19 | r__CN2 | SCS runoff curve number for moisture condition II | [-0.3, 0.3] |
| 20 | v__CH_N2 | Manning's n value for main channel | [0, 0.3] |
| 21 | v__CH_K2 | Effective hydraulic conductivity in the main channel (mm/hr) | [0, 500] |

Note: "v" indicates the parameter value is replaced by a given value or absolute change; "r" means the parameter value is multiplied by (1± a given value) or relative change.

During calibration, the Latin Hypercube Sampling Technique within the SUFI2 algorithm generates samples of parameter sets based on the simulation number specified by the user. The samples of parameter sets can contain both realistic and unrealistic snow parameter combinations (i.e., those containing SMFMX<SMFMN) as SWATCUP does not control the relationship between various snow parameters. In this study, the parameter sets that contained unrealistic snow parameter combinations were removed, and the remaining realistic parameter sets were written into the SWATCUP files (par_val.txt and str.txt) for further calibration. R and batch scripting were used to automatically eliminate unrealistic parameter sets and perform simulations. This new automatic calibration process is referred as the modified SWATCUP hereafter to distinguish from the original one.

The workflow of this research is summarized in Figure 3.2. The CFSR, ECCC and ERA5 data were assessed by checking their magnitude, spatial patterns, and the model performance before calibration. The climate data that led to better pre-calibration result was used in the subsequent steps. Step 2 evaluates the various model calibration schemes using the original and modified SWATCUP. Step 3 compares the model performance with single-objective (streamflow) and multi-objective (SWE and streamflow) calibrations. For computational time efficiency, a parallel program developed by Du et al. (2020) was used to parallelize our simulations over multiple cores in an advanced computer.

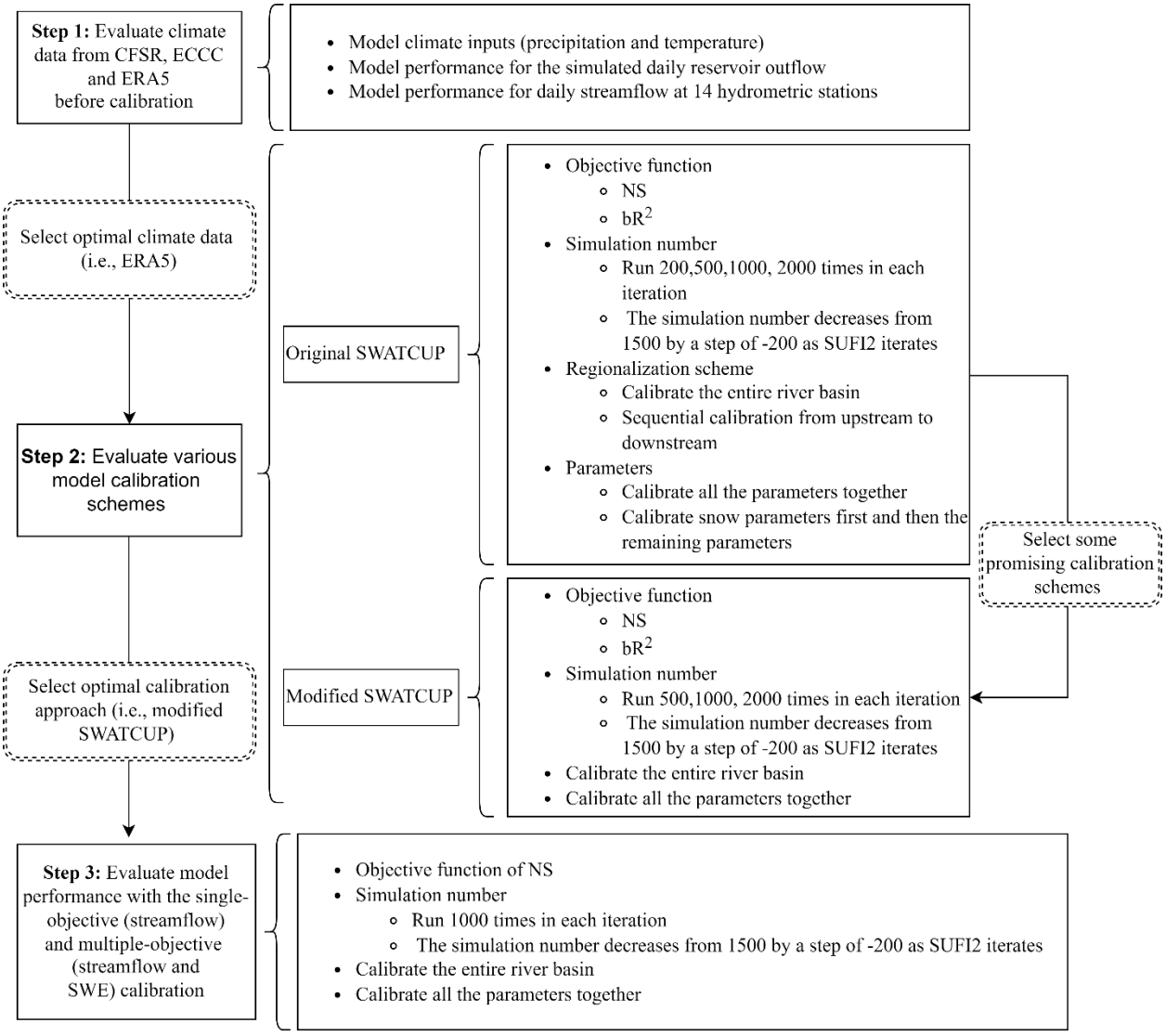


**Figure 3.2** Diagram of the methodology adopted for this study.

The model performance was evaluated using NS, coefficient of determination ($R^2$), and Percent Bias (PBIAS) (Moriasi et al., 2015). The evaluation criteria from Moriasi et al. (2015) was adapted and shown in Table 3.5.

**Table 3.5** SWAT model performance criteria for daily streamflow.

| Measure | Very Good | Good | Satisfactory | Unsatisfactory |
|---|---|---|---|---|
| $R^2$ | $R^2$>0.85 | 0.75<$R^2$<=0.85 | 0.6<$R^2$<=0.75 | $R^2$<=0.6 |
| NS | NS>0.8 | 0.7<NS<=0.8 | 0.5<NS<=0.7 | NS<=0.5 |
| PBIAS (%) | \|PBIAS\|<5 | 5<=\|PBIAS\|<10 | 10<=\|PBIAS\|<15 | \|PBIAS\|>=15 |

## 3.3 Results and discussion

### *3.3.1 Climate data evaluation*

SWAT uses the weather station closest to the centroid of each subbasin. The daily precipitation and temperature from CFSR, ECCC, and ERA5 were analyzed for modeled subbasins and displayed in Figure 3.3. Precipitation and temperature from the three sources in the western mountain regions (where observed data are sparse, see Figure 3.1) were significantly different. The average annual precipitation from gridded CFSR was larger than ECCC and ERA5, ranging from 358 to 1,762 mm per year. The observed annual mean precipitation of ECCC varied from 386 to 1,278 mm. Overall, the gridded ERA5 precipitation followed a similar pattern as the ECCC, ranging from 403 to 1,386 mm per year across the study region. The temperature difference among the three sources was not distinct in regions where there were relatively dense gauging stations. The annual average temperature of ECCC in the PRB varied from -1.8 to 3.9 ℃. The long-term average annual temperatures were lower in the gridded CFSR and ERA5 datasets than ECCC data. They varied from -4.8 to 3.6 ℃ and -4.3 to 4.2 ℃ across the basin for CFSR and ERA5, respectively. In addition,

the annual mean temperature of ECCC in the western Rocky Mountains was above zero and higher than CFSR and ERA5 data. It is probably due to very sparse ECCC stations available in the mountains, and SWAT used outlying stations for these subbasins.

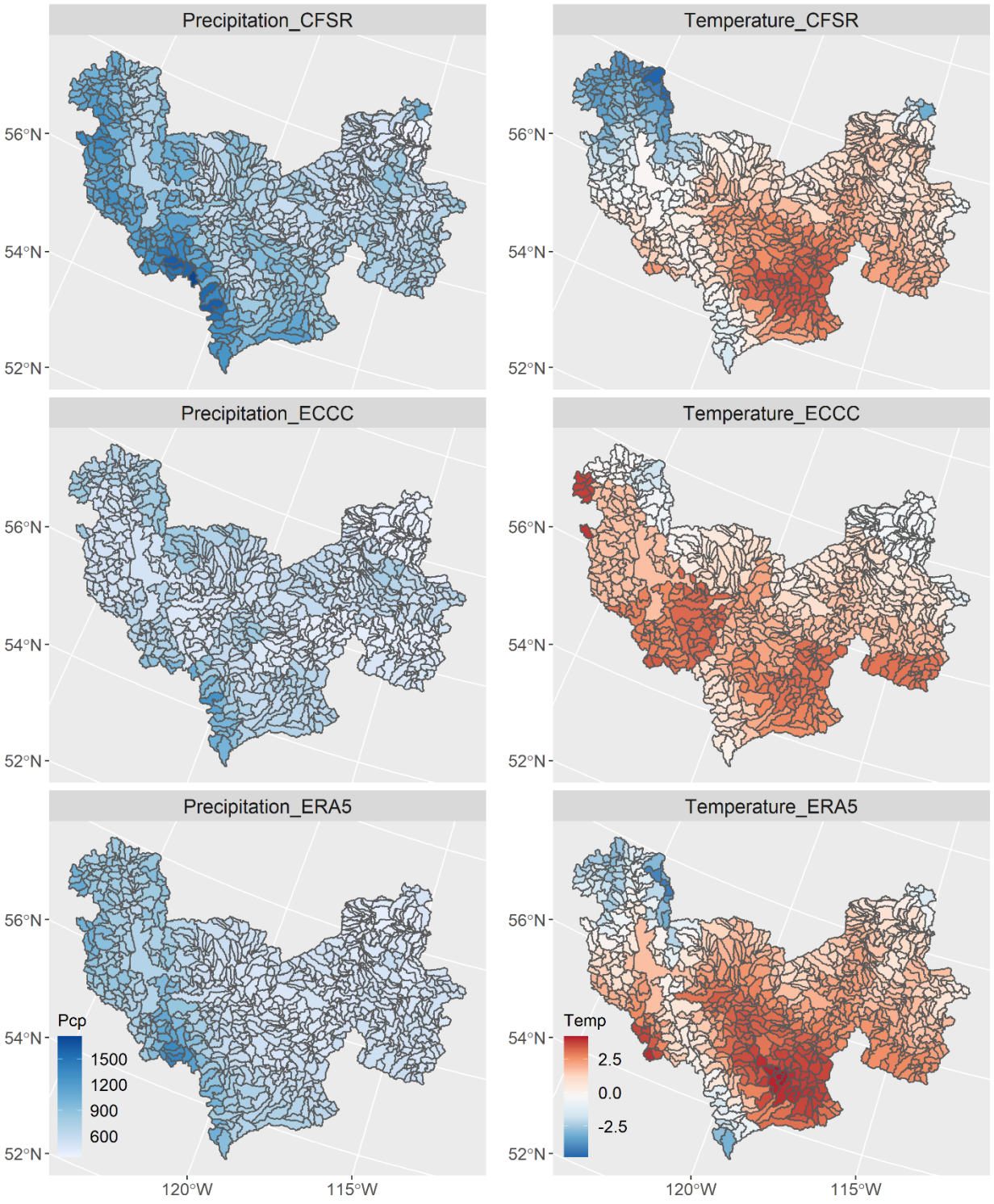


**Figure 3.3** Spatial distribution of the 10-year-average (2004-2013) annual total precipitation and mean air temperature. Note: pcp and temp indicate precipitation and temperature, respectively.

The three climate data sources were also assessed by comparing the pre-calibrated reservoir outflows (see Figure 3.4). The ERA5 data performed the best as most simulated reservoir outflow fit their measured counterparts. The ECCC data cannot generate enough runoff for the reservoir to discharge, while the CFSR data generated too much runoff exceeding the reservoir's capacity, likely due to the larger values of precipitation in this dataset.

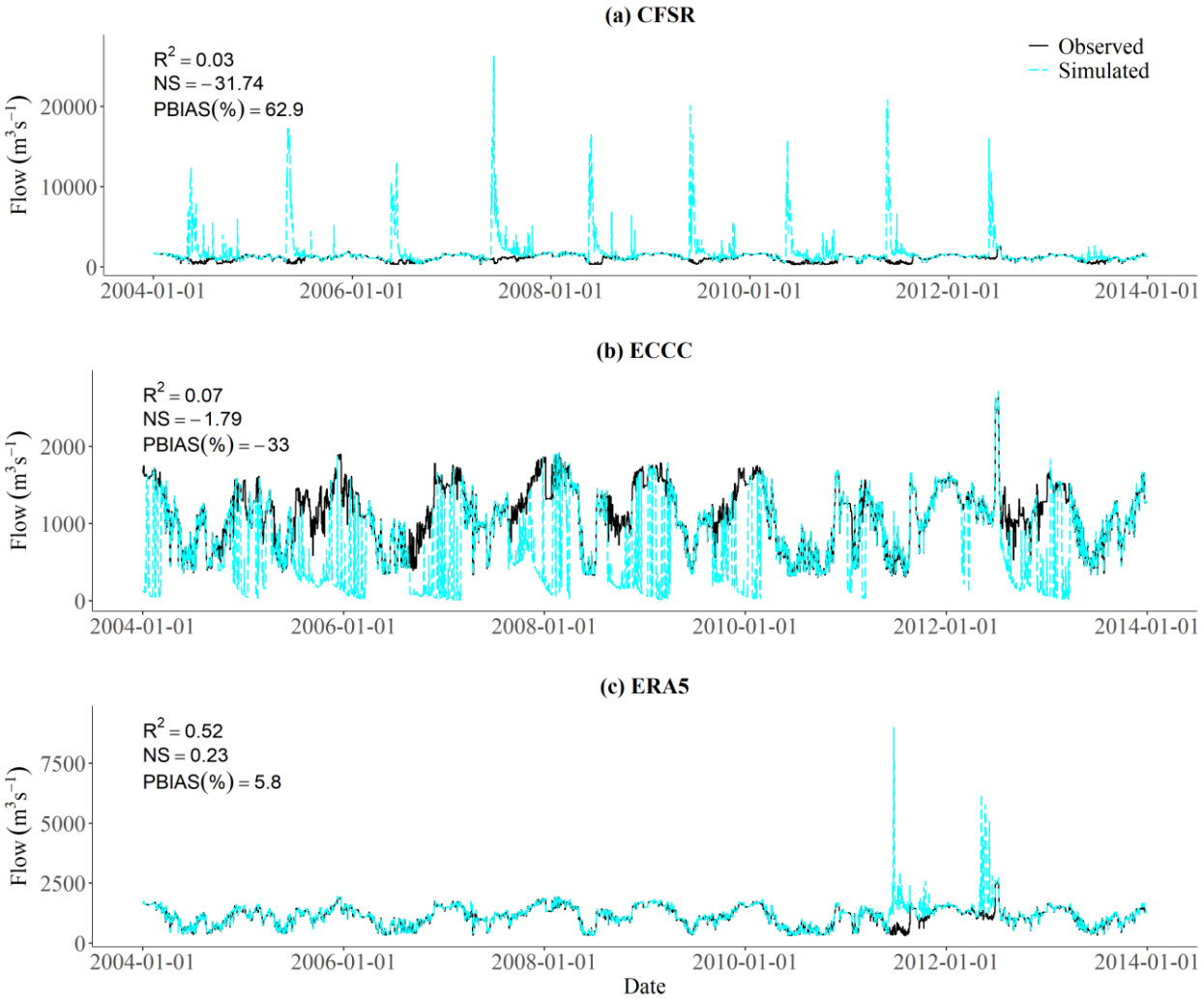


**Figure 3.4** Comparison of the observed and simulated reservoir outflow with various climate inputs.

Figure 3.5 shows the pre-calibration performance of the model based on the three climate data sources. The ERA5 data performed the best judged by any of the three efficiency criteria, i.e., $R^2$, NS, and PBIAS in the study. The CFSR data performed better when judged by $R^2$, but worse than the ECCC data according to the NS and PBIAS values. It can be seen from Figure 3.4 that using the CFSR data, the historical low flows were reproduced but the peak flows were significantly overestimated. This likely explained the acceptable $R^2$ values but significantly large negative values for NS and PBIAS. The poor performance of the CFSR data using various model efficiency criteria is likely due to its abnormally large precipitation (Faramarzi et al., 2015). In general, ERA5 climate data showed the best pre-calibration performance in driving the SWAT model simulating daily streamflow. This agrees with the findings of Tarek et al. (2020), which suggested that the lumped hydrologic model driven by the ERA5 data generally preforms well over most river basins in North America.

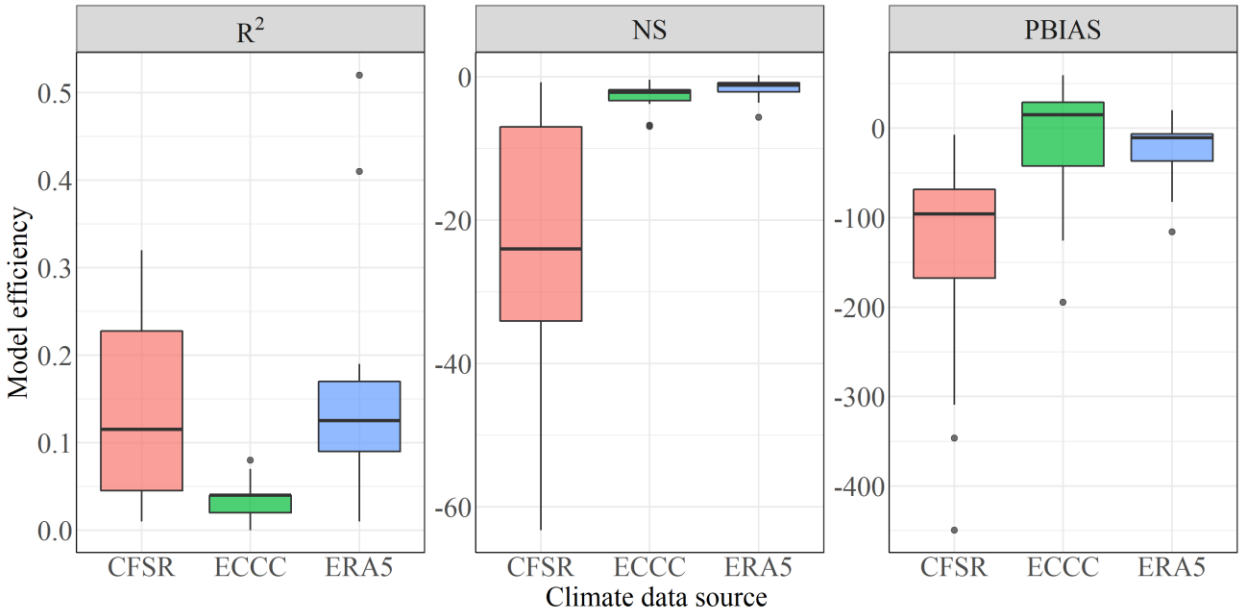


**Figure 3.5** Pre-calibration model performance of various climate data sources for daily streamflow during 2004-2013 at 14 hydrometric stations. The boxplots show model performance with $R^2$, NS, and PBIAS.

### *3.3.2 Evaluation of various model calibration schemes based on ERA5 data*

#### *3.3.2.1 Results from the original SWATCUP*

A total of 14 projects (the combinations of 2 objective functions and 7 calibration schemes, see Table 6) were built based on ERA5 climate data and calibrated using the original SWATCUP. A total of 14 projects of different calibration schemes (Table 3.6) were built based on ERA5 climate data. Figure 3.6 shows the calibration results, with the model performance evaluated by the three model efficiency criteria. The multi-site ccalibration results showed that the objective function of $bR^2$ was more sensitive to the use of various calibration schemes than NS. Calibration results based on the NS objective function were overall better than those using $bR^2$. The objective functions of NS and $R^2$ are both very sensitive to peak flows, but $R^2$ can produce very high values of streamflow for some bad model results (Krause et al., 2005). Although integrating $R^2$ with the gradient b ($bR^2$) can somewhat counteract that effect, our results showed that $bR^2$ still can produce very high values of streamflow for some poorly simulated stations. This partly explained why the objective function of NS outperformed the $bR^2$ here.

The results showed that larger number of simulations did not result in better model performance when $bR^2$ was used as the objective function (ERA5_$bR^2$ in Figure 3.6). In contrast, better model performance was achieved with more simulation numbers in each iteration when the objective function was NS (C1-C4 of ERA5_NS in Figure 3.6). C3 was an exception but its calibrated snow parameters were unreasonable with the objective function of NS (see Table 3.6). The calibration scheme C5 using NS as the objective function produced the best performance with reasonable snow parameters and smaller total number of simulations. During model calibration using SUFI2 of SWATCUP, the range of parameter set progressively reduces with more iterations. Therefore, calibrating SWAT with decreasing simulation number during the iteration process (C5) is probably

more effective than using equal number of simulations in each iteration.

The sequential calibration scheme from upstream to downstream (C6) performed well at the upstream hydrometric stations. Fixing the parameters of the upper basin and only calibrating those of the lower basin led to difficulty in simulating the downstream stations that are close to the upper basin. The overall performance of the sequential calibration was worse than that simultaneously calibrating all hydrometric stations across the entire basin (e.g., C3-C5 versus C6 of ERA5_NS in Figure 3.6). These results do not agree with Nkiaka et al. (2018), who found that sequential calibration outperformed simultaneous multi-site calibration. Apart from the different study sites, opposite results were probably due to difference of the location and number of calibrated hydrometric stations. Nkiaka et al. (2018) only used three stations to calibrate the SWAT model and they were mainly in the lower region of the watershed. A total of 14 hydrometric stations across the river basin were used for the calibration calibrated in this study. In addition, how to separate a river basin into various calibration segments may also greatly affect the model performance.

The author of SWATCUP commented that snow-related parameters (e.g., TLAPS, PLAPS, SFTMP, SMTMP, SMFMX, SMFMN, and TIMP) should not be calibrated together with other hydrological parameters because they could negatively affect the simulation results (Abbaspour et al., 2017). This was explored by C7 (Table 3.6), in which the snow-related parameters were calibrated first with fewer number of simulations (e.g., 100-300), and then fixed while calibrating the remaining parameters. Our results indicated that when examining fewer number of simulations (e.g., 300), SWATCUP generally suggested reasonable values for the snow-related parameters (SMFMX does not exceed SMFMN). In this case, the best calibrated parameter set did not contain unreasonable snow parameter combinations. However, the simulated results in the PRB based on the suggestion

from Abbaspour et al. (2017) were not satisfactory compared with other calibration schemes when NS was used as the objective function (see C7 in Figure 3.6). This was likely due to the effect of parameter interaction (Qi et al., 2016), which was not considered in this calibration scheme. C7 performed well among those calibration schemes when using the objective function $bR^2$, but the overall performance was still worse than those using the NS objective function. It was also noted that the optimal calibrated parameter sets resulting from both objective functions contained unreasonable parameter combinations (SMFMX<SMFMN) when the original SWATCUP was used (see Table 3.6). Those parameter sets may be mathematically optimal but not physically meaningful.

**Table 3.6** Calibration projects based on ERA5.

| Scenario | Objective Function | Calibration Scheme | | | | Total Simulation # | Are Par Set Reasonable? |
|---|---|---|---|---|---|---|---|
| | | ID | Calibration Stations | Calibration Parameters | Simulation Scheme | | |
| S1 | $bR^2$ | C1 | 14 streamflow stations | 21 parameters | 200*6 | 1200 | yes |
| S2 | | C2 | 14 streamflow stations | 21 parameters | 500*6 | 3000 | yes |
| S3 | | C3 | 14 streamflow stations | 21 parameters | 1000*6 | 6000 | no |
| S4 | | C4 | 14 streamflow stations | 21 parameters | 2000*6 | 12000 | yes |
| S5 | | C5 | 14 streamflow stations | 21 parameters | (1500, 500, -200) | 6000 | no |
| S6 | | C6 | 2 upstream stations + 12 downstream stations | 21 parameters | 1000*3+1000*4 | 7000 | yes |
| S7 | | C7 | 14 streamflow stations | (1) pars 6-7 (2) pars 1-5 (3) pars 8-21 | 100+300+1000*5 | 5400 | yes |
| S8 | NS | C1 | 14 streamflow stations | 21 parameters | 200*6 | 1200 | yes |
| S9 | | C2 | 14 streamflow stations | 21 parameters | 500*6 | 3000 | no |
| S10 | | C3 | 14 streamflow stations | 21 parameters | 1000*5 | 5000 | no |
| S11 | | C4 | 14 streamflow stations | 21 parameters | 2000*5 | 10000 | yes |
| S12 | | C5 | 14 streamflow stations | 21 parameters | (1500, 700, -200) | 5500 | yes |
| S13 | | C6 | 2 upstream stations + 12 downstream stations | 21 parameters | 1000*3+1000*4 | 7000 | no |
| S14 | | C7 | 14 streamflow stations | (1) pars 6-7 (2) pars 1-5 (3) pars 8-21 | 100+300+1000*5 | 5400 | yes |

Par is short for parameter; pars 6-7 indicate parameters of TLAPS and PLAPS; pars 1-5 are five snowfall parameters (SFTMP, SMTMP, SMFMX, SMFMN, and TIMP).

The title of last column denotes if the calibrated parameter set of each scenario is reasonable; if SMFMX is less than SMFMN in a calibrated parameter set, it is considered not reasonable.

$bR^2$ is an efficiency criterion defined by Krause et al. (2005) which integrates the slope of the regression line (b) and the coefficient of determination ($R^2$).

S5: use the objective function of $bR^2$, calibrate 14 stations of the watershed for all the 21 selected parameters for 5 iterations, the simulation number of each iteration decreasing from 1,500 to 500 by a step of -200.

S6: use the objective function of $bR^2$, the model is calibrated at 2 stations within the upstream river basin for 3 iterations, the simulation number of each iteration is 1,000, the 21 parameters upstream are fixed; then the model is calibrated at 12 downstream stations for 4 iterations and the simulation number of each iteration is 1,000.

S7: use the objective function of $bR^2$, simulate 100 times for the whole basin with TLAPS and PLAPS, choose the best parameter set and fix them; simulate 300 times for 5 snow parameters, choose the best parameter set and fix them; calibrate the remaining 14 parameters for 5 iterations and the simulation number of each iteration is 1,000.

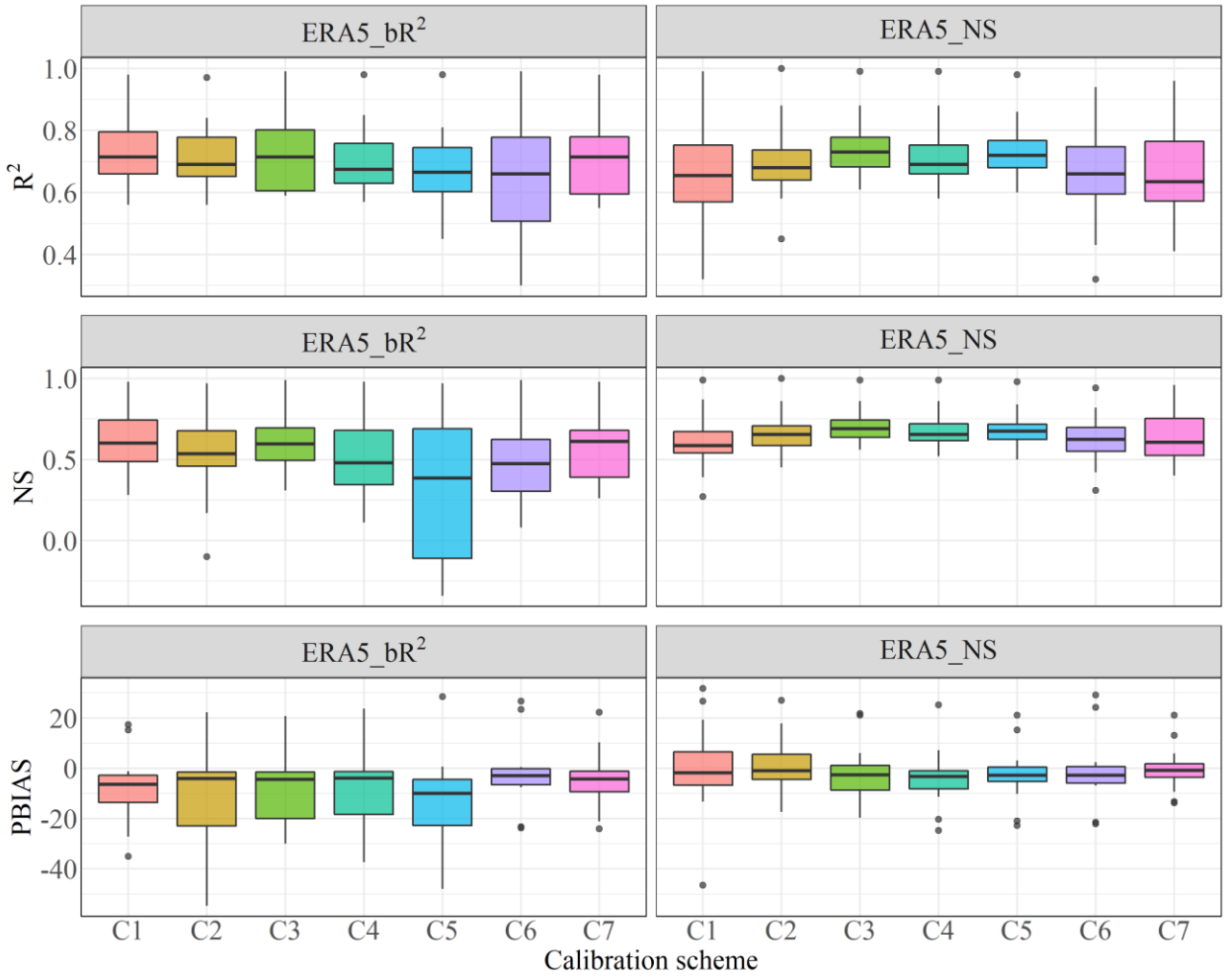


**Figure 3.6** Model performance of ERA5 data with various model calibration schemes for daily streamflow during 2004-2009 at 14 hydrometric stations. The boxplots show model performance with $R^2$, NS and PBIAS. The title of each boxplot indicates the climate data source and the objective function used during calibration.

*3.3.2.2 Results from the modified SWATCUP*

The calibration schemes C1, C6 and C7 did not show good potential based on the analysis of the results from the original SWATCUP. Therefore, only C2 to C5 were selected to evaluate the performance of the modified SWATCUP. All C2 to C5 calibration schemes (see Table 3.6) were recalibrated using the modified SWATCUP and compared with the results obtained from the

corresponding calibration schemes using the original SWATCUP (Figure 3.7). The model results of most calibration schemes using the modified SWATCUP were significantly improved after removing unreasonable snow parameter combinations. This suggested that the unreasonable snow parameter combinations can negatively affect the SUFI2 of SWATCUP, making it hard to search for the optimal parameter set while calibrating the hydrologic model. In addition, the models calibrated using NS as the objective function again outperformed those using $bR^2$ as the objective function.

The use of a smaller number of simulations (e.g., C2_2 in Figure 3.7) during calibration was more likely to cause a few poorly simulated stations. The calibration scheme with the highest number of simulations (2,000) in each iteration (C4_2) did not always give the best results. For example, model performance of C3_2, using 1,000 number of simulations in each iteration, performed better than that of C4_2 with $bR^2$ as the objective function. A possible reason is that the large number of simulations during early iterations can lead SUFI2 into local optimal (Mousavi et al., 2012). Using NS as the objective function, the C4_2 performed the best among all the calibration projects with reasonable calibrated parameters. However, C5_2 had similar performance to C4_2 but used only nearly half of the number of simulations. The total number of simulations during calibration significantly decreased with the modified SWATCUP as the unrealistic parameter combinations were automatically removed. As can be seen from Figure 3.8, a reduction of the total simulation number from 13.9% to 45.5% was seen among the four calibration schemes. This would be very efficient for large SWAT projects since it can notably save time.

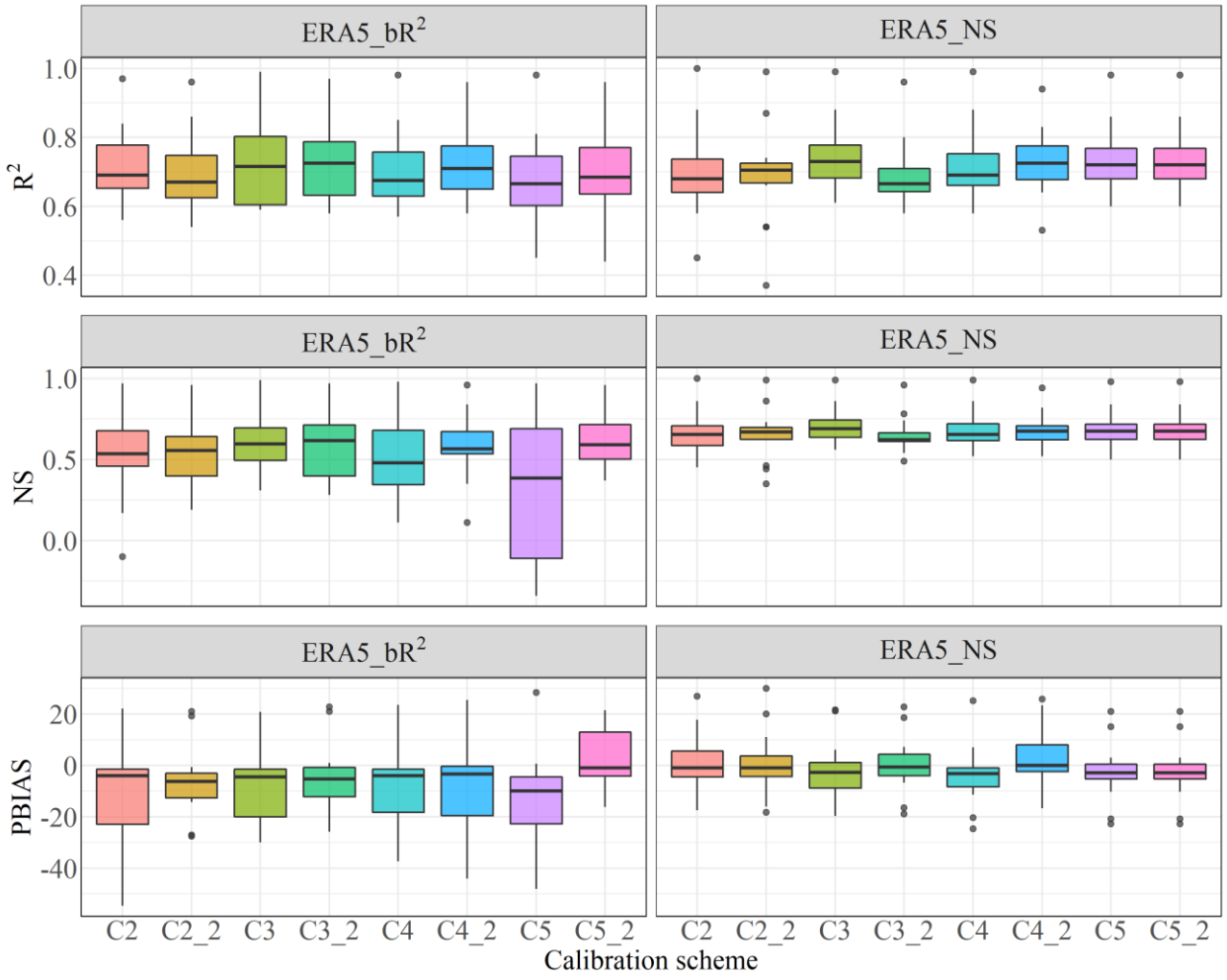


**Figure 3.7** Model performance of ERA5 data with various model calibration schemes for daily streamflow during 2004-2009 at 14 hydrometric stations using the original and modified SWATCUP. Symbols of C2_2-C5_2 refer to those calibrations conducted with the modified calibration method. The boxplots show model performance with $R^2$, NS and PBIAS. The title of each boxplot indicates the climate data source and the objective function used during calibration.

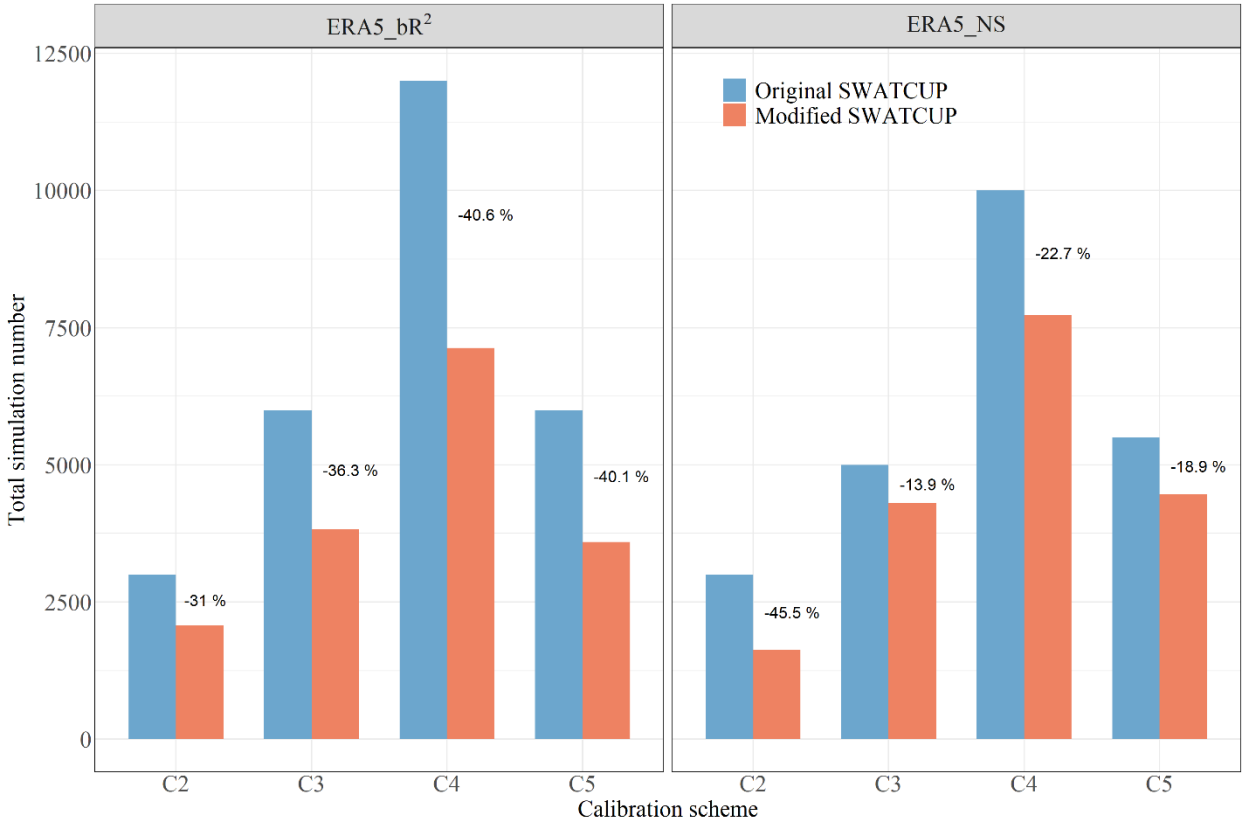


**Figure 3.8** Total number of simulations of various calibration schemes during calibration using the original and modified SWATCUP. The numbers above the bars show the percent change of the total number of simulations resulting from the modified SWATCUP compared with the original SWATCUP. The title of each bar plot indicates the climate data source used for modeling and the objective function used during calibration.

### *3.3.3 Model performance with single-objective and multi-objective calibration*

The modified SWATCUP with the objective function of NS was used to evaluate the model performance with single-objective (streamflow only) and multi-objective (streamflow and SWE) calibration. The calibration scheme C3 is often used in SWATCUP while C5 showed good potential in single-objective calibration (see details of C3 and C5 in Table 3.6). Therefore, the calibration schemes of C3 and C5 were further examined in multi-objective calibration. 14 stations were

calibrated for the single objective (streamflow), while 28 stations (14 stations of streamflow and 14 stations of SWE) were calibrated for the multi-objective calibration. Each station was given equal weight during the calibrations. The model results for both the calibration and the validation periods are shown in Table 3.7. The calibration scheme C5 used decreasing number of simulations during the iteration process. This calibration scheme performed better than when using the same number of simulations in each iteration (calibration scheme C3) for the single-objective calibration (P3) during the calibration and validation periods, but this was not the case in the multi-objective calibration (P3multi). Nonetheless, both calibration schemes can provide satisfactory performance for the single and multi-objective calibration. Given that the same calibration scheme could perform differently with the single and multi-objective calibration, it is advisable to use at least two calibration schemes (e.g., C3 and C5) in order to get more optimal result.

Figure 3.9 compares the subbasin SWE from the single and multi-objective calibration during the calibration and validation periods. It can be seen that the simulated SWE of multi-objective calibration matched well with the observed SWE at most stations as compared to using single-objective calibration. To further explore the significance of using multi-objective calibration with both streamflow and SWE, the observed and simulated spring streamflow of two mainstream hydrometric stations in 2007 (in the calibration period) and 2013 (in the validation period) are shown in Figure 3.10. The multi-objective calibration with the calibration scheme of either C3 or C5 had similar performance, and thus the calibration scheme C3 was selected to compare the spring flow simulated by the single-objective and multi-objective calibrations. It can be seen that the simulated spring streamflow (primarily the rising limb) based on the multi-objective calibration performed much better than using the single objective calibration during the calibration period. During the validation period, the multi-objective calibration model accurately simulated the rising

limb of spring flow, but underestimated the peaks. Without the constraint of SWE, the single-objective calibration tried to match the spring peak flow through magnifying the SWE and delaying the time of snow melting (see Figure 3.9). However, the simulated start of the spring freshet was significantly later than the observed for both the calibration and the validation periods. Moreover, it significantly overestimated the peak flow during the validation period (Figure 3.10).

In a snow-dominated river basin like the PRB, snow is vital in contributing to the streamflow, especially to the spring freshet. The calibrated parameters from single-objective (streamflow) cannot not properly represent the actual snow process, and thus cannot accurately simulate snow affected spring streamflow. Calibrating SWE together with streamflow can limit the uncertainty of snow-related parameters, and produce more reasonable parameter sets. Consequently, the spring streamflow simulated by multi-objective calibration notably outperformed that using single-objective calibration.

The poorer performance of simulating spring peak flow was likely due to uncertainties and/or errors in data source and model structure. The precipitation, temperature and SWE were from ERA5 reanalysis data. Although they have a good potential to replace the observations, deviations from real values still exist. Most of the streamflow is derived from the mountain headwaters of the Peace River, where the data errors can be more significant due to station scarcity in the mountainous regions. In addition, the method used to calculate the subbasin SWE was not very accurate because the snow is not evenly distributed in each subbasin, especially those in the mountainous regions. Peace River generally experiences spring peak flow during the river ice breakup period (late April to early May). For example, ice jam events were reported in major tributary (Smoky River) in late April 2013 and main reach (Fort Vermilion) in early May 2013 (Alberta Environment and Parks Peace River Ice Observation Reports 2013), which resulted in

spring peak flow combined with snow melting. However, river ice breakup effects are not appropriately accounted for in the routing process of SWAT. These issues above all increase the uncertainties and difficulties of accurately modelling the spring peak flow. The poor prediction of spring streamflow in the PRB was also noted by Toth et al. (2006) who attributed it to the inherent difficulties of hydrologic modelling of the complex snowmelt related physical processes. The underestimation of high streamflow due to snowmelt by the SWAT model was also noted by Tuo et al. (2018b) in the alpine catchments though they mainly ascribed it to the effects of river damming. This study showed the significance of including SWE as an additional calibration objective when simulating spring streamflow in snow-dominated river basins.

**Table 3.7** Model performance of calibration (2004-2009) and validation (2010-2013) periods at 14 hydrometric stations.

| Calibration Scheme | Station Number | P3 | | | | | | P3multi | | | | | |
|---|---|---|---|---|---|---|---|---|---|---|---|---|---|
| | | Calibration Period | | | Validation Period | | | Calibration Period | | | Validation Period | | |
| | | $R^2$ | NS | PBIAS (%) | $R^2$ | NS | PBIAS (%) | $R^2$ | NS | PBIAS (%) | $R^2$ | NS | PBIAS (%) |
| C3 | 07HF001 | 0.66 | 0.61 | -6.7 | 0.68 | 0.66 | -6.6 | 0.82 | 0.8 | -3.8 | 0.78 | 0.77 | -0.1 |
| | 07JD002 | 0.59 | 0.54 | 22.8 | 0.66 | 0.63 | 7.9 | 0.73 | 0.66 | 32.9 | 0.87 | 0.75 | 37.2 |
| | 07EF001 | 0.96 | 0.96 | -0.6 | 0.99 | 0.99 | -1.3 | 0.99 | 0.99 | -1 | 0.96 | 0.96 | -0.7 |
| | 07FA004 | 0.8 | 0.78 | -3.8 | 0.85 | 0.85 | -2 | 0.88 | 0.87 | -3.3 | 0.86 | 0.86 | 0 |
| | 07FD002 | 0.69 | 0.65 | -4.1 | 0.83 | 0.82 | -2.7 | 0.64 | 0.59 | -4 | 0.79 | 0.79 | -1.2 |
| | 07FC001 | 0.63 | 0.62 | 7.3 | 0.46 | 0.46 | -2.1 | 0.4 | 0.38 | 9.4 | 0.51 | 0.48 | 13.8 |
| | 07FD010 | 0.67 | 0.61 | -0.5 | 0.76 | 0.76 | 0.1 | 0.62 | 0.52 | -0.2 | 0.75 | 0.73 | 2.7 |
| | 07FB001 | 0.77 | 0.74 | 5.3 | 0.87 | 0.83 | 1.8 | 0.57 | 0.56 | 2.3 | 0.76 | 0.72 | 2.1 |
| | 07EE007 | 0.71 | 0.59 | 18.6 | 0.78 | 0.57 | 24.7 | 0.68 | 0.55 | 17.9 | 0.74 | 0.57 | 22 |
| | 07HA001 | 0.65 | 0.64 | -2.7 | 0.69 | 0.69 | 0 | 0.72 | 0.72 | -1.1 | 0.79 | 0.77 | 4.6 |
| | 07FD003 | 0.65 | 0.61 | -0.8 | 0.72 | 0.71 | 5.3 | 0.63 | 0.58 | 0.6 | 0.73 | 0.68 | 8.6 |
| | 07GJ001 | 0.71 | 0.67 | -16.5 | 0.75 | 0.72 | -17 | 0.86 | 0.85 | -10.6 | 0.87 | 0.87 | -6.5 |
| | 07GH002 | 0.58 | 0.49 | 1.2 | 0.5 | 0.49 | -6.8 | 0.58 | 0.56 | -1.4 | 0.52 | 0.5 | 4.2 |
| | 07GE001 | 0.64 | 0.62 | -18.9 | 0.72 | 0.67 | -29.2 | 0.73 | 0.72 | -16.2 | 0.8 | 0.77 | -23 |
| | Average | 0.69 | 0.65 | / | 0.73 | 0.70 | / | 0.70 | 0.67 | / | 0.77 | 0.73 | / |
| | Nr. of satisfactory stations | 12 | 13 | 10 | 12 | 12 | 11 | 11 | 13 | 11 | 12 | 13 | 11 |
| C5 | 07HF001 | 0.71 | 0.62 | -10.2 | 0.65 | 0.61 | -9.7 | 0.73 | 0.6 | -14.1 | 0.72 | 0.66 | -13.4 |
| | 07JD002 | 0.6 | 0.54 | 15.1 | 0.62 | 0.54 | 0.6 | 0.71 | 0.67 | 9.2 | 0.84 | 0.82 | -13.7 |
| | 07EF001 | 0.98 | 0.98 | -0.8 | 0.99 | 0.99 | -1.3 | 0.98 | 0.98 | -0.9 | 0.96 | 0.96 | -1.1 |
| | 07FA004 | 0.86 | 0.84 | -4.4 | 0.88 | 0.88 | -1.9 | 0.88 | 0.87 | -3.8 | 0.85 | 0.85 | -1.2 |
| | 07FD002 | 0.73 | 0.67 | -5.1 | 0.86 | 0.85 | -2.8 | 0.67 | 0.62 | -4.6 | 0.8 | 0.79 | -2.9 |
| | 07FC001 | 0.62 | 0.58 | -2.8 | 0.55 | 0.52 | -17.2 | 0.44 | 0.37 | -40 | 0.38 | 0.27 | -63.2 |
| | 07FD010 | 0.72 | 0.65 | -1.9 | 0.79 | 0.79 | -1 | 0.61 | 0.54 | -2.9 | 0.73 | 0.72 | -1.9 |

| | | | | | | | | | | | | | |
|---|---|---|---|---|---|---|---|---|---|---|---|---|---|
| | 07FB001 | 0.81 | 0.81 | 3.1 | 0.9 | 0.89 | 0.2 | 0.69 | 0.65 | 2.1 | 0.81 | 0.74 | 1.4 |
| | 07EE007 | 0.72 | 0.68 | 21 | 0.77 | 0.71 | 21.2 | 0.67 | 0.51 | 17.4 | 0.77 | 0.59 | 22.2 |
| | 07HA001 | 0.72 | 0.7 | -5.3 | 0.72 | 0.72 | -1.6 | 0.61 | 0.56 | -8.3 | 0.72 | 0.7 | -5.3 |
| | 07FD003 | 0.67 | 0.63 | -2.9 | 0.73 | 0.72 | 3.6 | 0.56 | 0.48 | -4 | 0.67 | 0.66 | 1.9 |
| | 07GJ001 | 0.78 | 0.72 | -20.9 | 0.79 | 0.77 | -16.6 | 0.74 | 0.69 | -26.2 | 0.82 | 0.78 | -23.4 |
| | 07GH002 | 0.67 | 0.5 | 0.9 | 0.44 | 0.37 | 3.3 | 0.57 | 0.44 | -24.5 | 0.38 | 0.32 | -14.4 |
| | 07GE001 | 0.73 | 0.71 | -22.7 | 0.81 | 0.76 | -30.8 | 0.71 | 0.66 | -25.6 | 0.77 | 0.72 | -34 |
| | Average | 0.74 | 0.69 | / | 0.75 | 0.72 | / | 0.68 | 0.62 | / | 0.73 | 0.68 | / |
| | Nr. of satisfactory stations | 14 | 14 | 10 | 12 | 13 | 10 | 11 | 11 | 9 | 12 | 12 | 10 |

The calibration scheme C5 is calibrated with the simulation number in a decreasing order during the iteration process (from 1,500 to 700 by -200) while the C3 has the same simulation number (1,000) of each iteration; P3 indicates the model is calibrated with streamflow while streamflow and SWE are both used to calibrate the model for P3multi; No. of satisfactory stations indicates the number of hydrometric stations that at least are rated as satisfactory (see the criteria in Table 3.5); The precipitation and temperature inputs for these projects are all from the ERA5 data; Here, only streamflow simulation results were shown for P3multi in order to compare with P3.

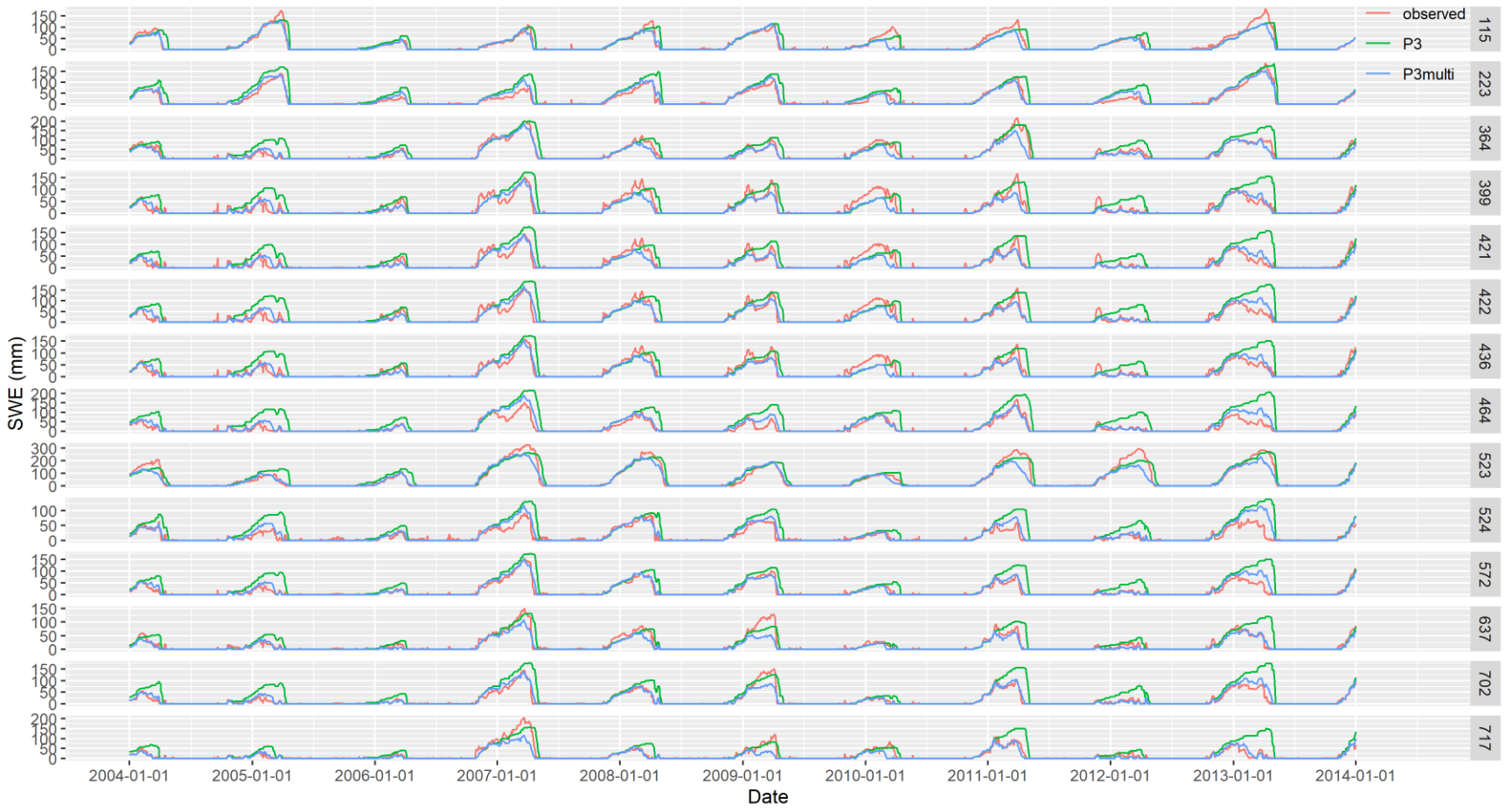


**Figure 3.9** Observed and simulated daily SWE at 14 stations (the right title indicates the subbasin that each station locates) during calibration and validation periods.

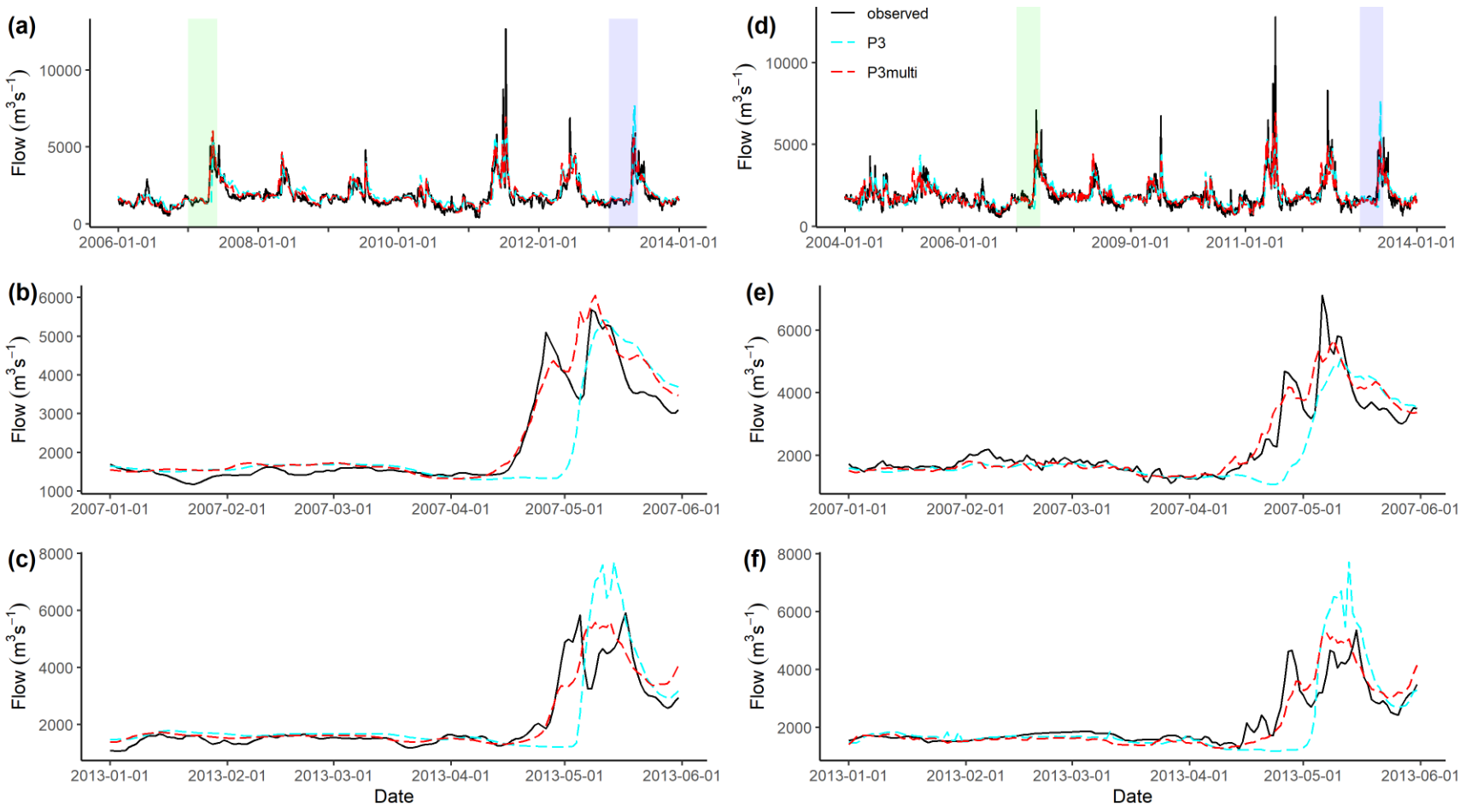


**Figure 3.10** Observed and simulated daily streamflow for two selected hydrometric stations, Peace River at Fort Vermilion (a) and Peace River at Peace River (d); Streamflow in 2007 (b & e) and in 2013 (c & f) were enlarged to display the spring streamflow during calibration and validation periods.

## 3.4 Conclusion

This study quantitatively assessed the uncertainties in various climate data sources (ECCC, CFSR and ERA5) and calibration schemes based on the semi-distributed hydrologic model SWAT. Assessment of the model performance using daily discharge data at 14 hydrometric stations and at the outlet of the reservoir in the study region showed that the gridded ERA5 precipitation and temperature data performed the best among these three data sources and can be used to drive the SWAT in simulating daily streamflow in the Peace River Basin. 14 calibration projects were built and calibrated to investigate the impacts of the objective function (NS and $bR^2$) and the simulation number of each iteration based on the SUFI2 of SWATCUP. The objective function of $bR^2$ had greater uncertainty than NS in guiding the SUFI2 to search for the best parameter set. It was found that the objective function of NS had overall better performance than the $bR^2$ during calibration as the objective function $bR^2$ can produce too high peak flow at some poorly simulated stations in multi-site calibration. Therefore, the objective function of NS is recommended to use in SUFI2 of SWATCUP. The number of simulations during calibration iterations had a notable influence on the model performance. Lower number of simulations in each iteration (such as 200 and 500) could lead to significant uncertainty, while larger number of model runs (e.g., 2,000) could lead to local optimal. The new calibration scheme using decreasing number of simulations (e.g., from 1,500 to 500 by -200) was shown to have good potential in calibrating the streamflow.

Sequential calibration from upstream to downstream did not improve the model performance as expected and could lead to worse performance than calibrating the river basin as a whole.

Calibrating the snow-related parameters separately from the other parameters did not perform well in comparison with calibrating all parameters together when the objective function of NS was used. This calibration scheme may have avoided unrealistic snow parameter combinations, but it was difficult to get an optimal model performance likely because parameter interactions were not accounted for. A modified SUFI2 of SWATCUP approach was developed to automatically remove the unrealistic snow parameter combinations generated by SWATCUP. The modified tool showed improved performance than the original SUFI2-SWATCUP under various calibration schemes, and was more computationally efficient as it greatly reduced the number of simulations.

To limit model equifinality and parameter uncertainty, multi-objective calibration (streamflow and SWE) was applied and compared with single-objective calibration. Modification of SWAT was done to automatically calibrate subbasin SWE and streamflow using SWATCUP, providing an efficient tool for calibrating large-scale SWAT models in snow-dominated regions. It was found that the multi-objective calibration better limited the parameter uncertainties and improved the reliability and robustness of the hydrologic model in simulating future streamflow. Simulation of the snow process was improved due to the additional calibration variable of SWE. Consequently, the simulated spring streamflow affected by snowmelt was in better agreement with the observed data. In addition, various calibration schemes (e.g., the choice of the simulation number) was shown to have significantly different performance in single-objective and multi-objective calibrations. It is therefore suggested to try at least two calibration schemes in calibrating a hydrologic model to find more optimal result. The work presented in this paper is expected to

contribute to water resources planning and management in the Peace River Basin, and provide insights for researchers on modelling and calibrating large-scale snow-dominated river basins. Future studies should focus on further improving the simulation of spring peak flow affected by snowmelt and river ice breakup.

## 3.5 Reference

Abbaspour, K.C., 2015. SWAT Calibration and Uncertainty Programs—A User Manual. Swiss Fed. Inst. Aquat. Sci. Technol. Eawag, Switz.

Abbaspour, K.C., Rouholahnejad, E., Vaghefi, S., Srinivasan, R., Yang, H., Kløve, B., 2015. A continental-scale hydrology and water quality model for Europe: Calibration and uncertainty of a high-resolution large-scale SWAT model. J. Hydrol. 524, 733–752. https://doi.org/10.1016/j.jhydrol.2015.03.027

Abbaspour, K.C., Vaghefi, S.A., Srinivasan, R., 2017. A guideline for successful calibration and uncertainty analysis for soil and water assessment: A review of papers from the 2016 international SWAT conference. Water (Switzerland) 10. https://doi.org/10.3390/w10010006

Abbaspour, K.C., Yang, J., Maximov, I., Siber, R., Bogner, K., Mieleitner, J., Zobrist, J., Srinivasan, R., 2007. Modelling hydrology and water quality in the pre-alpine/alpine Thur watershed using SWAT. J. Hydrol. 333, 413–430. https://doi.org/10.1016/j.jhydrol.2006.09.014

Anand, J., Gosain, A.K., Khosa, R., Srinivasan, R., 2018. Regional scale hydrologic modeling for prediction of water balance, analysis of trends in streamflow and variations in streamflow: The case study of the Ganga River basin. J. Hydrol. Reg. Stud. 16, 32–53. https://doi.org/10.1016/j.ejrh.2018.02.007

Arnold, J.G., Srinivasan, R., Muttiah, R.S., Williams, J.R., 1998. Large area hydrologic modeling and assesment Part I: Model development. JAWRA J. Am. Water Resour. Assoc. 34, 73–89.

https://doi.org/10.1111/j.1752-1688.1998.tb05961.x

Arsenault, R., Poulin, A., Côté, P., Brissette, F., 2014. Comparison of Stochastic Optimization Algorithms in Hydrological Model Calibration. J. Hydrol. Eng. 19, 1374–1384. https://doi.org/10.1061/(asce)he.1943-5584.0000938

Beven, K., 2006. A Manifesto for the Equifinality Thesis Keith Beven Lancaster University, UK. J. Hydrol. 320, 18–36.

Beven, K., Binley, A., 2014. GLUE: 20 years on. Hydrol. Process. 28, 5897–5918. https://doi.org/10.1002/hyp.10082

Beven, K.J., 2000. Uniqueness of place and process representations in hydrological modelling. Hydrol. Earth Syst. Sci. https://doi.org/10.5194/hess-4-203-2000

Cao, W., Bowden, W.B., Davie, T., Fenemor, A., 2006. Multi-variable and multi-site calibration and validation of SWAT in a large mountainous catchment with high spatial variability. Hydrol. Process. 20, 1057–1073. https://doi.org/10.1002/hyp.5933

Champagne, O., Arain, M.A., Wang, S., Leduc, M., Russell, H.A.J., 2021. Interdecadal variability of streamflow in the Hudson Bay Lowlands watersheds driven by atmospheric circulation. J. Hydrol. Reg. Stud. 36, 100868. https://doi.org/10.1016/j.ejrh.2021.100868

Cordeiro, M.R.C., Lelyk, G., Kröbel, R., Legesse, G., Faramarzi, M., Masud, M.B., McAllister, T., 2017. Deriving a country-wide soils dataset from the Soil Landscapes of Canada (SLC)

database for use in Soil and Water Assessment Tool (SWAT) simulations. Earth Syst. Sci. Data Discuss. 1–30. https://doi.org/10.1594/PANGAEA.877298.KEY

Dile, Y.T., Srinivasan, R., 2014. Evaluation of CFSR climate data for hydrologic prediction in data-scarce watersheds: An application in the blue nile river basin. J. Am. Water Resour. Assoc. 50, 1226–1241. https://doi.org/10.1111/jawr.12182

Du, X., Loiselle, D., Alessi, D.S., Faramarzi, M., 2020. Hydro-climate and biogeochemical processes control watershed organic carbon inflows: Development of an in-stream organic carbon module coupled with a process-based hydrologic model. Sci. Total Environ. 718, 137281. https://doi.org/10.1016/j.scitotenv.2020.137281

Faramarzi, M., Abbaspour, K.C., Adamowicz, W.L.V., Lu, W., Fennell, J., Zehnder, A.J.B., Goss, G.G., 2017. Uncertainty based assessment of dynamic freshwater scarcity in semi-arid watersheds of Alberta, Canada. J. Hydrol. Reg. Stud. 9, 48–68. https://doi.org/10.1016/j.ejrh.2016.11.003

Faramarzi, M., Srinivasan, R., Iravani, M., Bladon, K.D., Abbaspour, K.C., Zehnder, A.J.B., Goss, G.G., 2015. Setting up a hydrological model of Alberta: Data discrimination analyses prior to calibration. Environ. Model. Softw. 74, 48–65. https://doi.org/10.1016/j.envsoft.2015.09.006

Ficklin, D.L., Barnhart, B.L., 2014. SWAT hydrologic model parameter uncertainty and its implications for hydroclimatic projections in snowmelt-dependent watersheds. J. Hydrol. 519, 2081–2090. https://doi.org/10.1016/j.jhydrol.2014.09.082

Ficklin, D.L., Luo, Y., Stewart, I.T., Maurer, E.P., 2012. Development and application of a hydroclimatological stream temperature model within the Soil and Water Assessment Tool. Water Resour. Res. 48, 1–16. https://doi.org/10.1029/2011WR011256

Fischer, G., Nachtergaele, F., Prieler, S., Van Velthuizen, H.T., Verelst, L., Wiberg, D., 2008. Global agro-ecological zones assessment for agriculture (GAEZ 2008). IIASA, Laxenburg, Austria FAO, Rome, Italy 10.

Gizaw, M.S., Biftu, G.F., Gan, T.Y., Moges, S.A., Koivusalo, H., 2017. Potential impact of climate change on streamflow of major Ethiopian rivers. Clim. Change 143, 371–383. https://doi.org/10.1007/s10584-017-2021-1

Grusson, Y., Sun, X., Gascoin, S., Sauvage, S., Raghavan, S., Anctil, F., Sáchez-Pérez, J.M., 2015. Assessing the capability of the SWAT model to simulate snow, snow melt and streamflow dynamics over an alpine watershed. J. Hydrol. 531, 574–588. https://doi.org/10.1016/j.jhydrol.2015.10.070

Ha, L.T., Bastiaanssen, W.G.M., van Griensven, A., van Dijk, A.I.J.M., Senay, G.B., 2017. SWAT-CUP for Calibration of Spatially Distributed Hydrological Processes and Ecosystem Services in a Vietnamese River Basin Using Remote Sensing. Hydrol. Earth Syst. Sci. Discuss. 1–35. https://doi.org/10.5194/hess-2017-251

Hanzer, F., Helfricht, K., Marke, T., Strasser, U., 2016. Multilevel spatiotemporal validation of snow/ice mass balance and runoff modeling in glacierized catchments. Cryosphere 10, 1859–

1881. https://doi.org/10.5194/tc-10-1859-2016

Her, Y., Seong, C., 2018. Responses of hydrological model equifinality, uncertainty, and performance to multi-objective parameter calibration. J. Hydroinformatics 20, 864–885. https://doi.org/10.2166/hydro.2018.108

Hersbach, H., Bell, B., Berrisford, P., Hirahara, S., Horányi, A., Muñoz-Sabater, J., Nicolas, J., Peubey, C., Radu, R., Schepers, D., Simmons, A., Soci, C., Abdalla, S., Abellan, X., Balsamo, G., Bechtold, P., Biavati, G., Bidlot, J., Bonavita, M., De Chiara, G., Dahlgren, P., Dee, D., Diamantakis, M., Dragani, R., Flemming, J., Forbes, R., Fuentes, M., Geer, A., Haimberger, L., Healy, S., Hogan, R.J., Hólm, E., Janisková, M., Keeley, S., Laloyaux, P., Lopez, P., Lupu, C., Radnoti, G., de Rosnay, P., Rozum, I., Vamborg, F., Villaume, S., Thépaut, J.N., 2020. The ERA5 global reanalysis. Q. J. R. Meteorol. Soc. 146, 1999–2049. https://doi.org/10.1002/qj.3803

Jarvis, A., Reuter, H.I., Nelson, A., Guevara, E., 2008. Hole-filled SRTM for the globe Version 4. available from CGIAR-CSI SRTM 90m Database (http//srtm. csi. cgiar. org) 15, 25–54.

Kouchi, D.H., Esmaili, K., Faridhosseini, A., Sanaeinejad, S.H., Khalili, D., Abbaspour, K.C., 2017. Sensitivity of calibrated parameters and water resource estimates on different objective functions and optimization algorithms. Water (Switzerland) 9, 1–16. https://doi.org/10.3390/w9060384

Krause, P., Boyle, D.P., Bäse, F., 2005. Comparison of different efficiency criteria for hydrological

model assessment. Adv. Geosci. 5, 89–97. https://doi.org/10.5194/adgeo-5-89-2005

Liu, Z., Yin, J., E Dahlke, H., 2020. Enhancing Soil and Water Assessment Tool Snow Prediction Reliability with Remote-Sensing-Based Snow Water Equivalent Reconstruction Product for Upland Watersheds in a Multi-Objective Calibration Process. Water 12, 3190.

Loiselle, D., Du, X., Alessi, D.S., Bladon, K.D., Faramarzi, M., 2020. Projecting impacts of wildfire and climate change on streamflow, sediment, and organic carbon yields in a forested watershed. J. Hydrol. 590, 125403. https://doi.org/10.1016/j.jhydrol.2020.125403

McKenney, D.W., Hutchinson, M.F., Papadopol, P., Lawrence, K., Pedlar, J., Campbell, K., Milewska, E., Hopkinson, R.F., Price, D., Owen, T., 2011. Customized spatial climate models for North America. Bull. Am. Meteorol. Soc. 92, 1611–1622.

Molina-Navarro, E., Andersen, H.E., Nielsen, A., Thodsen, H., Trolle, D., 2017. The impact of the objective function in multi-site and multi-variable calibration of the SWAT model. Environ. Model. Softw. 93, 255–267. https://doi.org/10.1016/j.envsoft.2017.03.018

Moriasi, D.N., Gitau, M.W., Pai, N., Daggupati, P., 2015. Hydrologic and water quality models: Performance measures and evaluation criteria. Trans. ASABE 58, 1763–1785. https://doi.org/10.13031/trans.58.10715

Mousavi, S.J., Kamali, B., Abbaspour, K.C., Amini, M., Yang, H., 2012. Uncertainty-based automatic calibration of HEC-HMS model using sequential uncertainty fitting approach. J.

Hydroinformatics 14, 286–309. https://doi.org/10.2166/hydro.2011.071

Muleta, M.K., 2012. Model Performance Sensitivity to Objective Function during Automated Calibrations. J. Hydrol. Eng. 17, 756–767. https://doi.org/10.1061/(asce)he.1943-5584.0000497

Musau, J., Sang, J., Gathenya, J., Luedeling, E., 2015. Hydrological responses to climate change in Mt. Elgon watersheds. J. Hydrol. Reg. Stud. 3, 233–246. https://doi.org/10.1016/j.ejrh.2014.12.001

Neitsch, S.., Arnold, J.., Kiniry, J.., Williams, J.., 2011. Soil & Water Assessment Tool Theoretical Documentation Version 2009. Texas Water Resour. Inst. 1–647. https://doi.org/10.1016/j.scitotenv.2015.11.063

Neupane, R.P., Adamowski, J.F., White, J.D., Kumar, S., 2018. Future streamflow simulation in a snow-dominated rocky mountain headwater catchment. Hydrol. Res. 49, 1172–1190. https://doi.org/10.2166/nh.2017.024

Nkiaka, E., Nawaz, N.R., Lovett, J.C., 2018. Effect of single and multi-site calibration techniques on hydrological model performance, parameter estimation and predictive uncertainty: a case study in the Logone catchment, Lake Chad basin. Stoch. Environ. Res. Risk Assess. 32, 1665–1682. https://doi.org/10.1007/s00477-017-1466-0

Peker, I.B., Sorman, A.A., 2021. Application of SWAT using snow data and detecting climate

change impacts in the mountainous eastern regions of Turkey. Water (Switzerland) 13. https://doi.org/10.3390/w13141982

Pomeroy, J.W., Gray, D.M., Brown, T., Hedstrom, N.R., Quinton, W.L., Granger, R.J., Carey, S.K., 2007. The cold regions hydrological model: a platform for basing process representation and model structure on physical evidence. Hydrol. Process. 21, 2650–2667.

Puertes, C., Lidón, A., Echeverría, C., Bautista, I., González-Sanchis, M., del Campo, A.D., Francés, F., 2019. Explaining the hydrological behaviour of facultative phreatophytes using a multi-variable and multi-objective modelling approach. J. Hydrol. 575, 395–407. https://doi.org/10.1016/j.jhydrol.2019.05.041

Qi, W., Zhang, C., Fu, G., Zhou, H., 2016. Quantifying dynamic sensitivity of optimization algorithm parameters to improve hydrological model calibration. J. Hydrol. 533, 213–223. https://doi.org/10.1016/j.jhydrol.2015.11.052

Rajib, M.A., Merwade, V., Yu, Z., 2016. Multi-objective calibration of a hydrologic model using spatially distributed remotely sensed/in-situ soil moisture. J. Hydrol. 536, 192–207. https://doi.org/10.1016/j.jhydrol.2016.02.037

Rientjes, T.H.M., Muthuwatta, L.P., Bos, M.G., Booij, M.J., Bhatti, H.A., 2013. Multi-variable calibration of a semi-distributed hydrological model using streamflow data and satellite-based evapotranspiration. J. Hydrol. 505, 276–290. https://doi.org/10.1016/j.jhydrol.2013.10.006

Scheepers, H., Wang, J., Gan, T.Y., Kuo, C.C., 2018. The impact of climate change on inland waterway transport: Effects of low water levels on the Mackenzie River. J. Hydrol. 566, 285–298. https://doi.org/10.1016/j.jhydrol.2018.08.059

Schuol, J., Abbaspour, K.C., Yang, H., Srinivasan, R., Zehnder, A.J.B., 2008. Modeling blue and green water availability in Africa. Water Resour. Res. 44, 1–18. https://doi.org/10.1029/2007WR006609

Sospedra-Alfonso, R., Melton, J.R., Merryfield, W.J., 2015. Effects of temperature and precipitation on snowpack variability in the Central Rocky Mountains as a function of elevation. Geophys. Res. Lett. 42, 4429–4438. https://doi.org/10.1002/2015GL063898

Tarek, M., Brissette, F.P., Arsenault, R., 2020. Evaluation of the ERA5 reanalysis as a potential reference dataset for hydrological modelling over North America. Hydrol. Earth Syst. Sci. 24, 2527–2544. https://doi.org/10.5194/hess-24-2527-2020

Toth, B., Pietroniro, A., Conly, F.M., Kouwen, N., 2006. Modelling climate change impacts in the Peace and Athabasca catchment and delta: I—hydrological model application. Hydrol. Process. An Int. J. 20, 4197–4214.

Tuo, Y., Duan, Z., Disse, M., Chiogna, G., 2016. Evaluation of precipitation input for SWAT modeling in Alpine catchment: A case study in the Adige river basin (Italy). Sci. Total Environ. 573, 66–82. https://doi.org/10.1016/j.scitotenv.2016.08.034

Tuo, Y., Marcolini, G., Disse, M., Chiogna, G., 2018a. Calibration of snow parameters in SWAT: comparison of three approaches in the Upper Adige River basin (Italy). Hydrol. Sci. J. 63, 657–678. https://doi.org/10.1080/02626667.2018.1439172

Tuo, Y., Marcolini, G., Disse, M., Chiogna, G., 2018b. A multi-objective approach to improve SWAT model calibration in alpine catchments. J. Hydrol. 559, 347–360. https://doi.org/10.1016/j.jhydrol.2018.02.055

Xiang, Y., Chen, J., Li, L., Peng, T., Yin, Z., 2021. Evaluation of eight global precipitation datasets in hydrological modeling. Remote Sens. 13, 1–20. https://doi.org/10.3390/rs13142831

Yan, B., Fang, N.F., Zhang, P.C., Shi, Z.H., 2013. Impacts of land use change on watershed streamflow and sediment yield: An assessment using hydrologic modelling and partial least squares regression. J. Hydrol. 484, 26–37. https://doi.org/10.1016/j.jhydrol.2013.01.008

Yang, J., Reichert, P., Abbaspour, K.C., Xia, J., Yang, H., 2008. Comparing uncertainty analysis techniques for a SWAT application to the Chaohe Basin in China. J. Hydrol. 358, 1–23. https://doi.org/10.1016/j.jhydrol.2008.05.012

Zaremehrjardy, M., Razavi, S., Faramarzi, M., 2021. Assessment of the cascade of uncertainty in future snow depth projections across watersheds of mountainous, foothill, and plain areas in northern latitudes. J. Hydrol. 598, 125735. https://doi.org/10.1016/j.jhydrol.2020.125735

# Chapter 4. A Hydrologic and River Ice Modeling Framework for Assessing the Impact of Ungauged Subbasins on Open Water and River Ice Breakup Peak Flow in a Large Cold-region River Basin

## 4.1 Introduction

Disastrous river floods have caused fatalities, displacement, and huge economic loss globaly (Merz et al., 2021), and it is projected that more global population will be exposed to floods in the future (Tellman et al., 2021). In addition to heavy rainfall, flood dynamics could also be driven by snowmelt and river ice processes in cold region rivers (Das et al., 2020; Mishra et al., 2022). Snow and ice are major components of the hydrological regime in northern latitudes, and their combined effects can greatly affect streamflow. During spring, significantly increased streamflow due to rapid melting of large snowpacks can result in mechanical breakup of a river ice cover (Beltaos and Prowse, 2009). Unlike a thermal breakup, during which the ice cover deteriorates in place with minimal movement, the mechanical breakup is often associated with ice jams formed by broken ice arrested by downstream intact ice cover or constrictions such as bridge piers and islands (Beltaos, 2008). Breakup ice jams can lead to fast rising water levels and cause severe flooding even at lower streamflow as compared to open water floods (Beltaos and Prowse, 2001; Burrell et al., 2021). The anuual cost of ice jam related damages in North America is nearly 300 million CAD (French, 2017).

The hydrologic and hydraulic modelling framework has been widely used for flood forecasting and risk assessment (Bonnifait et al., 2009; Grimaldi et al., 2019; W. Li et al., 2019; Nguyen et al.,

2016). Previous studies mostly focused on open water floods, while ice-induced floods are more complex and chaotic (Turcotte et al., 2019). The effects of ice should be taken into consideration in order to correctly simulate the river hydraulic conditions. A number of hydraulic models have the capability of simulating various river ice processses, herein refered as river ice models, such as River1D (Blackburn and She, 2019), CRISSP (Chen et al., 2006; Liu et al., 2006), Mike-Ice (Thériault et al., 2010), and RIVICE (Lindenschmidt, 2017). Few studies have used hydrologic model in conjunction with river ice model to assess future ice regime and ice-jam flood risk. Timalsina et al. (2013) evaluated the impact of climate change on river ice regime using the indices of water temperature, frazil ice and ice cover in a Norwegian regulated medium-scale river using Mike-Ice and the HBV hydrologic model. Lindenschmidt et al. (2019) and Das et al. (2020) used RIVICE and MESH hydrologic model for operational real-time and future ice jam flood hazard assessment and flood mapping. The focus was on the simulation of water level profiles caused by ice jams instead of peak flow during river ice breakup period. More work is needed to improve the capability of the hydrologic and river ice modelling framework for simulating snow and ice induced floods in cold-region river basins.

Many drainage basins of the world are ungauged or poorly gauged (Mishra and Coulibaly, 2009; Sivapalan, 2003; Sivapalan et al., 2003). Even for basins with a good number of well distributed gauge stations, flow from certain regions or subbasins can still be ungauged. For example, the hydrometric stations on tributaries are often located at a distance upstream the confluence to the mainstream, and thus the streamflow from the area between the hydrometric station and the

confluence is ungauged. Some catchments or subbasins in a river basin are often not gauged as they only have significant flows during flood periods. The total ungauged subbasins usually take a large portion of a river basin (Dessie et al., 2015; Viglione et al., 2013). However, the ungauged catchment streamflow is not easy to estimate and often not taken into account in modelling inputs (Zhang et al., 2017), which can introduce significant uncertainies and/or errors into hydraulic models for simulating flood events.

Estimation or prediction of ungauged streamflow is a challenging research field (Guo et al., 2021b; Hrachowitz et al., 2013; Sivapalan, 2003). The International Association of Hydrological Sciences (IAHS) launched the initiative for Predictions in Ungauged Basins (PUB) in 2003 to stimulate the development of new and advanced predictive approach (Sivapalan et al., 2003), and numerous studies have been carried out since then (Booker and Woods, 2014; Pagliero et al., 2019; Parajka et al., 2013; Salinas et al., 2013; Singh et al., 2022; Viglione et al., 2013; Zelelew and Alfredsen, 2014; Zhang and Chiew, 2009). Most of these studies are to identify donor gauged catchments that are hydrologically similar to the target ungauged catchments, and then transfer information (e.g., streamflow or calibrated hydologic model parameters) from gauged catchments to ungauged catchments. Such process is generally refered as regionalization (Blöschl and Sivapalan, 1995; He et al., 2011). The simplest regionalization method is probably the draninage-area ratio (DAR) method, which generally estimates the streamflow in an ungauged catchment using the streamflow information of nearby gauged catchment and the ratio of the drainage areas of the donor and target catchments (Asquith et al., 2006; Emerson et al., 2005; Ergen and Kentel, 2016; Gianfagna et al.,

2015; Q. Li et al., 2019; McCuen and Levy, 2000). The DAR method can produce reasonable results when the ungauged catchment and its donor gauged catchment have homogeous hydrological characteristics (Ergen and Kentel, 2016). The more sophisticated and widely used regionalization methods are based on hydrologic models (Guo et al., 2021b; Parajka et al., 2013; Razavi and Coulibaly, 2013), which generally use hydrologic model parameters calibrated for donor gauged catchment(s) to derive the model parameters for the target ungauged catchment, and estimate or predict the ungauged streamflow. However, it is not uncommon that these methods sometimes produce unsatisfactory simulation results and low prediction accuracy due to large heterogeneity of land surface conditions, spatial and temporal variability of climatic inputs, unclear hydrological similarity indicators, and uncertainties arising from model structures and calibrations (Guo et al., 2021b; Hrachowitz et al., 2013; Sivapalan, 2003).

A hydraulic model can be a useful tool to verify the hydrologic model simulated ungauged catchment streamflow. For example, Liu et al. (2015) coupled the SWAT (Soil and Water Assessment Tool) hydrologic model and the XSECT hydraulic model for estimating streamflow and water levels for ungauged subbasins in the Red River Basin (U.S. portion). The SWAT model was used to estimate streamflow to provide inflows to the XSECT model, which then simulates water levels and water surface area. By comparing to their observed values extracted from satellites, the XSECT model results provide a verification to the ungauged streamflow simulated by SWAT. Zhang et al. (2017) used the SWAT model to simulate the streamflow of the ungauged zones in the Poyang Lake Basin, and the verification was achieved with the Delft3D hydraulic model

through comparing the simulated flow and lake water levels with the observed. Although there are numerous studies on how to estimate and/or predict streamflow in ungauged catchments, and verify the estimated results using the hydrologic and hydraulic modelling framework, the effects of ungauged subbasins on peak flow, especially snow and ice induced peak flow during river ice breakup in large cold-region river basins, is yet to be explored through the hydrologic and river ice modelling framework.

The objectives of this study are to (1) assess ungauged subbasin streamflow estimation methods (i.e., the simple drainage-area ratio method and sophisticated hydrologic model); (2) investiagte the impacts of ungauged subbasins on peak flow simualtion under open water and river ice breakup conditions; and (3) analyze the peak flow contributions of the gauged and ungauged subbasins for open water and river ice breakup events. A modelling framework was established utilizing the public-domain hydrologic model SWAT and the hydraulic/river ice model River1D, and was applied to the Peace River Basin (PRB), a large cold-region watershed in western Canada. Two open water and three river ice breakup periods were simulated and the impacts of ungauged subbasin streamflow on peak flow of these periods were evaluated.

## 4.2 Data and methodology

The process for estimating and evaluating the ungauged subbasin streamflow in a river basin is shown in Figure 4.1, including (1) delineating a basin into gauged and ungauged subbasins, and simulate the streamflow of each subbasin using the hydrologic model; (2) coupling the hydrologic model outputs and river ice model inputs through: (a) allocating ungauged subbasins into various

inflow boundaries for the river ice model, (b) estimating ungauged subbasin streamflow using the DAR method and/or the hydrologic model, and (c) setting up different inflow boundary scenarios based on how the ungauged subbasin streamflow is considered (partly or fully) and/or estimated; and (3) evaluating ungauged subbasin streamflow with the river ice and hydrologic models. In the modelling framework, the river ice model simulated results can provide feedbacks for the hydrologic model, or the ungauged subbasin streamflow estimated by the hydrologic model can be verified by the simulated results of the river ice model. The hydrologic model would be further calibrated or tuned until the hydrologic model can provide satisfying simulated streamflow in ungauged subbasins for the river ice model.

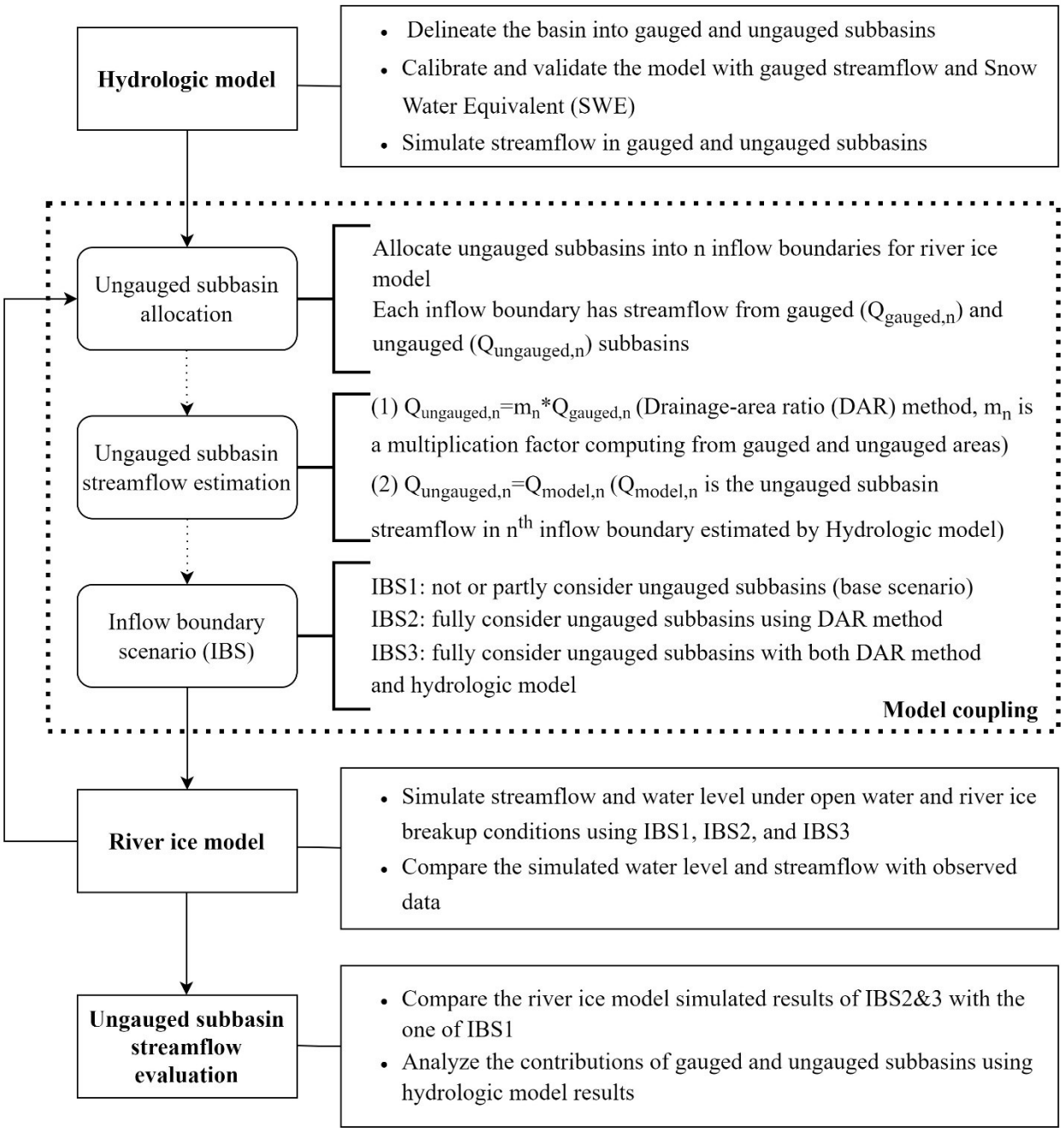


**Figure 4.1** Flow chart for estimating and evaluating ungauged subbasin streamflow in a river basin through combined use of hydrologic and river ice models.

### *4.2.1 Study area and data*

The Peace River originates in the Rocky Mountains, flowing ~1,923 km through the British Columbia and Northern Alberta before joining with the Athabasca River and forming the Slave River. The Peace River Basin (PRB) has an area of approximately 306,000 $km^2$, with the elevations ranging from approximately 3,286 m to about 200 m from upstream to downstream (Figure 4.2). The area enclosed by the black line indicates the modelled area in the hydrologic model in this study which has an area of around 277,286 $km^2$. The modelled reach in the rive ice model (blue line in Figure 4.2) extends from Hudson Hope to approximately 100 km downstream of Fort Vermilion for a total length of 932 km. The river stationing is the distance from the W.A.C. Bennett Dam.

Streamflow data are available from the Water Survey of Canada (WSC). 23 gauge stations were used for calibrating and validating the hydrologic model, shown as black dots in Figure 4.2. 14 of these stations (circled in red) were used to determine the inflow and tributary inflow boundary conditions for the river ice model. Water levels from 7 gauge stations located on the Peace River (hollow black squares) for calibrating and validating the river ice model. Details of the gauge stations used are summarized in Table 4.1.

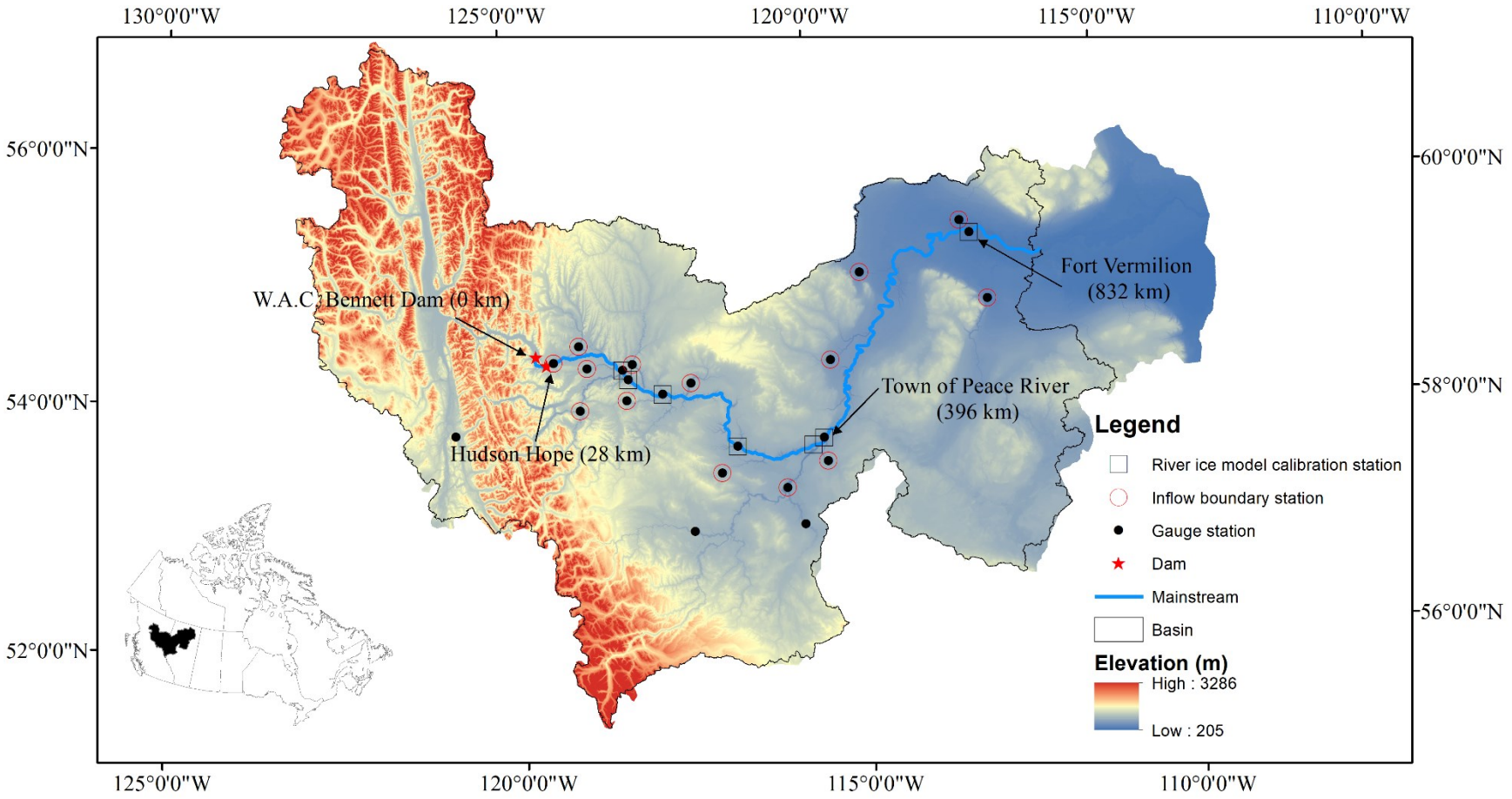


**Figure 4.2** Map of the Peace River Basin and study reach with location of hydrometric gauge stations used in this study.

**Table 4.1** Hydrometric stations in the Peace River Basin used in this study.

| ID | Station | Station Name | Longitude | Latitude | Data Used | Usage |
|---|---|---|---|---|---|---|
| 1 | 07EF001 | Peace River at Hudson Hope | -121.91 | 56.03 | Flow | Hydrologic model calibration/validation and River ice model inflow boundary |
| 2 | 07FA006 | Halfway River near Farrell Creek | -121.63 | 56.25 | Flow | |
| 3 | 07FB008 | Moberly River near Fort St. John | -121.37 | 56.09 | Flow | |
| 4 | 07FB001 | Pine River at East Pine | -121.21 | 55.72 | Flow | |
| 5 | 07FC001 | Beatton River near Fort St. John | -120.7 | 56.28 | Flow | |
| 6 | 07FD001 | Kiskatinaw River near Farmington | -120.56 | 55.96 | Flow | |
| 7 | 07FD009 | Clear River near Bear Canyon | -119.68 | 56.31 | Flow | |
| 8 | 07GJ001 | Smoky River at Watino | -117.62 | 55.72 | Flow | |
| 9 | 07GE001 | Wapiti River near Grande Prairie | -118.8 | 55.07 | Flow | |
| 10 | 07HA003 | Heart River near Nampa | -117.13 | 56.06 | Flow | |
| 11 | 07HC001 | Notikewin River at Manning | -117.62 | 56.92 | Flow | |
| 12 | 07HF002 | Keg River at Highway No. 35 | -117.63 | 57.75 | Flow | |
| 13 | 07JF003 | Ponton River above Boyer River | -116.26 | 58.46 | Flow | |
| 14 | 07JD002 | Wabasca River at Highway No. 88 | -115.39 | 57.88 | Flow | |
| 15 | 07EE007 | Parsnip River above Misinchinka River | -122.91 | 55.08 | Flow | Hydrologic model calibration/validation |
| 16 | 07FD006 | Saddle River near Woking | -118.7 | 55.64 | Flow | |
| 17 | 07GH002 | Little Smoky River near Guy | -117.16 | 55.46 | Flow | |
| 18 | 07FA004 | Peace River above Pine River | -120.82 | 56.2 | Flow & Level | Hydrologic model and river ice model calibration/validation |
| 19 | 07FD002 | Peace River near Taylor | -120.67 | 56.14 | Flow & Level | |
| 20 | 07FD010 | Peace River above Alces River | -120.06 | 56.13 | Flow & Level | |
| 21 | 07FD003 | Peace River at Dunvegan Bridge | -118.61 | 55.92 | Flow & Level | |
| 22 | 07HA001 | Peace River at Peace River | -117.31 | 56.25 | Flow & Level | |
| 23 | 07HF001 | Peace River at Fort Vermilion | -116.03 | 58.39 | Flow & Level | |
| 24 | 07FD901 | Peace River above Smoky River Confluence | -117.44 | 56.16 | Level | River ice model calibration/validation |

### *4.2.2 Hydrologic model*

The SWAT2012 model, a semi-distributed and river basin scale model (Arnold et al., 1998; Neitsch et al., 2011), was used to divide the river basin into gauged and ungauged subbasins, and to simulate streamflow. The model delineates a watershed into subbasins, which is further divided into hydrologic response units (HRUs). A HRU is a combination of unique soil, land cover, and slope. The watershed delineation is based on the digital elevation model (DEM). The ArcSWAT interface for the SWAT2012 model can automatically create streams and outlets for the watershed based on the DEM (Winchell et al., 2013). However, outlets are not necessary situated at the locations of the actual gauge stations. The ArcSWAT interface allows users to manually edit the outlets for the subbasins during watershed delineation. In this study, redundant outlets were deleted to reduce the model complexity. Meanwhile, additional outlets were added based on the locations of the gauge stations used in this study for delineating the gauged and ungauged subbasins, as well as for model calibration (see Table 4.1). Detailed model setup and calibration has been previously conducted for the PRB (see Section 3.2 in Chapter3).

The SWAT model was calibrated with both daily streamflow and Snow Water Equivalent (SWE) from 2004 to 2013 based on the widely used Sequential Fitting program (SUFI2) of SWATCUP (Abbaspour, 2015). Daily streamflow at the 23 selected stations shown in Table 4.1 were used and daily SWE at 23 point stations near the flow stations were obtained from ERA5 reanalysis data (Hersbach et al., 2020). Two commonly used efficiency coefficients, the Nash–Sutcliffe efficiency (NS) and a modified version of the efficiency criterion ($bR^2$) defined by Krause et al. (2005), were tested as the objective function for model calibration. Tests showed that the $bR^2$ performed better in capturing the peak flows and when there were many missing values in observed streamflow data. As the peak flow during open water and river ice breakup periods were the focus of this study and

some of the flow stations on the tributaries have many missing values, $bR^2$ was used as the objective function in SUFI2 of SWATCUP.

### *4.2.3 River ice model*

The open water and river ice hydraulic modeling was conducted with the University of Alberta's public-domain River1D model. The model originated as a hydrodynamic model (Hicks and Steffler, 1992, 1990), and gradually expanded to simulate various river ice processes (Andrishak and Hicks, 2008; Blackburn and She, 2019; She et al., 2009; She and Hicks, 2006). River1D can simulate the mechanical breakup of ice cover via different breakup criteria and a systematic evaluation was provided by Ye and She (2021). However, validation of these breakup criteria is limited. To reduce the uncertainties of simulating the progression of ice breakup and also because the ice front location on the Peace River has been observed relatively frequently, ice cover breakup was not modelled with a breakup criterion, but rather with the observed ice front locations provided to the River1D model. Ice front locations during river ice breakup were mainly obtained from the River Ice Observation Reports Archive of the Government of Alberta (https://rivers.alberta.ca/#), supplemented by information extracted from the Landsat Data (https://www.usgs.gov/landsat-missions/data).

A static ice cover was assumed to initially present in the study reach mimicking the pre-breakup condition. The initial ice thickness was set according to the observed stable ice thickness available at two WSC gauge stations on the Peace River from the Canadian River Ice Database (De Rham et al., 2020). At each time step, the model checks where the ice front is located. Upstream of the ice front, the ice cover was assumed to be fully broken up and offered no resistance to the flow. This was simulated by removing the ice resistance in the model. Following Ye and She (2021), a transition zone of five channel widths was assumed to exist between the freely flowing broken ice

and the intact ice cover, within which the ice offers reduced resistance to flow. The ice velocity within the transition zone was assumed to decrease linearly from open water velocity to zero from upstream to downstream.

The geometric model is a combination of surveyed and approximated cross sections (Blackburn and Hicks, 2002; Ye and She, 2021). Sub-daily discharge data was requested from Environment and Climate Change Canada (ECCC) and used as inflow boundary conditions at the upstream end of the study reach and incoming tributaries (see Table 4.1). The daily streamflow that is publicly available from the WSC Hydrometric database was used to fill in the missing values in the sub-daily dataset for some stations. No water level data was available at the downstream boundary of the modelled reach but since it is about 100 km downstream of the reach of interest (i.e., Hudson Hope to Fort Vermillion), a constant water level boundary could be assumed without impacting the hydraulic conditions in the reach of interest.

Sub-daily streamflow and water levels at 7 hydrometric stations on the Peace River (see Table 4.1) requested from ECCC, were employed to calibrate the river ice model for open water and river ice breakup events. Model calibration for open water events was completed by adjusting the main channel bed roughness values of the study reach. Once the bed roughness values were calibrated, the ice roughness values for the reach were adjusted for the river ice breakup periods. The model performance was evaluated using the Nash–Sutcliffe efficiency coefficient (NS) and the coefficient of determination ($R^2$) (Moriasi et al., 2015). The range of $R^2$ is 0 to 1 while NS is from $-\infty$ to 1. The perfect value of both $R^2$ and NS is 1.

### *4.2.4 Model coupling*

#### *4.2.4.1 Gauged and ungauged subbasins delineation*

The PRB was delineated into 818 subbasins using the SWAT model. The 14 hydrometric stations (Table 4.1) used to set the inflow boundaries for the river ice model were used to distinguish the ungauged subbasins from gauged subbasins (Figure 4.3a). The drainage area of a hydrometric station contains all the subbasins upstream of this station, and the 14 inflow boundary zones (colored area) for the River1D model are corresponding to the 14 hydrometric stations. The remaining (grey) area of the PRB covers all the ungauged subbasins, which takes about 26.54% of the whole modelled area. The ungauged subbasins were manually allocated into the nearby 14 inflow boundary zones so that the impacts of ungauged subbasin streamflow on the inflow boundaries of the river ice model can be evaluated (see Figure 4.3b). Manual allocation was mainly based on the final outlet location of each ungauged subbasin to the mainstream and the locations of the mainstream gauge stations.

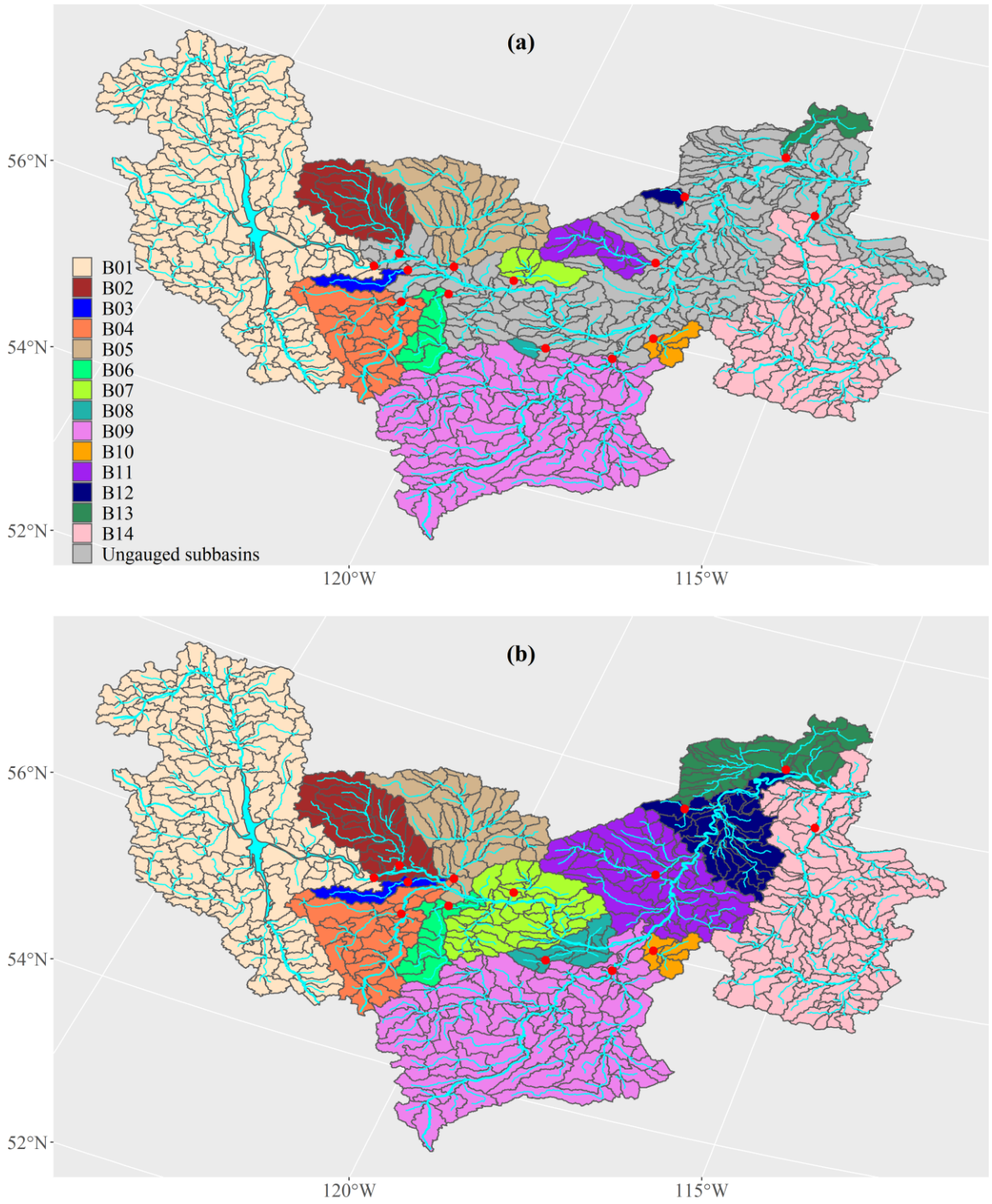


**Figure 4.3** Delineated subbasins of Peace River Basin (a) gauged inflow boundary zones (various colors) and ungauged subbasins (grey); (b) ungauged subbasins allocated into 14 inflow boundary zones.

*4.2.4.2 Ungauged subbasin streamflow estimation*

The inflow boundary hydrometric stations on the tributaries (Table 4.1) are not located right at the confluence to the Peace River (see Figure 4.3). The streamflow from subbasins between the tributary gauges and the confluence therefore is not considered if the gauge data is directly used as the inflow boundaries for the river ice model. To account for these ungauged flows, Hicks (1996) used a set of multiplication factors from Alberta Environment (Taggart, 1995) to adjust the tributary inflow boundaries of the Peace River when simulating open water flood events using the River1D model. These multiplication factors were computed based on the ratio of the catchment area at the confluence to the catchment area at the tributary gauge (i.e., the DAR method). These multiplication factors were used in this study as the base scenario (S1 in Table 4.2). Not all inflow boundaries were adjusted by the multiplication factors in the study of Hicks (1996). Additionally, this scenario does not consider the ungauged subbasins outside the subbasin between the tributary gauge station and the confluence of the mainstream.

A second scenario was constructed by manually allocating all the ungauged subbasins into the nearby gauged drainage area (Figure 4.3b) and re-calculating the multiplication factor for each inflow boundary using the DAR method:

$$m_i = \frac{\mathrm{A}_{gauged,i} + A_{ungauged,i}}{\mathrm{A}_{gauged,i}} \tag{4-1}$$

where $m_i$ is the multiplication factor for the $i^{\text{th}}$ inflow boundary ($i$ = 1, 2, …, 14); $A_{\text{gauged},i}$ and $A_{\text{ungauged},i}$ are the area of the gauged and ungauged drainage area for the $i^{\text{th}}$ inflow boundary zone, respectively.

As can be seen from Table 4.2, the ungauged subbasins are far greater than the gauged subbasins for some of the inflow boundary zones (e.g., B07, B08 and B11-B13). In this case, the simple DAR

method that amplifies the gauged streamflow by a multiplication factor could misestimate the ungauged subbasin streamflow to a great extent, while a hydrologic model may provide better estimate. Therefore, a third scenario was constructed by using the SWAT model to calculate the ungauged subbasin streamflow for these inflow boundary zones with large ungauged subbasins, while keeping the same multiplication factors from scenario 2 for all other inflow boundary zones.

**Table 4.2** The three scenarios of inflow boundaries of River1D.

| Boundary | Station | Gauged Area ($km^2$) | Ungauged Area ($km^2$) | Scenario (S1) | Scenario2 (S2) | Scenario3 (S3) |
|---|---|---|---|---|---|---|
| B01 | 07EF001 | 70,042.28 | 0 | $1*Q_{gauged01}$ | $1*Q_{gauged01}$ | $1*Q_{gauged01}$ |
| B02 | 07FA006 | 9,238.09 | 2,830.87 | $1*Q_{gauged02}$ | $1.306*Q_{gauged02}$ | $1.306*Q_{gauged02}$ |
| B03 | 07FB008 | 1,505.69 | 433.54 | $1.4*Q_{gauged03}$ | $1.288*Q_{gauged03}$ | $1.288*Q_{gauged03}$ |
| B04 | 07FB001 | 11,956.05 | 1,443.2 | $1*Q_{gauged04}$ | $1.121*Q_{gauged04}$ | $1.121*Q_{gauged04}$ |
| B05 | 07FC001 | 15,297.17 | 774.6 | $1.03*Q_{gauged05}$ | $1.051*Q_{gauged05}$ | $1.051*Q_{gauged05}$ |
| B06 | 07FD001 | 3,584.24 | 694.74 | $1.26*Q_{gauged06}$ | $1.194*Q_{gauged06}$ | $1.194*Q_{gauged06}$ |
| B07 | 07FD009 | 2,840.49 | 11,049.39 | $1*Q_{gauged07}$ | $\mathbf{4.89}*Q_{gauged07}$ | $Q_{gauged07}+Q_{ungauged07,\ swat}$ |
| B08 | 07FD006 | 523.44 | 3,275.62 | $1*Q_{gauged08}$ | $\mathbf{7.258}*Q_{gauged08}$ | $Q_{gauged08}+Q_{ungauged08,\ swat}$ |
| B09 | 07GJ001 | 48,553.39 | 2,385.76 | $1.02*Q_{gauged09}$ | $1.049*Q_{gauged09}$ | $1.049*Q_{gauged09}$ |
| B10 | 07HA003 | 1,737.2 | 473.55 | $1*Q_{gauged10}$ | $1.273*Q_{gauged10}$ | $1.273*Q_{gauged10}$ |
| B11 | 07HC001 | 4,636.73 | 16,352.69 | $1.39*Q_{gauged11}$ | $\mathbf{4.527}*Q_{gauged11}$ | $Q_{gauged11}+Q_{ungauged11,\ swat}$ |
| B12 | 07HF002 | 735.81 | 11,147.58 | $1*Q_{gauged12}$ | $\mathbf{16.15}*Q_{gauged12}$ | $Q_{gauged12}+Q_{ungauged12,\ swat}$ |
| B13 | 07JF003 | 2,370.11 | 8,869.65 | $1.26*Q_{gauged13}$ | $\mathbf{4.742}*Q_{gauged13}$ | $Q_{gauged13}+Q_{ungauged13,\ swat}$ |
| B14 | 07JD002 | 33,043.97 | 11,490.48 | $1.1*Q_{gauged14}$ | $1.348*Q_{gauged14}$ | $1.348*Q_{gauged14}$ |

**Note:** $Q_{gauged}$ is the streamflow data at each of the inflow gauge station; $Q_{ungauged,\ swat}$ indicates the ungauged streamflow in an inflow boundary zone simulated by SWAT; Number in the subscript indicates the number of the inflow boundary; A multiplication factor of 1 is used in S1 for those inflow boundary stations not found in Hicks (1996); The multiplication factors in S2 are computed from Equation 1; the multiplication factors greater than 1.5 in S2 are shown in bold.

*4.2.4.3 Evaluate the impacts of ungauged subbasin streamflow*

Two open water periods and three river ice breakup periods were selected to evaluate the impacts of ungauged subbasin streamflow on the River1D model in simulating the streamflow and water levels. For open water periods, both flood (June 10 to August 10, 2011) and non-flood (May 20 to June 20, 2012) years were selected to better evaluate the contribution of ungauged subbasins. For the breakup periods, the simulations started from the date when the ice front began to retreat. Two mechanical river ice breakup years (modeling period from March 28 to May 15, 2007 and February 7 to May 15, 2013) and one thermal breakup year (modeling period from March 3 to May 15, 2012) were simulated. In addition, the contributions of ungauged subbasins to streamflow in the PRB were roughly evaluated based on the simulated streamflow from the SWAT model.

## 4.3 Results and discussion

### *4.3.1 Open water periods*

The 2012 open water period has better data quality in terms of the amount of missing values, and thus was used to calibrate the bed roughness and the 2011 open water period was used for model validation. The bed roughness was calibrated for the three inflow boundary scenarios (S1-S3 in Table 4.2) separately and the used values are shown in Figure 4.4. The calibrated roughness values are in general agreement with those used in Andres (1996), which ranged from 0.017 to 0.03 for discharges between 1,000 and 10,000 $m^3/s$ at the station of Peace River at Fort Vermilion (PRFV), and 0.02 to 0.04 for discharges between 1,000 and 5,000 $m^3/s$ at the station of Peace River at Peace River (PRPR). The calibrated manning's *n* values also are also overall in line with those calibrated by Huang et al. (2021), whose calibrated bed roughness of the Peace River were mainly between 0.01 and 0.03.

The simulated results for the two open water periods are showed in Figures 4.5-4.8, in comparison

with the observed water levels and streamflow. In general, the simulated water level and streamflow in all three inflow boundary scenarios showed good agreement with the observed data. For water levels, the values of NS and $R^2$ at all stations were over 0.8. The values of NS and $R^2$ for streamflow at most stations were greater than 0.8 for the 2011 modelling period; however, for 2012 two of the three scenarios showed poor agreement with the observed flow at PRFV. Comparing the observed streamflow at PRPR and PRFV, a nearly 1,700 $m^3/s$ reduction of the peak flow occurred over this distance (~450 km). Such a reduction was not seen in any of the model routed hydrographs no matter which inflow boundary scenario was used. As the magnitude of peak flow is mainly affected by channel roughness (Blackburn and Hicks, 2002), the Manning's n value for the PRPR to PRFV reach was varied to see the change in the peak flow reduction. It was found that a flow reduction comparable to the observed can only be achieved by increasing the Manning's n value by over 0.02 for the nearly 450 km reach. Such an increase in roughness caused the water levels at both PRPR and PRFV to increase significantly, resulting in poor agreement with the observed water levels. It is therefore suspected that the observed flow at PRFV during this period was lower than the actual. This is also supported by the simulation of the 2011 open water flood period. It can be seen from Figure 4.6 that the routing of the two flood waves from PRPR to PRFV agreed very well between the modelled and observed.

Looking closely to the peak flows, S1, using the multiplication factors from Hicks (1996), significantly underestimated the peak flow at many hydrometric stations, especially during the 2011 open water flood period. For example, the observed largest peak flow at PRPR in 2011 was about 13,630 $m^3/s$ while the simulated value in S1 was only 8,966 $m^3/s$. This is likely due to streamflow from large parts of the ungauged subbasins was not taken into account in S1.

S2 used the updated multiplication factors which account for the streamflow from all the ungauged

subbasins. It significantly improved the open water peak flow simulations at most of the hydrometric stations as compared with S1 (see Figures 4.6 and 4.8). However, S2 still evidently underestimated the largest peak flow of the 2011 open water flood event with the simulated value at PRPR around 10,091 $m^3/s$. This could be due to the underestimation of streamflow in the inflow boundary zones of B07 and B08, located just before PRPR. Despite the underestimation of the largest peak flow at PRPR, the corresponding largest peak flow at the downstream station of PRFV showed good agreement with the observed. This may be due to the overestimation of ungauged subbasin streamflow in B11 and B12, located between PRPR and PRFV. As mentioned earlier, the ungauged area far exceeds the gauged area in B07, B08, B11 and B12 (see Table 4.2), and thus the runoff production mechanisms for the ungauged subbasins are probably very different from the gauged subbasins. In this case, the DAR method has large uncertainty and may significantly misestimate the ungauged subbasin streamflow. The uncertainty arising from applying the DAR method to large ungauged area was small during the 2012 open water period. It is likely due to the streamflow from the large ungauged subbasins (such as those in B07 and B08) had a small contrition to the peak flow in the non-flood period.

S3 used SWAT to estimate the ungauged streamflow for the inflow boundary zones containing large ungauged area (B07, B08, B11 and B12). Like S2, S3 overall improved the peak flow at most stations (see Figures 4.6 and 4.8). Moreover, S3 provided more reasonable simulation of the largest peak flow at both PRPR and PRFV in 2011, though the simulated value was still a little lower than the observed peak value. However, S3 significantly overestimated the second peak flow at the Peace River at Dunvegan Bridge (PRDB). These results suggested that the SWAT model may have overestimated the ungauged subbasin streamflow in B07, while somewhat underestimated the streamflow from those ungauged subbasins in B08 and B09 In addition, S3 overall tended to

overestimate during the first peak and low flow periods at PRPR and PRFV in 2011. The simulated rising times of the hydrographs and the peaking times were also earlier than the observed. These discrepancies are likely due to uncertainties and/or errors of both observed data and the SWAT model. The geometric data may be another source of uncertainty as hundreds of kilometers of the study reach used approximated geometry and many of the surveyed cross sections were obtained in the 1990s.

In general, the comparison of the three inflow boundary scenarios demonstrated that the streamflow from the ungauged subbasins greatly contributed to the open water flood. The hydrologic model is useful in simulating the streamflow in the ungauged area and has a good potential to provide inflow boundaries for the hydraulic model. Nevertheless, the hydrologic model still needs to be further improved to well capture open water flood.

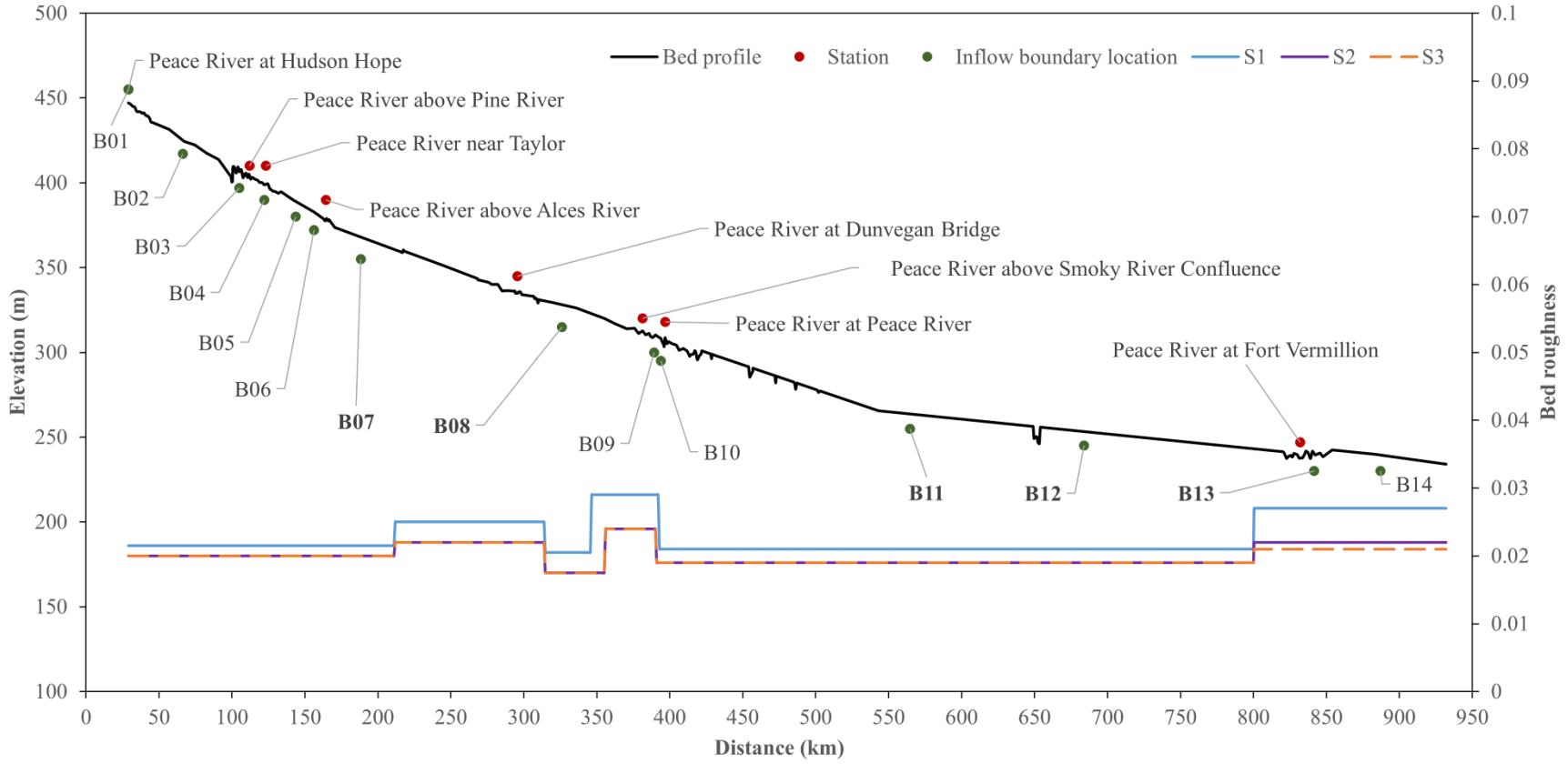


**Figure 4.4** Bed profile, bed roughness in three inflow boundary scenarios (S1-S3), inflow boundary and mainstream hydrometric station locations used in the River1D model; the inflow boundaries with larger ungauged subbasins are indicated in bold.

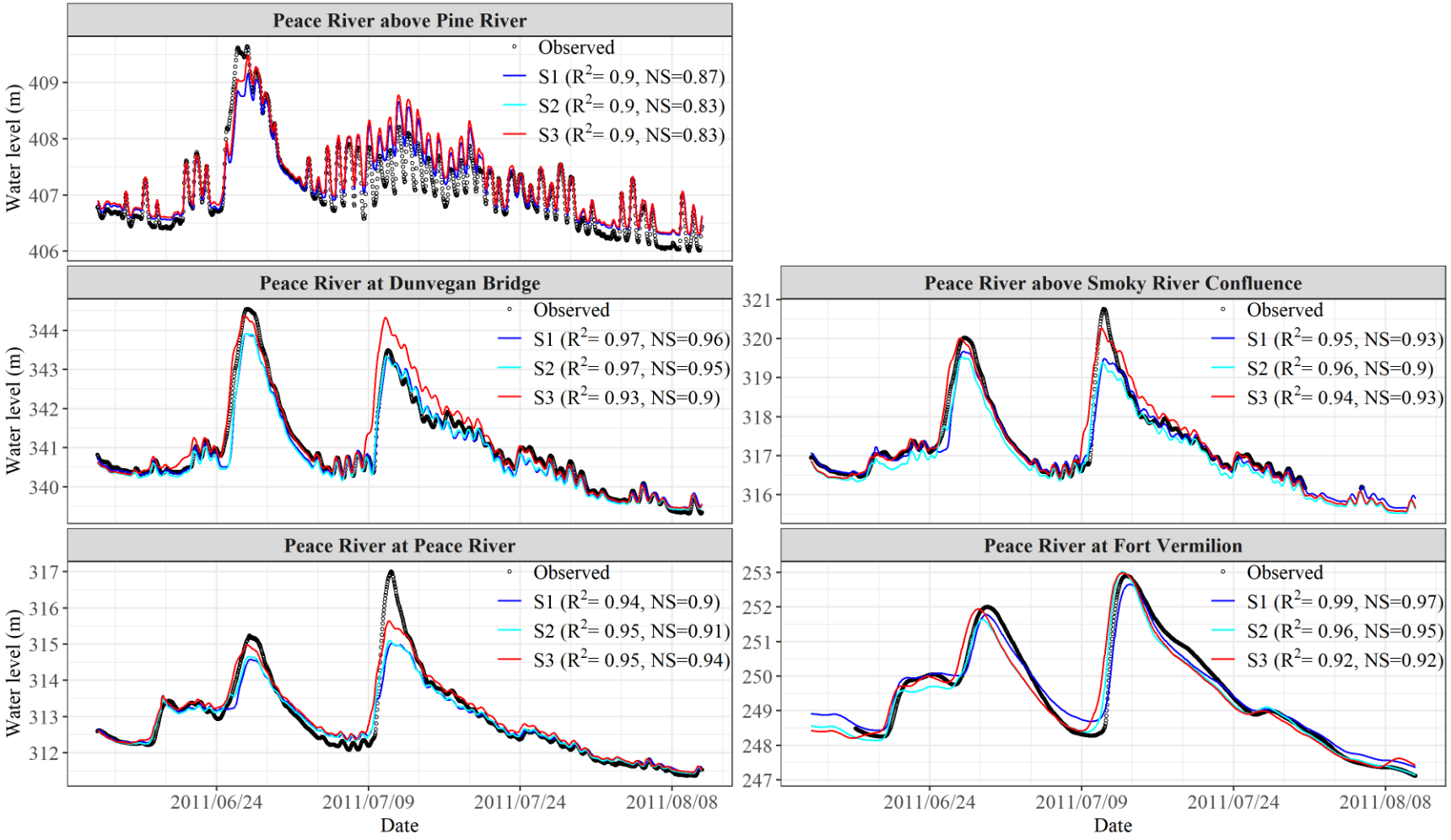


**Figure 4.5** Comparisons of observed and simulated water level for the 2011 open water period.

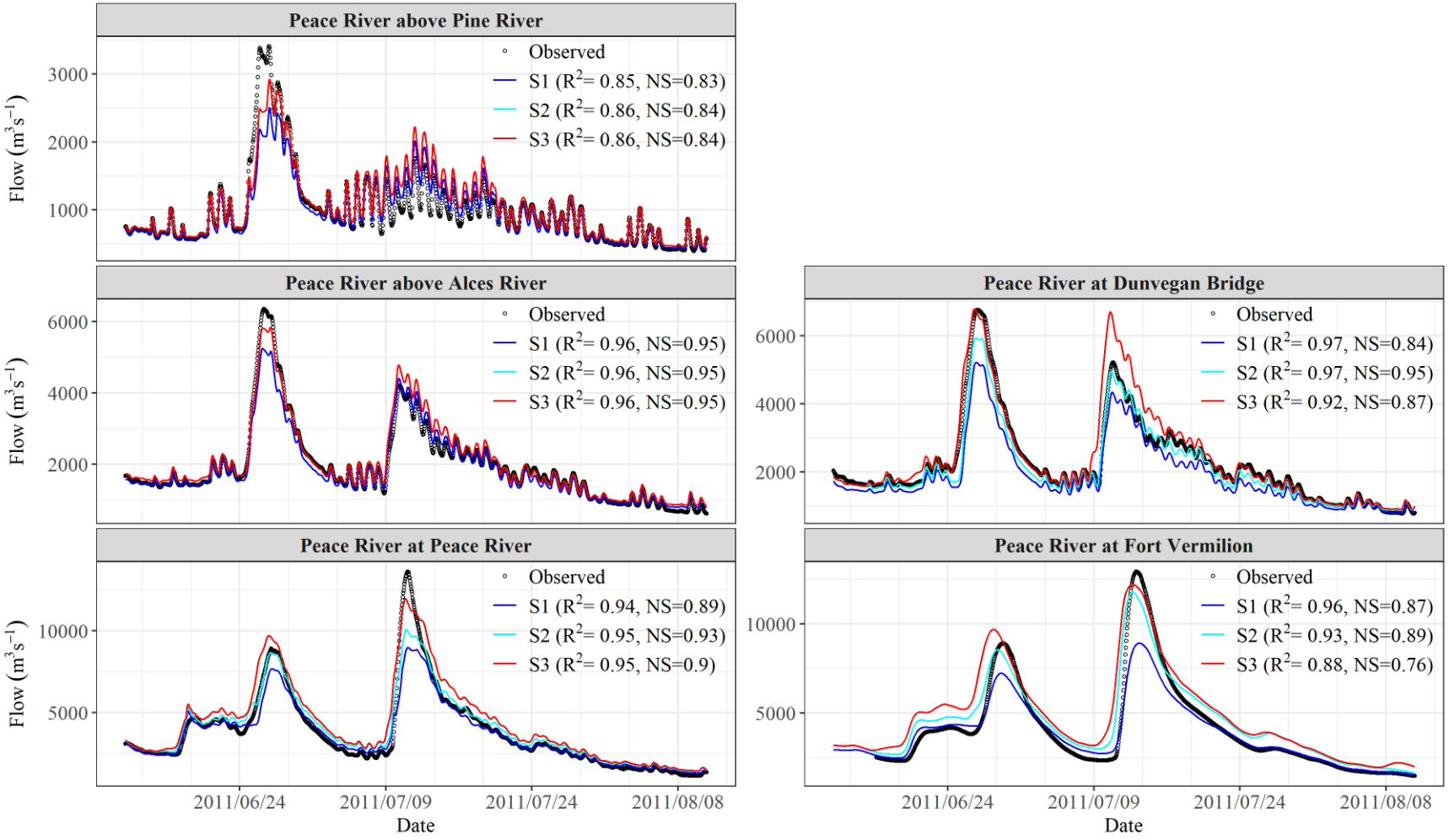


**Figure 4.6** Comparisons of observed and simulated streamflow for the 2011 open water period.

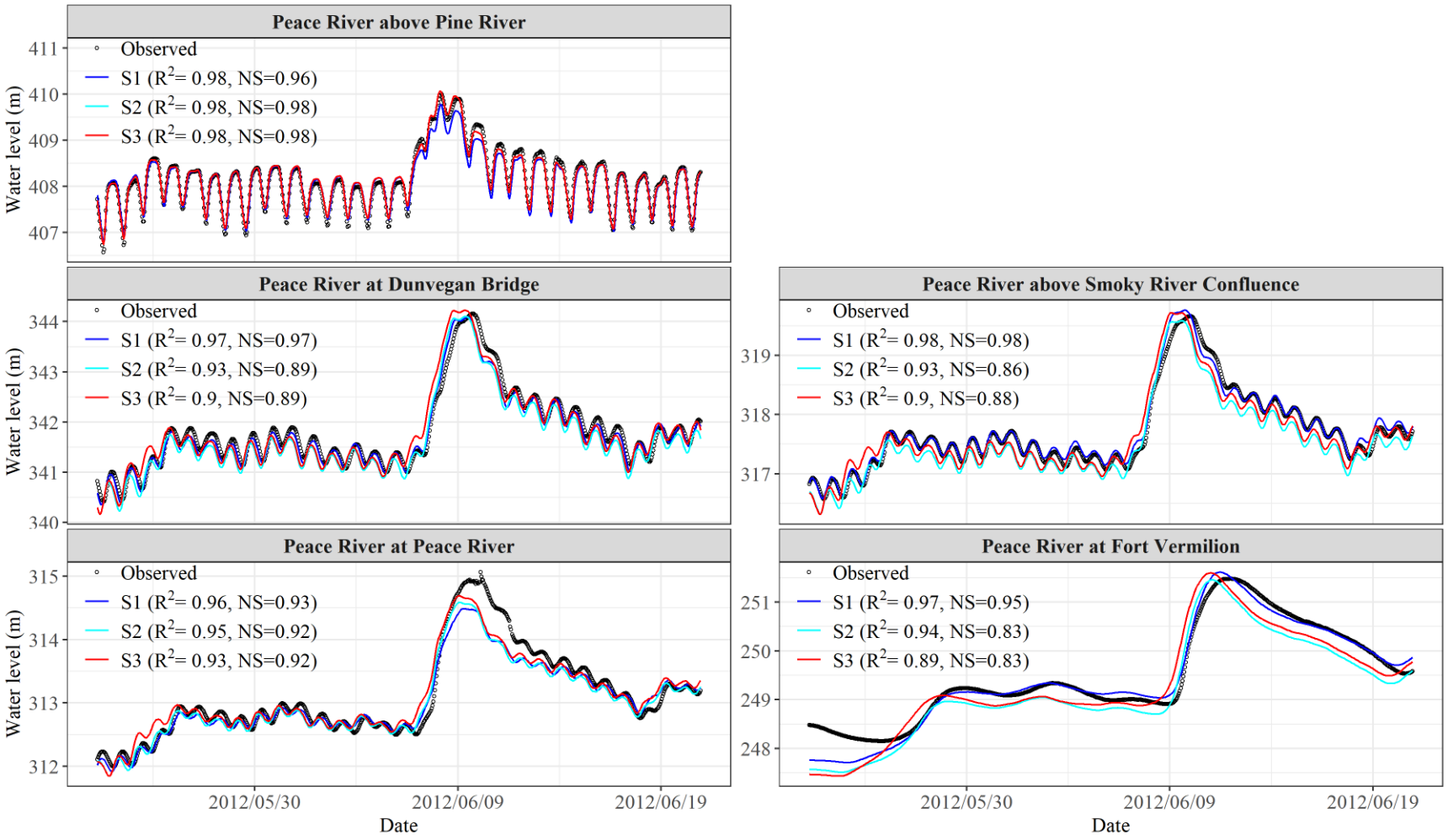


**Figure 4.7** Comparisons of observed and simulated water level for the 2012 open water period.

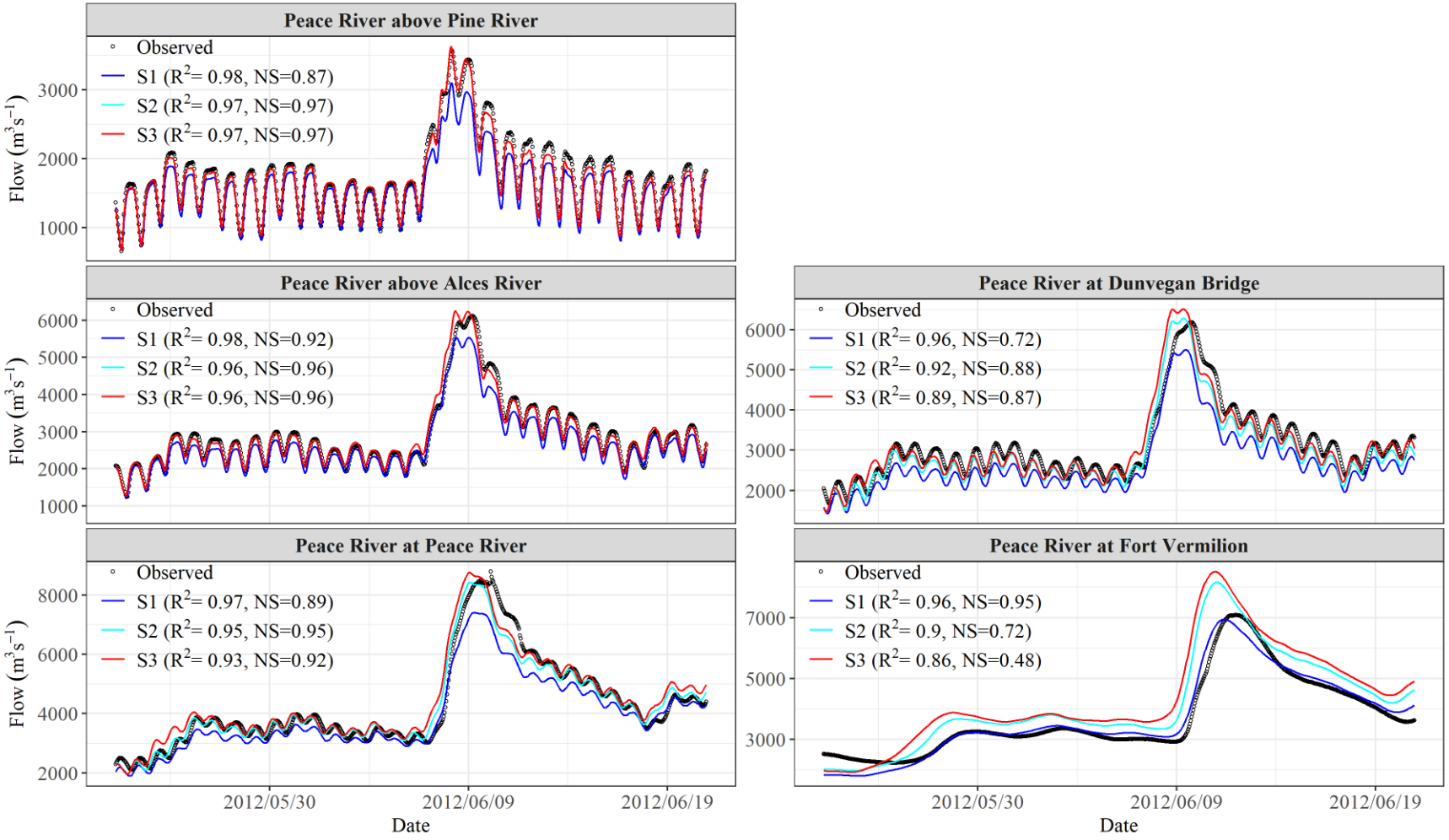


**Figure 4.8** Comparisons of observed and simulated streamflow for the 2012 open water period.

### *4.3.2 River ice breakup periods*

Before comparing the modelled results with observed, it is worth noting that the WSC flow data can contain greater uncertainty when the gauge is affected by ice. WSC uses station-specific open water rating curves (i.e., water level-discharge relationship) to derive flow from continuous measurement of water levels. However, the presence of ice causes the water level-discharge relationship to greatly deviate from the rating curve, and the flow derived from the rating curve only represents the maximum possible discharge in the presence of ice. Turcotte and Rainville (2022) explained the procedure that WSC takes to correct the derived discharge. Direct flow measurements provide a good basis for such correction but are only done a couple of times during winter when the ice cover is safe to work on. When such data is not available, the correction can be subjective. Figure 4.9 shows the observed retreat of the ice front during the three simulated years, which provides a rough idea on when a gauge station may have been affected by ice. In the upstream steeper reach where the ice caused backwater does not extend very far upstream from the ice front, stations Peace River above Pine River, Peace River near Taylor, and Peace River above Alces River were not affected by ice. In the downstream reach where the channel slope is mild, the backwater from ice can extend tens of kilometers upstream depending on the thickness and roughness of the ice cover. The date when the downstream gauge stations like PRDB, Peace River above Smoky River Confluence (PRSRC), PRPR and PRFV were not affected by ice was estimated based on ice front locations, the last “B” symbol in the flow data (used by WSC to indicate a gauge station is affected by ice), and available satellite images of the study reach. The dates when PRDB, PRSRC, PRPR and PRFV were not affected by ice were April 18, 25, 26 and

29 in 2007, April 2, 13, 15 and May 7 in 2013. In 2012, PRDB was not affected by ice since the beginning of the simulation while PRSRC, PRPR and PRFV were not affected by ice starting from March 16, 30 and April 29, respectively. These dates are shown in the result figures (Figures 4.10-4.15) where the simulated water levels and streamflow are compared with their observed values. Note that the streamflow during river ice breakup prior to these dates could have larger uncertainty than the rest of the simulated periods.

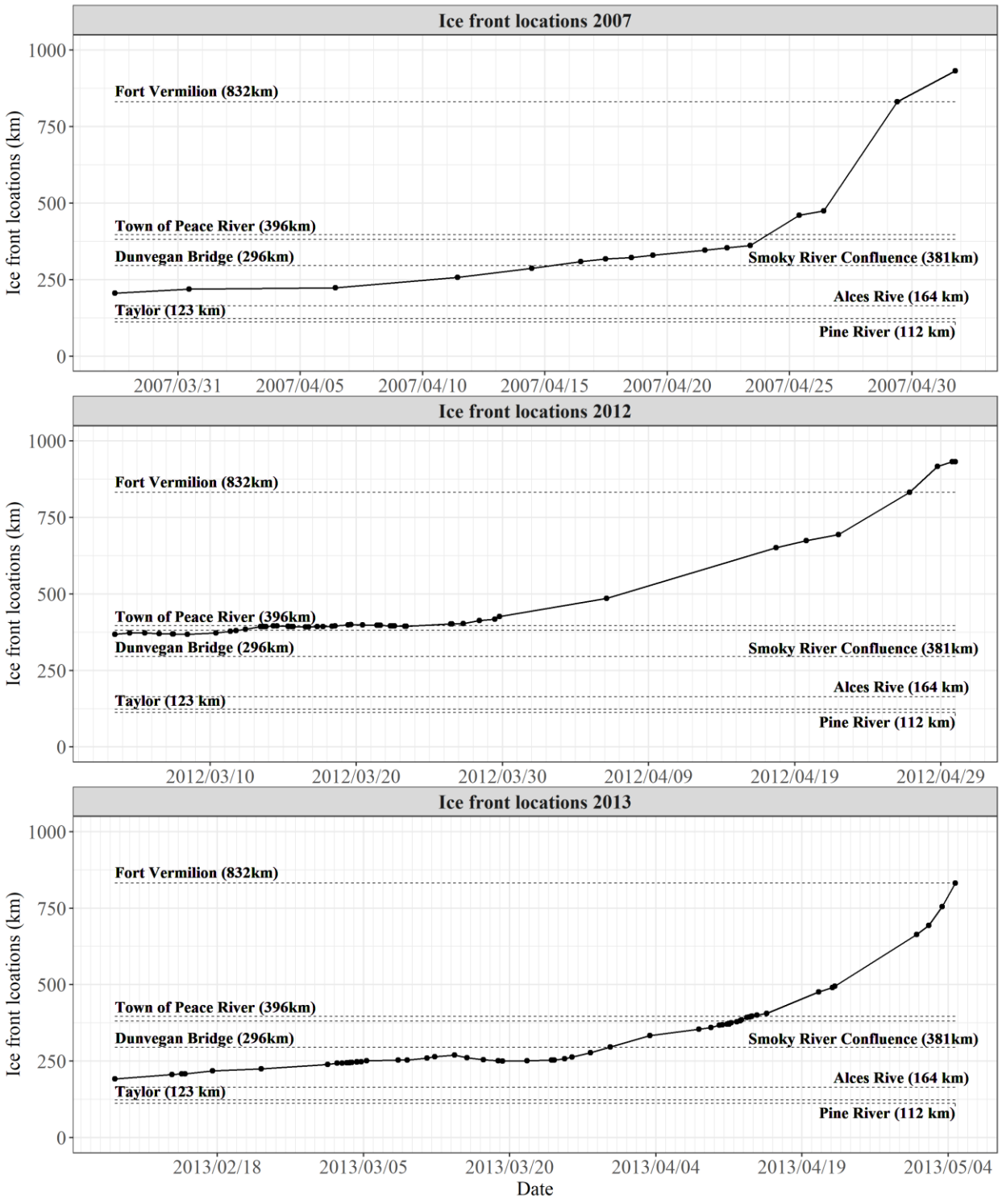


**Figure 4.9** Observed ice front locations of Peace River during the retreating period for 2007, 2012 and 2013.

Except for PRDB in 2012, the stations that were not affected by ice, i.e., Peace River above Pine River, Peace River above Taylor, and Peace River above Alces River, were well simulated regardless the inflow boundary scenario. The simulated water levels at most of the ice affected stations showed good agreement with observed, and the water level drop as the ice front passed a gauge station was also well captured. The less satisfactory water level simulations were mainly in three situations: (1) when an ice jam formed or released as such events are not accounted for in the river ice model. For example, an ice jam formed near PRPR on April 21, 2007 (Alberta Environment Peace River Ice Observation Report NO. 52 – 2006/2007), which caused water level of PRPR to increase by 0.5 to 1 m. This water level increase and later the sharp drop due to the jam release was not well simulated by the River1D (see PRPR in Figure 4.10); (2) when the ice front moved long distance in relatively short period, or when the ice front location was not observed for longer time. For example, Figure 4.9 shows that in 2007 the ice front moved nearly 100 km near PRPR and PRSRC between April 23 and April 25, and its location was not tracked between April 26 and April 29 during which the ice front moved about 357 km from near PRPR to PRFV. In the former case, the ice breakup was very dynamic and cannot be well represented by a fixed length transition zone and specified ice velocity. In the latter case, the ice front may have stalled and restarted during the period without ice front location data, and thus linearly interpolating the ice front location between the known data points led to errors in simulating the hydraulic conditions. As a result, the simulated water levels showed poor agreement with the observed data at PRSRC, PRPR and PRFV during the above mentioned time periods; (3) when the ice cover had broken up at a gauge station. The simulated water level was relatively high as

compared to the observed values after the ice cover had broken up and the hydraulic conditions near the gauge had returned to near open water conditions. For example, the simulated water levels at PRDB in 2007, PRSRC, PRPR, and PRFV in 2012 were all overestimated after the water level dropped significantly. This is likely due to the effect of remnant ice in the river channel. Additionally, the bed morphology and roughness may have changed due to ice caused sediment deposition and scouring, while these changes were not accounted for in the model.

Figures 4.11, 4.13 and 4.15 show the comparison of simulated and observed streamflow during the three breakup periods. The streamflow was well simulated at all the gauge stations that were not affected by ice. The only exception was PRDB in 2012, where the simulated flow with either of the three inflow boundary scenarios was lower than the observed. This is likely due to snowmelt in ungauged subbasins upstream this station was not well simulated in 2012. Compared with the other two simulated breakup periods, late winter to early spring of 2012 had higher temperature. By checking snow depth data, it was found that the inflow boundary zones (e.g., B07) just before PRDB experienced two large snowmelt events from early March to early April. The River1D simulated streamflow at PRDB should be underestimated if the streamflow from the two large snow melting was not properly considered in the inflow boundaries. The SWAT model was calibrated with multiple years of data, and the calibrated parameters can well represent the snow processes of most years. But the SWAT model probably cannot provide good simulation for one or few years that has obvious different snowmelt conditions than others. This likely explains the underestimation of streamflow from early March to late April in 2012.

For the ice affected stations, the inflow boundary scenario S1 again significantly underestimated the peak flow. The only exception was PRFV flow in 2007 where S1 simulated flow better matched the observed than the other two scenarios. Based on a satellite image from LANDSAT7, the river condition near PRFV was in complete open water in 2007-05-01 18:36:44. Therefore, the streamflow at PRFV should have not been affected by ice from 2007-05-01. The streamflow after this date should have been calculated using open water rating curve but was found to be significantly lower than the values computed from the rating curves of PRFV. The WSC published peak flow was about 5,760 $m^3/s$ on 2007-05-08 while the value computed from the rating curve was about 7,135 $m^3/s$. Therefore, the discrepancy between simulated and observed flow at PRFV is likely due to error in observed data.

S2 improved the peak flow at some stations (e.g., PRPR and PRFV in 2013), but significantly underestimated the snow and ice affected peak flow while overestimated the peak flow when river just turned into open water conditions at many stations (e.g., PRFV in both 2012 and 2013). S2 had a large uncertainty in estimating snow and ice affected streamflow for the ungauged subbasins. S3 generally performed the best as it captured the snow and ice affected peak flow at most stations very well (e.g., PRDB and PRPR in 2007, PRFV in 2012, PRPR and PRFV in 2013). Nevertheless, the discrepancy was still obvious at some stations (e.g., PRPR in 2012) as there were still some deviations for the streamflow provided by the SWAT model. Moreover, the daily streamflow calculated by SWAT model was probably not fine enough to capture the very dynamic flood occurring during river ice breakup. However, the comparison among the three inflow boundary

scenarios still demonstrated that the ungauged subbasins did contribute a large amount of streamflow and can greatly affect the peak flow during snow melting and river ice breakup period.

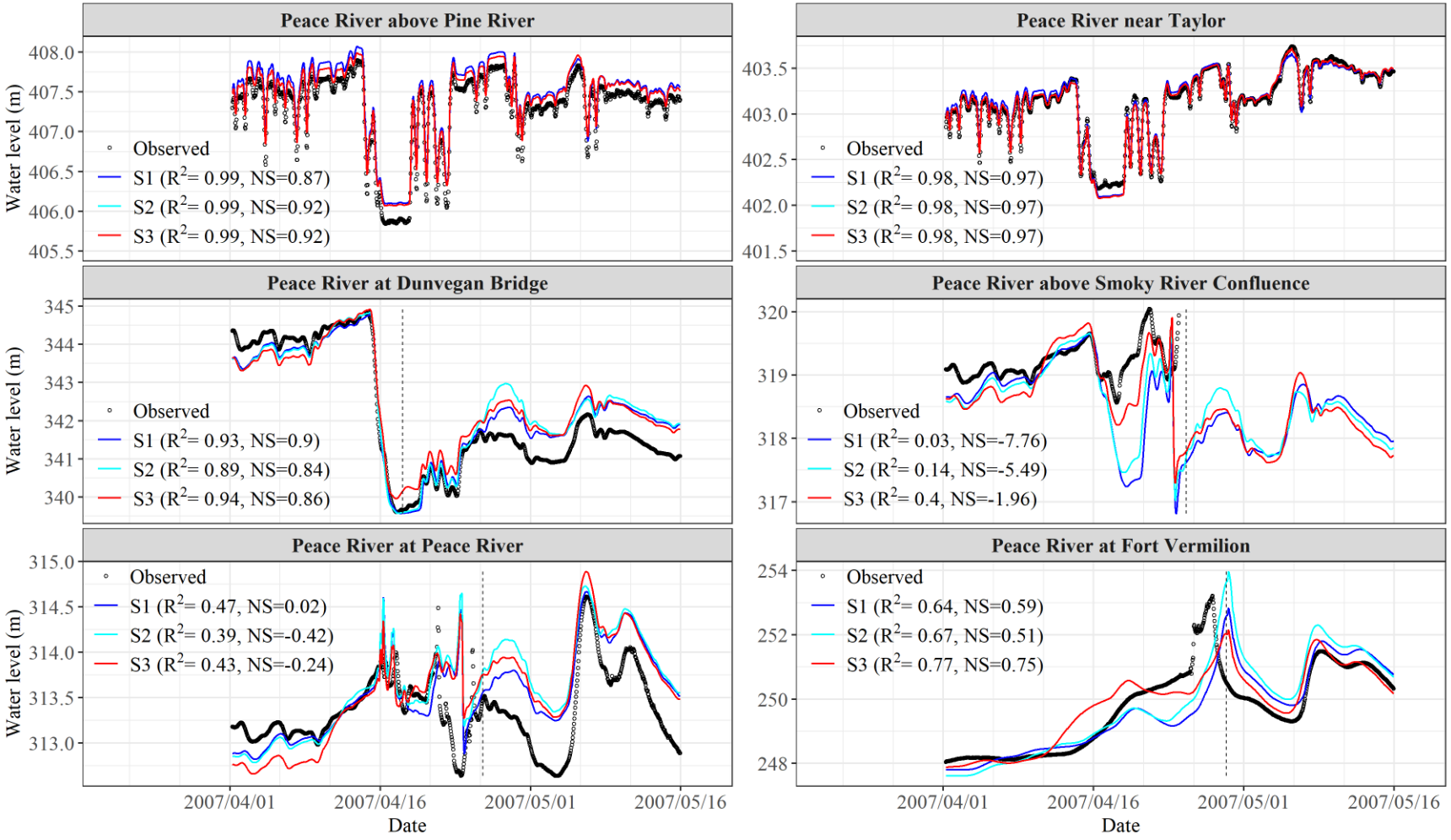


**Figure 4.10** Comparisons of observed and simulated water level for the 2007 river ice breakup period (vertical dashed line indicates the rough date when the station is not affected by ice).

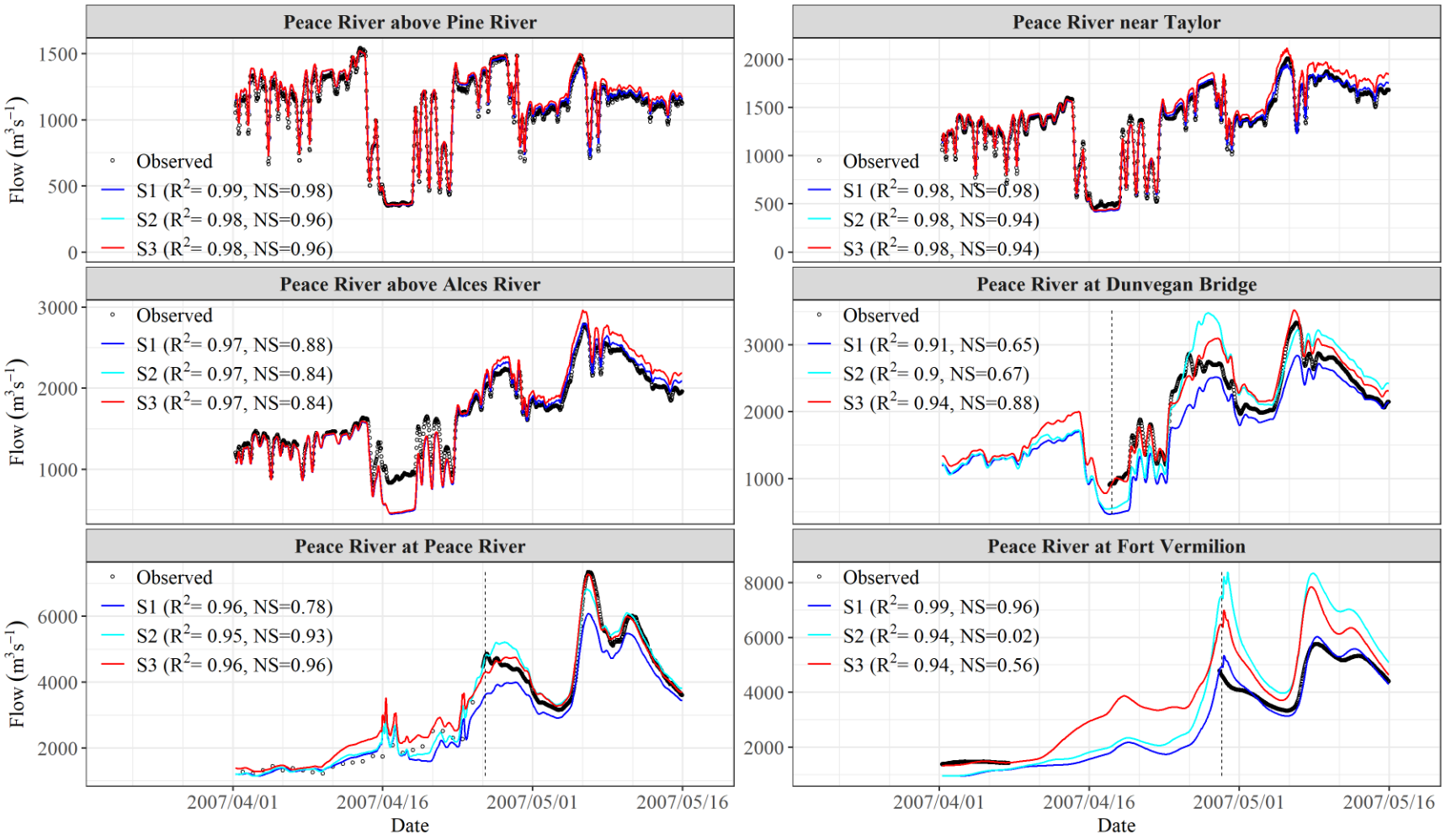


**Figure 4.11** Comparisons of observed and simulated streamflow for the 2007 river ice breakup period (vertical dashed line indicates the rough date when the station is not affected by ice).

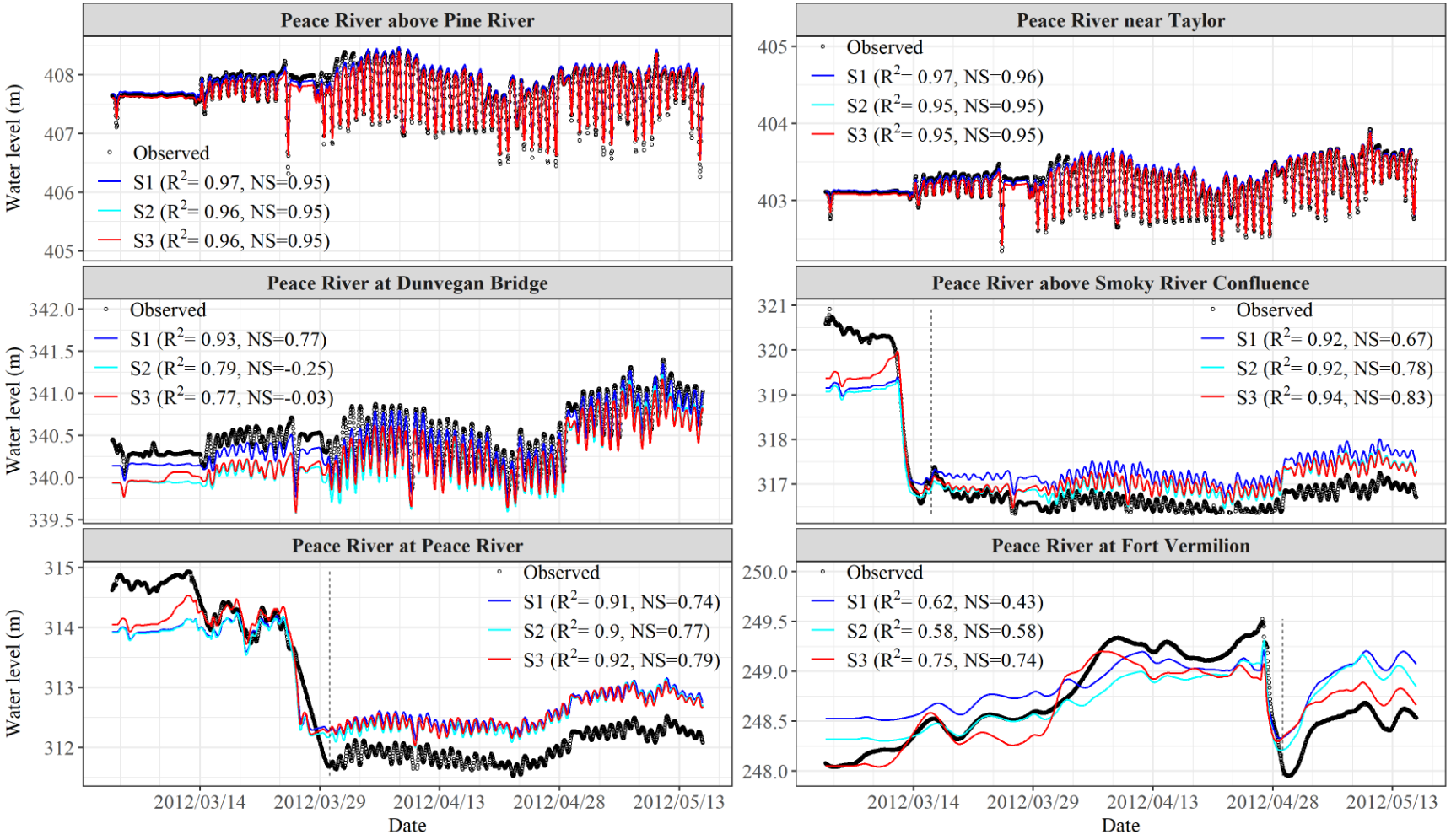


**Figure 4.12** Comparisons of observed and simulated water level for the 2012 river ice breakup period (vertical dashed line indicates the rough date when the station is not affected by ice).

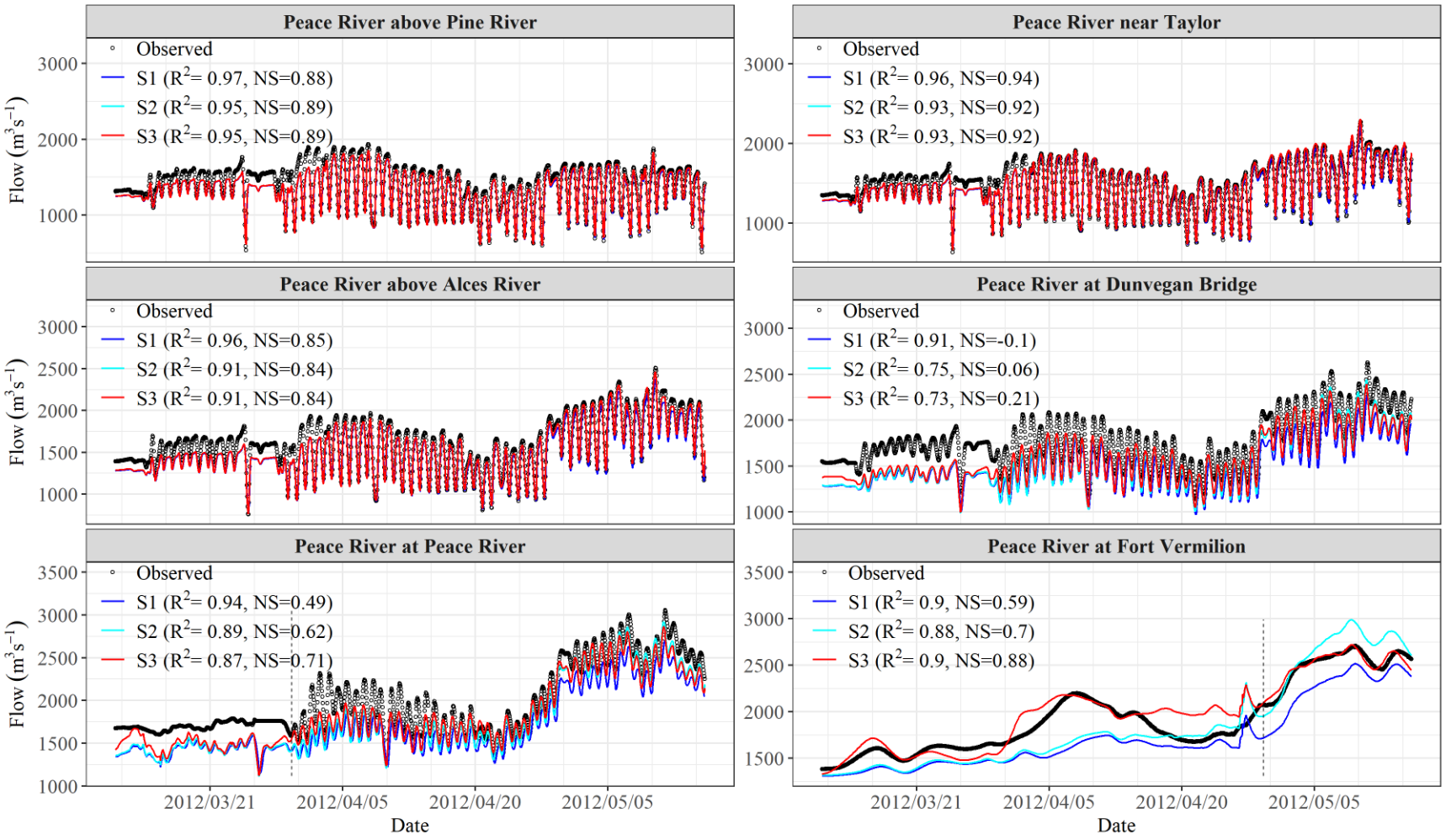


**Figure 4.13** Comparisons of observed and simulated streamflow for the 2012 river ice breakup period (vertical dashed line indicates the rough date when the station is not affected by ice).

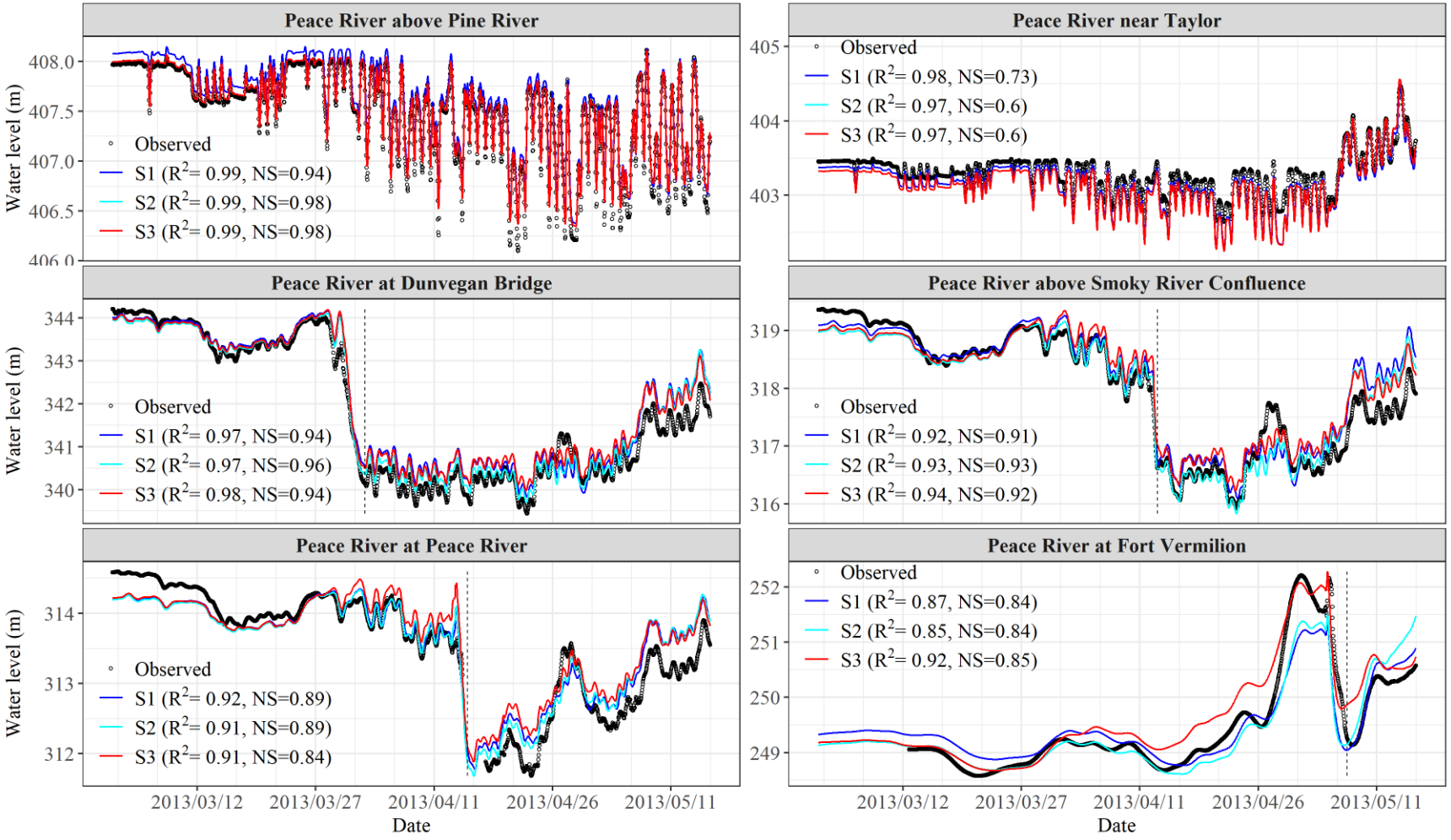


**Figure 4.14** Comparisons of observed and simulated water level for the 2013 river ice breakup period (vertical dashed line indicates the rough date when the station is not affected by ice).

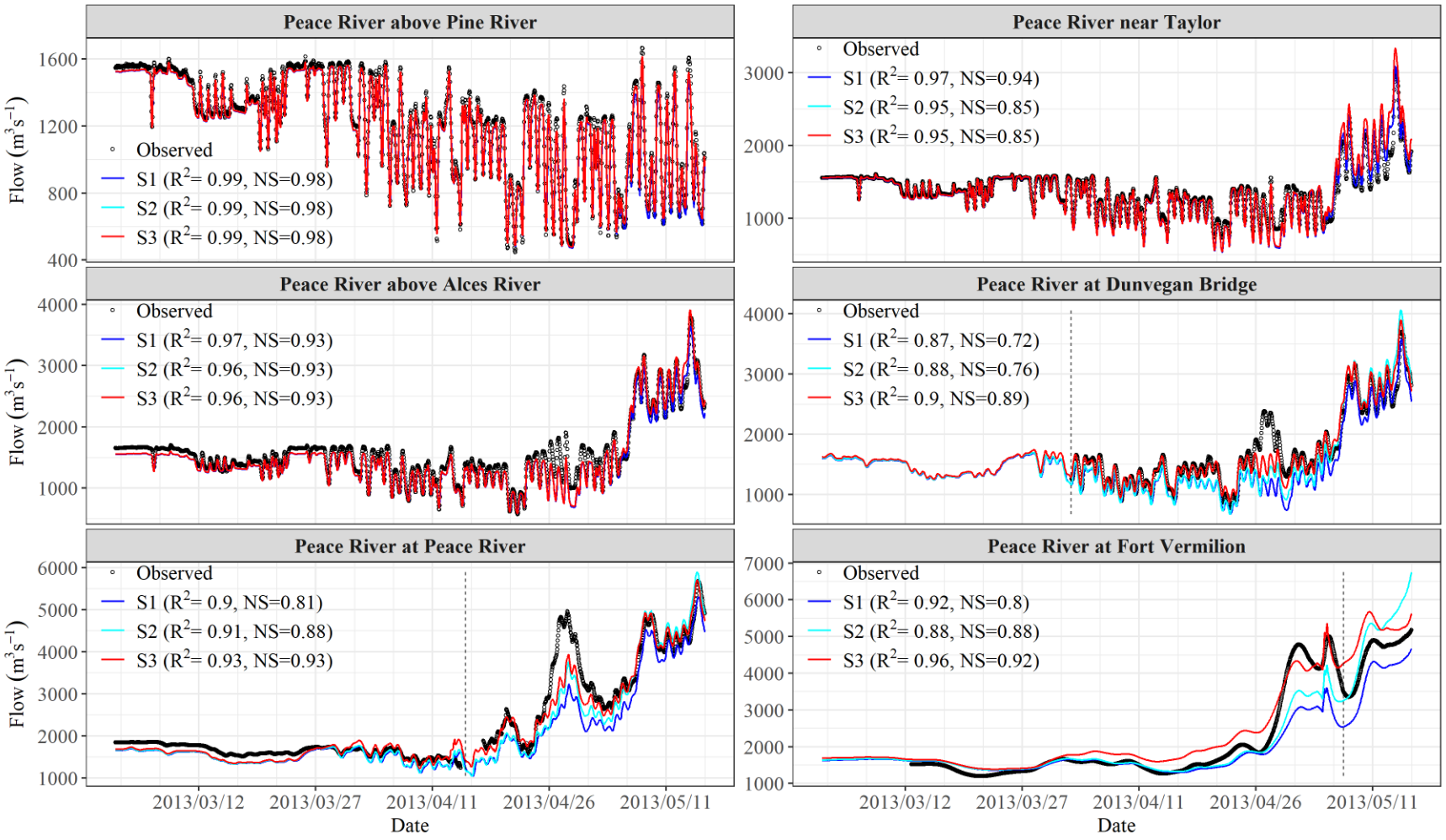


**Figure 4.15** Comparisons of observed and simulated streamflow for the 2013 river ice breakup period (vertical dashed line indicates the rough date when the station is not affected by ice).

### *4.3.3 Streamflow in gauged and ungauged subbasins*

In previous sections, it was demonstrated that the calibrated SWAT model generally performed good in providing inflows for the River1D model. Before the calibrated SWAT model was used to investigate the streamflow contributions of gauged and ungauged subbasins across the PRB, it was further evaluated by comparing the simulated gauged subbasin streamflow in the 14 inflow boundary zones with the corresponding observed data (Table 4.3). Based on the index of multi-year (2004-2013) average annual mean streamflow (MAMS) and annual peak streamflow (MAPS), the streamflow contributions of each inflow boundary zone were roughly quantified. For the observed gauged streamflow, the MAMS index indicated that B01 contributed the most, followed by B09 and B04. However, the most contributing inflow boundary became B09 based on the MAPS. This is because B01 is regulated by the dam and its outflow is reduced during flood season. A similar contributing pattern was also seen in the SWAT model simulated results. The relative errors between the observed and simulated gauged subbasins in each inflow boundary zone were also computed (Table 4.3). The absolute relative errors for the first three most contributing inflow boundaries were less than 35%. The large deviations were often seen in less contributing inflow boundaries. In general, the calibrated SWAT model had a good performance and can provide reasonable streamflow for both gauged and ungauged subbasins across the PRB.

The contribution from the gauged and ungauged subbasins to the peak flow during the simulated open water and river ice breakup periods are shown in Figure 4.16. It is important to note that near the end of each simulated river ice breakup periods the river had returned to open water condition, and these open water periods were excluded when determining the peak flow during river ice breakup. For the non-flood periods, such as the 2012 open water and breakup periods, the ungauged subbasins both contributed about 26% and 27% of the peak flow, respectively. This is

nearly the same as the percentage area of the ungauged subbasins to the whole modelled area, which is ~26.54%. However, the ungauged subbasins contributed 41% to 42% of the peak flow for the 2011 flood period and the mechanical river ice breakup periods (i.e., 2007 and 2013). The inflow boundary zones for which the ungauged area far exceeds the gauged area, such as B07, B08, B11 and B12, contributed a large amount of streamflow for the open water and breakup flood years. Given the peak flow simulated by Scenario 3 during river ice breakup was still underestimated, the ungauged subbasins could have contributed more to the peak flow. This emphasized the importance of considering the ungauged subbasin streamflow when setting up a river ice model or hydraulic model.

**Table 4.3** The summarize of observed and simulated multi-year (2004-2013) average annual mean streamflow (MAMS) and annual peak streamflow (MAPS) for gauged area in each inflow boundary zone.

| Boundary | Station | Gauged Area ($km^2$) | Observed Gauged Streamflow | | | | SWAT Simulated Streamflow | | | | Relative Error (%) | |
|---|---|---|---|---|---|---|---|---|---|---|---|---|
| | | | MAMS ($m^3/s$) | Ratio (%) | MAPS ($m^3/s$) | Ratio (%) | MAMS ($m^3/s$) | Ratio (%) | MAPS ($m^3/s$) | Ratio (%) | MAMS | MAPS |
| B01 | 07EF001 | 70,042 | 1,115.8 | **59.64** | 1,881 | **23.49** | 1,122.7 | **55.12** | 1,879.7 | **26.94** | 0.62 | -0.07 |
| B02 | 07FA006 | 9,238 | 64.4 | 3.44 | 717.5 | **8.96** | 89.2 | 4.38 | 726.9 | **10.42** | 38.44 | 1.30 |
| B03 | 07FB008 | 1,506 | 11.6 | 0.62 | 84.1 | 1.05 | 14.2 | 0.70 | 218.9 | 3.14 | 22.58 | 160.39 |
| B04 | 07FB001 | 11,956 | 190.3 | **10.17** | 1,539.3 | **19.22** | 182.2 | **8.95** | 1,003.1 | **14.38** | -4.27 | -34.84 |
| B05 | 07FC001 | 15,297 | 45.3 | 2.42 | 528.3 | **6.60** | 93.1 | 4.57 | 448.5 | **6.43** | 105.57 | -15.10 |
| B06 | 07FD001 | 3,584 | 9.9 | 0.53 | 167.4 | 2.09 | 19.4 | 0.95 | 128.1 | 1.84 | 95.27 | -23.47 |
| B07 | 07FD009 | 28,40 | 6.2 | 0.33 | 84.5 | 1.05 | 11.8 | 0.58 | 122.8 | 1.76 | 89.82 | 45.43 |
| B08 | 07FD006 | 523 | 1.6 | 0.08 | 36.5 | 0.46 | 4.0 | 0.20 | 59.6 | 0.85 | 153.16 | 63.14 |
| B09 | 07GJ001 | 48,553 | 327.4 | **17.50** | 2,242 | **28.00** | 401.6 | **19.72** | 1,848.1 | **26.49** | 22.66 | -17.57 |
| B10 | 07HA003 | 1,737 | 2.6 | 0.14 | 46.1 | 0.58 | 8.6 | 0.42 | 91.1 | 1.31 | 227.27 | 97.51 |
| B11 | 07HC001 | 4,637 | 10.9 | 0.58 | 158.2 | 1.98 | 8.0 | 0.39 | 29.2 | 0.42 | -26.70 | -81.52 |
| B12 | 07HF002 | 736 | 2.7 | 0.14 | 29.4 | 0.37 | 1.0 | 0.05 | 9.9 | 0.14 | -61.57 | -66.21 |
| B13 | 07JF003 | 2,370 | 15.6 | 0.83 | 104.8 | 1.31 | 11.3 | 0.55 | 112.5 | 1.61 | -27.80 | 7.35 |
| B14 | 07JD002 | 33,044 | 66.7 | 3.57 | 388.3 | 4.85 | 69.8 | 3.43 | 298.7 | 4.28 | 4.62 | -23.07 |

Note: The ratio indicates the percentage of MAMS and MAPS of each boundary gauged area to the total gauged area; the ratio over 5% is indicated in bold; the relative error is computed from the simulated and observed MAMS and MAPS.

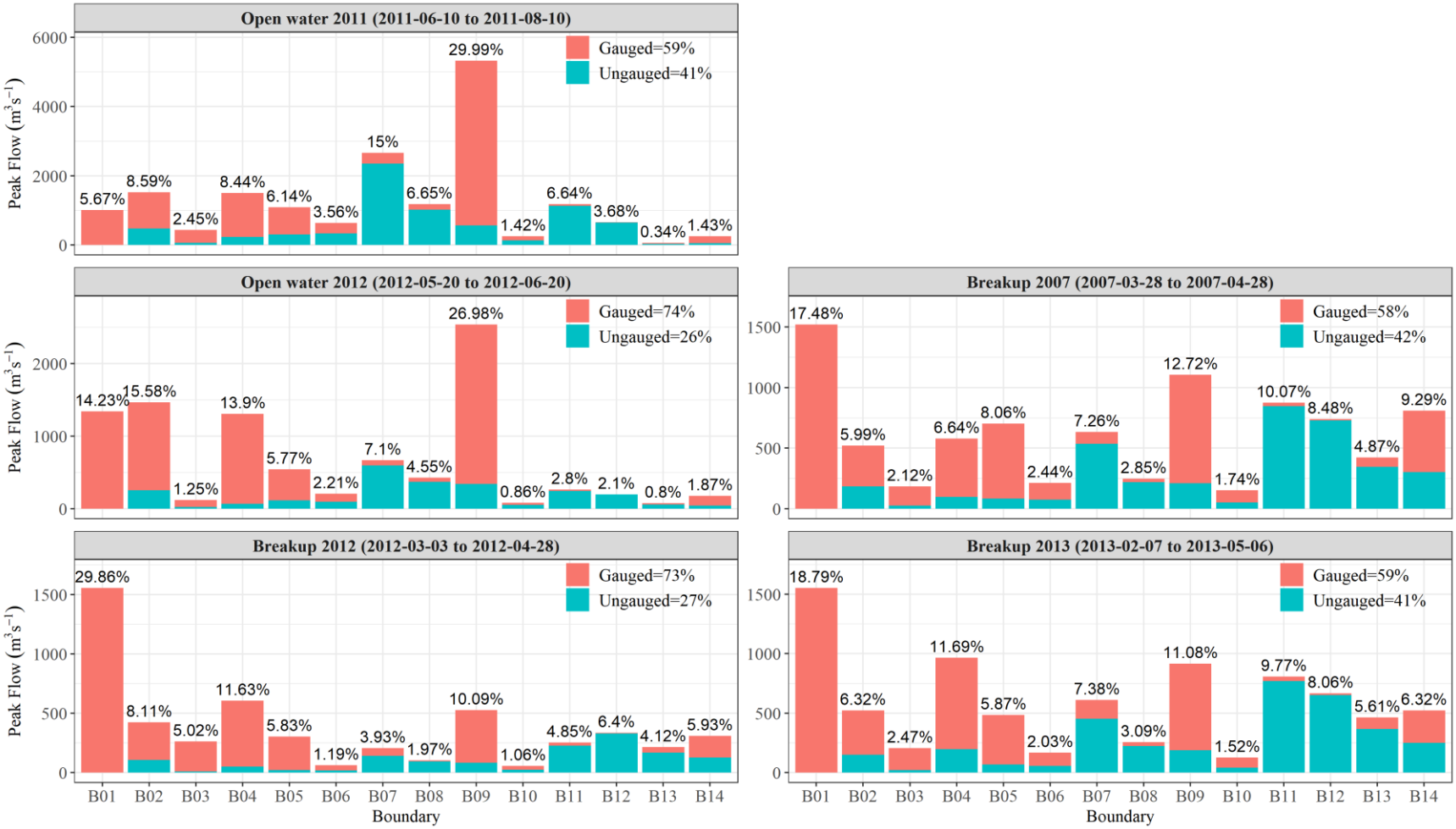


**Figure 4.16** Peak flow contributions of gauged and ungauged subbasins in various inflow boundary zones; the values on top of each column show the peak flow contrition of each inflow boundary zone.

## 4.4 Conclusions and recommendations

This study constructed a hydrologic and river ice modelling framework with SWAT and River1D to investigate the impact of the streamflow from ungauged subbasins on peak flows during open water and river ice breakup periods in the Peace River Basin (PRB). In the framework, the drainage-area ratio (DAR) method and the hydrologic model were employed to estimate the ungauged subbasin streamflow within the PRB and improve the inflow boundaries for the River1D model. Comparing to the simple DAR method, it was shown that the hydrologic model can provide more accurate estimation of the ungauged subbasin streamflow for regions with large ungauged subbasin area during flood events. In particular, the SWAT model outperformed the DAR method for simulating the ungauged streamflow during river ice breakup periods, which is mainly due to the SWAT model can reasonably simulate snow affected streamflow. Nevertheless, there were still some discrepancies because of the uncertainties in both the observed data and model structures. In general, both the DAR method and the hydrologic modelling method can significantly improve the River1D model in capturing the peak flow when the ungauged subbasins within the PRB were fully considered. Meanwhile, the River1D simulation results demonstrated that the streamflow from the ungauged subbasins of the PRB can greatly affect the peak flow simulation of the river ice model for both open water and river ice breakup flood events. Based on the simulated streamflow from the SWAT model, it was found that the ungauged subbasins can contribute to nearly half of the peak flow for the open water and river ice breakup flood events even though they are only about 26.5% of the whole study area. Overall, the findings in this study can contribute to open water and river ice breakup flood simulation, and water resources planning and management in the Peace River Basin. The proposed methods also can provide insights on modelling flood events in other ungauged or partially ungauged basins.

The hydrologic and river ice modelling framework can be a useful tool for forecasting snow and ice related flood events. The hydrologic model can provide necessary inflow boundaries for the river ice model while the channel routing method used in the river ice model can be used to simulate the ice affected streamflow. In this study, the river ice breakup conditions were only considered in the mainstream of the Peace River. The effects of river ice breakup on streamflow should be considered in the whole Peace River networks through deeply coupling the physics-based river ice models with hydrologic models in future work, to better simulate snow and ice affected spring streamflow. The SWAT model developed in this study can only provide daily scale streamflow which is probably not enough for capturing the more dynamic flood events such as those associated with mechanical breakup. The hydrologic model with the capability of providing high temporal resolution streamflow data in large cold-region watersheds should be developed in future studies. Calibrating a sub-daily hydrologic model in a large river basin can be super computationally expensive and time consuming. Therefore, more efforts should also be devoted into improving the efficiency of hydrologic model calibration. The ability of river ice models for simulating the onset of the mechanical breakup and determining whether, when and where an ice jam may form can be further developed. Furthermore, the uncertainties in the observed streamflow data due to ice effects will need to be reduced in order to better calibrate and validate the modelling framework.

## 4.5 Reference

Abbaspour, K.C., 2015. SWAT Calibration and Uncertainty Programs—A User Manual. Swiss Fed. Inst. Aquat. Sci. Technol. Eawag, Switz.

Andres, D., 1996. Ice formation and breakup at the Town of Peace River-a study of regulated conditions, 1969-1994. A Rep. Prep. T. Peace River, BC Hydro Alberta Environ. Prot. by Trillium Eng. Hydrogr. Inc., Northwest Hydraul. Consult. Ltd. Thurber Eng. Ltd.

Andrishak, R., Hicks, F., 2008. Simulating the effects of climate change on the ice regime of the Peace River. Can. J. Civ. Eng. 35, 461–472. https://doi.org/10.1139/L07-129

Arnold, J.G., Srinivasan, R., Muttiah, R.S., Williams, J.R., 1998. Large area hydrologic modeling and assesment Part I: Model development. JAWRA J. Am. Water Resour. Assoc. 34, 73–89. https://doi.org/10.1111/j.1752-1688.1998.tb05961.x

Asquith, W.H., Roussel, M.C., Vrabel, J., 2006. Statewide analysis of the drainage-area ratio method for 34 streamflow percentile ranges in Texas. US Geological Survey.

Beltaos, S., 2008. Progress in the study and management of river ice jams. Cold Reg. Sci. Technol. 51, 2–19. https://doi.org/10.1016/j.coldregions.2007.09.001

Beltaos, S., Prowse, T., 2009. River‐ice hydrology in a shrinking cryosphere. Hydrol. Process. 23, 122‐144.

Beltaos, S., Prowse, T.D., 2001. Climate impacts on extreme ice-jam events in Canadian rivers. Hydrol. Sci. J. 46, 157–181. https://doi.org/10.1080/02626660109492807

Blackburn, J., Hicks, F.E., 2002. Combined flood routing and flood level forecasting. Can. J. Civ.

Eng. 29, 64–75.

Blackburn, J., She, Y., 2021. One-dimensional channel network modelling and simulation of flow conditions during the 2008 ice breakup in the Mackenzie Delta, Canada. Cold Reg. Sci. Technol. 189, 103339. https://doi.org/10.1016/j.coldregions.2021.103339

Blackburn, J., She, Y., 2019. A comprehensive public-domain river ice process model and its application to a complex natural river. Cold Reg. Sci. Technol. 163, 44–58. https://doi.org/10.1016/j.coldregions.2019.04.010

Blöschl, G., Sivapalan, M., 1995. Scale issues in hydrological modelling: a review. Hydrol. Process. 9, 251–290.

Bonnifait, L., Delrieu, G., Lay, M. Le, Boudevillain, B., Masson, A., Belleudy, P., Gaume, E., Saulnier, G.M., 2009. Distributed hydrologic and hydraulic modelling with radar rainfall input: Reconstruction of the 8-9 September 2002 catastrophic flood event in the Gard region, France. Adv. Water Resour. 32, 1077–1089. https://doi.org/10.1016/j.advwatres.2009.03.007

Booker, D.J., Woods, R.A., 2014. Comparing and combining physically-based and empirically-based approaches for estimating the hydrology of ungauged catchments. J. Hydrol. 508, 227–239. https://doi.org/10.1016/j.jhydrol.2013.11.007

Burrell, B.C., Beltaos, S., Turcotte, B., 2021. Effects of Climate Change on River-Ice Processes and Ice Jams. Int. J. River Basin Manag. 1–78. https://doi.org/10.1080/15715124.2021.2007936

Chen, F., Shen, H.T., Jayasundara, N., 2006. A one-dimensional comprehensive river ice model,

in: Proceedings of 18th International Association of Hydraulic Research Symposium on Ice, Sapporo, Japan. Citeseer.

Das, A., Rokaya, P., Lindenschmidt, K.E., 2020. Ice-Jam Flood Risk Assessment and Hazard Mapping under Future Climate. J. Water Resour. Plan. Manag. 146, 1–12. https://doi.org/10.1061/(ASCE)WR.1943-5452.0001178

De Rham, L., Dibike, Y., Beltaos, S., Peters, D., Bonsal, B., Prowse, T., 2020. A Canadian River Ice Database from the National Hydrometric Program Archives. Earth Syst. Sci. Data 12, 1835–1860. https://doi.org/10.5194/essd-12-1835-2020

Dessie, M., Verhoest, N.E.C., Pauwels, V.R.N., Adgo, E., Deckers, J., Poesen, J., Nyssen, J., 2015. Water balance of a lake with floodplain buffering: Lake Tana, Blue Nile Basin, Ethiopia. J. Hydrol. 522, 174–186. https://doi.org/10.1016/j.jhydrol.2014.12.049

Emerson, D.G., Vecchia, A. V, Dahl, A.L., 2005. Evaluation of drainage-area ratio method used to estimate streamflow for the Red River of the North Basin, North Dakota and Minnesota. US Department of the Interior, US Geological Survey.

Ergen, K., Kentel, E., 2016. An integrated map correlation method and multiple-source sites drainage-area ratio method for estimating streamflows at ungauged catchments: A case study of the Western Black Sea Region, Turkey. J. Environ. Manage. 166, 309–320. https://doi.org/10.1016/j.jenvman.2015.10.036

French, H.M., 2017. The periglacial environment. John Wiley & Sons.

Gianfagna, C.C., Johnson, C.E., Chandler, D.G., Hofmann, C., 2015. Watershed area ratio

accurately predicts daily streamflow in nested catchments in the Catskills, New York. J. Hydrol. Reg. Stud. 4, 583–594. https://doi.org/10.1016/j.ejrh.2015.09.002

Grimaldi, S., Schumann, G.J.P., Shokri, A., Walker, J.P., Pauwels, V.R.N., 2019. Challenges, Opportunities, and Pitfalls for Global Coupled Hydrologic-Hydraulic Modeling of Floods. Water Resour. Res. 55, 5277–5300. https://doi.org/10.1029/2018WR024289

Guo, Y., Zhang, Y., Zhang, L., Wang, Z., 2021. Regionalization of hydrological modeling for predicting streamflow in ungauged catchments: A comprehensive review. Wiley Interdiscip. Rev. Water 8, 1–32. https://doi.org/10.1002/wat2.1487

He, Y., Bárdossy, A., Zehe, E., 2011. A review of regionalisation for continuous streamflow simulation. Hydrol. Earth Syst. Sci. 15, 3539–3553. https://doi.org/10.5194/hess-15-3539-2011

Hersbach, H., Bell, B., Berrisford, P., Hirahara, S., Horányi, A., Muñoz-Sabater, J., Nicolas, J., Peubey, C., Radu, R., Schepers, D., Simmons, A., Soci, C., Abdalla, S., Abellan, X., Balsamo, G., Bechtold, P., Biavati, G., Bidlot, J., Bonavita, M., De Chiara, G., Dahlgren, P., Dee, D., Diamantakis, M., Dragani, R., Flemming, J., Forbes, R., Fuentes, M., Geer, A., Haimberger, L., Healy, S., Hogan, R.J., Hólm, E., Janisková, M., Keeley, S., Laloyaux, P., Lopez, P., Lupu, C., Radnoti, G., de Rosnay, P., Rozum, I., Vamborg, F., Villaume, S., Thépaut, J.N., 2020. The ERA5 global reanalysis. Q. J. R. Meteorol. Soc. 146, 1999–2049. https://doi.org/10.1002/qj.3803

Hicks, F.E., 1996. Hydraulic flood routing with minimal channel data: Peace River, Canada. Can. J. Civ. Eng. 23, 524–535. https://doi.org/10.1139/l96-057

Hicks, F.E., Steffler, P.M., 1992. Characteristic dissipative Galerkin scheme for open-channel flow. J. Hydraul. Eng. 118, 337–352.

Hicks, F.E., Steffler, P.M., 1990. Finite element modeling of open channel flow. Department of Civil Engineering, University of Alberta, Edmonton, Alta. Water Resour. Eng. Rep.

Hrachowitz, M., Savenije, H.H.G., Blöschl, G., McDonnell, J.J., Sivapalan, M., Pomeroy, J.W., Arheimer, B., Blume, T., Clark, M.P., Ehret, U., Fenicia, F., Freer, J.E., Gelfan, A., Gupta, H. V., Hughes, D.A., Hut, R.W., Montanari, A., Pande, S., Tetzlaff, D., Troch, P.A., Uhlenbrook, S., Wagener, T., Winsemius, H.C., Woods, R.A., Zehe, E., Cudennec, C., 2013. A decade of Predictions in Ungauged Basins (PUB)-a review. Hydrol. Sci. J. 58, 1198–1255. https://doi.org/10.1080/02626667.2013.803183

Huang, F., Jasek, M., Shen, H.T., 2021. Simulation of the 2014 Dynamic Ice Breakup on the Peace River 1–19.

Krause, P., Boyle, D.P., Bäse, F., 2005. Comparison of different efficiency criteria for hydrological model assessment. Adv. Geosci. 5, 89–97. https://doi.org/10.5194/adgeo-5-89-2005

Li, Q., Peng, Y., Wang, G., Wang, H., Xue, B., Hu, X., 2019. A combined method for estimating continuous runoff by parameter transfer and drainage area ratio method in ungauged catchments. Water 11, 1104.

Li, W., Lin, K., Zhao, T., Lan, T., Chen, X., Du, H., Chen, H., 2019. Risk assessment and sensitivity analysis of flash floods in ungauged basins using coupled hydrologic and hydrodynamic models. J. Hydrol. 572, 108–120. https://doi.org/10.1016/j.jhydrol.2019.03.002

Lindenschmidt, K.E., 2017. RIVICE-A non-proprietary, open-source, one-dimensional river-ice model. Water (Switzerland) 9. https://doi.org/10.3390/w9050314

Lindenschmidt, K.E., Rokaya, P., Das, A., Li, Z., Richard, D., 2019. A novel stochastic modelling approach for operational real-time ice-jam flood forecasting. J. Hydrol. 575, 381–394. https://doi.org/10.1016/j.jhydrol.2019.05.048

Liu, G., Schwartz, F.W., Tseng, K., Shum, C.K., 2015. Discharge and water‐depth estimates for ungauged rivers: Combining hydrologic, hydraulic, and inverse modeling with stage and water‐area measurements from satellites. Water Resour. Res. 51, 6017‐6035.

Liu, L., Li, H., Shen, H.T., 2006. A Two-Dimensional Comprehensive River Ice Model. Proc. 18th IAHR Int. Symp. Ice 69–76.

McCuen, R.H., Levy, B.S., 2000. Evaluation of peak discharge transposition. J. Hydrol. Eng. 5, 278–289.

Merz, B., Blöschl, G., Vorogushyn, S., Dottori, F., Aerts, J.C.J.H., Bates, P., Bertola, M., Kemter, M., Kreibich, H., Lall, U., 2021. Causes, impacts and patterns of disastrous river floods. Nat. Rev. Earth Environ. 2, 592–609.

Mishra, A., Mukherjee, S., Merz, B., Singh, V.P., Wright, D.B., Villarini, G., Paul, S., Kumar, D.N., Khedun, C.P., Niyogi, D., Schumann, G., Stedinger, J.R., 2022. An Overview of Flood Concepts, Challenges, and Future Directions. J. Hydrol. Eng. 27, 1–30. https://doi.org/10.1061/(asce)he.1943-5584.0002164

Mishra, A.K., Coulibaly, P., 2009. Developments in hydrometric network design: A review. Rev.

Geophys. 47.

Moriasi, D.N., Gitau, M.W., Pai, N., Daggupati, P., 2015. Hydrologic and water quality models: Performance measures and evaluation criteria. Trans. ASABE 58, 1763–1785. https://doi.org/10.13031/trans.58.10715

Neitsch, S.., Arnold, J.., Kiniry, J.., Williams, J.., 2011. Soil & Water Assessment Tool Theoretical Documentation Version 2009. Texas Water Resour. Inst. 1–647. https://doi.org/10.1016/j.scitotenv.2015.11.063

Nguyen, P., Thorstensen, A., Sorooshian, S., Hsu, K., AghaKouchak, A., Sanders, B., Koren, V., Cui, Z., Smith, M., 2016. A high resolution coupled hydrologic–hydraulic model (HiResFlood-UCI) for flash flood modeling. J. Hydrol. 541, 401–420. https://doi.org/10.1016/j.jhydrol.2015.10.047

Pagliero, L., Bouraoui, F., Diels, J., Willems, P., McIntyre, N., 2019. Investigating regionalization techniques for large-scale hydrological modelling. J. Hydrol. 570, 220–235. https://doi.org/10.1016/j.jhydrol.2018.12.071

Parajka, J., Viglione, A., Rogger, M., Salinas, J.L., Sivapalan, M., Blöschl, G., 2013. Comparative assessment of predictions in ungauged basins-Part 1: Runoff-hydrograph studies. Hydrol. Earth Syst. Sci. 17, 1783–1795. https://doi.org/10.5194/hess-17-1783-2013

Razavi, T., Coulibaly, P., 2013. Streamflow Prediction in Ungauged Basins: Review of Regionalization Methods. J. Hydrol. Eng. 18, 958–975. https://doi.org/10.1061/(asce)he.1943-5584.0000690

Salinas, J.L., Laaha, G., Rogger, M., Parajka, J., Viglione, A., Sivapalan, M., Blöschl, G., 2013. Comparative assessment of predictions in ungauged basins-Part 2: Flood and low flow studies. Hydrol. Earth Syst. Sci. 17, 2637–2652. https://doi.org/10.5194/hess-17-2637-2013

She, Y., Andrishak, R., Hicks, F., Morse, B., Stander, E., Krath, C., Keller, D., Abarca, N., Nolin, S., Tanekou, F.N., Mahabir, C., 2009. Athabasca River ice jam formation and release events in 2006 and 2007. Cold Reg. Sci. Technol. 55, 249–261. https://doi.org/10.1016/j.coldregions.2008.02.004

She, Y., Hicks, F., 2006. Modeling ice jam release waves with consideration for ice effects. Cold Reg. Sci. Technol. 45, 137–147. https://doi.org/10.1016/j.coldregions.2006.05.004

Shen, H.T., 2010. Mathematical modeling of river ice processes. Cold Reg. Sci. Technol. 62, 3–13. https://doi.org/10.1016/j.coldregions.2010.02.007

Singh, L., Mishra, P.K., Pingale, S.M., Khare, D., Thakur, H.P., 2022. Streamflow regionalisation of an ungauged catchment with machine learning approaches. Hydrol. Sci. J. 67, 886–897. https://doi.org/10.1080/02626667.2022.2049271

Sivapalan, M., 2003. Prediction in ungauged basins: a grand challenge for theoretical hydrology. Hydrol. Process. 17, 3163–3170.

Sivapalan, M., Takeuchi, K., Franks, S.W., Gupta, V.K., Karambiri, H., Lakshmi, V., Liang, X., McDonnell, J.J., Mendiondo, E.M., O'Connell, P.E., Oki, T., Pomeroy, J.W., Schertzer, D., Uhlenbrook, S., Zehe, E., 2003. IAHS Decade on Predictions in Ungauged Basins (PUB), 2003-2012: Shaping an exciting future for the hydrological sciences. Hydrol. Sci. J. 48, 857–880. https://doi.org/10.1623/hysj.48.6.857.51421

Taggart, J., 1995. The Peace River natural flow and regulated flow scenarios-daily flow data report. Surf. Water Assess. Branch, Alberta Environ. Prot. Edmonton, AB.

Tellman, B., Sullivan, J.A., Kuhn, C., Kettner, A.J., Doyle, C.S., Brakenridge, G.R., Erickson, T.A., Slayback, D.A., 2021. Satellite imaging reveals increased proportion of population exposed to floods. Nature 596, 80–86. https://doi.org/10.1038/s41586-021-03695-w

Thériault, I., Saucet, J.-P., Taha, W., 2010. Validation of the Mike-Ice model simulating river flows in presence of ice and forecast of changes to the ice regime of the Romaine river due to hydroelectric project, in: Proceedings of the 20th IAHR International Symposium on Ice, Lahti, Finland. pp. 14–17.

Timalsina, N.P., Charmasson, J., Alfredsen, K.T., 2013. Simulation of the ice regime in a Norwegian regulated river. Cold Reg. Sci. Technol. 94, 61–73. https://doi.org/10.1016/j.coldregions.2013.06.010

Turcotte, B., Burrell, B.C., Beltaos, S., 2019. The Impact of Climate Change on Breakup Ice Jams in Canada : State of knowledge and research approaches.

Turcotte, B., Rainville, F., 2022. A new winter discharge estimation procedure: Yukon proof of concept, in: In 26th IAHR International Symposium on Ice, Montréal, Canada.

Viglione, A., Parajka, J., Rogger, M., Salinas, J.L., Laaha, G., Sivapalan, M., Blöschl, G., 2013. Comparative assessment of predictions in ungauged basins - Part 3: Runoff signatures in Austria. Hydrol. Earth Syst. Sci. 17, 2263–2279. https://doi.org/10.5194/hess-17-2263-2013

Winchell, M., Srinivasan, R., Di Luzio, M., Arnold, J., 2013. ArcSWAT interface for SWAT2012:

User's guide. Blackl. Res. Center, Texas AgriLife Res. Coll. Stn. 1–464.

Ye, Y., She, Y., 2021. A systematic evaluation of criteria for river ice breakup initiation using River1D model and field data. Cold Reg. Sci. Technol. 189, 103316. https://doi.org/10.1016/j.coldregions.2021.103316

Zelelew, M.B., Alfredsen, K., 2014. Use of Cokriging and Map Correlation to Study Hydrological Response Patterns and Select Reference Stream Gauges for Ungauged Catchments. J. Hydrol. Eng. 19, 388–406. https://doi.org/10.1061/(asce)he.1943-5584.0000803

Zhang, L., Lu, J., Chen, X., Liang, D., Fu, X., Sauvage, S., Perez, J.M.S., 2017. Stream flow simulation and verification in ungauged zones by coupling hydrological and hydrodynamic models: A case study of the Poyang Lake ungauged zone. Hydrol. Earth Syst. Sci. 21, 5847–5861. https://doi.org/10.5194/hess-21-5847-2017

Zhang, Y., Chiew, F.H.S., 2009. Relative merits of different methods for runoff predictions in ungauged catchments. Water Resour. Res. 45. https://doi.org/10.1029/2008WR007504

# Chapter 5. Conclusions and Recommendations

## 5.1 Summary and conclusions

Both the observed and projected warming in Canada are about double the magnitude of the average global warming (Bush and Lemmen, 2019), which can greatly affect the snow and river ice regime, as well as the timing and magnitude of snow and ice induced spring peak flow. A good understanding of river ice breakup and a reliable prediction of snowmelt and river ice breakup induced spring peak flow is vital in helping cold region communities mitigate snow and ice related damages and adapt to climate change. This study investigated the trends and drivers of river ice breakup timing through constructing and analyzing long-term river ice breakup timing data across Canada, and improved snow and ice affected spring streamflow in a large cold-region river basin, the Peace River Basin (PRB) in western Canada, through the development and application of the physics-based hydrologic model SWAT and the river ice model River1D.

This study provides several key original contributions as follows:

1. Constructed a long-term and uniform dataset of river ice breakup timing for Canada and investigated the breakup timing patterns and how various factors (e.g., climatic factors, elevation and flow regulation) affect river ice breakup over Canada. This study provided evidence for climate change and theoretical support for modelling river ice breakup processes.

2. Proposed a multi-objective hydrologic model calibration framework that can automatically remove unrealistic snow parameter combinations and calibrate streamflow and Snow Water Equivalent (SWE) simultaneously. The proposed multi-objective calibration framework

effectively limited the uncertainty of snow-related parameters and provided better prediction of snow-affected spring streamflow in the PRB. It can be applied in other snow-dominated river basins to help improve the simulation of snow affected spring streamflow. This study evaluated various climate data sources and calibration schemes, which can help limit and/or reduce the uncertainties/errors of model inputs and calibrations and provide insights in modelling cold region river basins and calibrating hydrologic models.

3. Constructed a hydrologic and river ice modelling framework and improved the snow and ice affected peak streamflow though properly considering and estimating ungauged subbasin streamflow in the PRB. The study greatly contributes to open water and river ice breakup flood simulation, and water resources planning and management in the PRB. The hydrologic and river ice modelling framework developed in this study can be applied to other cold region river basins to investigate impacts of the ungauged subbasins and/or forecast snow and ice induced flood events.

The details of these contributions were discussed and presented below.

### *5.1.1 Trends and drivers of river ice breakup timing across Canada*

River ice records often differ in length, observation site, and documented event among various sources, making large-scale spatial and temporal analyses challenging and scarce. In Chapter 2, nearly 200 hydrometric stations form Water Survey of Canada HYDAT database were used to construct a long record of river ice breakup timing from 1950 to 2016. Based on the constructed river ice breakup timing dataset, the spatial and temporal variations of river ice breakup timing over terrestrial ecozones and five selected river basins of Canada were explored, and the drivers, such as air temperature, rainfall, snowfall, elevation and human activities, behind the identified

breakup patterns were analyzed. Like previous studies (Fu and Yao, 2015; Lacroix et al., 2005; Obyazov and Smakhtin, 2014; Zhang et al., 2001), it was found that Canada presented a general earlier breakup trend and the air temperature was the most contributing factor behind the river ice breakup. However, this research found that the river ice breakup timing was mainly correlated with spring air temperature even though the winter warming trend across Canada was the most pronounced. Less strong and/or weak spring warming trend can even result in many stations showing later and significant later breakup in some periods. Spring snowfall usually delayed breakup while rainfall can both advance and delay breakup depending on whether they were in spring or winter. Breakup timing appeared to be more sensitive to climatic warming in lower latitude regions than in higher latitude regions likely due to the increased snowfall in the north and increased rainfall in the south. In comparison with main streams and large rivers, river ice breakup in headwaters and small tributaries was found to be more sensitive to climate change. Elevation and human activities (e.g., flow regulation and fragmentation) also contributed to the changes of river ice breakup. Chapter 2 provides a way for researchers to construct long-time and uniform records of river ice breakup timing, and an opportunity to conduct large-scale spatial and temporal analyses of breakup timing trends. Moreover, the findings from Chapter 2 can provide evidence for climate change, and theoretical support for modelling the river ice breakup processes.

### *5.1.2 The effects of climate data inputs and model calibration on streamflow simulation*

Chapter 3 aimed to improve the performance of the hydrologic model in simulating snow affected spring streamflow in a large-scale regulated and snow-dominated river basin (PRB). Through the application and modifications of the hydrologic model SWAT and the calibration tool SWATCUP, Chapter 3 (1) evaluated the observed and two commonly used gridded climate data, (2) proposed a multi-objective calibration framework that can automatically remove unrealistic snow parameter

combinations, and calibrate both streamflow and subbasin-scale SWE, and (3) investigated the uncertainties of various model calibration schemes, such as the choice of objective functions, number of simulations, single-objective (streamflow) versus multi-objective calibration (streamflow and SWE). The results showed that the gridded ERA5 climate data performed the best in driving the SWAT model in the PRB. The proposed multi-objective calibration framework was shown to effectively limit the uncertainty of snow-related parameters and provide better prediction of snow-affected spring streamflow in the PRB. It has a good potential to be applied in other snow-dominated river basins to help improve the simulation of snow affected spring streamflow. The workflow of evaluating climate data sources and calibration schemes developed in this study can help limit and/or reduce the uncertainties/errors of model inputs and calibrations and provide insights for researchers in modelling cold region river basins and calibrating the hydrologic models.

### *5.1.3 A hydrologic and river ice modeling framework for assessing the impact of ungauged subbasins on open water and river ice breakup peak flow*

Work towards improving the simulation of snow and ice induced spring peak flow, and particularly reliable estimation of ungauged subbasin streamflow, through the hydrologic and river ice modelling framework are challenging and in great demand. In the proposed modelling framework, the hydrologic model is used to simulate streamflow and provide inflow boundaries for the river ice model while the river ice model is utilized to simulate ice affected streamflow and water levels. Based on the hydrologic model SWAT and the river ice model River1D, Chapter 4 explored the effects of ungauged subbasin streamflow on peak flow simulation under open water and rive ice breakup conditions in the PRB. The results showed that the simple drainage-area ratio (DAR) method had a large uncertainty in estimating the ungauged subbasin streamflow (especially during river ice breakup period) while the sophisticated hydrologic model SWAT can be a promising and robust tool for estimating ungauged subbasin streamflow for the river ice model. It was found that

the peak flow simulation was significantly improved when the ungauged subbasin streamflow was properly considered and/or estimated. Moreover, the ungauged subbasins of the PRB can contribute nearly half of the peak flow for the open water and river ice breakup flood events with around a quarter of the whole modelled area. The findings from Chapter 4 are of great importance to open water and river ice breakup flood simulation, and water resources planning and management in the PRB. The hydrologic and river ice modelling framework developed in this study can be applied into other cold region river basins to investigate the impact of the ungauged subbasins and/or forecast snow and ice induced flood events.

## 5.2 Recommendations for future work

The large-scale teleconnections, such as El Niño/Southern Oscillation (ENSO), the Pacific Decadal Oscillation (PDO), the Pacific North American (PNA) pattern, the North Pacific (NP) index, the North Atlantic Oscillation (NAO), and the Arctic Oscillation (AO), could also greatly impact river ice breakup dates (Bonsal et al., 2006, 2005). The impacts of large-scale teleconnections on the river ice breakup timing across Canada should be analyzed based on the constructed long-time and uniform river ice breakup timing records (1950-2016) in the future.

The breakup of the ice cover is a common hydrological regime in cold region rivers. However, river ice breakup processes are seldom considered in hydrologic models due to their complex thermal and dynamic processes and the simplicity of river geometries in hydrologic models. River ice models can consider the detailed physical characteristics of river geometries, provide better flow routing methods for both open water and river ice breakup periods and simulate various river ice processes (Blackburn and Hicks, 2003, 2002; Blackburn and She, 2019). The effects of river ice breakup on streamflow in the whole Peace River and tributary networks should be considered through deeper coupling of the physics-based river ice models with hydrologic models

in future work, to better simulate snow and ice affected spring streamflow.

The hydrologic modelling was conducted on a daily scale in this study, which may not be adequate for capturing highly dynamic flood events. There have been many studies to simulate sub-daily hydrological process with the SWAT model and the calibration tool SWAT-CUP (Koltsida et al., 2021; Maharjan et al., 2013; Meaurio et al., 2021; Shannak, 2017; Yang et al., 2016; Yu et al., 2018). However, these studies mainly focused on simulating and calibrating sub-daily streamflow in small-scale river basins. More work will need to be done for modifying the SWAT model and developing and/or improving the calibration tool before applying to large-scale regulated snow-dominated river basins. For example, the reservoir module in the SWAT model is specific for simulating daily or larger scale streamflow (Neitsch et al., 2011), and thus will need to be modified for better simulating sub-daily streamflow. To limit the uncertainty of snow-related parameters in the SWAT model, Chapter 3 realized automatic multi-objective calibration with both daily streamflow and subbasin-scale SWE but new calibration tool will need to be developed to calibrate sub-daily streamflow with SWE. In addition, calibrating a sub-daily hydrologic model in a large river basin can be computationally expensive and time consuming. Therefore, more efforts should also be devoted into improving the efficiency of calibrating the hydrologic models.

Existing river ice models have some limitations in simulating mechanical river ice breakup, mainly in terms of predicting the onset of the mechanical breakup, whether, when and where an ice jam may form (Shen, 2010). River ice models still evolve along with the progress in theory. Future work should go toward advancing the development of the River1D and improving its capability of simulating mechanical breakup events and in a more automatic way.

## 5.3 Reference

Blackburn, J., Hicks, F., 2003. Suitability of dynamic modeling for flood forecasting during ice jam release surge events. J. Cold Reg. Eng. 17, 18–36. https://doi.org/10.1061/(ASCE)0887-381X(2003)17:1(18)

Blackburn, J., Hicks, F.E., 2002. Combined flood routing and flood level forecasting. Can. J. Civ. Eng. 29, 64–75.

Blackburn, J., She, Y., 2019. A comprehensive public-domain river ice process model and its application to a complex natural river. Cold Reg. Sci. Technol. 163, 44–58. https://doi.org/10.1016/j.coldregions.2019.04.010

Bonsal, B.R., Prowse, T.D., Duguay, C.R., Lacroix, M.P., 2006. Impacts of large-scale teleconnections on freshwater-ice break/freeze-up dates over Canada. J. Hydrol. 330, 340–353. https://doi.org/10.1016/j.jhydrol.2006.03.022

Bonsal, B.R., Prowse, T.D., Duguay, C.R., Lacroix, M.P., 2005. Impacts of Large-Scale Teleconnections on River-Ice Duration over Canada.

Bush, E., Lemmen, D.S., 2019. Canada's changing climate report. Government of Canada= Gouvernement du Canada.

Fu, C., Yao, H., 2015. Trends of ice breakup date in south‐central Ontario. J. Geophys. Res. Atmos. 120, 9220–9236.

Koltsida, E., Mamassis, N., Kallioras, A., 2021. Hydrological modeling using the SWAT Model in urban and peri- urban environments : The case of Kifissos experimental sub-basin. Hydrol.

Earth Syst. Sci. 1–24.

Lacroix, M.P., Prowse, T.D., Bonsal, B.R., Duguay, C.R., Ménard, P., 2005. River ice trends in Canada, in: 13th Workshop on the Hydraulics of Ice Covered Rivers. pp. 41–55.

Maharjan, G.R., Park, Y.S., Kim, N.W., Shin, D.S., Choi, J.W., Hyun, G.W., Jeon, J.H., Ok, Y.S., Lim, K.J., 2013. Evaluation of SWAT sub-daily runoff estimation at small agricultural watershed in Korea. Front. Environ. Sci. Eng. China 7, 109–119. https://doi.org/10.1007/s11783-012-0418-7

Meaurio, M., Zabaleta, A., Srinivasan, R., Sauvage, S., Sánchez-Pérez, J.M., Lechuga-Crespo, J.L., Antiguedad, I., 2021. Long-term and event-scale sub-daily streamflow and sediment simulation in a small forested catchment. Hydrol. Sci. J. 66, 862–873. https://doi.org/10.1080/02626667.2021.1883620

Neitsch, S.., Arnold, J.., Kiniry, J.., Williams, J.., 2011. Soil & Water Assessment Tool Theoretical Documentation Version 2009. Texas Water Resour. Inst. 1–647. https://doi.org/10.1016/j.scitotenv.2015.11.063

Obyazov, V.A., Smakhtin, V.K., 2014. Ice regime of Transbaikalian rivers under changing climate. Water Resour. 41, 225–231. https://doi.org/10.1134/S0097807814030130

Shannak, S., 2017. Calibration and validation of SWAT for sub-hourly time steps using SWAT-CUP. Int. J. Sustain. Water Environ. Syst. 9, 21–27.

Shen, H.T., 2010. Mathematical modeling of river ice processes. Cold Reg. Sci. Technol. 62, 3–13. https://doi.org/10.1016/j.coldregions.2010.02.007

Yang, X., Liu, Q., He, Y., Luo, X., Zhang, X., 2016. Comparison of daily and sub-daily SWAT models for daily streamflow simulation in the Upper Huai River Basin of China. Stoch. Environ. Res. Risk Assess. 30, 959–972. https://doi.org/10.1007/s00477-015-1099-0

Yu, D., Xie, P., Dong, X., Hu, X., Liu, J., Li, Y., Peng, T., Ma, H., Wang, K., Xu, S., 2018. Improvement of the SWAT model for event-based flood simulation on a sub-daily timescale. Hydrol. Earth Syst. Sci. 22, 5001–5019. https://doi.org/10.5194/hess-22-5001-2018

Zhang, X., David Harvey, K., Hogg, W.D., Yuzyk, T.R., 2001. Trends in Canadian streamflow. Water Resour. Res. 37, 987–998. https://doi.org/10.1029/2000WR900357

Blackburn, J., Hicks, F., 2003. Suitability of dynamic modeling for flood forecasting during ice jam release surge events. J. Cold Reg. Eng. 17, 18–36. https://doi.org/10.1061/(ASCE)0887-381X(2003)17:1(18)

Blackburn, J., Hicks, F.E., 2002. Combined flood routing and flood level forecasting. Can. J. Civ. Eng. 29, 64–75.

Blackburn, J., She, Y., 2019. A comprehensive public-domain river ice process model and its application to a complex natural river. Cold Reg. Sci. Technol. 163, 44–58. https://doi.org/10.1016/j.coldregions.2019.04.010

Bonsal, B.R., Prowse, T.D., Duguay, C.R., Lacroix, M.P., 2006. Impacts of large-scale teleconnections on freshwater-ice break/freeze-up dates over Canada. J. Hydrol. 330, 340–353. https://doi.org/10.1016/j.jhydrol.2006.03.022

Bonsal, B.R., Prowse, T.D., Duguay, C.R., Lacroix, M.P., 2005. Impacts of Large-Scale

Teleconnections on River-Ice Duration over Canada.

Bush, E., Lemmen, D.S., 2019. Canada's changing climate report. Government of Canada= Gouvernement du Canada.

Fu, C., Yao, H., 2015. Trends of ice breakup date in south‐central Ontario. J. Geophys. Res. Atmos. 120, 9220–9236.

Koltsida, E., Mamassis, N., Kallioras, A., 2021. Hydrological modeling using the SWAT Model in urban and peri- urban environments : The case of Kifissos experimental sub-basin. Hydrol. Earth Syst. Sci. 1–24.

Lacroix, M.P., Prowse, T.D., Bonsal, B.R., Duguay, C.R., Ménard, P., 2005. River ice trends in Canada, in: 13th Workshop on the Hydraulics of Ice Covered Rivers. pp. 41–55.

Maharjan, G.R., Park, Y.S., Kim, N.W., Shin, D.S., Choi, J.W., Hyun, G.W., Jeon, J.H., Ok, Y.S., Lim, K.J., 2013. Evaluation of SWAT sub-daily runoff estimation at small agricultural watershed in Korea. Front. Environ. Sci. Eng. China 7, 109–119. https://doi.org/10.1007/s11783-012-0418-7

Meaurio, M., Zabaleta, A., Srinivasan, R., Sauvage, S., Sánchez-Pérez, J.M., Lechuga-Crespo, J.L., Antiguedad, I., 2021. Long-term and event-scale sub-daily streamflow and sediment simulation in a small forested catchment. Hydrol. Sci. J. 66, 862–873. https://doi.org/10.1080/02626667.2021.1883620

Neitsch, S.., Arnold, J.., Kiniry, J.., Williams, J.., 2011. Soil & Water Assessment Tool Theoretical Documentation Version 2009. Texas Water Resour. Inst. 1–647.

https://doi.org/10.1016/j.scitotenv.2015.11.063

Obyazov, V.A., Smakhtin, V.K., 2014. Ice regime of Transbaikalian rivers under changing climate. Water Resour. 41, 225–231. https://doi.org/10.1134/S0097807814030130

Shannak, S., 2017. Calibration and validation of SWAT for sub-hourly time steps using SWAT-CUP. Int. J. Sustain. Water Environ. Syst. 9, 21–27.

Shen, H.T., 2010. Mathematical modeling of river ice processes. Cold Reg. Sci. Technol. 62, 3–13. https://doi.org/10.1016/j.coldregions.2010.02.007

Yang, X., Liu, Q., He, Y., Luo, X., Zhang, X., 2016. Comparison of daily and sub-daily SWAT models for daily streamflow simulation in the Upper Huai River Basin of China. Stoch. Environ. Res. Risk Assess. 30, 959–972. https://doi.org/10.1007/s00477-015-1099-0

Yu, D., Xie, P., Dong, X., Hu, X., Liu, J., Li, Y., Peng, T., Ma, H., Wang, K., Xu, S., 2018. Improvement of the SWAT model for event-based flood simulation on a sub-daily timescale. Hydrol. Earth Syst. Sci. 22, 5001–5019. https://doi.org/10.5194/hess-22-5001-2018

Zhang, X., David Harvey, K., Hogg, W.D., Yuzyk, T.R., 2001. Trends in Canadian streamflow. Water Resour. Res. 37, 987–998. https://doi.org/10.1029/2000WR900357

## Bibliography

Abbaspour, K.C., 2015. SWAT Calibration and Uncertainty Programs—A User Manual. Swiss Fed. Inst. Aquat. Sci. Technol. Eawag, Switz.

Abbaspour, K.C., Rouholahnejad, E., Vaghefi, S., Srinivasan, R., Yang, H., Kløve, B., 2015. A continental-scale hydrology and water quality model for Europe: Calibration and uncertainty of a high-resolution large-scale SWAT model. J. Hydrol. 524, 733–752. https://doi.org/10.1016/j.jhydrol.2015.03.027

Abbaspour, K.C., Vaghefi, S.A., Srinivasan, R., 2017. A guideline for successful calibration and uncertainty analysis for soil and water assessment: A review of papers from the 2016 international SWAT conference. Water (Switzerland) 10. https://doi.org/10.3390/w10010006

Abbaspour, K.C., Yang, J., Maximov, I., Siber, R., Bogner, K., Mieleitner, J., Zobrist, J., Srinivasan, R., 2007. Modelling hydrology and water quality in the pre-alpine/alpine Thur watershed using SWAT. J. Hydrol. 333, 413–430. https://doi.org/10.1016/j.jhydrol.2006.09.014

Adam, J.C., Hamlet, A.F., Lettenmaier, D.P., 2009. Implications of global climate change for snowmelt hydrology in the twenty-first century. Hydrol. Process. An Int. J. 23, 962–972.

Anand, J., Gosain, A.K., Khosa, R., Srinivasan, R., 2018. Regional scale hydrologic modeling for prediction of water balance, analysis of trends in streamflow and variations in streamflow: The case study of the Ganga River basin. J. Hydrol. Reg. Stud. 16, 32–53. https://doi.org/10.1016/j.ejrh.2018.02.007

Andres, D., 1996. Ice formation and breakup at the Town of Peace River-a study of regulated

conditions, 1969-1994. A Rep. Prep. T. Peace River, BC Hydro Alberta Environ. Prot. by Trillium Eng. Hydrogr. Inc., Northwest Hydraul. Consult. Ltd. Thurber Eng. Ltd.

Andrishak, R., Hicks, F., 2008. Simulating the effects of climate change on the ice regime of the Peace River. Can. J. Civ. Eng. 35, 461–472. https://doi.org/10.1139/L07-129

Ariano, S.S., Brown, L.C., 2019. Ice processes on medium-sized north-temperate lakes. Hydrol. Process. 33, 2434–2448.

Arnold, J.G., Srinivasan, R., Muttiah, R.S., Williams, J.R., 1998. Large area hydrologic modeling and assesment Part I: Model development. JAWRA J. Am. Water Resour. Assoc. 34, 73–89. https://doi.org/10.1111/j.1752-1688.1998.tb05961.x

Arsenault, R., Poulin, A., Côté, P., Brissette, F., 2014. Comparison of Stochastic Optimization Algorithms in Hydrological Model Calibration. J. Hydrol. Eng. 19, 1374–1384. https://doi.org/10.1061/(asce)he.1943-5584.0000938

Ashmore, P., Church, M.A., 2001. The impact of climate change on rivers and river processes in Canada. Geological Survey of Canada Ottawa, Ontario.

Ashton, G.D., 2011. River and lake ice thickening, thinning, and snow ice formation. Cold Reg. Sci. Technol. 68, 3–19. https://doi.org/10.1016/j.coldregions.2011.05.004

Asquith, W.H., Roussel, M.C., Vrabel, J., 2006. Statewide analysis of the drainage-area ratio method for 34 streamflow percentile ranges in Texas. US Geological Survey.

Barnett, T.P., Adam, J.C., Lettenmaier, D.P., 2005. Potential impacts of a warming climate on water availability in snow-dominated regions. Nature 438, 303–309.

https://doi.org/10.1038/nature04141

Barry, R.G., Gan, T.Y., 2022. The global cryosphere: past, present, and future. Cambridge University Press.

Beltaos, S., 2013. Hydrodynamic and climatic drivers of ice breakup in the lower Mackenzie River. Cold Reg. Sci. Technol. 95, 39–52. https://doi.org/10.1016/j.coldregions.2013.08.004

Beltaos, S., 2008. Progress in the study and management of river ice jams. Cold Reg. Sci. Technol. 51, 2–19. https://doi.org/10.1016/j.coldregions.2007.09.001

Beltaos, S., 2003. Threshold between mechanical and thermal breakup of river ice cover. Cold Reg. Sci. Technol. 37, 1–13. https://doi.org/10.1016/S0165-232X(03)00010-7

Beltaos, S., 2002. Effects of climate on mid-winter ice jams. Hydrol. Process. 16, 789–804.

Beltaos, S., Burrell, B.C., 2003. Climatic change and river ice breakup. Can. J. Civ. Eng. 30, 145–155. https://doi.org/10.1139/l02-042

Beltaos, S., Miller, L., Burrell, B.C., Sullivan, D., 2007. Hydraulic effects of ice breakup on bridges. Can. J. Civ. Eng. 34, 539–548. https://doi.org/10.1139/L06-145

Beltaos, S., Prowse, T., 2009. River-ice hydrology in a shrinking cryosphere. Hydrol. Process. 23, 122–144.

Beltaos, S., Prowse, T., Bonsal, B., MacKay, R., Romolo, L., Pietroniro, A., Toth, B., 2006. Climatic effects on ice-jam flooding of the Peace-Athabasca Delta. Hydrol. Process. An Int. J. 20, 4031–4050.

Beltaos, S., Prowse, T.D., 2001. Climate impacts on extreme ice-jam events in Canadian rivers. Hydrol. Sci. J. 46, 157–181. https://doi.org/10.1080/02626660109492807

Benson, B.J., Magnuson, J.J., Jensen, O.P., Card, V.M., Hodgkins, G., Korhonen, J., Livingstone, D.M., Stewart, K.M., Weyhenmeyer, G.A., Granin, N.G., 2012. Extreme events, trends, and variability in Northern Hemisphere lake-ice phenology (1855-2005). Clim. Change 112, 299–323. https://doi.org/10.1007/s10584-011-0212-8

Beven, K., 2006. A Manifesto for the Equifinality Thesis Keith Beven Lancaster University, UK. J. Hydrol. 320, 18–36.

Beven, K., Binley, A., 2014. GLUE: 20 years on. Hydrol. Process. 28, 5897–5918. https://doi.org/10.1002/hyp.10082

Beven, K.J., 2000. Uniqueness of place and process representations in hydrological modelling. Hydrol. Earth Syst. Sci. https://doi.org/10.5194/hess-4-203-2000

Blackadar, R.J., Baxter, C. V., Davis, J.M., Harris, H.E., 2020. Effects of river ice break-up on organic-matter dynamics and feeding ecology of aquatic insects. River Res. Appl. 36, 480–491. https://doi.org/10.1002/rra.3585

Blackburn, J., Hicks, F., 2003. Suitability of dynamic modeling for flood forecasting during ice jam release surge events. J. Cold Reg. Eng. 17, 18–36. https://doi.org/10.1061/(ASCE)0887-381X(2003)17:1(18)

Blackburn, J., Hicks, F.E., 2002. Combined flood routing and flood level forecasting. Can. J. Civ. Eng. 29, 64–75.

Blackburn, J., She, Y., 2019. A comprehensive public-domain river ice process model and its application to a complex natural river. Cold Reg. Sci. Technol. 163, 44–58. https://doi.org/10.1016/j.coldregions.2019.04.010

Blöschl, G., Sivapalan, M., 1995. Scale issues in hydrological modelling: a review. Hydrol. Process. 9, 251–290.

Bonnifait, L., Delrieu, G., Lay, M. Le, Boudevillain, B., Masson, A., Belleudy, P., Gaume, E., Saulnier, G.M., 2009. Distributed hydrologic and hydraulic modelling with radar rainfall input: Reconstruction of the 8-9 September 2002 catastrophic flood event in the Gard region, France. Adv. Water Resour. 32, 1077–1089. https://doi.org/10.1016/j.advwatres.2009.03.007

Bonsal, B.R., Prowse, T.D., Duguay, C.R., Lacroix, M.P., 2006. Impacts of large-scale teleconnections on freshwater-ice break/freeze-up dates over Canada. J. Hydrol. 330, 340–353. https://doi.org/10.1016/j.jhydrol.2006.03.022

Bonsal, B.R., Prowse, T.D., Duguay, C.R., Lacroix, M.P., 2005. Impacts of Large-Scale Teleconnections on River-Ice Duration over Canada.

Booker, D.J., Woods, R.A., 2014. Comparing and combining physically-based and empirically-based approaches for estimating the hydrology of ungauged catchments. J. Hydrol. 508, 227–239. https://doi.org/10.1016/j.jhydrol.2013.11.007

Brown, G., 2019. Application of a Hydrological Model for Predicting River Ice Breakup.

Burrell, B.C., Beltaos, S., Turcotte, B., 2021. Effects of Climate Change on River-Ice Processes and Ice Jams. Int. J. River Basin Manag. 1–78.

https://doi.org/10.1080/15715124.2021.2007936

Bush, E., Lemmen, D.S., 2019. Canada's changing climate report. Government of Canada= Gouvernement du Canada.

Cao, W., Bowden, W.B., Davie, T., Fenemor, A., 2006. Multi-variable and multi-site calibration and validation of SWAT in a large mountainous catchment with high spatial variability. Hydrol. Process. 20, 1057–1073. https://doi.org/10.1002/hyp.5933

Champagne, O., Arain, M.A., Wang, S., Leduc, M., Russell, H.A.J., 2021. Interdecadal variability of streamflow in the Hudson Bay Lowlands watersheds driven by atmospheric circulation. J. Hydrol. Reg. Stud. 36, 100868. https://doi.org/10.1016/j.ejrh.2021.100868

Chen, F., Shen, H.T., Jayasundara, N., 2006. A one-dimensional comprehensive river ice model, in: Proceedings of 18th International Association of Hydraulic Research Symposium on Ice, Sapporo, Japan. Citeseer.

Chen, Y., Guan, Y., Shao, G., Zhang, D., 2016. Investigating trends in streamflow and precipitation in Huangfuchuan basin with wavelet analysis and the Mann-Kendall test. Water (Switzerland) 8. https://doi.org/10.3390/w8030077

Chen, Y., She, Y., 2019. Temporal and Spatial Variations of River Ice Breakup Timing across Canada, in: 20th Workshop on the Hydraulics of Ice Covered Rivers.

Clark, D.G., Ford, J.D., Berrang-Ford, L., Pearce, T., Kowal, S., Gough, W.A., 2016. The role of environmental factors in search and rescue incidents in Nunavut, Canada. Public Health 137, 44–49. https://doi.org/10.1016/j.puhe.2016.06.003

Cordeiro, M.R.C., Lelyk, G., Kröbel, R., Legesse, G., Faramarzi, M., Masud, M.B., McAllister, T., 2017. Deriving a country-wide soils dataset from the Soil Landscapes of Canada (SLC) database for use in Soil and Water Assessment Tool (SWAT) simulations. Earth Syst. Sci. Data Discuss. 1–30. https://doi.org/10.1594/PANGAEA.877298.KEY

Craig, J.R., Brown, G., Chlumsky, R., Jenkinson, W., Jost, G., Lee, K., Mai, J., Serrer, M., Snowdon, A.P., Sgro, N., 2020. Flexible watershed simulation with the Raven hydrological modelling framework. Environ. Model. Softw. 104728.

Das, A., Rokaya, P., Lindenschmidt, K.E., 2020. Ice-Jam Flood Risk Assessment and Hazard Mapping under Future Climate. J. Water Resour. Plan. Manag. 146, 1–12. https://doi.org/10.1061/(ASCE)WR.1943-5452.0001178

De Rham, L., Dibike, Y., Beltaos, S., Peters, D., Bonsal, B., Prowse, T., 2020. A Canadian River Ice Database from the National Hydrometric Program Archives. Earth Syst. Sci. Data 12, 1835–1860. https://doi.org/10.5194/essd-12-1835-2020

de Rham, L.P., Prowse, T.D., Bonsal, B.R., 2008. Temporal variations in river-ice break-up over the Mackenzie River Basin, Canada. J. Hydrol. 349, 441–454. https://doi.org/10.1016/j.jhydrol.2007.11.018

Dessie, M., Verhoest, N.E.C., Pauwels, V.R.N., Adgo, E., Deckers, J., Poesen, J., Nyssen, J., 2015. Water balance of a lake with floodplain buffering: Lake Tana, Blue Nile Basin, Ethiopia. J. Hydrol. 522, 174–186. https://doi.org/10.1016/j.jhydrol.2014.12.049

Dile, Y.T., Srinivasan, R., 2014. Evaluation of CFSR climate data for hydrologic prediction in data-scarce watersheds: An application in the blue nile river basin. J. Am. Water Resour. Assoc.

50, 1226–1241. https://doi.org/10.1111/jawr.12182

Doyle, P.F., Ball, J.F., 2008. Changing ice cover regime in southern British Columbia due to changing climate, in: Proceedings of the 19th IAHR International Symposium on Ice. St Joseph Communications, Vancouver, Canada. pp. 51–61.

Du, X., Loiselle, D., Alessi, D.S., Faramarzi, M., 2020. Hydro-climate and biogeochemical processes control watershed organic carbon inflows: Development of an in-stream organic carbon module coupled with a process-based hydrologic model. Sci. Total Environ. 718, 137281. https://doi.org/10.1016/j.scitotenv.2020.137281

Duguay, C.R., Prowse, T.D., Bonsal, B.R., Brown, R.D., Lacroix, M.P., Ménard, P., 2006. Recent trends in Canadian lake ice cover. Hydrol. Process. 20, 781–801. https://doi.org/10.1002/hyp.6131

Dynesius, M., Nilsson, C., 1994. Fragmentation and flow regulation of river systems in the northern third of the world. Science (80-. ). 266, 753–762.

Emerson, D.G., Vecchia, A. V, Dahl, A.L., 2005. Evaluation of drainage-area ratio method used to estimate streamflow for the Red River of the North Basin, North Dakota and Minnesota. US Department of the Interior, US Geological Survey.

Ergen, K., Kentel, E., 2016. An integrated map correlation method and multiple-source sites drainage-area ratio method for estimating streamflows at ungauged catchments: A case study of the Western Black Sea Region, Turkey. J. Environ. Manage. 166, 309–320. https://doi.org/10.1016/j.jenvman.2015.10.036

Faramarzi, M., Abbaspour, K.C., Adamowicz, W.L.V., Lu, W., Fennell, J., Zehnder, A.J.B., Goss, G.G., 2017. Uncertainty based assessment of dynamic freshwater scarcity in semi-arid watersheds of Alberta, Canada. J. Hydrol. Reg. Stud. 9, 48–68. https://doi.org/10.1016/j.ejrh.2016.11.003

Faramarzi, M., Srinivasan, R., Iravani, M., Bladon, K.D., Abbaspour, K.C., Zehnder, A.J.B., Goss, G.G., 2015. Setting up a hydrological model of Alberta: Data discrimination analyses prior to calibration. Environ. Model. Softw. 74, 48–65. https://doi.org/10.1016/j.envsoft.2015.09.006

Ficklin, D.L., Barnhart, B.L., 2014. SWAT hydrologic model parameter uncertainty and its implications for hydroclimatic projections in snowmelt-dependent watersheds. J. Hydrol. 519, 2081–2090. https://doi.org/10.1016/j.jhydrol.2014.09.082

Ficklin, D.L., Luo, Y., Stewart, I.T., Maurer, E.P., 2012. Development and application of a hydroclimatological stream temperature model within the Soil and Water Assessment Tool. Water Resour. Res. 48, 1–16. https://doi.org/10.1029/2011WR011256

Fischer, G., Nachtergaele, F., Prieler, S., Van Velthuizen, H.T., Verelst, L., Wiberg, D., 2008. Global agro-ecological zones assessment for agriculture (GAEZ 2008). IIASA, Laxenburg, Austria FAO, Rome, Italy 10.

French, H.M., 2017. The periglacial environment. John Wiley & Sons.

Fu, C., Yao, H., 2015. Trends of ice breakup date in south-central Ontario. J. Geophys. Res. Atmos. 120, 9220–9236.

Ghanbari, R.N., Bravo, H.R., Magnuson, J.J., Hyzer, W.G., Benson, B.J., 2009. Coherence

between lake ice cover, local climate and teleconnections (Lake Mendota, Wisconsin). J. Hydrol. 374, 282–293. https://doi.org/10.1016/j.jhydrol.2009.06.024

Gianfagna, C.C., Johnson, C.E., Chandler, D.G., Hofmann, C., 2015. Watershed area ratio accurately predicts daily streamflow in nested catchments in the Catskills, New York. J. Hydrol. Reg. Stud. 4, 583–594. https://doi.org/10.1016/j.ejrh.2015.09.002

Gizaw, M.S., Biftu, G.F., Gan, T.Y., Moges, S.A., Koivusalo, H., 2017. Potential impact of climate change on streamflow of major Ethiopian rivers. Clim. Change 143, 371–383. https://doi.org/10.1007/s10584-017-2021-1

Goulding, H.L., Prowse, T.D., Beltaos, S., 2009b. Spatial and temporal patterns of break-up and ice-jam flooding in the Mackenzie Delta, NWT. Hydrol. Process. An Int. J. 23, 2654–2670.

Goulding, H.L., Prowse, T.D., Bonsal, B., 2009a. Hydroclimatic controls on the occurrence of break-up and ice-jam flooding in the Mackenzie Delta, NWT, Canada. J. Hydrol. 379, 251–267. https://doi.org/10.1016/j.jhydrol.2009.10.006

Grimaldi, S., Schumann, G.J.P., Shokri, A., Walker, J.P., Pauwels, V.R.N., 2019. Challenges, Opportunities, and Pitfalls for Global Coupled Hydrologic-Hydraulic Modeling of Floods. Water Resour. Res. 55, 5277–5300. https://doi.org/10.1029/2018WR024289

Grusson, Y., Sun, X., Gascoin, S., Sauvage, S., Raghavan, S., Anctil, F., Sáchez-Pérez, J.M., 2015. Assessing the capability of the SWAT model to simulate snow, snow melt and streamflow dynamics over an alpine watershed. J. Hydrol. 531, 574–588. https://doi.org/10.1016/j.jhydrol.2015.10.070

Guo, Y., Zhang, Y., Zhang, L., Wang, Z., 2021a. Regionalization of hydrological modeling for predicting streamflow in ungauged catchments: A comprehensive review. Wiley Interdiscip. Rev. Water 8, e1487.

Guo, Y., Zhang, Y., Zhang, L., Wang, Z., 2021b. Regionalization of hydrological modeling for predicting streamflow in ungauged catchments: A comprehensive review. Wiley Interdiscip. Rev. Water 8, 1–32. https://doi.org/10.1002/wat2.1487

Ha, L.T., Bastiaanssen, W.G.M., van Griensven, A., van Dijk, A.I.J.M., Senay, G.B., 2017. SWAT-CUP for Calibration of Spatially Distributed Hydrological Processes and Ecosystem Services in a Vietnamese River Basin Using Remote Sensing. Hydrol. Earth Syst. Sci. Discuss. 1–35. https://doi.org/10.5194/hess-2017-251

Hanzer, F., Helfricht, K., Marke, T., Strasser, U., 2016. Multilevel spatiotemporal validation of snow/ice mass balance and runoff modeling in glacierized catchments. Cryosphere 10, 1859–1881. https://doi.org/10.5194/tc-10-1859-2016

He, Y., Bárdossy, A., Zehe, E., 2011. A review of regionalisation for continuous streamflow simulation. Hydrol. Earth Syst. Sci. 15, 3539–3553. https://doi.org/10.5194/hess-15-3539-2011

Her, Y., Seong, C., 2018. Responses of hydrological model equifinality, uncertainty, and performance to multi-objective parameter calibration. J. Hydroinformatics 20, 864–885. https://doi.org/10.2166/hydro.2018.108

Hersbach, H., Bell, B., Berrisford, P., Hirahara, S., Horányi, A., Muñoz-Sabater, J., Nicolas, J., Peubey, C., Radu, R., Schepers, D., Simmons, A., Soci, C., Abdalla, S., Abellan, X., Balsamo,

G., Bechtold, P., Biavati, G., Bidlot, J., Bonavita, M., De Chiara, G., Dahlgren, P., Dee, D., Diamantakis, M., Dragani, R., Flemming, J., Forbes, R., Fuentes, M., Geer, A., Haimberger, L., Healy, S., Hogan, R.J., Hólm, E., Janisková, M., Keeley, S., Laloyaux, P., Lopez, P., Lupu, C., Radnoti, G., de Rosnay, P., Rozum, I., Vamborg, F., Villaume, S., Thépaut, J.N., 2020. The ERA5 global reanalysis. Q. J. R. Meteorol. Soc. 146, 1999–2049. https://doi.org/10.1002/qj.3803

Hicks, F., 2009. An overview of river ice problems: CRIPE07 guest editorial.

Hicks, F.E., 2016. An introduction to river ice engineering for civil engineers and geoscientists. CreateSpace Independent Publishing Platform.

Hicks, F.E., 1996. Hydraulic flood routing with minimal channel data: Peace River, Canada. Can. J. Civ. Eng. 23, 524–535. https://doi.org/10.1139/l96-057

Hicks, F.E., Steffler, P.M., 1992. Characteristic dissipative Galerkin scheme for open-channel flow. J. Hydraul. Eng. 118, 337–352.

Hicks, F.E., Steffler, P.M., 1990. Finite element modeling of open channel flow. Department of Civil Engineering, University of Alberta, Edmonton, Alta. Water Resour. Eng. Rep.

Hodgkins, G.A., Dudley, R.W., Huntington, T.G., 2005. Changes in the number and timing of days of ice-affected flow on northern New England rivers, 1930-2000. Clim. Change 71, 319–340. https://doi.org/10.1007/s10584-005-5926-z

Hori, Y., Cheng, V.Y.S., Gough, W.A., Jien, J.Y., Tsuji, L.J.S., 2018a. Implications of projected climate change on winter road systems in Ontario’s Far North, Canada. Clim. Change 148,

109–122. https://doi.org/10.1007/s10584-018-2178-2

Hori, Y., Gough, W.A., Tam, B., Tsuji, L.J.S., 2018b. Community vulnerability to changes in the winter road viability and longevity in the western James Bay region of Ontario's Far North. Reg. Environ. Chang. 18, 1753–1763. https://doi.org/10.1007/s10113-018-1310-1

Hrachowitz, M., Savenije, H.H.G., Blöschl, G., McDonnell, J.J., Sivapalan, M., Pomeroy, J.W., Arheimer, B., Blume, T., Clark, M.P., Ehret, U., Fenicia, F., Freer, J.E., Gelfan, A., Gupta, H. V., Hughes, D.A., Hut, R.W., Montanari, A., Pande, S., Tetzlaff, D., Troch, P.A., Uhlenbrook, S., Wagener, T., Winsemius, H.C., Woods, R.A., Zehe, E., Cudennec, C., 2013. A decade of Predictions in Ungauged Basins (PUB)-a review. Hydrol. Sci. J. 58, 1198–1255. https://doi.org/10.1080/02626667.2013.803183

Huang, F., Jasek, M., Shen, H.T., 2021. Simulation of the 2014 Dynamic Ice Breakup on the Peace River 1–19.

IPCC, 2013. IPCC, 2013: climate change 2013: the physical science basis. Contribution of working group I to the fifth assessment report of the intergovernmental panel on climate change.

Jakkila, J., Leppäranta, M., Kawamura, T., Shirasawa, K., Salonen, K., 2009. Radiation transfer and heat budget during the ice season in Lake Pääjärvi, Finland. Aquat. Ecol. 43, 681–692. https://doi.org/10.1007/s10452-009-9275-2

Janowicz, J.R., 2010. Observed trends in the river ice regimes of northwest Canada. Hydrol. Res. 41, 462. https://doi.org/10.2166/nh.2010.145

Jarvis, A., Reuter, H.I., Nelson, A., Guevara, E., 2008. Hole-filled SRTM for the globe Version 4.

available from CGIAR-CSI SRTM 90m Database (http//srtm. csi. cgiar. org) 15, 25–54.

Jasek, M.J., Shen, H.T., 1999. 1998 break-up and flood on the Yukon River at Dawson–did El Niño and climate change play a role? Ice Surf. Waters, Balkema, Rotterdam 761–768.

Jensen, O.P., Benson, B.J., Magnuson, J.J., Card, V.M., Futter, M.N., Soranno, P.A., Stewart, K.M., 2007. Spatial analysis of ice phenology trends across the Laurentian Great Lakes region during a recent warming period. Limnol. Oceanogr. 52, 2013–2026. https://doi.org/10.4319/lo.2007.52.5.2013

Jobe, A., Bhandari, S., Kalra, A., Ahmad, S., 2017. Ice-Cover and Jamming Effects on Inline Structures and Upstream Water Levels. World Environ. Water Resour. Congr. 2017 Hydraul. Waterw. Water Distrib. Syst. Anal. - Sel. Pap. from World Environ. Water Resour. Congr. 2017 270–279. https://doi.org/10.1061/9780784480625.025

Koltsida, E., Mamassis, N., Kallioras, A., 2021. Hydrological modeling using the SWAT Model in urban and peri- urban environments : The case of Kifissos experimental sub-basin. Hydrol. Earth Syst. Sci. 1–24.

Kouchi, D.H., Esmaili, K., Faridhosseini, A., Sanaeinejad, S.H., Khalili, D., Abbaspour, K.C., 2017. Sensitivity of calibrated parameters and water resource estimates on different objective functions and optimization algorithms. Water (Switzerland) 9, 1–16. https://doi.org/10.3390/w9060384

Krause, P., Boyle, D.P., Bäse, F., 2005. Comparison of different efficiency criteria for hydrological model assessment. Adv. Geosci. 5, 89–97. https://doi.org/10.5194/adgeo-5-89-2005

Lacroix, M.P., Prowse, T.D., Bonsal, B.R., Duguay, C.R., Ménard, P., 2005. River ice trends in Canada, in: 13th Workshop on the Hydraulics of Ice Covered Rivers. pp. 41–55.

Li, Q., Peng, Y., Wang, G., Wang, H., Xue, B., Hu, X., 2019. A combined method for estimating continuous runoff by parameter transfer and drainage area ratio method in ungauged catchments. Water 11, 1104.

Li, W., Lin, K., Zhao, T., Lan, T., Chen, X., Du, H., Chen, H., 2019. Risk assessment and sensitivity analysis of flash floods in ungauged basins using coupled hydrologic and hydrodynamic models. J. Hydrol. 572, 108–120. https://doi.org/10.1016/j.jhydrol.2019.03.002

Lindenschmidt, K.E., 2017. RIVICE-A non-proprietary, open-source, one-dimensional river-ice model. Water (Switzerland) 9. https://doi.org/10.3390/w9050314

Lindenschmidt, K.E., Das, A., Rokaya, P., Chu, T., 2016. Ice-jam flood risk assessment and mapping. Hydrol. Process. 30, 3754–3769. https://doi.org/10.1002/hyp.10853

Lindenschmidt, K.E., Rokaya, P., Das, A., Li, Z., Richard, D., 2019. A novel stochastic modelling approach for operational real-time ice-jam flood forecasting. J. Hydrol. 575, 381–394. https://doi.org/10.1016/j.jhydrol.2019.05.048

Liu, G., Schwartz, F.W., Tseng, K., Shum, C.K., 2015. Discharge and water-depth estimates for ungauged rivers: Combining hydrologic, hydraulic, and inverse modeling with stage and water-area measurements from satellites. Water Resour. Res. 51, 6017–6035.

Liu, L., Li, H., Shen, H.T., 2006. A Two-Dimensional Comprehensive River Ice Model. Proc. 18th IAHR Int. Symp. Ice 69–76.

Liu, Z., Yin, J., E Dahlke, H., 2020. Enhancing Soil and Water Assessment Tool Snow Prediction Reliability with Remote-Sensing-Based Snow Water Equivalent Reconstruction Product for Upland Watersheds in a Multi-Objective Calibration Process. Water 12, 3190.

Livingstone, D.M., 2000. Large-scale climatic forcing detected in historical observations of lake ice break-up. Int. Vereinigung für Theor. und Angew. Limnol. Verhandlungen 27, 2775–2783.

Loiselle, D., Du, X., Alessi, D.S., Bladon, K.D., Faramarzi, M., 2020. Projecting impacts of wildfire and climate change on streamflow, sediment, and organic carbon yields in a forested watershed. J. Hydrol. 590, 125403. https://doi.org/10.1016/j.jhydrol.2020.125403

Lopez, L.S., Hewitt, B.A., Sharma, S., 2019. Reaching a breaking point: How is climate change influencing the timing of ice breakup in lakes across the northern hemisphere? Limnol. Oceanogr. 1–11. https://doi.org/10.1002/lno.11239

Magnuson, J.J., Robertson, D.M., Benson, B.J., Wynne, R.H., Livingstone, D.M., Arai, T., Assel, R.A., Barry, R.G., Card, V., Kuusisto, E., 2000. Historical trends in lake and river ice cover in the Northern Hemisphere. Science (80-. ). 289, 1743–1746.

Mahabir, Chandra, Hicks, F., Fayek, A.R., 2006. Neuro-fuzzy river ice breakup forecasting system. Cold Reg. Sci. Technol. 46, 100–112. https://doi.org/10.1016/j.coldregions.2006.08.009

Mahabir, C., Hicks, F.E., Fayek, A.R., 2007. Transferability of a neuro-fuzzy river ice jam flood forecasting model. Cold Reg. Sci. Technol. 48, 188–201. https://doi.org/10.1016/j.coldregions.2006.12.004

Mahabir, C., Hicks, F.E., Robichaud, C., Fayek, A.R., 2006. Forecasting breakup water levels at

Fort McMurray, Alberta, using multiple linear regression. Can. J. Civ. Eng. 33, 1227–1238. https://doi.org/10.1139/L06-067

Maharjan, G.R., Park, Y.S., Kim, N.W., Shin, D.S., Choi, J.W., Hyun, G.W., Jeon, J.H., Ok, Y.S., Lim, K.J., 2013. Evaluation of SWAT sub-daily runoff estimation at small agricultural watershed in Korea. Front. Environ. Sci. Eng. China 7, 109–119. https://doi.org/10.1007/s11783-012-0418-7

McCuen, R.H., Levy, B.S., 2000. Evaluation of peak discharge transposition. J. Hydrol. Eng. 5, 278–289.

McKenney, D.W., Hutchinson, M.F., Papadopol, P., Lawrence, K., Pedlar, J., Campbell, K., Milewska, E., Hopkinson, R.F., Price, D., Owen, T., 2011. Customized spatial climate models for North America. Bull. Am. Meteorol. Soc. 92, 1611–1622.

Meaurio, M., Zabaleta, A., Srinivasan, R., Sauvage, S., Sánchez-Pérez, J.M., Lechuga-Crespo, J.L., Antiguedad, I., 2021. Long-term and event-scale sub-daily streamflow and sediment simulation in a small forested catchment. Hydrol. Sci. J. 66, 862–873. https://doi.org/10.1080/02626667.2021.1883620

Merz, B., Blöschl, G., Vorogushyn, S., Dottori, F., Aerts, J.C.J.H., Bates, P., Bertola, M., Kemter, M., Kreibich, H., Lall, U., 2021. Causes, impacts and patterns of disastrous river floods. Nat. Rev. Earth Environ. 2, 592–609.

Mishra, A., Mukherjee, S., Merz, B., Singh, V.P., Wright, D.B., Villarini, G., Paul, S., Kumar, D.N., Khedun, C.P., Niyogi, D., Schumann, G., Stedinger, J.R., 2022. An Overview of Flood Concepts, Challenges, and Future Directions. J. Hydrol. Eng. 27, 1–30.

https://doi.org/10.1061/(asce)he.1943-5584.0002164

Mishra, A.K., Coulibaly, P., 2009. Developments in hydrometric network design: A review. Rev. Geophys. 47.

Molina-Navarro, E., Andersen, H.E., Nielsen, A., Thodsen, H., Trolle, D., 2017. The impact of the objective function in multi-site and multi-variable calibration of the SWAT model. Environ. Model. Softw. 93, 255–267. https://doi.org/10.1016/j.envsoft.2017.03.018

Morales-Marín, L.A., Sanyal, P.R., Kadowaki, H., Li, Z., Rokaya, P., Lindenschmidt, K.E., 2019. A hydrological and water temperature modelling framework to simulate the timing of river freeze-up and ice-cover breakup in large-scale catchments. Environ. Model. Softw. 114, 49–63. https://doi.org/10.1016/j.envsoft.2019.01.009

Moriasi, D.N., Gitau, M.W., Pai, N., Daggupati, P., 2015. Hydrologic and water quality models: Performance measures and evaluation criteria. Trans. ASABE 58, 1763–1785. https://doi.org/10.13031/trans.58.10715

Mousavi, S.J., Kamali, B., Abbaspour, K.C., Amini, M., Yang, H., 2012. Uncertainty-based automatic calibration of HEC-HMS model using sequential uncertainty fitting approach. J. Hydroinformatics 14, 286–309. https://doi.org/10.2166/hydro.2011.071

Muleta, M.K., 2012. Model Performance Sensitivity to Objective Function during Automated Calibrations. J. Hydrol. Eng. 17, 756–767. https://doi.org/10.1061/(asce)he.1943-5584.0000497

Musau, J., Sang, J., Gathenya, J., Luedeling, E., 2015. Hydrological responses to climate change

in Mt. Elgon watersheds. J. Hydrol. Reg. Stud. 3, 233–246. https://doi.org/10.1016/j.ejrh.2014.12.001

Neitsch, S.., Arnold, J.., Kiniry, J.., Williams, J.., 2011. Soil & Water Assessment Tool Theoretical Documentation Version 2009. Texas Water Resour. Inst. 1–647. https://doi.org/10.1016/j.scitotenv.2015.11.063

Neupane, R.P., Adamowski, J.F., White, J.D., Kumar, S., 2018. Future streamflow simulation in a snow-dominated rocky mountain headwater catchment. Hydrol. Res. 49, 1172–1190. https://doi.org/10.2166/nh.2017.024

Newton, B.W., Prowse, T.D., de Rham, L.P., 2017. Hydro-climatic drivers of mid-winter break-up of river ice in western Canada and Alaska. Hydrol. Res. 48, 945–956. https://doi.org/10.2166/nh.2016.358

Nguyen, P., Thorstensen, A., Sorooshian, S., Hsu, K., AghaKouchak, A., Sanders, B., Koren, V., Cui, Z., Smith, M., 2016. A high resolution coupled hydrologic–hydraulic model (HiResFlood-UCI) for flash flood modeling. J. Hydrol. 541, 401–420. https://doi.org/10.1016/j.jhydrol.2015.10.047

Nilsson, C., Reidy, C.A., Dynesius, M., Revenga, C., 2005. Fragmentation and flow regulation of the world's large river systems. Science (80-. ). 308, 405–408.

Nkiaka, E., Nawaz, N.R., Lovett, J.C., 2018. Effect of single and multi-site calibration techniques on hydrological model performance, parameter estimation and predictive uncertainty: a case study in the Logone catchment, Lake Chad basin. Stoch. Environ. Res. Risk Assess. 32, 1665–1682. https://doi.org/10.1007/s00477-017-1466-0

Nõges, P., Nõges, T., 2014. Weak trends in ice phenology of Estonian large lakes despite significant warming trends. Hydrobiologia 731, 5–18. https://doi.org/10.1007/s10750-013-1572-z

Obyazov, V.A., Smakhtin, V.K., 2014. Ice regime of Transbaikalian rivers under changing climate. Water Resour. 41, 225–231. https://doi.org/10.1134/S0097807814030130

Pagliero, L., Bouraoui, F., Diels, J., Willems, P., McIntyre, N., 2019. Investigating regionalization techniques for large-scale hydrological modelling. J. Hydrol. 570, 220–235. https://doi.org/10.1016/j.jhydrol.2018.12.071

Parajka, J., Viglione, A., Rogger, M., Salinas, J.L., Sivapalan, M., Blöschl, G., 2013. Comparative assessment of predictions in ungauged basins-Part 1: Runoff-hydrograph studies. Hydrol. Earth Syst. Sci. 17, 1783–1795. https://doi.org/10.5194/hess-17-1783-2013

Peker, I.B., Sorman, A.A., 2021. Application of SWAT using snow data and detecting climate change impacts in the mountainous eastern regions of Turkey. Water (Switzerland) 13. https://doi.org/10.3390/w13141982

Pomeroy, J.W., Gray, D.M., Brown, T., Hedstrom, N.R., Quinton, W.L., Granger, R.J., Carey, S.K., 2007. The cold regions hydrological model: a platform for basing process representation and model structure on physical evidence. Hydrol. Process. 21, 2650–2667.

Poulin, A., Brissette, F., Leconte, R., Arsenault, R., Malo, J.S., 2011. Uncertainty of hydrological modelling in climate change impact studies in a Canadian, snow-dominated river basin. J. Hydrol. 409, 626–636. https://doi.org/10.1016/j.jhydrol.2011.08.057

Prowse, T., Alfredsen, K., Beltaos, S., Bonsal, B., Duguay, C., Korhola, A., McNamara, J., Pienitz,

R., Vincent, W.F., Vuglinsky, V., Weyhenmeyer, G.A., 2011. Past and future changes in arctic lake and river ice. Ambio 40, 53–62. https://doi.org/10.1007/s13280-011-0216-7

Prowse, T., Bonsal, B.R., Duguay, C.R., Lacroix, M.P., 2007. River-ice break-up/freeze-up: A review of climatic drivers, historical trends and future predictions. Ann. Glaciol. 46, 443–451. https://doi.org/10.3189/172756407782871431

Prowse, T.D., Bonsal, B.R., Lacroix, M.P., 2002. Trends in River-Ice Breakup and Related Temperature Controls 2–6.

Prowse, T.D., Conly, F.M., 1998. Effects of climatic variability and flow regulation on ice-jam flooding of a northern delta. Hydrol. Process. 12, 1589–1610.

Puertes, C., Lidón, A., Echeverría, C., Bautista, I., González-Sanchis, M., del Campo, A.D., Francés, F., 2019. Explaining the hydrological behaviour of facultative phreatophytes using a multi-variable and multi-objective modelling approach. J. Hydrol. 575, 395–407. https://doi.org/10.1016/j.jhydrol.2019.05.041

Qi, W., Zhang, C., Fu, G., Zhou, H., 2016. Quantifying dynamic sensitivity of optimization algorithm parameters to improve hydrological model calibration. J. Hydrol. 533, 213–223. https://doi.org/10.1016/j.jhydrol.2015.11.052

Rajib, M.A., Merwade, V., Yu, Z., 2016. Multi-objective calibration of a hydrologic model using spatially distributed remotely sensed/in-situ soil moisture. J. Hydrol. 536, 192–207. https://doi.org/10.1016/j.jhydrol.2016.02.037

Rantanen, M., Karpechko, A.Y., Lipponen, A., Nordling, K., Hyvärinen, O., Ruosteenoja, K.,

Vihma, T., Laaksonen, A., 2022. The Arctic has warmed nearly four times faster than the globe since 1979. Commun. Earth Environ. 3, 1–10.

Razavi, T., Coulibaly, P., 2013. Streamflow Prediction in Ungauged Basins: Review of Regionalization Methods. J. Hydrol. Eng. 18, 958–975. https://doi.org/10.1061/(asce)he.1943-5584.0000690

Rientjes, T.H.M., Muthuwatta, L.P., Bos, M.G., Booij, M.J., Bhatti, H.A., 2013. Multi-variable calibration of a semi-distributed hydrological model using streamflow data and satellite-based evapotranspiration. J. Hydrol. 505, 276–290. https://doi.org/10.1016/j.jhydrol.2013.10.006

Rokaya, P., Budhathoki, S., Lindenschmidt, K.-E., 2018. Trends in the Timing and Magnitude of Ice-Jam Floods in Canada. Sci. Rep. 8, 5834.

Rokaya, P., Morales-Marín, L., Bonsal, B., Wheater, H., Lindenschmidt, K.E., 2019a. Climatic effects on ice phenology and ice-jam flooding of the Athabasca River in western Canada. Hydrol. Sci. J. 64, 1265–1278. https://doi.org/10.1080/02626667.2019.1638927

Rokaya, P., Morales-Marin, L., Lindenschmidt, K.E., 2020. A physically-based modelling framework for operational forecasting of river ice breakup. Adv. Water Resour. 139, 103554. https://doi.org/10.1016/j.advwatres.2020.103554

Rokaya, P., Peters, D.L., Bonsal, B., Wheater, H., Lindenschmidt, K.E., 2019b. Modelling the effects of climate and flow regulation on ice-affected backwater staging in a large northern river. River Res. Appl. 35, 587–600. https://doi.org/10.1002/rra.3436

Salinas, J.L., Laaha, G., Rogger, M., Parajka, J., Viglione, A., Sivapalan, M., Blöschl, G., 2013.

Comparative assessment of predictions in ungauged basins-Part 2: Flood and low flow studies. Hydrol. Earth Syst. Sci. 17, 2637–2652. https://doi.org/10.5194/hess-17-2637-2013

Scheepers, H., Wang, J., Gan, T.Y., Kuo, C.C., 2018. The impact of climate change on inland waterway transport: Effects of low water levels on the Mackenzie River. J. Hydrol. 566, 285–298. https://doi.org/10.1016/j.jhydrol.2018.08.059

Schmidt, D.F., Grise, K.M., Pace, M.L., 2019. High-frequency climate oscillations drive ice-off variability for Northern Hemisphere lakes and rivers. Clim. Change 152, 517–532. https://doi.org/10.1007/s10584-018-2361-5

Schuol, J., Abbaspour, K.C., Yang, H., Srinivasan, R., Zehnder, A.J.B., 2008. Modeling blue and green water availability in Africa. Water Resour. Res. 44, 1–18. https://doi.org/10.1029/2007WR006609

Sen, P.K., 1968. Estimates of the regression coefficient based on Kendall's tau. J. Am. Stat. Assoc. 63, 1379–1389.

Shannak, S., 2017. Calibration and validation of SWAT for sub-hourly time steps using SWAT-CUP. Int. J. Sustain. Water Environ. Syst. 9, 21–27.

Shaw, J.K.E., Lavender, S.T., Stephen, D., Jamieson, K., 2013. Ice Jam Flood Risk Forecasting at the Kashechewan FN Community on the North Albany River. Proc. 17th Work. River Ice 20 pages.

She, Y., Andrishak, R., Hicks, F., Morse, B., Stander, E., Krath, C., Keller, D., Abarca, N., Nolin, S., Tanekou, F.N., Mahabir, C., 2009. Athabasca River ice jam formation and release events

in 2006 and 2007. Cold Reg. Sci. Technol. 55, 249–261. https://doi.org/10.1016/j.coldregions.2008.02.004

She, Y., Hicks, F., 2006. Modeling ice jam release waves with consideration for ice effects. Cold Reg. Sci. Technol. 45, 137–147. https://doi.org/10.1016/j.coldregions.2006.05.004

Shen, H.T., 2010. Mathematical modeling of river ice processes. Cold Reg. Sci. Technol. 62, 3–13. https://doi.org/10.1016/j.coldregions.2010.02.007

Singh, L., Mishra, P.K., Pingale, S.M., Khare, D., Thakur, H.P., 2022. Streamflow regionalisation of an ungauged catchment with machine learning approaches. Hydrol. Sci. J. 67, 886–897. https://doi.org/10.1080/02626667.2022.2049271

Sivapalan, M., 2003. Prediction in ungauged basins: a grand challenge for theoretical hydrology. Hydrol. Process. 17, 3163–3170.

Sivapalan, M., Takeuchi, K., Franks, S.W., Gupta, V.K., Karambiri, H., Lakshmi, V., Liang, X., McDonnell, J.J., Mendiondo, E.M., O'Connell, P.E., Oki, T., Pomeroy, J.W., Schertzer, D., Uhlenbrook, S., Zehe, E., 2003. IAHS Decade on Predictions in Ungauged Basins (PUB), 2003-2012: Shaping an exciting future for the hydrological sciences. Hydrol. Sci. J. 48, 857–880. https://doi.org/10.1623/hysj.48.6.857.51421

Sospedra-Alfonso, R., Melton, J.R., Merryfield, W.J., 2015. Effects of temperature and precipitation on snowpack variability in the Central Rocky Mountains as a function of elevation. Geophys. Res. Lett. 42, 4429–4438. https://doi.org/10.1002/2015GL063898

Sun, W., Trevor, B., 2018. Multiple model combination methods for annual maximum water level

prediction during river ice breakup. Hydrol. Process. 32, 421–435.

Taggart, J., 1995. The Peace River natural flow and regulated flow scenarios-daily flow data report. Surf. Water Assess. Branch, Alberta Environ. Prot. Edmonton, AB.

Tarek, M., Brissette, F.P., Arsenault, R., 2020. Evaluation of the ERA5 reanalysis as a potential reference dataset for hydrological modelling over North America. Hydrol. Earth Syst. Sci. 24, 2527–2544. https://doi.org/10.5194/hess-24-2527-2020

Tellman, B., Sullivan, J.A., Kuhn, C., Kettner, A.J., Doyle, C.S., Brakenridge, G.R., Erickson, T.A., Slayback, D.A., 2021. Satellite imaging reveals increased proportion of population exposed to floods. Nature 596, 80–86. https://doi.org/10.1038/s41586-021-03695-w

Thériault, I., Saucet, J.-P., Taha, W., 2010. Validation of the Mike-Ice model simulating river flows in presence of ice and forecast of changes to the ice regime of the Romaine river due to hydroelectric project, in: Proceedings of the 20th IAHR International Symposium on Ice, Lahti, Finland. pp. 14–17.

Timalsina, N.P., Charmasson, J., Alfredsen, K.T., 2013. Simulation of the ice regime in a Norwegian regulated river. Cold Reg. Sci. Technol. 94, 61–73. https://doi.org/10.1016/j.coldregions.2013.06.010

Toth, B., Pietroniro, A., Conly, F.M., Kouwen, N., 2006. Modelling climate change impacts in the Peace and Athabasca catchment and delta: I—hydrological model application. Hydrol. Process. An Int. J. 20, 4197–4214.

Tuo, Y., Duan, Z., Disse, M., Chiogna, G., 2016. Evaluation of precipitation input for SWAT

modeling in Alpine catchment: A case study in the Adige river basin (Italy). Sci. Total Environ. 573, 66–82. https://doi.org/10.1016/j.scitotenv.2016.08.034

Tuo, Y., Marcolini, G., Disse, M., Chiogna, G., 2018a. Calibration of snow parameters in SWAT: comparison of three approaches in the Upper Adige River basin (Italy). Hydrol. Sci. J. 63, 657–678. https://doi.org/10.1080/02626667.2018.1439172

Tuo, Y., Marcolini, G., Disse, M., Chiogna, G., 2018b. A multi-objective approach to improve SWAT model calibration in alpine catchments. J. Hydrol. 559, 347–360. https://doi.org/10.1016/j.jhydrol.2018.02.055

Turcotte, B., Burrell, B.C., Beltaos, S., 2019. The Impact of Climate Change on Breakup Ice Jams in Canada : State of knowledge and research approaches.

Turcotte, B., Morse, B., 2015. River ice breakup forecast and annual risk distribution in a climate change perspective, in: 18th Workshop on the Hydraulics of Ice Covered Rivers, CGU HS Committee on River Ice Processes and the Environment, Quebec.

Turcotte, B., Rainville, F., 2022. A new winter discharge estimation procedure: Yukon proof of concept, in: In 26th IAHR International Symposium on Ice, Montréal, Canada.

Vavrus, S.J., Wynne, R.H., Foley, J.A., 1996. Measuring the sensitivity of southern Wisconsin lake ice to climate variations and lake depth using a numerical model. Limnol. Oceanogr. 41, 822–831.

Viglione, A., Parajka, J., Rogger, M., Salinas, J.L., Laaha, G., Sivapalan, M., Blöschl, G., 2013. Comparative assessment of predictions in ungauged basins - Part 3: Runoff signatures in

Austria. Hydrol. Earth Syst. Sci. 17, 2263–2279. https://doi.org/10.5194/hess-17-2263-2013

Vincent, L.A., Milewska, E.J., Wang, X.L., Hartwell, M.M., 2018. Uncertainty in homogenized daily temperatures and derived indices of extremes illustrated using parallel observations in Canada. Int. J. Climatol. 38, 692–707. https://doi.org/10.1002/joc.5203

Vincent, L.A., Wang, X.L., Milewska, E.J., Wan, H., Yang, F., Swail, V., 2012. A second generation of homogenized Canadian monthly surface air temperature for climate trend analysis. J. Geophys. Res. Atmos. 117, 1–13. https://doi.org/10.1029/2012JD017859

Vincent, L.A., Zhang, X., Brown, R.D., Feng, Y., Mekis, E., Milewska, E.J., Wan, H., Wang, X.L., 2015. Observed trends in Canada's climate and influence of low-frequency variability modes. J. Clim. 28, 4545–4560. https://doi.org/10.1175/JCLI-D-14-00697.1

Weyhenmeyer, G.A., Livingstone, D.M., Meili, M., Jensen, O., Benson, B., Magnuson, J.J., 2011. Large geographical differences in the sensitivity of ice-covered lakes and rivers in the Northern Hemisphere to temperature changes. Glob. Chang. Biol. 17, 268–275. https://doi.org/10.1111/j.1365-2486.2010.02249.x

White, K.D., 2008. Breakup ice jam forecasting (Chapter 10). River ice Break. 327–348.

Williams, S.G., Stefan, H.G., 2006. Modeling of lake ice characteristics in North America using climate, geography, and lake bathymetry. J. Cold Reg. Eng. 20, 140–167. https://doi.org/10.1061/(ASCE)0887-381X(2006)20:4(140)

Winchell, M., Srinivasan, R., Di Luzio, M., Arnold, J., 2013. ArcSWAT interface for SWAT2012: User's guide. Blackl. Res. Center, Texas AgriLife Res. Coll. Stn. 1–464.

Xiang, Y., Chen, J., Li, L., Peng, T., Yin, Z., 2021. Evaluation of eight global precipitation datasets in hydrological modeling. Remote Sens. 13, 1–20. https://doi.org/10.3390/rs13142831

Yan, B., Fang, N.F., Zhang, P.C., Shi, Z.H., 2013. Impacts of land use change on watershed streamflow and sediment yield: An assessment using hydrologic modelling and partial least squares regression. J. Hydrol. 484, 26–37. https://doi.org/10.1016/j.jhydrol.2013.01.008

Yang, J., Reichert, P., Abbaspour, K.C., Xia, J., Yang, H., 2008. Comparing uncertainty analysis techniques for a SWAT application to the Chaohe Basin in China. J. Hydrol. 358, 1–23. https://doi.org/10.1016/j.jhydrol.2008.05.012

Yang, X., Liu, Q., He, Y., Luo, X., Zhang, X., 2016. Comparison of daily and sub-daily SWAT models for daily streamflow simulation in the Upper Huai River Basin of China. Stoch. Environ. Res. Risk Assess. 30, 959–972. https://doi.org/10.1007/s00477-015-1099-0

Ye, Y., She, Y., 2021. A systematic evaluation of criteria for river ice breakup initiation using River1D model and field data. Cold Reg. Sci. Technol. 189, 103316. https://doi.org/10.1016/j.coldregions.2021.103316

Yu, D., Xie, P., Dong, X., Hu, X., Liu, J., Li, Y., Peng, T., Ma, H., Wang, K., Xu, S., 2018. Improvement of the SWAT model for event-based flood simulation on a sub-daily timescale. Hydrol. Earth Syst. Sci. 22, 5001–5019. https://doi.org/10.5194/hess-22-5001-2018

Zaremehrjardy, M., Razavi, S., Faramarzi, M., 2021. Assessment of the cascade of uncertainty in future snow depth projections across watersheds of mountainous, foothill, and plain areas in northern latitudes. J. Hydrol. 598, 125735. https://doi.org/10.1016/j.jhydrol.2020.125735

Zelelew, M.B., Alfredsen, K., 2014. Use of Cokriging and Map Correlation to Study Hydrological Response Patterns and Select Reference Stream Gauges for Ungauged Catchments. J. Hydrol. Eng. 19, 388–406. https://doi.org/10.1061/(asce)he.1943-5584.0000803

Zhang, L., Lu, J., Chen, X., Liang, D., Fu, X., Sauvage, S., Perez, J.M.S., 2017. Stream flow simulation and verification in ungauged zones by coupling hydrological and hydrodynamic models: A case study of the Poyang Lake ungauged zone. Hydrol. Earth Syst. Sci. 21, 5847–5861. https://doi.org/10.5194/hess-21-5847-2017

Zhang, X., David Harvey, K., Hogg, W.D., Yuzyk, T.R., 2001. Trends in Canadian streamflow. Water Resour. Res. 37, 987–998. https://doi.org/10.1029/2000WR900357

Zhang, Y., Chiew, F.H.S., 2009. Relative merits of different methods for runoff predictions in ungauged catchments. Water Resour. Res. 45. https://doi.org/10.1029/2008WR007504

Zhao, L., Hicks, F.E., Fayek, A.R., 2012. Applicability of multilayer feed-forward neural networks to model the onset of river breakup. Cold Reg. Sci. Technol. 70, 32–42. https://doi.org/10.1016/j.coldregions.2011.08.011